UNIVERSIDADE FEDERAL DO RIO GRANDE DO SUL
INSTITUTO DE GEOCIÊNCIAS
PROGRAMA DE PÓS-GRADUAÇÃO EM GEOCIÊNCIAS

GEOLOGIA E PETROLOGIA DAS ROCHAS HIPABISSAIS ASSOCIADAS À PROVÍNCIA MAGMÁTICA PARANÁ-ETENDEKA E A SUA CORRELAÇÃO PETROGENÉTICA COM O VULCANISMO DA CALHA DE TORRES NO SUL DO BRASIL

CARLA CECÍLIA TREIB SARMENTO

ORIENTADOR – Prof. Dr. Carlos Augusto Sommer
COORIENTADOR – Prof. Dr. Evandro Fernandes de Lima

Porto Alegre – 2017

UNIVERSIDADE FEDERAL DO RIO GRANDE DO SUL
INSTITUTO DE GEOCIÊNCIAS
PROGRAMA DE PÓS-GRADUAÇÃO EM GEOCIÊNCIAS

GEOLOGIA E PETROLOGIA DAS ROCHAS HIPABISSAIS ASSOCIADAS À PROVÍNCIA MAGMÁTICA PARANÁ-ETENDEKA E A SUA CORRELAÇÃO PETROGENÉTICA COM O VULCANISMO DA CALHA DE TORRES NO SUL DO BRASIL

CARLA CECÍLIA TREIB SARMENTO

ORIENTADOR – Prof. Dr. Carlos Augusto Sommer
CO-ORIENTADOR – Prof. Dr. Evandro Fernandes de Lima

BANCA EXAMINADORA

Profa. Dra. Adriane Machado – UFS

Prof. Dr. Breno Leitão Waichel – UFSC

Profa. Dra. Márcia Elisa Boscato Gomes – UFRGS

Tese de Doutorado apresentada como requisito parcial para a obtenção do Título de Doutor em Ciências

Porto Alegre – 2017

Sarmento, Carla Cecília Treib

Geologia e petrologia das rochas hipabissais associadas à província magmática Paraná-Etendeka e a sua correlação petrogenética com o vulcanismo da Calha de Torres no Sul do Brasil/ Carla Cecília Treib Sarmento. – 2017.

186 f. ; 30 cm.

Tese (doutorado) – Universidade Federal do Rio Grande do Sul, Programa de Pós-Graduação em Geociências da UFRGS, Porto Alegre, 2017.

Orientador: Prof. Dr. Carlos Augusto Sommer.
Co-orientador: Prof. Dr. Evandro Fernandes de Lima

1. Petrologia. 2. Vulcanismo. 3. Petrogenética. I. Sommer, Carlos Augusto. II. Lima, Evandro Fernandes de. III. Universidade Federal do Rio Grande do Sul. IV. Título.

CDD 552

Catalogação na Publicação
Biblioteca Instituto de Geociências -
UFRGS Sibila F. T. Binotto CRB
10/1743

Universidade Federal do Rio Grande do Sul - Campus do Vale Av. Bento Gonçalves, 9500 - Porto Alegre - RS - Brasil
CEP: 91501-970 / Caixa Postal: 15001.
Fone: +55 51 3308-6329 Fax: +55 51 3308-6337
E-mail: bibgeo@ufrgs.br

AGRADECIMENTOS

Gostaria de agradecer aos meus orientadores Carlos Augusto Sommer e Evandro Fernandes de Lima pela dedicação e ensinamentos ao longo do período de doutorado.

Agradeço à amiga Dra. Carla J. Santos Barreto pela preparação das amostras e obtenção dos resultados de isótopos realizadas no Laboratório de Geologia Isotópica da Universidade Federal do Pará com o apoio de Jean-Michel Lafon e pela participação no segundo artigo.

Agradeço a Edinei Koester pelo apoio na preparação das amostras e resultados de isótopos realizadas no Laboratório de Geologia Isotópica da Universidade Federal do Rio Grande do Sul.

Meus agradecimentos também aos geólogos Diego Skieresz de Oliveira, Suzana Benites, Roberto Noll Filho e Hemeli Ligabue pela ajuda na coleta das amostras.

Por fim, quero agradecer também à CAPES por fornecer a minha bolsa de estudos durante o doutorado.

RESUMO

O estudo das intrusões máficas subvulcânicas pertencentes a Província Magmática Paraná-Etendeka foi efetuado no extremo sul do Brasil. Esses corpos subvulcânicos cortam as Formações Torres, Vale do Sol e Palmas, Grupo Serra Geral, na ombreira sul da Calha de Torres e as rochas sedimentares que bordejam a Bacia do Paraná. A direção preferencial dos diques intrusivos nas rochas sedimentares (NE-SW) coincide com lineamentos tectono-magmáticos que serviram de dutos para enxames de diques paralelos à costa brasileira e também a mesma direção do enxame de diques da costa da Namíbia, sugerindo que esses diques fizeram parte do sistema de junção tríplice relacionado à abertura do Atlântico Sul. As direções preferenciais dos diques que cortam derrames de lava (NW-SE) são similares às direções dos Arcos de Ponta Grossa, Rio Grande e da Calha de Torres e podem ter feito parte ou serem causados por um ou mais dos ciclos geotectônicos que originaram essas estruturas. Em relação à morfologia, os diques foram separados em dois grupos distintos: simétricos e assimétricos. As rochas foram divididas em dois termos: Toleíto Supersaturado em Sílica (SST) – diques e sills constituídos por plagioclásio e clinopiroxênios como minerais essenciais; e Olivina Toleíto Saturado em Sílica (SSOT) - diques constituídos principalmente por plagioclásio, clinopiroxênio e olivina. Os dados geoquímicos de elementos maiores e elementos-traço permitem classificar esses corpos hipabissais como basaltos (SSOT), andesitos basálticos e traquiandesitos (SST) de afinidade toleítica. Os diques SSOT têm assinaturas geoquímicas e apresentam variações isotópicas restritas ($^{87}Sr/^{86}Sr_i$ = 0.70570 a 0.70585; εNd_i = -1.01 a -4.49; $^{206}Pb/^{204}Pb$ = 18.0306), sem magma-tipo LTi equivalente na Província do Paraná, mas mais próximas das razões isotópicas dos magmas-tipo LTi com MgO > 7w% como o Nil Desperandum, na Província Etendeka. Os diques SST mostram variações isotópicas mais amplas ($^{87}Sr/^{86}Sr_i$ = 0.70787 a 0.71336; εNd_i = - 2.51 a - 8.65; $^{206}Pb/^{204}Pb$ = 18.578 a 19.049) e assinaturas geoquímicas similares ao magma-tipo Gramado, na Província do Paraná e também ao magma-tipo Tafelbeg no lado africano. Quando os diques são confrontados com os fluxos de lava divididos em associações de litofácies, conforme o comportamento dos elementos geoquímicos e das razões isotópicas Sr-Nd-Pb, é

observado que os diques fazem parte de um sistema de abastecimento dos derrames básicos, estratigraficamente posicionados acima das lavas encaixantes. A variação dessas razões isotópicas pode ter ocorrido pela contaminação no momento da ascensão e extrusão do magma. A partir do modelamento dos diques mais primitivos SSOT com os derrames de lava da ombreira sul da Calha de Torres, o processo de cristalização fracionada seguida de assimilação crustal teve um papel importante desde a ascensão dos magmas pelos condutos até a extrusão das lavas. O comportamento dos elementos-traço revela que a assimilação de rochas com idades tanto Paleoproterozoica quanto Neoproterozoica pode ser considerada, porém de acordo com modelamento de razões isotópicas, uma maior contribuição de crosta Neoproterozoica foi constatada.

ABSTRACT

The study of the mafic subvolcanic intrusions from Paraná-Etendeka Igneous Province was performed in the extreme south of Brazil. These subvolcanic bodies are intrusive in the Torres, Vale do Sol and Palmas Formations, which belong to the Serra Geral Group, in the south hinge of the Torres Syncline and sedimentary rocks bordering the Paraná Basin. The preferred direction of the intrusive dikes in the sedimentary rocks (NE-SW) coincides with tectonic-magmatic that served as vents for dike swarms parallel to the Brazilian coast, with the same direction as the Namibia coast dike swarm. This suggests that these dikes were part of the triple junction system related to the opening of the South Atlantic Ocean. The preferred directions of the intrusive dikes in the lava flows (NE-SW) are similar to the directions of the Ponta Grossa and Rio Grande Arcs and the Torres Syncline. They may have been a part of, or been caused by one or more geotectonic cycles that originated these structures. Regarding the morphology, the dikes were separated into two different groups: symmetrical and asymmetrical. The rocks were divided into two types: Silica Supersaturated Tholeiite (SST) - dikes and sills consisting of plagioclase and clinopyroxene as essential minerals; and Silica Saturated Olivine Tholeiite (SSOT) - dikes consisting mainly of plagioclase, clinopyroxene and olivine. The major and trace element geochemistry allows classifying these hypabyssal bodies as basalts (SSOT), basaltic andesites and trachyandesites (SST) of tholeiitic affinity. The SSOT dikes show restricted isotopic ranges ($^{87}Sr/^{86}Sr_i$ = 0.70570 to 0.70585; εNd_i = -1.01 to -4.49; $^{206}Pb/^{204}Pb$ = 18.0306), with no equivalent LTi magma type in the Paraná Province, but are closer to the isotopic ratios of LTi magma types with MgO > 7w% such as Nil Desperandum in the Etendeka Province. The SST dikes show broader isotopic ranges ($^{87}Sr/^{86}Sr_i$ = 0.70787 to 0.71336; εNd_i = -2.51 to -8.65; $^{206}Pb/^{204}Pb$ = 18.578 to 19.049), similar to the Gramado magma type in the Paraná Province and also to the Tafelberg magma type in the African side. When the dikes are compared with the lava flows that are divided into lithofacies associations according to the behavior of the geochemical elements and Sr-Nd-Pb isotopic ratios, it is observed that the dikes are part of a supply system of basic lava flows stratigraphically positioned above the host lavas. The variation of these isotopic ratios may have

occurred due to the contamination at the moment of magma rise and extrusion. Based on the trace element modeling of the SSOT dikes with the lava flows of the south hinge of the Torres Syncline, the fractional crystallization process followed by crustal assimilation played an important role, from the magma rise through the conduits to the extrusion of the lavas. The behavior of the trace elements revealed that the assimilation of rocks with both Palaeoproterozoic and Neoproterozoic ages can be considered, but according to isotopic modeling, a greater contribution of the Neoproterozoic crust was verified.

LISTA DE FIGURAS

LISTA DE TABELAS

SUMÁRIO

ESTRUTURA E ORGANIZAÇÃO DA TESE

Esta tese está estruturada em formato de artigos científicos, publicados e/ou submetidos em periódicos. Consequentemente, sua organização compreende as seguintes partes:

Capítulo 1: É apresentada a introdução com os principais temas que motivaram este estudo, bem como os objetivos propostos para esta tese. Em seguida, é apresentada a área de estudo e os materiais e métodos utilizados.

Capítulo 2: É apresentada uma contextualização teórica sobre as Grandes Províncias Ígneas (LIPs), Províncias Basálticas Continentais com destaque para Província Magmática Paraná-Etendeka. Também são apresentados aspectos gerais sobre os corpos intrusivos associados a algumas das principais Províncias Basálticas Continentais como as províncias do Deccan, Karoo, Columbia River e Paraná-Etendeka, além de tópicos sobre a morfologia e os condicionantes físicos relacionados aos mecanismos de intrusão dos corpos hipabissais.

Capítulo 3: São apresentados três artigos científicos submetidos a periódicos internacionais, atendendo as normas estabelecidas pelo Programa de Pós-Graduação em Geociências da Universidade Federal do Rio Grande do Sul.

O primeiro artigo intitulado *"Mafic subvolcanic intrusions and their petrologic relation with the volcanism in the south hinge Torres Syncline, Paraná-Etendeka Igneous Province, southern Brazil"* foi aceito e publicado no periódico: *Journal of South American Earth Sciences.* O Segundo artigo intitulado *"Sr-Nd-Pb isotopic insights of the mafic subvolcanic intrusions from Paraná-Etendeka Igneous Province: Petrologic and isotopic relationship with the volcanism of the southern Brazil"* foi submetido no periódico: *Journal of Volcanology and Geothermal Research* e o terceiro artigo intitulado: *"Petrogenesis of mafic sills from Paraná-Etendeka Igneous Province in southernmost Brazil: Trace element and isotope geochemistry"* foi submetido no periódico: *Geological Journal*.

Capítulo 4: Estão reunidas as considerações finais da tese com a síntese integradora das principais conclusões obtidas com os artigos científicos. Para finalizar, as referências bibliográficas citadas nos capítulos que antecedem os artigos, permanecendo as referências dos artigos listados nos mesmos.

1. INTRODUÇÃO

A investigação das intrusões básicas/intermediárias (diques e soleiras) tem se mostrado de fundamental importância para o entendimento da gênese e evolução das Grandes Províncias Ígneas (Large Igneous Province - LIPs), principalmente as Províncias Basálticas Continentais como as Províncias do Deccan Traps, Columbia River, Siberian Traps e Paraná-Etendeka.

A Província Magmática do Paraná-Etendeka, vinculada ao Cretáceo Inferior, ocorre na porção centro-sul da Placa Sul-Americana, principalmente no Brasil, onde concentra-se cerca de 90% desta província, sendo o restante localizado na África. No Brasil estes vulcanitos são reunidos e denominados estratigraficamente como Grupo Serra Geral (GSG) que abrange toda a região centro-sul do país.

As intrusões de rochas básicas e intermediárias toleíticas correlacionadas aos derrames do GSG são fenômenos comuns na Bacia do Paraná. Estudos recentes demonstram que o volume referente a esses corpos intrusivos do tipo soleira é de pelo menos 112.000 km^3 (Frank et al., 2009). Por outro lado, não há uma estimativa em relação ao volume vinculado aos diques. Os sills ocorrem com maior concentração no limite leste da Bacia do Paraná, eles também são relativamente abundantes em toda sua extensão, normalmente intrusivos nos sedimentos paleozóicos (Almeida, 1986; Zalán et al., 1985) nos Estados de São Paulo (Machado et al., 2007) e do Paraná (Maniesi & Oliveira, 1997; Petersohn et al., 2007; Petersohn & Gouvea, 2009). Muitas vezes essas intrusões estão agrupadas na forma de enxames, cujas ocorrências têm maior concentração no estado de Paraná (enxame de diques de Ponta Grossa), Santa Catarina (enxame de diques de Florianópolis) (Raposo et al., 1998; Deckart et al., 1998; Marques & Ernesto, 2004; Tomazzoli & Lima, 2006; Florisbal et al., 2014, 2017; Tomazzoli & Pellerin, 2015), São Paulo e Rio de Janeiro (enxame de diques da Serra do Mar)) (Turner et al.,1994; Stewart et al., 1996; Corval et al., 2008; Valente et al., 2007; Corval, 2009).

Alguns corpos intrusivos têm sido investigados ao longo dos anos no extremo sul do Brasil, principalmente no contexto das unidades sedimentares da Bacia do Paraná. Entre estes, destacam-se o Complexo Básico Lomba Grande (Viero &

Roisenberg, 1992) de composição picrítica a andesito basáltica, as soleiras de composição andesito-basáltica localizadas nas regiões de Manoel Viana e Agudo (Renner et al., 2008; Renner, 2010) e as soleiras básicas/intermediárias da região do Cerro do Coronel, Pantano Grande (Sarmento et al., 2014).

A importância das intrusões na evolução das Grandes Províncias Magmáticas Basáticas Continentais tem sido demonstrada em alguns trabalhos, destacando-se Bryan (2007), Bryan & Ernst (2008), Sheth et al. (2013), Vanderkluysen et al. (2011); Florisbal et al., (2014, 2017). No entanto, poucas investigações têm sido realizadas com o intuito de apresentar um panorama estatístico das intrusões básicas/intermediárias e qual a sua relação geológica e petrológica com os depósitos vulcânicos associados, levando-se em conta questões estratigráficas e de tipologia dos derrames, num contexto estrutural da Bacia do Paraná (e.g. vulcanismo e sedimentação preenchendo a Calha de Torres).

Uma importante questão ainda em debate é a origem dos magmas da Província Magmática Paraná-Etendeka e a influência da contaminação crustal. O processo de contaminação tem sido bem documentado para os basaltos de baixo Ti da Província Magmática Paraná-Etendeka (Cox & Hawkesworth, 1985; Mantovani et al., 1985; Petrini et al., 1987; Hawkesworth et al., 1988; Piccirillo et al., 1989; Peate & Hawkesworth, 1996; Ewart et al., 1998; Barreto et al., 2016), embora ainda sejam poucos os estudos quantitativos do grau de contaminação e dos possíveis contaminantes no sul da Província Paraná.

1.1. OBJETIVOS

Os objetivos gerais do presente trabalho envolvem a caracterização geológica, petrográfica e geoquímica das rochas hipabissais básicas/intermediádias associadas ao Grupo Serra Geral na região centro-leste do Rio Grande do Sul, visando o aprimoramento dos conhecimentos que se tem respeito à relação entres os corpos intrusivos e e as rochas vulcânicas distribuídas ao longo da Calha de

Torres e, consequentemente, sobre o magmatismo toleítico da Província Magmática do Paraná-Etendeka no Sul do Brasil.

Como objetivos específicos, destacam-se:

1) Mapeamento geológico de detalhe dos corpos hipabissais: controle estrutural e disposição espacial das intrusões; Observação das estruturas internas e aspectos de colocação (*emplacement*) das rochas intrusivas nas encaixantes;

2) Caracterização petrográfica e geoquímica dos diques e *sills* estudados, com o intuito de investigar aspectos petrogenéticos para tecer considerações sobre os aspectos genéticos e evolutivos destas;

3) Discutir as variações geoquímicas e isotópicas Sr-Nd-Pb dos diques e sills;

4) Estabelecer vínculos petrogenéticos com os derrames de acordo com as associações de litofácies do Grupo Serra Geral, proposto par a Calha de Torres, no sul do Brasil.

5) Avaliar a importância da assimilação crustal e discutir hipóteses sobre a origem e evolução do magmatismo durante sua ascensão e extrusão, bem como estimar os possíveis contaminantes envolvidos;

6) Discutir semelhanças petrogenéticas entre as intrusões investigadas e as intrusões básicas de baixo Ti da Província Etendeka, Namíbia.

1.2. LOCALIZAÇÃO DA ÁREA

A área de estudo abrange parte da sub-província sul do Grupo Serra Geral, ombreira sul da Sinclinal de Torres, centro-leste no Rio Grande do Sul, como também o limite com as rochas sedimentares da Bacia do Paraná no Estado (Figura 1).

Geograficamente a área do projeto abrange uma região desde centro-leste até o extremo nordeste do Rio Grande do Sul, envolvendo politicamente municípios

de importantes macroregiões do estado: Vales, Grande Porto Alegre, Litoral Norte e Serra Gaúcha. Os principais acessos à região, partindo-se de Porto Alegre são as rodovias BR 290, BR 101, BR 116 e BR 020, utilizando-se, também, muitos acessos não pavimentados.

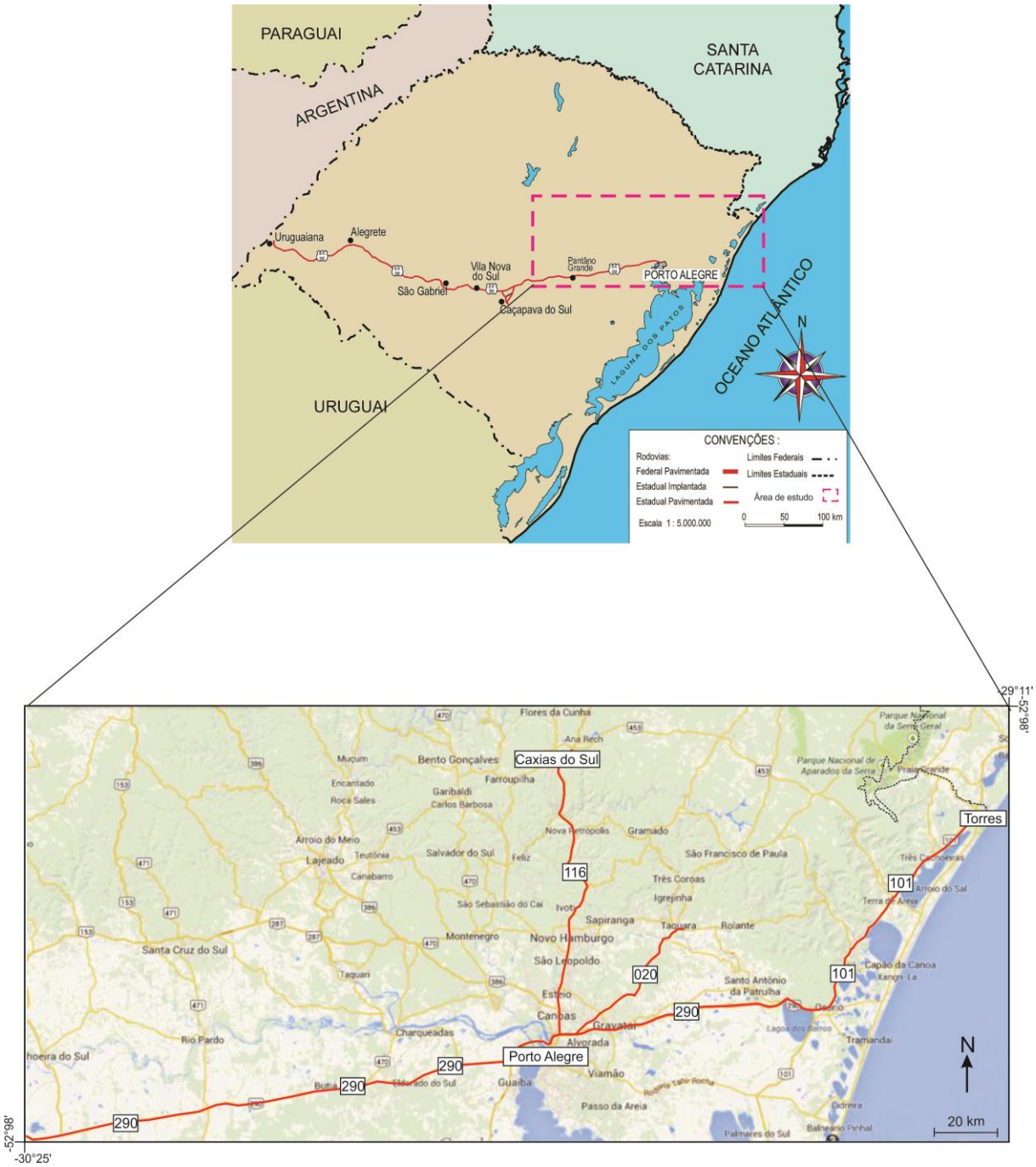

Figura 1. Localização da área de estudo e as principais vias de acesso.

1.3. MÉTODOS E INSTRUMENTOS

1.3.1. Levantamento Bibliográfico

Envolveu a compilação de publicações referentes às áreas relacionadas ao estudo e temas afins a pesquisa, reunindo assim um conjunto de informações úteis sobre os objetivos a serem alcançados e métodos a serem utilizados no decorrer deste trabalho. Nesta etapa, foram adquiridas informações acerca da geologia, petrografia e petrogênese das rochas que caracterizam a Província Magmática do Paraná-Etendeka. Também foram levantadas bibliografias referentes aos estudos geoquímicos e petrográficos das rochas relacionadas ao vulcanismo que se manifestou na forma de derrames e corpos intrusivos.

1.3.2.Trabalhos De Campo

Foram realizadas etapas de trabalho que consistiram em visitações de afloramentos em cortes de estrada com exposição de perfil de derrames basálticos que continham intrusões e pedreiras e ao longo da borda da Bacia do Paraná na região. Para isso, foram utilizadas as folhas de 1:250 000 de Gravatai SH.22-X-C e D, Cachoeira do Sul SH.22-Y-A, Caxias do Sul SH.22-V-D e Porto Alegre SH.22-Y-B.

Foram descritos pontos que orientaram uma coleta seletiva de amostras para estudo petrográficos e geoquímicos. Em cada ponto fez-se o uso de receptores *GPS* para a obtenção de coordenadas UTM precisas. Os afloramentos foram descritos detalhadamente, fotografados e amostrados. Amostras das bordas e dos núcleos dos diques e soleiras foram coletadas sempre que possível. Utilizou-se uma bússola para medidas de atitude dos diques.

1.3.3.Petrografia

A etapa de preparação de amostras foi executada no Laboratório de Apoio Analítico e Preparação de Amostras do CPGq (Centro de Estudos em Petrologia e Geoquímica – IG) da UFRGS.

Para os estudos petrográficos foram confeccionadas lâminas delgadas para análise com o auxílio de microscópio petrográfico de luz polarizada convencional. Estas análises compreendem a identificação e quantificação da mineralogia modal, da textura e estrutura das amostras coletadas. É feito o corte da rocha em fatias de aproximadamente 2 cm de espessura. Na etapa seguinte, uma fatia fina é separada, lixada com lixas de distintos potenciais de desbaste (120, 220, 600, 1.200, 2.500 e 4.000 grana) é submetida a processos de abrasão com abrasivos de carbeto de silício (900µm) e óxido de alumínio (9,5µm). O polimento das lâminas é feito com politriz com a aplicação de 100 rotações por minuto (rpm) durante aproximadamente 5 minutos com abrasivo composto por alumina (0,3µm).

Nesta etapa também foi realizada a obtenção de fotomicrografias das amostras mais representativas, destacando os vários tipos de textura e ocorrência mineralógica, através da utilização do “Microscópio de Aquisição de Imagens Leica”.

1.3.4. Geoquímica De Rocha Total

Os dados foram obtidos junto ao laboratório com excelente precisão analítica e credibilidade internacional ACME. Para a realização das análises geoquímicas, são preparadas as amostras para análise geoquímica de rocha total para caracterizar as unidades estudadas a partir da determinação da composição dos elementos maiores, traços e terras raras. As análises geoquímicas são feitas no *Acme Laboratories Ltda* (Canadá) por Espectrometria de Emissão de Plasma (*Inductively Coupled Plasma – Emission Spectometer* - ICP-ES) para os elementos maiores, com limite de detecção de 0,01% e para Sc, Be, V, Ba, Sr, Y e Zr, com limite de detecção de 1 a 5 ppm. Para os demais elementos-traço e elementos terras raras foi utilizado a técnica Espectrometria de Emissão de Plasma com

Espectrometria de Massa (*Inductively Coupled Plasma – Mass Spectrometer - ICP-MS)* com limite de detecção de 0,005 a 2 ppm.

1.3.5. Microssonda Eletrônica

Esta etapa foi realizada no Laboratórios de Microssonda Eletrônica do CPGq/IG/UFRGS. Dados de química mineral serão utilizados como apoio na definição da afinidade geoquímica e evolução petrogenética. Foram feitas análises de piroxênios, plagioclásio e olivina. O equipamento de Microssonda eletrônica utilizado para obtenção de dados quantitativos e qualitativos é uma CAMECA SX-5 equipada com cinco espectrômetros tipo WDS e um espectrômetro tipo EDS situado no Laboratório de Microssonda Eletrônica do CPGq – IGEO – UFRGS. As lâminas delgadas são revestidas com película de carbono para que o feixe de elétrons seja condutivo na superfície das amostras. As condições analíticas para análise de silicatos inclui diâmetro de feixe de elétrons em 1µm, corrente *Faraday* em 15 nA com aceleração de voltagem em 15 kV. Espectrômetros SP1- TAP (Na e Mg), SP2 - LLIF (Fe, Ni e V), SP3 – LPET (Ti, Cr e Mn), SP4 – TAP (Na e Mg) e SP5 – PET (K e Ca).

Os resultados das análises foram disponibilizados pela equipe técnica do laboratório na forma de planilhas do Microsoft Excel, os quais foram tratados e interpretados em planilhas específicas para cálculo de estequiometria mineral, disponíveis em *http://www.gabbrosoft.org/spreadsheets.html*.

1.3.6. Geoquímica isotópica

Foram submetidas 6 amostras a análises isotópicas de Sr, Nd e Pb no Laboratório de Geologia Isotópica da Universidade Federal do Rio Grande do Sul (LGI-UFRGS) e 15 amostras no Laboratório de Geologia Isotópica da Universidade Federal do Pará (Pará-Iso UFPA).

No LGI-UFRGS, foi utilizado um espectrômetro de massa multi-coletor por ionização térmica (*Thermal Ionization Mass Spectrometer – TIMS*), modelo VG

Sector 54. Foram obtidos dados isotópicos Rb-Sr, Sm-Nd e Pb-Pb, através da moagem da rocha total em gral de ágata, a fim de se obter uma fração < 200 *mesh*. Após estes procedimentos, as amostras foram pesadas, adicionados traçadores (*spikes*) mistos $^{149}Sm/^{150}Nd$ e $^{87}Rb/^{84}Sr$ e foram dissolvidas com misturas de HF e HNO_3, concentrados e soluções de HCl 6N, em frascos de teflon (Savilex) de 7mL, onde foram aquecidas em chapa quente a temperatura de 40°C durante sete dias, passando por procedimentos periódicos de agitação para que os possíveis problemas de dissolução e homogeneização entre as amostras e os *spikes* fossem minimizados. Depois de completa a dissolução, as amostras foram secas e redissolvidas em HCl 2,5N. Rb, Sr e ETR foram separados usando colunas preenchidas por resina de troca catiônica Dowex AG-50-X8 (200-400 *mesh*), utilizando HCl 2,5N para Rb e Sr e HCl 6N para os ETR. Nd e Sm foram separados dos demais ETR usando colunas de troca com resina HDEHP LN (50-100μm) e HCl 0,18N para Nd e HCl 0,5N para Sm. Pb foi separado através de colunas de resina de troca catiônica Dowex AG-1X8 (200-400 *mesh*), diluídas com HBr 0,6N e coletadas com HCl 6N. As razões isotópicas foram determinadas no modo *static multi-coletor*, utilizando coletores Faraday. Rb, Sr, Sm e Pb foram secos e depositados sobre filamentos simples de Re, enquanto os isótopos de Nd, em filamentos triplos de Ta-Re-Ta. Rb foi seco e depositado com auxílio de HNO_3, enquanto Sr, Sm, Nd e Pb com H_3PO_4, e o primeiro também foi depositado com sílica gel. As medidas dos padrões NIST foram: NBS 987 ($^{87}Sr/^{86}Sr$ = 0,71026 ± 0,000011; 1σ; n = 100) e as razões isotópicas foram normalizadas para $^{86}Sr/^{88}Sr$ = 0,1194; La Jolla (0,511848 ± 0,000021; 1σ; n = 100) e normalizadas para $^{146}Nd/^{147}Nd$ = 0,7219. O Pb foi corrigido para o efeito de fracionamento em 0,1% amu-1 com base em 38 análises do padrão NBS-981. Os valores de brancos totais para Rb e Sm foram < 500 pg, para Sr < 60 pg, para Nd < 150 pg e para Pb < 100 pg. Os erros analíticos típicos para $^{87}Rb/^{86}Sr$, $^{147}Sm/^{144}Nd$ e a razão $^{206}Pb/^{204}Pb$ foram iguais ou melhores do que 0,1%. A idade Rb-Sr foi calculada seguindo Ludwig (2001). As idades modelo Nd foram calculadas de acordo com De Paolo (1981). As constantes de decaimento utilizadas foram aquelas recomendadas por Steiger *&* Jäger (1977) e Wasserburg *et al.* (1981). Os erros para todos os dados isotópicos apresentados na tabela 30 são melhores do que 0,0010 (SD absoluta) para $^{87}Rb/^{86}Sr$, 0,00020 (SD absoluta) para $^{87}Sr/^{86}Sr$, 25

ppm para Sm/Nd, 20 ppm para $^{143}Nd/^{144}Nd$ e inferior a 0,0020 (SD absoluta) para Pb, e a média das análises foi, em geral, 10 blocos de 10 análises (n = 100).

No Pará-Iso UFPA, o equipamento utilizado foi o espectrômetro de massa ICP multi-coletor Thermo-Finnigan Neptune equipado com um sistema de nove coletores de íons em modo Faraday. Aproximadamente 100 mg de amostra de rocha foi misturada a um *spike* de $^{149}Sm/^{150}Nd$ e dissolvida nos ácidos HNO_3, HCl e bombas de Teflon Savillex em forno microondas. Um procedimento cromatográfico de troca iônica de duplo estágio foi utilizado para a purificação do elementos Pb, Sr, Nd, e Sm. A primeira etapa consistiu na elutriação das amostras de colunas de Teflon preenchidas com resina catiônica (Biorad Dowex AG 50W-X8) usando os ácidos HCl e HNO_3. O pb é coletado após elutriação com 3,9 ml de HCl 2N e Sr coletado após elutriação com 13 ml de HCl 2N. O grupo dos ETRs foi extraído após elutriação com 2 ml de HCl 2N e 12 ml de HNO_3 3N. No estágio seguinte, oso elemantos Sm e Nd foram separados dos outros ETRs com o objetivo de evitar interferências isobáricas dos ETRP (Yang et al., 2012). A solução de ETR foi adicionada a colunas de Teflon preenchidas por resina Eichrom Ln, sendo que a fração de Nd foi coletada após elutriação de 7,3 ml de HCl 0,2N e o Sm foi coletado após elutriação de 5 ml de HCl 0,2N e 7 ml de HCl 0,3N. Para a segunda etapa de separação deo Sr, a solução de amostra foi carregada em colunas de Teflon preenchidas por resina Eichron Ln, no qual o Sr é coletado após adição de 2 ml de HNO_3 3,5N. Para a segunda separação cromatagráfica de Pb, a solução de amostra foi adicionada à colunas de Teflon preenchidas do Eichron Ln, onde foram adicionados 3 ml de HCl 2N. O Pb foi coletado após adição de 3 ml de HCl 6N. A fração de Pb coletada na segunda separação foi dissolvida em 500 µl de HNO_3 3% +Tl (tálio) 50 ppb e então analisada. Os elementos Sr, Sm e Nd foram dissolvidos para análise em 2 ml de HNO_3 3%. Os cálcuos de incerteza para as razões Sm/Nd e $^{143}Nd/^{144}Nd$ são baseados nas análises repetidas dos materiais de referência BCR-1 e La Jolla, respectivamente (Oliveira et al., 2008). As razões isotópicas de Sr foram normalizadas para $^{86}Sr/^{88}Sr$= 0,1194. As composições isotópicas de Sr foram normalizadas para $^{146}Nd/^{144}Nd$= 0,7219, cuja constante de decaimento utilizada foi o valor revisado por Lugmair & Marti (1978) de $6,54 \times 10^{-12.y-1}$.

2. CONTEXTUALIZAÇÃO TEÓRICA

2.1. GRANDES PROVÍNCIAS ÍGNEAS (LIPs)

O termo “Large Igneous Provinces” (LIPs) foi proposto por Coffin & Eldholm (1994) para definir uma variedade de províncias ígneas máficas com grande extensão territorial (> 0,1 Mkm^2), formadas a partir de anômalos eventos ígneos de curta duração de colocação (<1-5 Ma), resultando em rápida acumulação de um grande volume (> 1000 Km^3) de rochas extrusivas e intrusivas. A base de dados no qual o termo LIP foi definido se resume quase que exclusivamente aos registros preservados do Mesozóico e Cenozóico, com composição predominantemente básica, que compreendem as províncias basálticas continentais, os platôs oceânicos e basaltos de fundo oceânico.

A maioria da LIPs é composicional e volumetricamente dominada por rochas máficas, em geral toleíticas, que afloram como sucessões de derrames basáltivos. Entratanto, volumes consideráveis de magmatismo ácido estão fraquentemente associados à LIPs continentais. Em outros casos, as LIPs são dominantemente ácidas sendo denominadas Grandes Privíncias ìgneas Félsicas (*Silicic Large Igneous Provinces* – *SLIPs*) (Figura 2).

Bryan & Ernst (2008) (Figura 3) propuseram uma revisão da definição de LIPs e enfatizaram que a classificação de uma província ígnea como LIP, baseada somente na sua extensão (Sheth, 2007) poderia agrupar incorretamente províncias ígneas de diferentes origens, contexto tectônico, contexto geodinâmico, condições de colocação dos magmas e duração do evento ígneo. Dessa forma, volume, duração e taxas de colocação do magma são características igualmente importantes que necessitam ser consideradas para que haja uma definição mais precisa das LIPs.

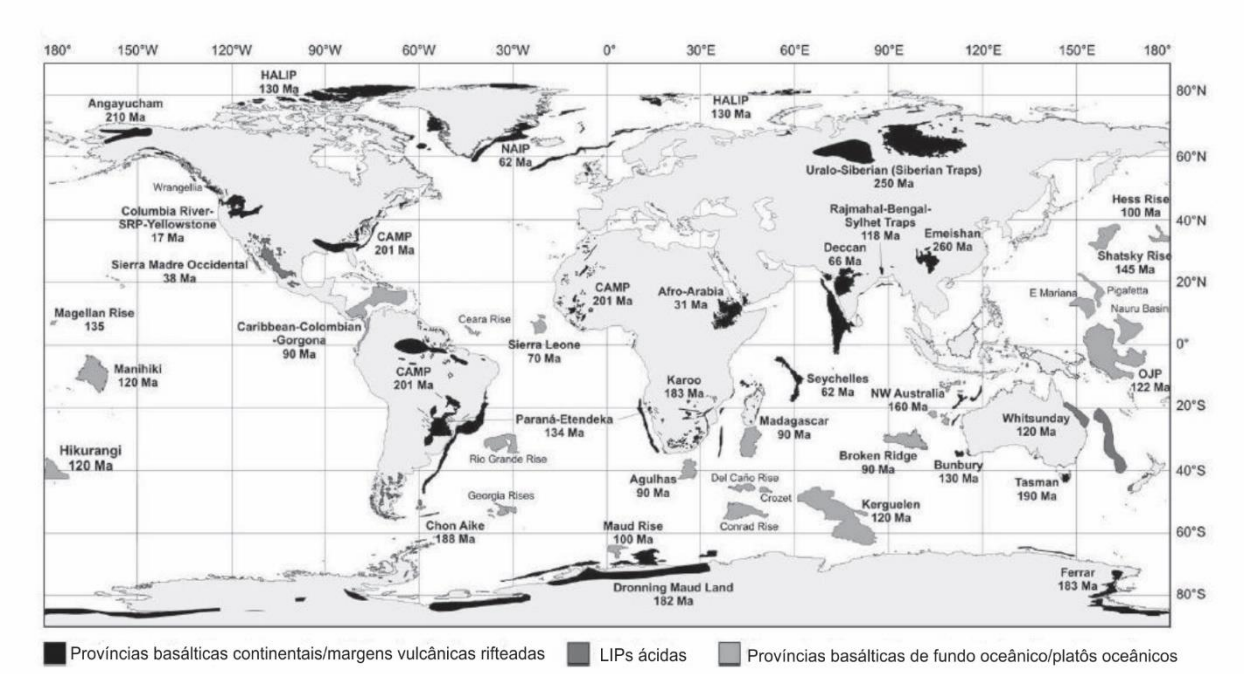

Figura 2. Distribuição global das grandes províncias ígneas (Fonte: traduzido de Bryan & Ernst (2008)).

A frequência dessas erupções e o volume total de magma liberado durante os principais pulsos magmáticos indicam que as LIPs são eventos excepcionais na história geológica da Terra e muitas vezes responsáveis por mudanças ambientais regionais ou globais incluindo mudanças climáticas, eventos de extinção, mudanças topográficas regionais e quebras de supercontinentes (Courtillot et al., 1986; Rampino & Stothers, 1988; Courtillot, 1990, 1995, 1999; Glen, 1994; Rampino & Haggerty, 1996; Wignall, 2001, 2005; Courtillot & Renne, 2003; Kelley, 2007).

As LIPs, tanto básicas quanto ácidas, foram definidas ou caracterizadas por um conjunto de atributos além de extensão: 1) idade (Arqueano, Proterozoico, Fanerozoico); 2) volume; 3) contexto crustal (continental versus oceânico); 4) contexto tectônico; 5) duração ou rapidez de colocação do magma; 6) caráter intrusivo ou extrusivo (Sheth, 2007); 7) composição (ácidas ou básicas (Bryan & Ernst, 2006)). Com isso, foram incluídas nessa divisão as LIPs ácidas, além de LIPs mais antigas, como complexos intrusivos máfico-ultramáficos e greenstone belts arqueanos.

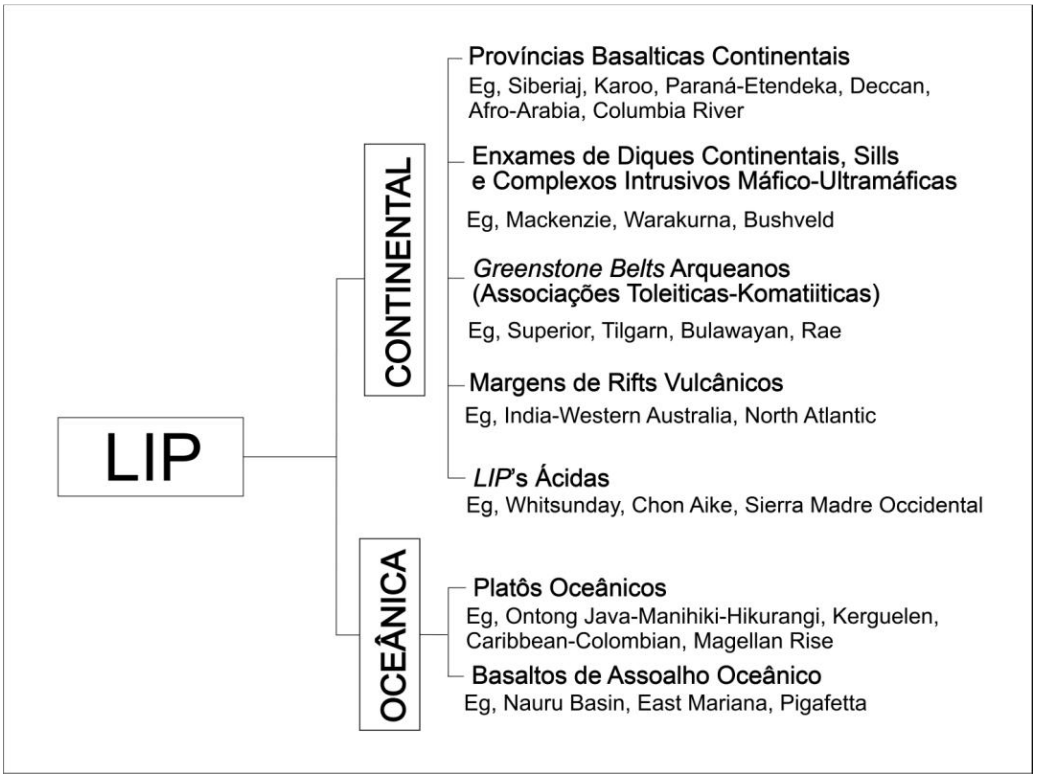

Figura 3. Classificação das grandes províncias ígneas incluindo LIPs antigas e LIPs ácidas (Fonte: traduzido de Bryan & Ernst (2008)).

2.2. PROVÍNCIAS BASÁLTICAS CONTINENTAIS

As Províncias Basálticas Continentais (PBCs) resultam do derramamento de enormes volumes de lava de composições predominantemente toleíticas (Coffin & Eldholm, 1992), em períodos de tempo relativamente curtos (Self et al., 1998) (Figura 4). Em geral, constituem imensos platôs que antecedem a quebra dos supercontinentes e a formação de riftes (White & McKenzie, 1989; Coffin & Eldhom, 1994). A maior parte das PBCs foi formada durante os períodos Mesozóico e Cenozóico e extravasaram em um curto espaço de tempo, na ordem de 1 Ma (Bryan & Ernst, 2008), e são aparentemente sincrônicos com as grandes crises climáticas globais e extinções em massa. Estas províncias estão presentes em todos os continentes do planeta, destacando-se as Províncias do Deccan (Índia), Paraná-Etendeka (Brasil/Namíbia), Karoo (África do Sul), Columbia River (EUA) e Traps Siberianos (Rússia) (Tabela 1).

Foram propostos diversos modelos que procuram explicar a origem dos derrames e das intrusões associadas. Algumas PBCs estão relacionadas à superplumas e sua relação com a formação e fragmentação de supercontinentes (White & McKenzie, 1995; Kumagai & Kurita, 2005). De acordo com o modelo de plumas mantélicas (Gibson et al., 1995, 1999; Milner & Le Roex, 1996), as assinaturas geoquímicas e isotópicas deveriam ser compatíveis com uma contribuição dominante de manto astenosférico na gênese dos basaltos (Campbell & Griffiths, 1990; Arndt & Christensen, 1992). Por outro lado, White & McKenzie (1989) e Coffin & Eldhom (1994), propõem que a atividade ígnea estaria relacionada a processos distensivos, que poderiam evoluir para a abertura de oceanos, sendo que neste caso, a distensão da litosfera precederia o magmatismo, ocasionando alívio de pressão em regiões do manto anomalamente quentes. Alguns autores propõem uma origem no manto litosférico, sem assinatura geoquímica e isotópica típicas de plumas para explicar características dos basaltos baixo e alto-Ti, por exemplo, da PBC Paraná-Etendeka (Piccirillo & Melfi, 1988; Peate & Hawkesworth, 1996; Comin-Chiaramonti et al., 1997; Marques et al., 1999).

Tabela 1 - Características das principais províncias basálticas continentais.

	Idade (Ma)	Área (km^2)	Volume atual (km^3)	Volume original (km^3)	Espessura max (m)	Pluma
Columbia River	16	1.6×10^5	1.8×10^5	1.8×10^5	> 1500	Yellowstone
Deccan	66	5×10^5	5.2×10^5	$1\text{-}2 \times 10^6$	> 2000	Reunion
Paraná	132	1.2×10^6	8×10^5	1.5×10^6	1800	Tristão da Cunha
Karoo	183	3×10^6	não definido	$1\text{-}2 \times 10^6$	9000	Bouvet
Trapes Siberianos	248	3.4×10^5	3.4×10^5	$> 2 \times 10^6$	3500	Jan Mayen

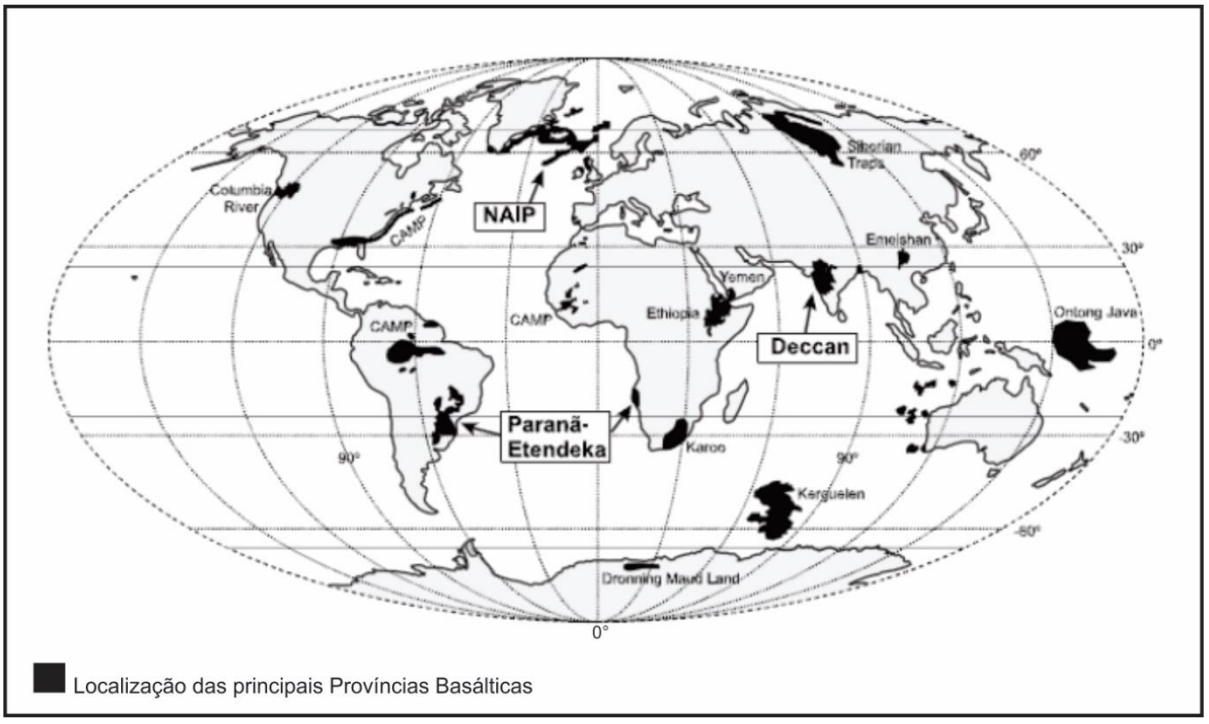

Figura 4. Distribuição global das províncias Basálticas Continentais. Modificado de Coffin & Eldholm (1994).

Bryan et al. (2010) propuseram um modelo com quatro membros finais (A, B, C, D) para a evolução petrogenética dos magmas básicos e ácidos das PBCs. Esses autores demonstraram em relação ao armazenamento dos magmas, que em pressões crustais elevadas poderiam ocorrer processos como cristalização fracionada e assimilação crustal, enquanto que em profundidades rasas seria comum a presença de complexos de sills colocados previamente à extrusão final (Figura 5).

Na trajetória A, os magmas basálticos deveriam mostrar pouca ou nenhuma evidência para armazenamento crustal ou assimilação, preservando as assinaturas isotópicas e geoquímicas de manto. A transferência desses magmas seria diretamente a partir das regiões fontes do manto superior através de fissuras até a superfície. Alternativamente, esses magmas poderiam ter residido temporariamente em reservatórios no manto superior ou em underplate máfico, evitando dessa forma oportunidades para assimilação crustal.

Nas trajetórias B1 e B3, é possível que o grande volume de magmas basálticos baixo-TiO2 seja submetido a um armazenamento em profundidades crustais inferiores e superiores, resultando em assimilação crustal, cristalização e degaseificação. Desta forma, poderiam ser produzidas lavas basálticas com conteúdos menores de MgO e andesito-basálticos afíricos ou com fenocristais de plagioclásio. Na trajetória B2, os basaltos seriam do tipo alto-TiO_2 e possuiriam evidências para armazenamento crustal. No entanto, seriam gerados pela fusão de intrusões máficas (underplate máfico) que poderiam diluir os indicadores geoquímicos de contaminação crustal, sendo dominantes a cristalização fracionada e a mistura de magmas.

Na trajetória C, os riolitos de alta temperatura e grande volume que ocorrem comumente nas LIPs continentais, teriam a origem explicada por processos de AFC de grande escala, envolvendo fusão e assimilação de crosta granulítica inferior e/ou refusão de underplate basáltico. Além disso, poderiam ter um adicional input de magmas ácidos e básicos e prolongamento da cristalização fracionada para gerar magmas ácidos pobres em cristais, anidros e de alta temperatura. Na superfície, essas erupções seriam expressas por meio de estruturas sag regionais (Ewart et al., 2002) ou condutos fissurais, onde seriam ausentes as feições de caldeiras devido os reservatórios de magmas de alta temperatura residirem em níveis crustais profundos. Na trajetória C1 são descritos os riolitos baixo-TiO_2 que teriam um maior envolvimento crustal, com ocorrência de fusão crustal inferior e assimilação em resposta ao underplating basáltico com recarga máfica adicional. Além disso, esses magmas poderiam ficar armazenados nas porções médias e superiores da crosta, onde ocorreria assimilação de materiais crustais graníticos e cristalização fracionada. Na trajetória C2 seria comum a presença de riolitos alto-TiO_2 que possuem envolvimento crustal mínimo, onde ocorre fracionamento ou refusão de basaltos alto-TiO2 próximo ao limite manto-crosta com adicional recarga de magma máfico. Nesta trajetória poderia ocorrer o armazenamento em níveis crustais médios, com possível mistura de magma ácido ou contaminação resultante de assimilação crustal ou interação com magmas ácidos que não extravasaram.

Na trajetória D1 poderiam ser descritos os ignimbritos riolíticos de grande volume e temperatura baixa, ricos em cristais, os quais seriam encontrados principalmente em LIPs ácidas (Bryan, 2007) e ambientes de margens continentais extensionais. Esses ignimbritos refletem o processo de formação de batólitos na crosta superior, através de intrusões rasas e underplating de magmas máficos basálticos. Estes magmas poderiam fornecer o input termal e de voláteis necessários para desencadear as erupções das câmaras crustais superiores e o desenvolvimento de caldeiras bem definidas. Na trajetória D2 seriam descritas intrusões de basaltos em profundidades crustais superiores. Estes magmas seriam gerados rapidamente e extravasariam volumes moderados de riolitos pobres em cristais através da refusão de rochas plutônicas altamente diferenciadas e solidificadas, as quais foram formadas durante as fases precoces do magmatismo no evento LIP.

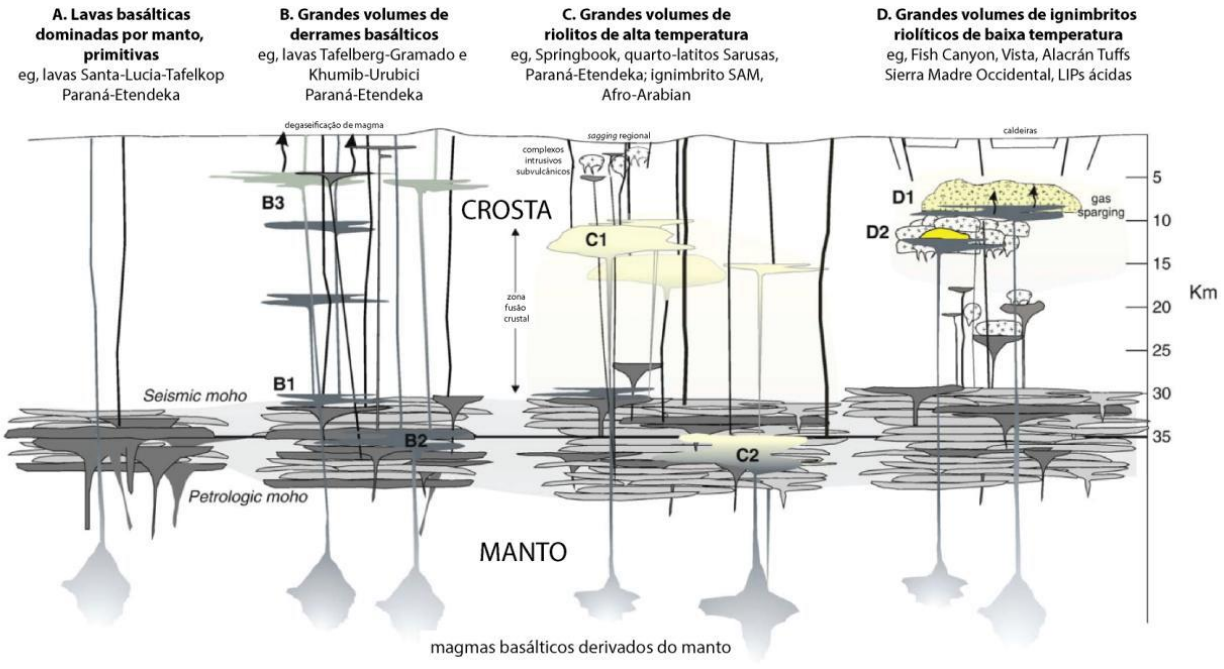

Figura 5. Visão crustal conceitual dos quatro membros finais de caminhos petrogenéticos para erupções de grande magnitude (basálticas e ácidas) principalmente em LIPs continentais (Fonte: traduzido de Bryan et al., 2010).

2.3. PROVÍNCIA MAGMÁTICA PARANÁ-ETENDEKA

Esta província abrange os estados do Rio Grande do Sul, Paraná, Santa Catarina, São Paulo, sudoeste de Minas Gerais, sudeste do Mato Grosso do Sul, sul de Goiás, sudeste do Mato Grosso, parte ocidental do Uruguai, nordeste da Argentina e extremo leste do Paraguai além do oeste da Namíbia. Cerca de 90% da PBC Paraná-Etendeka está localizada no continente Sul Americano. Estudos recentes sobre a extensão areal e o volume dessa província sugerem que a área correspondente as rochas vulcânicas na Bacia do Paraná seja de aproximadamente 917.000 km^2, com um volume de cerca de 450.000 km^3. O volume referente aos corpos intrusivos do tipo soleira é de pelo menos 112.000 km^3 (Frank et al., 2009). No Brasil, na estratigrafia da Bacia do Paraná é representada pela Grupo Serra Geral (GSG), sendo muitas vezes denominada de Vulcanismo Serra Geral. É considerada uma das maiores manifestações vulcânicas máficas continentais do planeta (Milani 2004; Milani et al., 2007).

O GSG é caracterizada por uma sequência de derrames com espessura máxima de 1.700 metros, na qual ocorre o predomínio de basaltos e andesitos-basálticos de afinidade toleítica. Rochas ácidas (riolitos, riodacitos) ocorrem subordinadamente no topo da sequência vulcânica, principalmente no extremo sul do Brasil. É comum a ocorrência de uma grande quantidade de corpos intrusivos (soleiras e diques) de composição básica a ácida, geralmente associados a descontinuidades estruturais da Bacia do Paraná.

Na parte sul da bacia os derrames foram depositados principalmente sobre os arenitos da Formação Botucatu, preservando localmente morfologias originais de dunas e feições sedimentares, sugerindo contemporaneidade entre os primeiros episódios vulcânicos e o sistema eólico ativo desta unidade (Scherer, 2002; Waichel et al., 2008).

Recentes pesquisas, enfocando uma escala de trabalho de maior detalhe, têm sugerido novos modelos estratigráficos, fundamentados em arquitetura de fácies. Estes modelos têm sido propostos para a região da Sinclinal de Torres (Lima et al., 2012b; Waichel et al., 2012) e se fundamentam na morfologia dos derrames básicos

e ácidos, paleotopografia e taxas de efusão, complementando estudos similares baseados na estratigrafia no vulcanismo na Província Etendeka (e.g. Mountney et al., 1998; Jerram et al., 1999, 2000) na Bacia de Huab, Namíbia. Como este enfoque, esta região seria constituída nas suas porções inferiores, principalmente por lavas básicas com morfologia *pahoehoe* espessas (*ponded*) que ocupam os espaços interdunas da Formação Botucatu. As porções intermediárias desta província seriam compostas de derrames do tipo *pahoehoe* e tipo ***a'a'*** no topo, sendo as ocorrências de corpos intrusivos básicos/intermediários menos frequentes. Derrames e domos ácidos são predominantes nas as unidades superiores desta sequência vulcânica (Lima et al., 2012a; Waichel et al. 2012).

Barreto et al. (2014) e Rossetti et al. (2014) realizaram uma análise detalhada das condições de colocação de estas rochas vulcânicas básicas das regiões de Santa Cruz do Sul /Herveiras e Estância Velha/Caxias do Sul, ombreira sul da Calha de Torres, aplicando o método de análise de fácies integrado a dados petrográficos e geoquímicos. Os derrames foram divididos em associações de litofácies: Lava tipo *pahoehoe pounded* (derrames confinados interdunas), *compound pahoehoe* (pequenos lobos de lava *pahoehoe* empilhados em um padrão complexo), *simple* (*sheet) pahoehoe* (lobos tabulares com estrutura interna constituída de zona basal, núcleo maciço e zona vesiculada) e *rubbly* (derrames espessos com geometria tabular, núcleo maciço e topo com auto brechas).

Uma nomenclatura formal foi proposta para a litoestratigrafia e vulcanologia da Formação Serra Geral (Rossetti et al., 2017), elevando esta unidade de hierarquia, sendo denominada de Grupo Serra Geral (GSG). Devido à heterogeneidade dos pacotes de lava, esses foram divididos em quatro Formações: Formação Torres - caracterizada por derrames basálticos tipo *compound pahoehoe* quimicamente mais primitivos (> 5% em peso de MgO) e pacotes andesitos-basásticos a andesiticos *ponded pahoehoe*; Formação Vale do Sol - caracterizada por derrames andesito-basálticos tipo *rubbly e pahoehoe* (SiO_2> 51% em peso, MgO <5% em peso); Dacitos e riolitos da Formação de Palmas que sobrepõe diretamente sobre as lavas da Formação do Vale do Sol e no oeste da área estudada, a Formação Esmeralda - unidade estratigráfica formada por um campo basáltico de

derrames *pahoehoe* colocados no topo da sequência de lavas durante a fase decrescente da atividade vulcânica de TiO_2 baixa.

Diversos trabalhos baseados em dados químicos (Melfi et al., 1988; Bellieni et al., 1984; Mantovani et al., 1985; Piccirillo et al.,1989; Marques et al., 1989) sugeriram a divisão das rochas vulcânicas básicas em dois grandes grupos: basaltos alto-Ti, com teores de TiO_2 superiores a 2% e basaltos baixo-Ti, com teores inferiores a 2%. Subdivisões destes grupos em magmas-tipo foram propostas por Peate et al. (1992) e Peate (1997), tendo-se como base principalmente a abundância de elementos-traço e razões entre estes. Os magmas-tipo que ocorrem, dominantemente, na porção norte da província foram denominados de Pitanga (TiO_2>3%; Ti/Y>350), Paranapanema (2< TiO_2 < 3%; 200<Sr<450 ppm; Ti/Y>330) e Ribeira (TiO_2<2%; 200<Sr<375 ppm; Ti/Y >310). Os magmas-tipo Gramado (TiO_2< 2%; 140<Sr<400 ppm; Ti/Y<310), Esmeralda (TiO_2< 2%; 120<Sr<250 ppm; Ti/Y< 310) e Urubici (Ti>3%; Sr>550 ppm; Ti/Y>500) ocorrem predominantemente na porção sul da província. No entanto, trabalhos mais recentes têm reconhecido derrames do tipo Urubici também na região setentrional da província (Machado et al., 2007). Os grupos e suas principais características são apresentados na tabela 2.

Tabela 2 – Características principais da composição química dos diferentes magmas-tipo segundo a classificação de Peate et al. (1992).

Magma Tipo	Características	TiO_2	Ti/Y	Ti/Zr	$^{87}Sr/^{86}Sr_i$
Gramado	BTi/Y *e* Ti	0,7 – 1,9	< 310	< 60	0,7075-0,7167
Esmeralda	BTi/Y *e* Ti	1,1 – 2,3	< 310	> 60	0,7046-0,7086
Ribeira	ATi/Y *e* BTi	1,5 – 2,3	> 310	> 65	0,7055-0,7060
Paranapanema	ATi/Y *e* Ti	1,7 – 3,2	> 310	> 65	0,7055-0,7063
Pitanga	ATi/Y *e* Ti	> 2,9	> 350	> 60	0,7055-0,7060
Urubici	ATi/Y *e* Ti	> 3,3	> 500	> 57	0,7048-0,7065

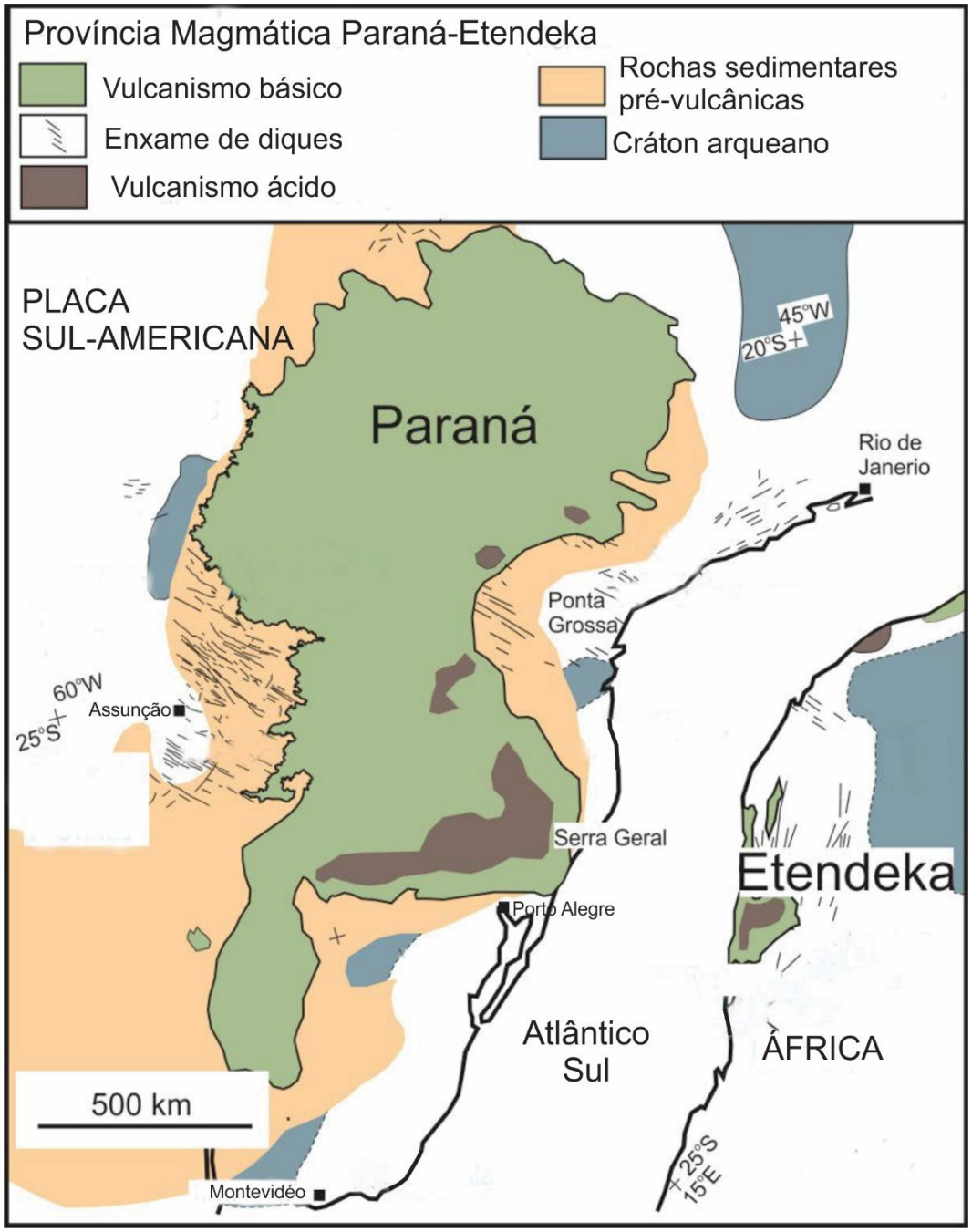

Figura 6. Reconstrução da PBC Paraná-Etendeka durante a fase inicial de abertura da porção sul do Oceano Atlântico, mostrando a grande extensão desse vulcanismo na Província Paraná quando comparado com a Província Etendeka (Fonte: modificado de Gibson et al., 2006).

As rochas vulcânicas ácidas foram subdivididas nas fácies Palmas (Caxias do Sul e Santa Maria) e Chapecó (Guarapuava e Ourinhos). As rochas ácidas do tipo Chapecó são concentradas no centro da Bacia do Paraná e são representadas por

dacitos, riodacitos, quartzo latitos e riolitos, hipohialinos, porfiríticos a fortemente porfiríticos. As rochas ácidas do tipo Palmas correspondem a riolitos e riodacitos, tipicamente afíricos, com estrutura “sal-e-pimenta”, holohialinos a hipocristalinos. De maneira geral, as rochas de composição ácida estão preferencialmente presentes nos estados de Rio Grande do Sul, Santa Catarina e Paraná. (Bellieni et al., 1986; Piccirillo et al., 1989; Nardy, 1995). O principal fator de distinção destes grupos é a abundância de elementos incompatíveis. A fácies Chapecó tem valores de Zr > 500ppm, Ba > 900 ppm e and Sr >250 ppm, enquanto a fácies Palmas apresenta valores de Zr < 400 ppm, Ba < 800 ppm e Sr < 170 ppm (Peate et al., 1992).

Estudos paleomagnéticos realizados nos derrames da Província do Paraná-Etendeka mostram registros de numerosas inversões de polaridade, com predomínio de tempos de polaridade normal. No Cretáceo inferior, a duração média dos intervalos de polaridade ficou abaixo de 1Ma, tornando relativamente frequentes as inversões de polaridade. Isso indica que o intervalo de tempo transcorrido para acumular esses pacotes de derrames foi relativamente curto, como indicado por algumas datações radiométricas (Ernesto et al., 1999). O caráter intermitente do vulcanismo dificulta o registro de transição da polaridade, considerando-se que é um processo relativamente rápido. Em alguns locais, a declinação magnética chega a 90°, caracterizando um campo magnético anômalo durante a inversão (Marques & Ernesto, 2004).

Renne et al. (1992) sugerem que as idades das rochas básicas e ácidas da porção sul da Bacia do Paraná situam-se entre 131,4 ± 1,6 e 132,9 Ma, tornando-se mais jovens nas regiões norte e central (129,9 ± 0,1 e 131,9 ± 0,9 Ma). Thiede & Vasconcelos (2010) obtiveram resultados que confirmam as idades obtidas por Renne et al. (1992) através do método geocronológico $^{40}Ar/^{39}Ar$ (134.7 ± 1Ma) para os basaltos da região sul da bacia. Os valores obtidos na porção norte da Bacia do Paraná são semelhantes aos do Etendeka, por estes mesmos autores. Recentemente, Janasi et al. (2011) obtiveram uma idade de 134,3 ± 0,8 Ma para um dacito do Grupo Chapecó (tipo Ourinhos) pela sistemática U-Pb em baddeleita/zircão. Segundo esses autores, o dacito é ligeiramente mais velho do que os basaltos Alto-Ti sobrejacentes (133,6-131,5 Ma) e os dados obtidos indicam um

período de tempo ~ 3 Ma para a construção da sequência alto-Ti da Bacia do Paraná. Esses autores destacam também o fato dos valores encontrados no dacito coincidirem com os de $^{40}Ar/^{39}Ar$ (134,8-134,1 Ma) obtidos nos basaltos Baixo-Ti (Gramado e Esmeralda) e nos dacitos e riolitos tipo de Palmas do sul do Brasil. O conjunto dos dados é, portanto, consistente com a curta duração do vulcanismo e rápida sucessão pela sequência de alto-TiO_2.

Barreto et al., (2016), conduziu um estudo sobre variações geoquimicas e isotópicas de derrames basálticos (com razões isotópicas iniciais (132 Ma) de Sr 0.707798 – 0.715751, εNd de −8.36 à −5.41 e variações isotópicas de $^{206}Pb/^{204}Pb$ = 18.42 – 18.86), pertencentes ao magmatismo de Baixo-Ti, tipo Gramado no extremo sul do Brasil, usando a estratigrafia em escala local como guia. Foi discutido a petrogênese desses fluxos em um único magma-tipo e avaliado qualitativamente e quantitativamente o papel da contaminação crustal e os potenciais contaminantes envolvidos nos derrames de lava nas regiões de Santa Cruz/ Herveiras, Lajeado e Morro da Cruz.

2.4.. CORPOS INTRUSIVOS E A EVOLUÇÃO DAS PROVÍNCIAS BASÁLTICAS CONTINENTAIS

2.4.1. Enxames de diques Província Basáltica Continental do Deccan

A Província Basáltica do Deccan recobre cerca de 500.000 km2 do território Indiano e possui um volume estimado em (1-3) x 10^6 km^3 (Sen, 2001; Jay et al., 2009) (Figura 7). Essa província magmática é composta principalmente por sucessivos derrames toleíticos que alcançam uma grande extensão lateral. Nas duas últimas décadas foram realizados muitos trabalhos sobre a PBC do Deccan, o que permitiu dividi-la em três subgrupos e onze formações. Cada formação é constituída por um conjunto de derrames que possuem características físicas, texturais e petrológicas semelhantes, correlacionáveis com a seção tipo Western Ghats (Peng et al., 1998; Subbarao et al, 1999; Mahoney et al., 2000).

Três grandes sistemas de enxames de diques estão expostos nos derrames basálticos da PBC do Deccan: enxame de diques Narmada-Tapi, com orientação predominantemente de ENE–WSW; enxame de diques Coastal, com orientação predominante de N-S; e o enxame de diques Nasik-Pune, no centro-oeste do Deccan, sem orientação definida. Vários estudos foram feitos correlacionando esses sistemas de diques com os derrames da província (Bondre et al., 2006; Ray et al., 2007; Sheth et al., 2009; Hooper et al., 2010; Vanderkluysen et al., 2011; Sheth et al., 2013).

Conforme estudos geoquímicos dos derrames e diques toleíticos expostos na região de Ghatkopar-Powai, cidade de Mumbai, situado na zona de flexão Panvel, os derrames foram originados antes desse evento tectônico extensional Cenozóico, enquanto que os diques foram originados após esse evento (Hooper et al., 2010; Sheth et al., 2013). As assinaturas geoquímicas da maioria dos derrames e diques dessa região não estão representadas na sequência Western Ghats. Os derrames são muito semelhantes à Formação Mahabaleshwar dessa seção tipo em razões isotópicas de Sr-Nd e padrões multielementares, mas diferente em relação a elementos-traço incompatíveis. Em geral, as assinaturas geoquímicas do Ghatkopar-Powai dos derrames e diques não estão representadas na estratigrafia Western Ghats. Dois dos diques se assemelham a Formação Ambenali em todas as características geoquímicas, embora eles não sejam propensos de serem alimentadores dos derrames dessa formação. Dez outros diques da região não exibem qualquer semelhança geoquímica com as unidades da seção tipo Western Ghats. Os padrões de ETR de seis dos quatorze diques analisados mostram um enriquecimento dos ETR leves em relação aos pesados, o que pode indicar anfibólio residual e, portanto, uma fonte litosférica. Três deles exibem razões isotópicas de Sr/Nd idênticas às da Formação Mahabaleshwar (Sheth et al., 2013). Os autores deduzem que derrames e diques sofreram pouca ou nenhuma contaminação da crosta continental inferior. As tendências estruturais dos diques indicam uma considerável extensão tardia da litosfera na direção leste-oeste, embora o magmatismo ainda se apresentasse vigoroso neste estágio de vulcanismo do Deccan (Sheth et al., 2013).

Vanderkluysen et al. (2011) combinaram as assinaturas geoquímicas e isotópicas dos três principais sistemas de enxames de diques da PBC do Deccan. Isso permitiu correlacionar um número substancial de diques com as conhecidas formações de derrames que compõem grande parte da província. Os resultados colocam limites sobre a localização, geometria e evolução dos principais sistemas de alimentação e sobre a correlação temporal relativa da colocação dos diques com relação à extensão litosférica dirigida regional.

As análises dos elementos maiores, elementos-traço e dados isotópicos de Sr- Nd -Pb revelam que os prováveis diques alimentadores das três principais formações da porção superior do pacote de lava (Formações Poladpur, Ambenali e Mahabaleshwar) estão abundantemente representadas no enxame de diques Nasik - Pune e enxames costeiros. Como um grupo, estes diques não têm tendência de preferência clara. Dentre os diques altamente orientados de Narmada -Tapi e áreas costeiras a oeste, alguns têm afinidades com a porção inferior do pacote de lava (Formações Jawhar, Igatpuri, Thakurvadi e Bushe) e estes parecem ter sido intrudidos sob a influência das extensões regionais norte-sul e leste-oeste, respectivamente.

Outros diques do enxame Narrada-Tapi têm altas razões de $^{206}Pb/^{204}Pb$, mesmas características dos derrames no extremo nordeste do Deccan. Estes dados sugerem que os derrames de lava do Deccan podem ter atingido cerca de 700 km de extensão. A extensão dirigida da litosfera parece ter sido um importante fator de controle sobre a colocação dos diques alimentadores e para as formações de derrames inferiores e intermediárias. Em contrapartida, a colocação das volumosas formações superiores, que abrangem o limite Cretáceo - Terciário e estima-se que compõem 50% do volume de lava do Deccan, não seria controlada pelo evento tectônico (Self et al., 2006). Essa conclusão contradiz as predições de modelos baseados em rifteamento para o vulcanismo do Deccan. Mesmo parecendo que outro mecanismo tenha sido necessário para explicar as volumosas formações superiores, não se pode descartar que o rifteamento tenha desencadeado o início do derramamento vulcânico (Ray et al., 2007; Vanderkluysen et al., 2011).

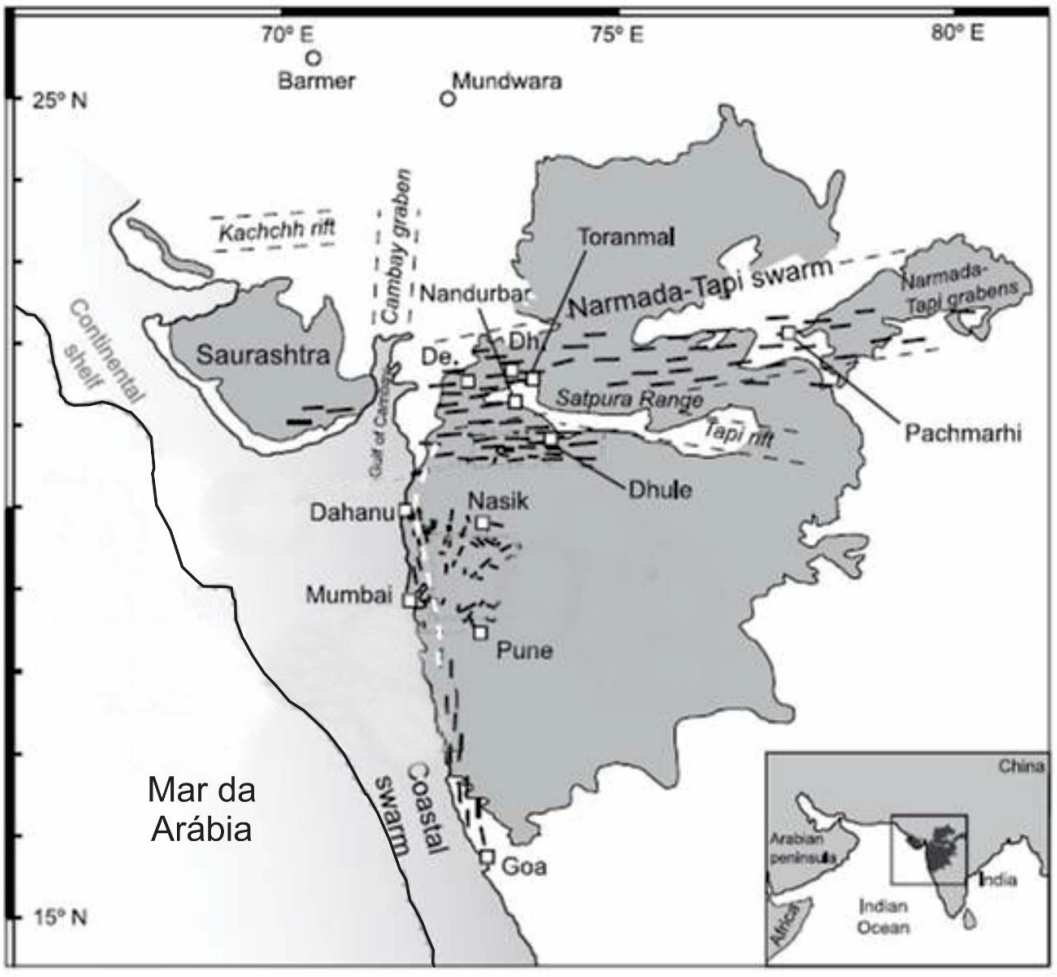

Figura 7. Mapa do Deccan Traps (cinza) e os três principais enxames dique (mostrado esquematicamente). A linha pontilhada branca perto da costa oeste representa a flexão Panvel. Modificado de Vanderkluysen et al. (2011).

2.4.2. Enxames de diques Província Basáltica Continental do Karoo

A grande Província Ígnea do Karoo se estende por toda a África do Sul, cobrindo aproximadamente 3×10^6 km^2 (Eales et al., 1984) (Figura 8). Com base em dados de U-Pb (baddeleíta/zircão) e $^{40}Ar/^{39}Ar$, foi constatado que a PBC do Karoo tem aproximadamente 184 Ma e seu magmatismo talvez tenha durado em torno de 1 milhão de anos. Essa grande província é contemporânea a outras províncias ígneas, incluindo a Província de Ferrar na Antártica (Encarnación et al, 1996; Zhang et al, 2003) e associados aos Basaltos Kirkpatrick e a vários componentes intrusivos

no oeste de Dronning Maud Land e dos Diabásios de Tasman da Australásia (Elliot, 1975; Fleming et al., 1995).

Existem três principais enxames de diques associados à tripla junção do Karoo (Save-Limpopo, Northern Lebombo e Okavango) (Jourdan et al., 2004b), quatro enxames mais isolados (Rooi Rand, Underberg, Lesoto do Sul e Botswana do Sul) (Armstrong et al, 1984.; Riley et al, 2006.; Jourdan et al., 2007) e em pelo menos cinco enxames de diques em Dronning Maud Land (Curtis et al., 2008). A junção tripla do Karoo em Mwenezi está situada dentro do Cinturão de Limpopo e compreende tanto as primeiras (nefelinitos e picritos) quanto as mais recentes (Complexo ígneo Mwenezi) manifestações do magmatismo da PBC do Karoo.

Ernst & Duncan (1995), invertigaram três enxames de diques proeminentes na PBC do Karoo. Estes incluem os enxames de Botswana, Lebombo e Orange River, que formam um padrão convergente abrangendo de 100° de arco. Por meio de estimativas preliminares com medidas de anisotropia de suscetibilidade magnética, que indicaram fluxo vertical no extremo leste do enxame de diques de Botswana e fluxo predominantemente horizontal mais a oeste, concluíram que essa observação é consistente com uma fonte de pluma subjacente à região.

Hastie et al. (2014) revisaram estudos de campo, estrutura e geocronologia dos enxames de diques e o magmatismo relacionado, no que se refere às fontes magmáticas e a hipótese de pluma mantélica para a PBC do Karoo. Especificamente, por meio de anisotropia de susceptibilidade magnética, a trama dos minerais máficos do fluxo do magma relacionados com 90 diques de cinco destes enxames, com especial atenção para aqueles que convergem para as junções triplas do sul da África e Antártica.

Esses autores concluíram que o padrão de fluxo total nos diques da PBC do Karoo é consistente com a junção tripla, sendo uma importante fonte de magma. No entanto, o Cinturão de Limpopo e o Cráton Kaapvaal controlaram de forma significativa a estrutura e distribuição dos Monoclinos Lebombo e Save -Limpopo e do enxame de diques Okavango. O locus do fluxo de magma nos diques de Dronning Maud Land está a aproximadamente 500 km de distância da junção tripla

do Karoo, assim como está o locus aparente do enxame de diques Rooi Rand. Em comparação com a modelagem recente de junção continental, a estrutura e o fluxo dos enxames de diques, vinculado com a geocronologia e geoquímica, sugerem que a incubação térmica durante a montagem do Gondwana levou ao magmatismo da PBC do Karoo. Por não haver provas de uma fonte profunda de pluma mantélica, a tectônica de placas é mais razoavelmente aplicável para o desenvolvimento da PBC do Karoo, ao invés de uma explicação por meio da dinâmica de fluidos de pluma mantélica.

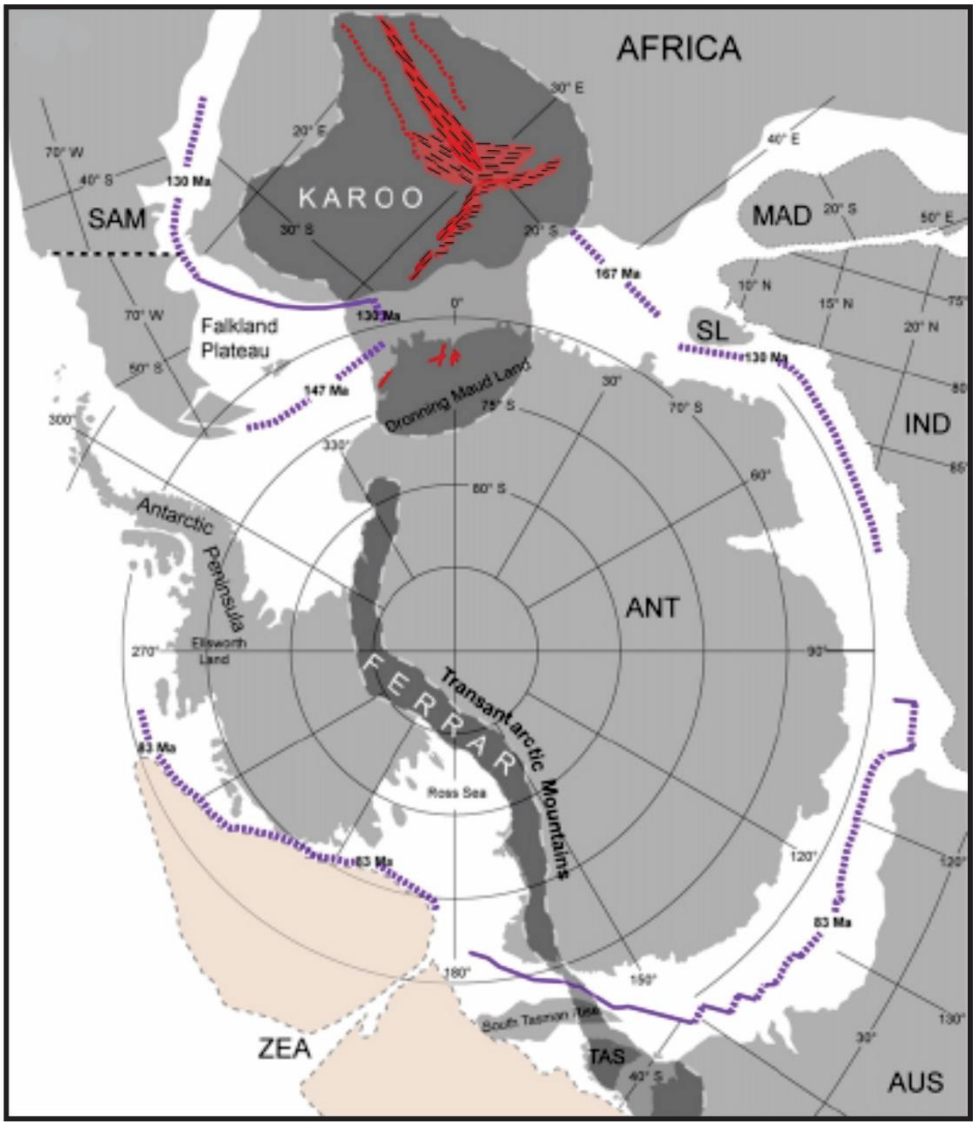

Figura 8. Mapa com as posições dos continentes do sul do Gondwana em ~ 180 Ma com a extensão inferida de dos magmatismo Karoo e Ferrar (cinza escuro com

linhas brancas tracejadas) em toda a África do Sul, Dronning Maud Land, e o restante das Montanhas Transantárti Mapa com as posições dos continentes do sul do Gondwana em ~ 180 Ma com a extensão inferida de dos magmatismo Karoo e Ferrar (cinza escuro com linhas brancas tracejadas) em toda a África do Sul, Dronning Maud Land, e o restante das Montanhas Transantárticas e Australásia. Os Grandes enxames de diques da África do Sul e Dronning Maud Land são mostrados. (ANT = Antártica, AUS = Austrália, IND = Índia, MAD = Madagascar, SAM = América do Sul, SL = Sri Lanka, TAS = Tasmânia, ZEA = Zelândia). Modificado de Hastie et al. (2014).

2.4.3. Diques da Província Basáltica Continental Columbia River

A Província Basáltica Continental Columbia River se localiza no noroeste dos Estados Unidos e compreende cerca de 230 mil quilômetros cúbicos de rocha (Figura 9). O vulcanismo que gerou essa PBC ocorreu entre 17,5 a 6 Ma. Diferenças litológicas, composicionais e de polaridade magnética dos derrames permitiram a divisão estratigráfica dessa sequência magmática (Swanson et al., 1979). Exibem padrões incomuns de distribuição de lava, geoquímica e aparente relação com a tectônica regional. Consequentemente há pouco consenso sobre a origem de seus magmas (Camp & Ross, 2004; Hooper et al., 2007). Alguns autores supõem que essa província ígnea pode estar relacionada à chegada de uma pluma mantélica centralizada a várias centenas de quilômetros a sul, que posteriormente migrou para o leste-nordeste de sua posição atual sob Yellowstone (Smith & Braile, 1993; Parsons et al., 1994; Jordan et al., 2004a). A atividade para o sul ao longo do Rift Nevada tem sido relacionada ao rifteamento da litosfera associada à mesma pluma (Zoback et al, 1994.; Parsons et al., 1994). Os diques associados ao Rift Nevada tendem a sul do centro da pluma e são datadas em 17-14 Ma (K/Ar) (Zoback et al., 1994).

A maior parte do volume de lava (Steens, Imnaha e Grande Ronde Basalts) eclodiu entre 16,7 e 16 Ma, através de aberturas associadas aos enxames de diques Steens e Chief Joseph no leste de Oregon e Washington, com uma área subsidiária da erupção no centro-norte de Oregon (Picture Gorge Basalts) associados ao enxame diques Monument. Durante esta fase principal, os condutos migraram

rapidamente para a área norte de Steens Montain, do leste de Oregon a sudeste de Washington, o que resultou numa idade progressiva dos derrames: Steens (mais velho), Imnaha e Grande Ronde (mais jovens) (Camp & Ross, 2004; Hooper et al., 2007).

A maior parte dos diques do enxame Chief Joseph, alimentadores das lavas do Grande Ronde Basalt, estão localizados em terrenos acrescidos a oeste do Cráton, limite definido pela razão $^{87}Sr/^{86}Sr$ = 0,706. Estes terrenos consistem em arcos de ilha Paleozóicos a Mesozóicos que foram extraídos do manto muito recentemente de acordo com as razões isotópicas de Sr e de Nd. Mesmas razões encontradas nesse enxame de diques e derrames basálticos. Só a crosta cratônica tem essa assinatura geoquímica e essas propriedades (Leeman et al., 1992).

Já nos derrames Steens e Picture Gorge não há nenhuma evidência geoquímica para a presença de significativas quantidades de crosta cratônica. Suas características isotópicas distintas são inconsistentes com a derivação das mesmas câmaras magmáticas crustais como as de Imnaha e Grande Ronde Basalts, mas se os derrames foram alimentados por magma em movimento lateral por meio de diques, como já constatado pelas distribuições dos enxames de diques e derrames Grande Ronde, Steens e Monument, então, sugerem que os seus sistemas de fonte de magma também estariam dentro da mesma "zona de convergência". Se assim for, as câmaras magmáticas que originaram dos basaltos Picture Gorge e Steens, provavelmente foram hospedadas dentro terrenos crustais acrescidos que fornecem pouca influência isotópica nos magmas e é, portanto, difícil de detectar. Apesar das ligeiras variações nas razões $^{87}Sr/^{86}Sr$ e $^{143}Nd/^{144}Nd$ entre as lavas Picture Gorge são, provavelmente, devido a contaminação crustal. As lavas superiores do Steens Basalt eclodiram de vários centros no sudeste de Oregon (Brandon et al., 1993). Esses centros podem ter sido alimentados por diques que irradiaram de um sistema principal localizado na crosta acrescida dentro da "zona de convergência" (Brueseke et al., 2007; Wolff et al., 2008).

Wolff et al. (2008) concluiu que a geoquímica do Columbia River, em particular dos derrames volumetricamente dominantes Imnaha e Grande Ronde, é simplesmente explicada pela derivação dos magmas a partir de um único sistema de

armazenamento centralizado de crosta. Isto exige transporte lateral de magma através de condutos agora representados pelos enxames de diques expostos.

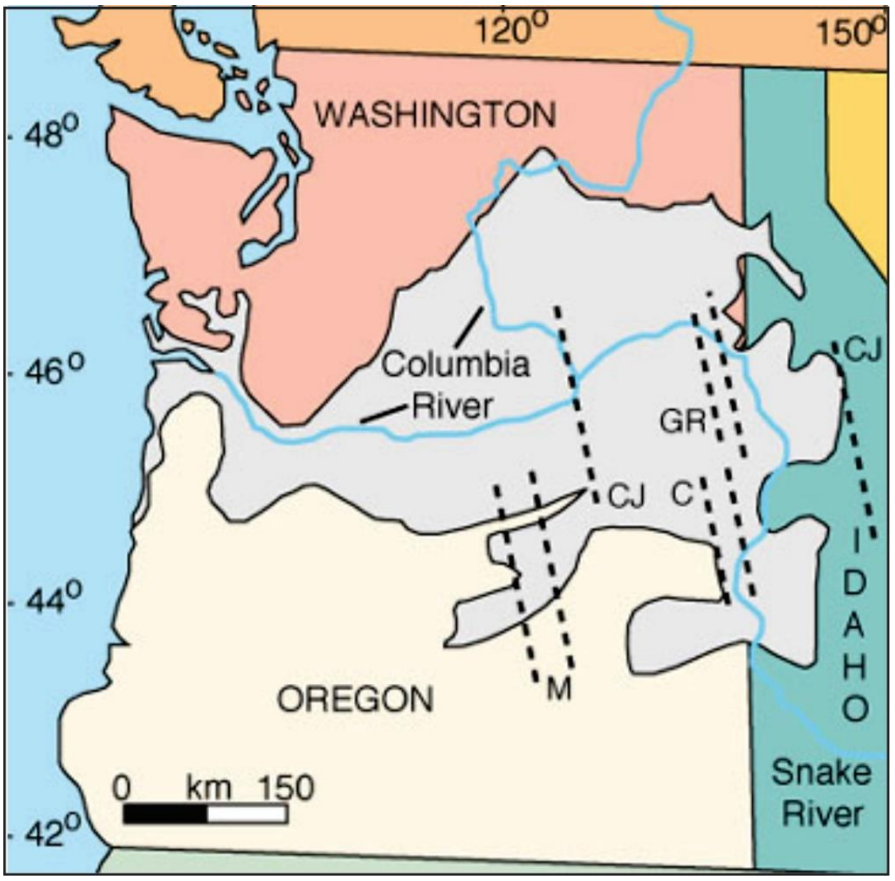

Figura 9. Área coberta PBC Columbia River em cinza. As linhas tracejadas são enxames de diques. Os limites exteriores do enxame diques Chief Joseph são marcados por CJ (condutos dos derrames das Formações Imhaha, Grande Ronde e Wanapum e Saddle Mountains). Os enxames de diques Grande Ronde (GR) e Cornucópia (C) estão incluídos no enxame de diques Chief Joseph. O enxame de diques Monument (M) foi o conduto da Formação Picture Gorge. A Bacia Paso está perto da confluência do Columbia e Snake River. Mapa baseado em Hooper (1997).

2.4.4. Intrusões associadas à Província Magmática Paraná-Etendeka

Para alguns autores (Piccirillo et al., 1990; Coutinho, 2008), os principais enxames de diques costeiros são constituintes dos braços norte, sul e leste de um sistema de junção tríplice centrado na costa do Estado do Paraná e relacionado à

abertura inicial do Atlântico Sul. O magma máfico introduziu-se ao longo das direções: N-S (braço sul, na costa Paraná-Santa Catarina), NW-SE (arco de Ponta Grossa) e NE-SW (braço norte na costa de São Paulo-Paraná) Figura 10.

2.4.4.1. Intrusões básicas associadas à Província Etendeka

O Enxame de Diques Henties Bay-Outjo no cinturão de Damara, Namíbia, é interpretado como um braço abortado de uma junção tripla centrada na borda da Walvis Bay. Tem um range composicional de basalto a riolito com composição basáltica predominante e Baixo-Ti (Duncan et al., 1990; Trumbull et al., 2004). Fazem parte desse enxame diques com termos picríticos ao redor de Spitzkoppe, oeste de Namíbia, com até de 20% de MgO, o que sugere que o magma provavelmente se originou da fusão de uma fonte mantélica do tipo mid-ocean ridge basalt (MORB), seguido pela reação limitante do manto litosférico subcontinental metassomatizado imediatamente antes da formação desses magmas. (Thompson et al., 2001; 2007). Os diques olivina-toleítos de magma-tipo Baixo-Ti Nil Desperandum, proposto por Thompson et al. (2001), pertencentes ao enxame de diques Nil Desperandum-Twyfelfontei exibem padrões de elementos-traço, quando normalizados com Manto Primitivo similares, mas mais uniformes com o magma-tipo Tafelberg e (baixo Pb, Rb, U, Th) e razões isotópicas menos radiogênicas.

Os doleritos Horingbaai têm afinidade pelos magmas do tipo MORB, com padrões planos de ETR e dados isotópicos que plotam dentro do quadrante do manto empobrecido no diagrama εSr vs.εNd (Erlank et al., 1984; Hawkesworth et al., 1984). O complexo de sills do Vale de Huab River e diques associados são separados em quatro tipos de magma doleríticos que se distinguem uns dos outros por diferentes razões de abundância de elementos incompatíveis (Duncan et al., 1989). Quando comparados os doleritos de Huab com os basaltos da Formação Etendeka, mostram mais semelhança com os tipos de Baixo-Ti Tafelberg and Albin (Erlank et al., 1984) e com o basalto tipo Huab (Duncan et al., 1990) que pode ser uma variação mais básica do tipo Tafelberg.

O Complexo de Doros é uma intrusão máfica estratificada dentro da Suíte Intrusiva Damaraland, nordeste da Namíbia que faz parte da Província Magmática Paraná-Etendeka com idades 134-132 Ma ($^{40}Ar/^{39}Ar$) (Marsh, 2013). Com base em dados de campo, petrológicos e geofísicos, Owen-Smith & Ashwal (2015) propuseram a origem do Complexo de Doros como resultante de no mínimo sete pulsos magmáticos espaçados. Os autores sugerem um grande e complexo sistema de condutos interligados e câmaras que hospedaram uma gama de magmas de diferentes composições.

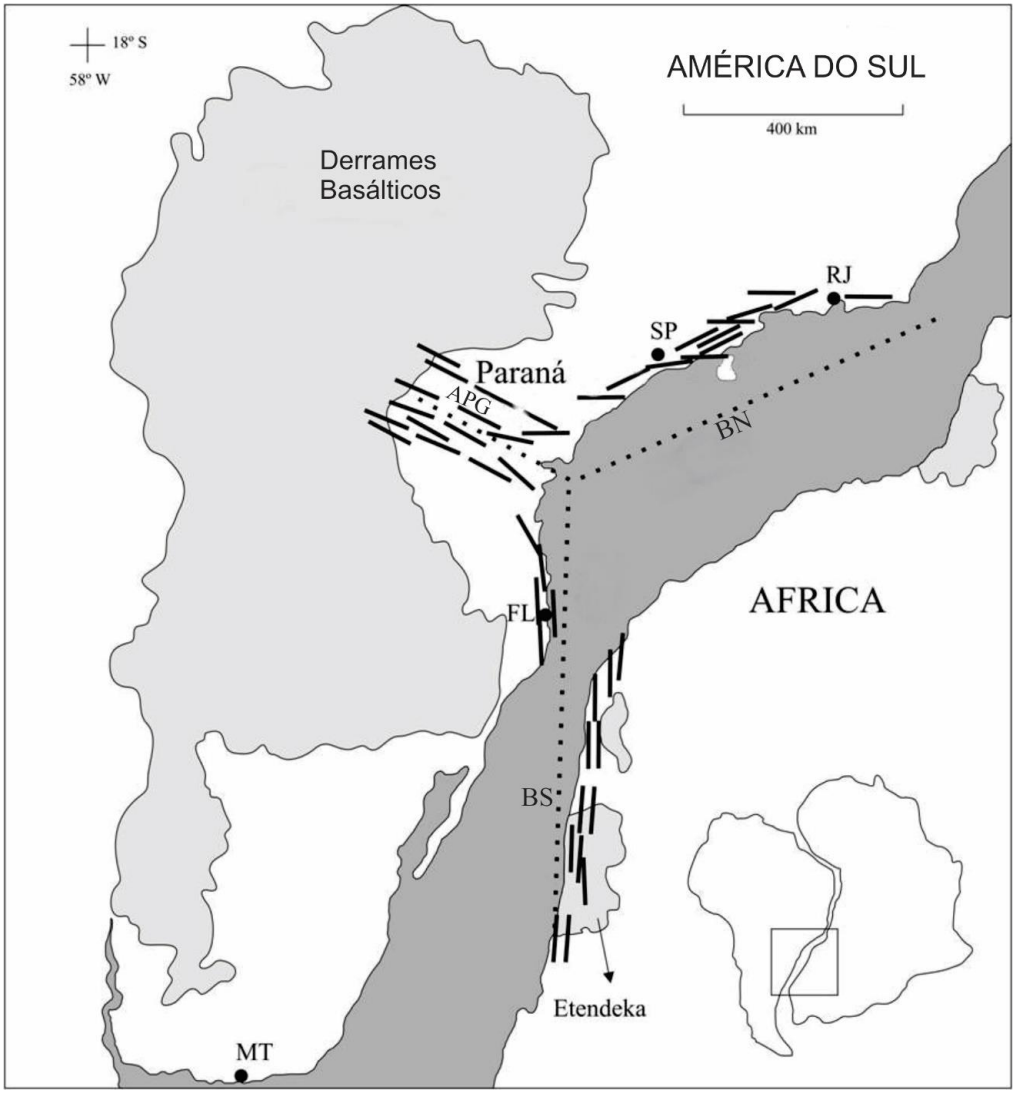

Figura 10. Reconstrução do pré-rift da América do Sul e África, mostrando a junção tripla Paraná e a correlação dos enxames de diques em ambos os continentes. APG: Arco de Ponta Grossa; BN: Braço Norte; BS: Braço Sul; RJ: Rio de Janeiro; SP: São Paulo; FL: Florianópolis; MT: Montevidéu; Barras: Direções generalizadas dos diques. Modificado de Coutinho (2008).

2.4.4.2. Intrusões básicas associados à Província Paraná

Enxame de Diques de Ponta Grossa

O Enxame de Diques de Ponta Grossa é a feição magmática mais significativa do arco de Ponta Grossa. Os diques estão orientados preferencialmente na direção NW-SE e, subordinadamente, NE-SW. Segundo Piccirillo & Melfi (1988). O magma basáltico intrudiu, sob forma de diques, rochas de idade Pré-Devoniana por meio de fraturas e falhas de distensão transversais às estruturas do embasamento. Os diques distribuem-se desde a região costeira Atlântica até as bordas da Província Magmática do Paraná, cortando o embasamento cristalino da Bacia do Paraná e rochas sedimentares Paleozóicas, principalmente da Formação Itararé e do Grupo Passa Dois (Almeida, 1986). Piccirillo et al. (1990) sugerem que a colocação desses corpos intrusivos tenha ocorrido nas fases iniciais do rifteamento.

Petrograficamente, o Enxame de Diques de Ponta Grossa é constituído predominantemente de rochas básicas, raramente por ácidas. Estas rochas são de textura afanítica a porfirítica com granulometria variando de muito fina (< 0,3 mm) a média (± 1,0 mm). Os dados geoquímicos demonstram que os diques do Arco de Ponta Grossa são composicionalmente semelhantes aos derrames alto-Ti Paranapanema da Província Magmática Paraná-Etendeka. Subordinadamente ocorrem diques com assinatura química semelhante aos derrames baixo-TiO_2 tipo Gramado e Esmeralda (Piccirillo et al., 1989, 1990; Marques, 2001). Piccirillo et al. (1990) sugerem que a geração dos diferentes grupos de diques no enxame pode estar relacionada a diferentes graus de fusão parcial de um manto peridotítico, sendo 9% e 20% de fusão para os toleítos de alto-TiO_2 e baixo-TiO_2, respectivamente. Dados geoquímicos e isotópicos mostram que componentes astenosféricos não foram significantes na gênese desses diques e que os mesmos podem ser considerados pouco afetados por processos de contaminação crustal (Marques & Ernesto, 2004).

As idades dos diques do Enxame de Ponta Grossa estão entre 131 e 129 Ma ($^{40}Ar/^{39}Ar$), temporalmente correlacionáveis aos derrames basálticos da Província Paraná-Etendeka. Renne et al. (1996) observaram idades próximas a 120 Ma em

diques próximos a margem continental, corroborando a hipótese proposta por Piccirillo et al. (1990) que sugerem que esses diques foram alimentadores dos derrames da sub-província norte, mais novos, dos quais não há afloramentos remanescentes devido à erosão posterior.

Enxame de Diques da Serra do Mar

O Enxame de Diques da Serra do Mar ocorre ao longo da região costeira dos Estados de São Paulo, Rio de Janeiro e uma parte do Estado do Espírito Santo. Os diabásios intrudem, principalmente, gnaisses e granitóides do Orógeno Ribeira de idade Neoproterozóico/Cambro-Ordoviciano (Heilbron et al., 2004). Esses diques estão associados à fragmentação do Gondwana no Cretáceo Inferior. Os diques que compõem esse enxame ocorrem, em geral, com atitudes subverticais, alguns tendo uma extensão superior a 15 km e podem exibir várias dezenas de metros de espessura. Mas, em geral, as espessuras ocorrem em torno de 1,0 a 3,0 metros. Estes diques orientam predominantemente a N40-50°E (Almeida, 1986).

Os diabásios do Enxame de Diques Serra do Mar são compostos por andesitos basálticos, latibasaltos e aqueles que transitam no limite andesitos basálticos/latibasaltos. Dados petrográficos e mineralógicos mostram que estes diques exibem caráter transicional e afinidade toleítica (Valente et al., 1998; Corval et al., 2008; Corval, 2009; Coutinho 2008). Os diabásios do Enxame de Diques da Serra do Mar no Estado do Rio de Janeiro compreendem predominantemente suítes de alto-Ti com razões Ti/Y>310 e, subordinadamente, suítes de baixo-TiO_2 e razões Ti/Y<310 (Valente et al., 1998; Valente et al., 2002; Corval, 2009). Os diabásios de baixo-Ti ocorrem principalmente na parte oriental do Estado do Rio de Janeiro. Valente et al. (2002), descriminaram duas suítes de baixo-Ti com base na geoquímica. Uma delas, chamada de Suíte Costa Azul, aflora predominantemente na região de Búzios e Cabo Frio, enquanto a outra, denominada Suíte Serrana, aflora na região serrana do Estado (Valente et al., 2002; Corval et al., 2008).

Os diques que afloram no litoral do Estado de São Paulo possuem características litoquímicas que permitiram discriminá-las em dois diferentes tipos de

magmas. Os diabásios Paraíba e Ubatuba são do Cretáceo Inferior (134-130 Ma; $^{40}Ar/^{39}Ar$), semelhantes aos diques de Ponta Grossa e aos derrames basálticos da Província Magmática do Paraná (Turner et al., 1994; Stewart et al., 1996). A maioria dos diques, cerca de 85%, é caracterizada por altos teores de TiO_2 (TiO_2>3% peso), bem como altas concentrações de P, Zr, Ba, Sr e Rb, sendo raros os diques com teores de TiO_2 entre 2% e 3% (Comin-Chiaramonti et al., 1983). Diques basálticos toleíticos de baixo-Ti (TiO_2<2%) são ainda mais raros, perfazendo cerca de 10% dos afloramentos (Marques & Ernesto, 2004).

Enxame de Diques de Florianópolis

O Enxame de Diques de Florianópolis está localizado na Ilha de Santa Catarina e na área continental adjacente. Os diques cortam sequências de derrames da Província Magmática do Paraná e granitóides neoproterozoicos. Esses diques são subverticais e orientados preferencialmente segundo as direções N30-55°E, subordinadamente, N15-45°W. Possuem espessuras que variam de 10 cm a 70 m, sendo mais comum espessuras entre 5 cm e 10 m. Esses diques são constituídos predominantemente de diabásios alto-Ti. Os termos baixo–Ti são representados por basaltos e traquiandesitos basálticos e os dacitos são geoquimicamente semelhantes às rochas vulcânicas ácidas do tipo Chapecó da Província Magmática do Paraná (Tomazzoli & Lima, 2006; Tomazzoli & Pellerin, 2015). Diques compostos ocorrem no sul de Florianópolis, com bordas de andesito basáltico e núcleo de traquiandesito contendo enxame de enclaves máficos magmáticos.

Estas rochas são compostas predominantemente por diques básicos com altos teores de TiO_2 (TiO_2>3%), representadas por latiandesitos e andesitos basálticos toleíticos, lati-basaltos e latitos. De maneira subordinada, diques exibindo baixos teores de TiO_2 (TiO_2<2%) representados por basaltos, andesitos basálticos e andesitos toleíticos. Dados litoquímicos mostram que os diques de Florianópolis são semelhantes aos derrames basálticos da Província Magmática do Paraná e aos diabásios do Enxame de Diques de Ponta Grossa. Os diques com teores baixos de TiO_2 possuem características geoquímicas similares às dos derrames do tipo

Gramado e Esmeralda, enquanto os litotipos com alto-Ti deste enxame se assemelham aos derrames do tipo Urubici e, em menor quantidade, aos derrames do tipo Pitanga (Marques & Ernesto, 2004). Porém, estes diques apresentam enriquecimento em elementos incompatíveis de grande raio iônico. Tal característica indica a ocorrência de processos de contaminação crustal dos magmas que originaram estas rochas, mascarando suas características geoquímicas originais.

O Enxame de Diques de Florianópolis foi formado no intervalo de 128,3 + 0,5 a 119,0 + 0,9 Ma ($^{40}Ar/^{39}Ar$), o pico magmático ocorreu nos intervalos de 128 e 126 Ma e de 122 e 119 Ma (Raposo et al., 1998; Deckart et al., 1998). No entanto, dados paleomagnéticos indicam que a maioria desses diques estão associados ao intervalo mais recente, sugerindo a associação desses diques à distensão crustal nos estágios finais que antecederam a formação da crosta oceânica nessa latitude (Marques & Ernesto, 2004). No entanto, em publicação recente de Florisbal et al. (2014, 2017) apresenta idades U-Pb em badeleíta de 134.7 ± 0.3 a 133.9 ± 0.7 Ma, ou seja, mais antigas que as indicadas por $^{40}Ar/^{39}Ar$ e opõe-se a uma ligação direta com o magmatismo sin-rifte associado a abertura sul do Oceano Atlântico.

Soleiras no Estado do Paraná

As soleiras de diabásio de Reserva e Salto do Itararé no Estado do Paraná estão associadas ao falhamento e grande lineamento magnético denominado Rio Alonzo (Ferreira et al. 1982). A soleira de Reserva, uma das mais expressivas soleiras do Estado do Paraná intrude rochas sedimentares da Bacia do Paraná (Formações Palermo e Irati). A soleira do Salto do Itararé encontra-se alojada nos arenitos, siltitos e folhelhos da Formação Rio Bonito. Os litotipos que compõem as soleiras são representados principalmente por basalto subalcalino seguido por lati-basalto, andesi-basalto, dacito e riolito. São caracterizadas petrograficamente como diabásio vitrofírico, olivina diabásio, pigeonita diabásio, diabásio granofírico e granófiro.

Os dados químicos e petrográficos mostram que a cristalização fracionada foi o principal processo responsável de seus diversos litotipos, com exceção dos termos

ácidos que são veios pegmatóides granofíricos e representam o líquido residual associado a fases minerais em desequilíbrio, incorporados por algum processo mecânico durante sua migração para zonas de mais baixa pressão. As rochas dessas soleiras exibem maior proximidade composicional com os basaltos de alto-Ti da região norte da Bacia do Paraná (Maniesi & Oliveira, 1997; Petersohn & Gouvea, 2009). Modelos construídos para a soleira de Reserva demonstram a distribuição das variáveis geoquímicas, nos quais se constata uma equivalência direta entre os parâmetros analisados.

As soleiras encaixadas nas Formações Irati e Ponta Grossa na Bacia do Paraná nas regiões de Reserva, Prudentópolis, Irati, Rebouças e Ponta Grossa são constituídas por rochas de composição básica a intermediária, variando de basaltos andesíticos a andesitos, lati-andesitos, latitos e um quartzo latito (Petersohn et al. 2007). Estas rochas apresentam elevadas concentrações de TiO_2 (>2%) e são classificadas como sendo dos tipos Pitanga e Paranapanema. Diagramas de variação apontam a cristalização fracionada como importante mecanismo na evolução e gênese destas rochas (Petersohn & Gouvea, 2009).

Soleiras no Estado de São Paulo

A maioria das soleiras da borda leste da Bacia do Paraná, no estado de São Paulo são intrusivas nos sedimentitos do Grupo Itararé (Machado, 2005). Contudo, os corpos superficialmente mais extensos, estão localizados no intervalo estratigráfico que compreende as rochas mecanicamente menos resistentes, sendo a porção superior do Super grupo Tubarão (siltitos e diamictitos do Grupo Itararé e siltitos arenosos da Formação Tatuí), Formação Irati (principalmente os folhelhos do Membro Taquaral) e Formação Corumbataí (siltitos, argilitos e folhelhos). Além disso, também ocorrem, soleiras intrudidas nos arenitos síltico-argilosos da Formação Pirambóia, raramente chegando até a Formação Botucatu.

Dados geoquímicos indicaram que as rochas intrusivas são constituidas por basalto, traqui-basalto e traqui-andesito de afinidade toleítica e podem ser

classificadas como pertencentes ao grupo de alto-Ti (TiO_2≥2%) (Machado et al., 2007). Além disso, as diferenças geoquímicas também indicam que as intrusivas pertencem aos subgrupos (magmas-tipo) Paranapanema e Pitanga, mostrando que a distribuição destes magmas pela área estudada não se faz ao acaso. O tipo Paranapanema ocorre nos *sills* da região de Campinas, enquanto que Pitanga nas regiões de Cajuru, Leme e Iracemápolis. Para comparação geoquímica, os derrames próximos também foram investigados, onde se observou que as amostras coletadas nas regiões de Franca, Igarapava e Rifaina em São Paulo e São Sebastião do Paraíso, em Minas Gerais, são pertencentes ao magma-tipo Urubici e aquelas da região de Brotas e Ribeirão Preto são do tipo Pitanga. Contudo, as concentrações de elementos terras raras, para as amostras representativas dos três magmas-tipo, mostraram que, embora as rochas intrusivas do tipo Paranapanema e Pitanga e derrames do tipo Urubici possam ter uma mesma fonte mantélica, foram submetidas a processos de evolução magmática distintos (Machado et al., 2007).

Soleiras no Estado do Rio Grande do Sul

Segundo Viero & Roisenberg (1992), o Complexo Básico de Lomba Grande, situado no município de Gravataí, RS é constituído por três corpos hipabissais de afinidade toleítica encaixados em rochas sedimentares das Formações Botucatu e Sanga do Cabral. Estes corpos foram designados informalmente de Olivina-Gabro (correspondendo a 95% do volume total do complexo), Diabásio Envolvente e Diabásio Oriental. As características químicas são de magmas relativamente primitivos com altos teores de MgO, Cr, Ni e Co e empobrecidos em elementos K, Rb, Ba, Zr e Elementos Terras Raras. As idades são da ordem de 160 Ma (K-Ar), representando, provavelmente uma das manifestações magmáticas mais precoces da Bacia do Paraná. Já o Diabásio Envolvente e o Oriental são mais jovens (125 Ma) e seus dados geoquímicos mostram baixos teores de elementos incompatíveis similaridade com as vulcânicas básicas de baixo-Ti da Bacia do Paraná. Viero et al. (1992) realizaram estudos de susceptibilidade magnética no Complexo Básico Lomba Grande identificando nas litologias correlação negativa com o MgO e positiva

com o SiO_2 e o FeO, o que contraria a concepção de que o magnetismo cresce com a basicidade da rocha.

Renner et al. (2008) e Renner (2010) compararam a geoquímica entre as soleiras da região de Manoel Viana e Agudo, RS, com soleiras da porção leste e norte da Bacia do Paraná nos Estado de Goiás, Paraná e São Paulo. Segundo os autores, as rochas estudadas no Rio Grande do Sul têm características químicas equivalentes à associação baixo-TiO_2, enquanto que as rochas dos estados do Paraná, São Paulo e Goiás apresentam afinidades com a associação alto-Ti.

A região do Cerro do Coronel, localizada no Vale do Rio Pardo, RS, é caracterizada pela presença de quatro soleiras de diabásio dispostas segundo uma direção preferencial NW-SE, intrusivas concordantemente em unidades sedimentares das Formações Rio Bonito e Irati, no limite norte do Escudo Sul-Rio-Grandense (Eick et al., 1984; UFRGS, 2006). As soleiras exibem textura holocristalina e são relativamente homogêneas com granulação fina. Bolsões gabróicos de pouca expressão são localizados na base do bloco norte do corpo de diabásio, sendo caracterizados pela textura fanerítica média a grossa.

Dados geoquímicos revelam que as rochas hipabissais da região do Cerro do Coronel são equivalentes a andesitos basálticos de afinidade toleítica. Todas as amostras estudadas apresentam concentrações de TiO_2 menores que 2%, o que permite relacioná-las aos magmas do tipo Baixo-Ti, característico da subprovíncia sul da Província Magmática do Paraná. Apresentam teores de Sr entre 185 e 244ppm, Zr/Y entre 4,1 e 5,9, Ti/Zr variando de 61 a 94, e Ti/Y entre 258 e 486, sugerindo assim uma correlação com o magma do tipo Esmeralda (Sarmento et al., 2014).

2.5. MORFOLOGIAS DAS INTRUSÕES

As intrusões básicas toleíticas associadas à PIPE são relacionadas principalmente ao Cretáceo Inferior e contemporâneas à atividade vulcânica. Ocorrem principalmente intrudidas nos sedimentos paleozóicos da Bacia do Paraná em seus diferentes níveis estratigráficos e são condicionadas por fatores

estratigráficos e tectônicos. O condicionamento estratigráfico é evidenciado pela existência de níveis preferenciais de intrusão, sendo em primeiro lugar a Formação Irati (em toda a bacia), a Formação Botucatu (em São Paulo e Rio Grande do Sul) e Formações Serra Alta e Terezina (Paraná e Santa Catarina). O condicionamento tectônico é caracterizado pelas áreas em que o esforço máximo favorece as intrusões concordantes, enquanto que a formação de diques é facilitada quando o esforço vertical é maior que o horizontal (Soares, 1981). Dentre os fatores tectônicos destacam-se os Arcos de Ponta Grossa, Rio Grande, Campo Grande e São Gabriel, além de lineamentos tectono/magmáticos, como Guapiara, São Jerônimo-Criúva, Rio Uruguai, Icamaquã e Piquiri (Ferreira, 1982). Os arcos são estruturas que podem ser reconhecidas por uma inflexão no embasamento cristalino. Entre os arcos de Ponta Grossa e Rio Grande ocorre a Sinclinal de Torres que, segundo Fúlfaro et al. (1982), estão associadas falhas escalonadas que rebaixaram os sedimentos da bacia, com alguns blocos situados abaixo do nível do mar, na atual plataforma continental. Deckart et al. (1998) sugerem que os lineamentos tectono/magmáticos mais importantes estariam conectados a sistemas de junção tríplice, relacionados a processos distensivos e de rifteamento sintracratônicos. Segundo estes autores, os sistemas de falhamentos constituiriam estruturas profundas que serviram de dutos para enxames de diques paralelos à costa (NE-SW) e coincidentes com a direção de abertura do Atlântico e com enxames de diques alimentadores para o sistema fissural responsável pelo vulcanismo e pela intrusão de um grande volume de soleiras (estruturas NW-SE) (Figura 11).

Utilizando dados de furos de sondagem e geofísicos, Zalán et. al. (1985) descreveram as principais estruturas na Bacia do Paraná relacionadas a esses corpos intrusivos, sendo estas destacadas na Figura 12 e descritas abaixo:

Soleira (Sill) – Trata-se de uma intrusão tabular concordante, ou seja, está posicionada paralelamente ou subparalelamente ao acamamento das rochas encaixantes. Suas espessuras horizontais são muito maiores do que as verticais e podem variar de poucas centenas de metros quadrados até centenas de quilômetros quadrados. As terminações das soleiras podem ser abruptas (na junção com o dique alimentador) ou graduais por afinamento;

Salto de Soleira (Sill Jump) – Dependendo da rocha encaixante e do volume do magma durante a intrusão do sill, o corpo pode mudar de nível estratigráfico através de porções inclinadas, que geralmente situam-se entre 10º até 40º. Sob essa denominação, inclui-se também qualquer língua de material magmático ejetado por uma soleira ou lacólito discordantemente ou a baixo ângulo, para cima ou para baixo, dentro das rochas encaixantes;

Lacólito – Corpo intrusivo concordante e de grande espessura, possuindo geralmente a base plana e topo arqueado. A característica mais importante deste tipo de intrusão é o arqueamento por elas produzido nas rochas encaixantes sobrepostas. Apresenta, em planta, uma forma circular ou oval. Consequentemente, os arqueamentos a ele associados são dômicos. Existe também, lacólitos de convexidade dupla, que apresentam uma forma grosseiramente lenticular em seções sísmicas;

Bismálito – Tipo especial de lacólito, sendo que neste caso as rochas encaixantes acima das intrusões são soerguidas por meio de falhamentos. A diferença principal entre um bismálito e um lacólito é a presença de ruptura de alçamento de seu teto, reflexo direto de sua geometria. São corpos grosseiramente semelhantes a cubos ou paralelepípedos, com terminações laterais íngremes e abruptas. Os bismálitos originam horsts.

Estrutura Gaivota (Sea-gull Structure) – Desenvolve-se nos contatos de certos diques de diabásio com as rochas sedimentares encaixantes e consiste em estratos arqueados que mergulham em direção ao dique. Embora a origem de tal estrutura seja ainda desconhecida, certas hipóteses podem ser tecidas: a) a estrutura resultaria do colapso dos estratos ao redor do dique, em consequência da diminuição de volume e aumento da densidade após o resfriamento da intrusão; b) a estrutura representaria o arrasto das camadas nas margens de diques injetados de cima para baixo, a partir de soleiras ou lacólitos situados em níveis superiores;

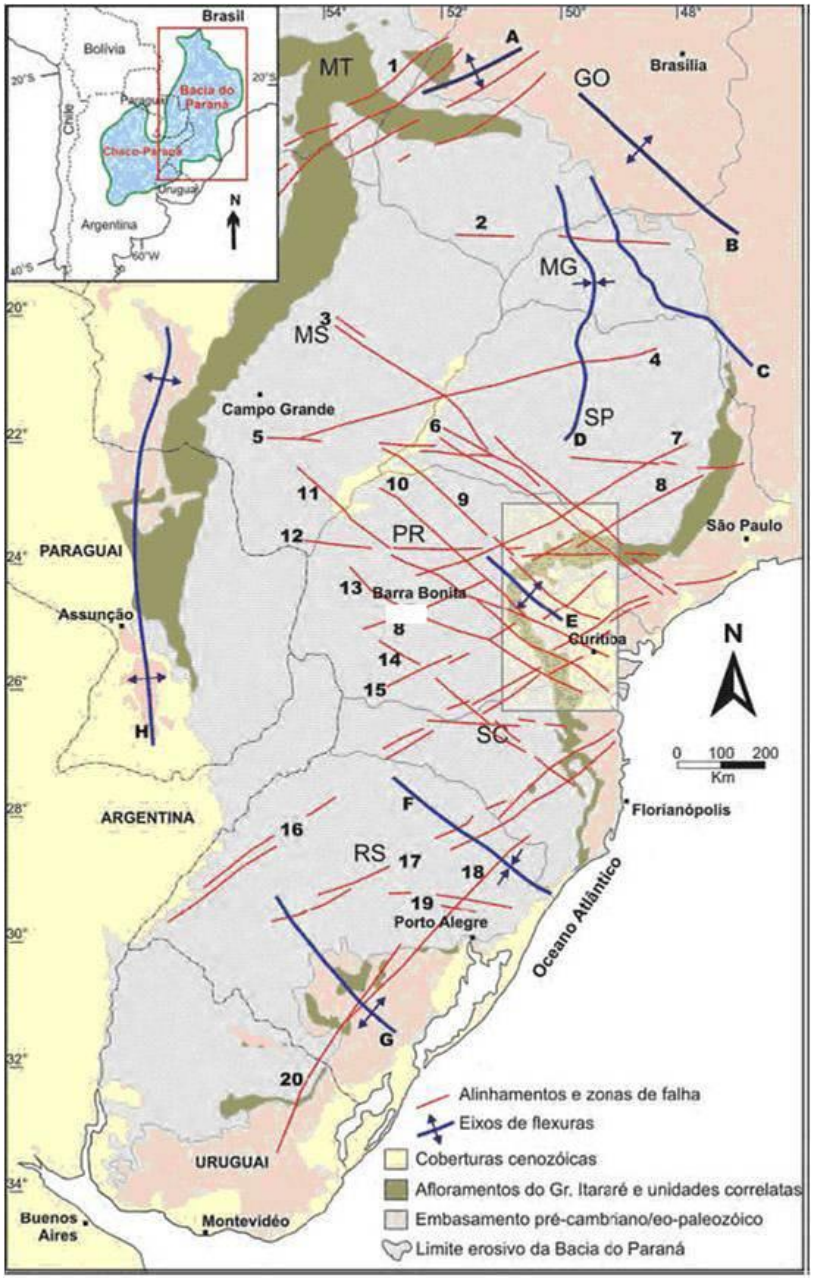

Figura 11. Mapa de localização da Bacia do Paraná e os principais elementos tectônicos definidos por Zalán et al. (1987): 1) Transbrasiliano; 2) Cassilândia; 3) Guapiara; 4) Araçatuba; 5) Moji-Guaçu/Dourados; 6) Santo Anastácio; 7) Guaxupé; 8) Jacutinga; 9) São Jerônimo/ Curiúva; 10) Rio Alonzo; 11) Cândido de Abreu/Campo Mourão; 12) São Sebastião; 13) Rio Piquiri; 14) Caçador; 15) Taxaquara; 16) Lancinha/Cubatão; 17) Blumenau/Soledade; 18) Leão; 19) Bento Gonçalves; 20) Açotea; a) Arco de Bom Jardim de Goiás; b) Arco do Alto Paranaíba; c) Flexura de Goiânia; d) Baixo de Ipiaçu/Campina Verde; e) Arco de Ponta Grossa; f) Sinclinal de Torres; g) Arco do Rio Grande; h) Arco de Assunção.

Dique – Intrusão vertical ou subvertical discordante, muitas vezes encaixado em planos de falha das rochas encaixantes. Alguns deles não apresentam deformação nas rochas encaixantes, ao passo que outras podem apresentar camadas subverticais em suas imediações, mergulhando para fora do dique. Muitas vezes os diques estão intrudidos ao longo de falhas, levantando a questão da idade das mesmas. Duas alternativas são viáveis: a) A falha foi formada em um evento tectônico anterior ao evento magmático; b) A falha formou-se durante o evento tectônico extencional relacionado ao magmatismo e simultaneamente preenchido por um dique;

Apófise – São feições relacionadas a diques ou a topo de soleiras. As deformações mais comumente associadas são dobramentos e flexuras nas rochas encaixantes.

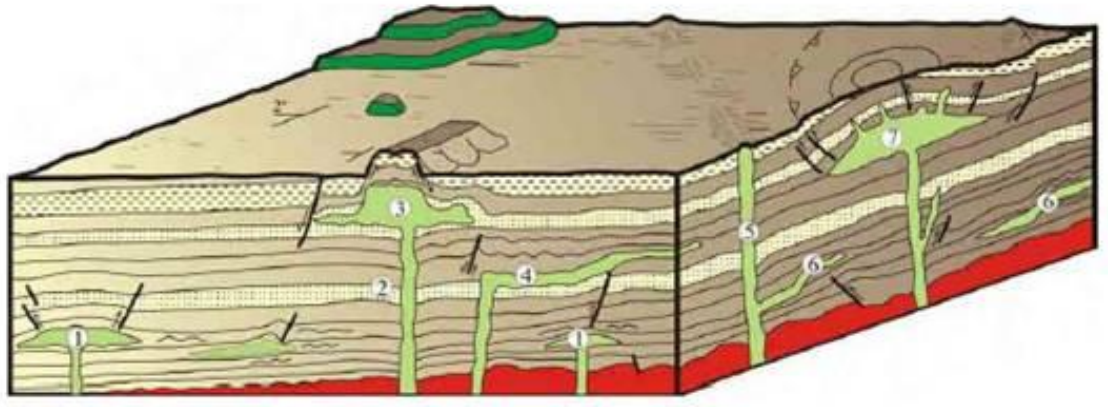

Figura 12. Figura esquemática mostrando diversos tipos de estruturas relacionadas a intrusões de diabásio e suas geometrias na Bacia do Paraná. Simplificado de Zalán et al. (1985). Legenda: Verde escuro - derrames; Verde claro – rochas intrusivas; Verde claro – rochas intrusivas; Vermelho – embasamento cristalino; Demais cores – rochas sedimentares da Bacia do Paraná; 1 – Estrutura do tipo Lacólito; 2 – Sea-gull Structure; 3 – Bismálito formando horst, com estruturas do tipo apófise nas laterais; 4 – Intrusão provocando flexuras na rocha encaixante; 5 – Dique; 6 – Sill Jump; 7 – Domo associado à lacólito.

2.6. CONDICIONANTES FÍSICOS RELACIONADOS AOS MECANISMOS DE INTRUSÃO

Os mecanismos de *emplacement* de soleiras e diques máficos na crosta é um assunto ainda muito debatido. Existe certa discussão sobre o fato da colocação dos diques ocorrer em fraturas pré-existentes ou se o alojamento e a propagação destes corpos ígneos podem gerar a sua própria fratura. A definição tradicional é baseada na idéia de que a intrusão de um magma ocorre mais facilmente ao longo dos sistemas de fraturas e zonas de fraqueza pré-existentes, do que por criação de novas fraturas (Billings, 1972). O modelo da entrada do magma ao longo de fraturas pré-existentes é amplamente aceito no Brasil. Para alguns autores, a presença de antigos sistemas de falhas no embasamento Pré-Cambriano é considerada um fator essencial para a ocorrência dos eventos magmáticos Fanerozóicos (Almeida, 1986; Ricommini, 1997; Ricommini et al., 2004; Schmitt & Stanton, 2007). Esses autores assumem que a crosta superior é altamente fraturada e que a pressão do magma não seria suficiente para fraturar a rocha encaixante. Alguns autores consideram o modelo de preenchimento de fraturas um importante mecanismo de intrusão de diques (Delaney et al., 1986; Bear et al., 1994; Delaney & Gartner, 1997; Valentine & Krogh, 2006).

Por outro lado, experimentos analíticos envolvendo conceitos de mecânica de rochas, ao aproximarem a geometria de diques para corpos elípticos alongados, demonstram que a tensão concentrada ao redor da ponta do dique seria suficientemente grande para fraturar a rocha encaixante mesmo sob baixas pressões de magma (Atkinson, 1987).

A morfologia de diques assimétricos e diques e *sills* secundários associados às intrusões principais tem sido atribuída modelo de fraturamento hidráulico, com gradientes de depressão magmática ou estresse regional e a magnitude de assimetria controlada pelo comprimento de fratura (sob pressão) e um gradiente de tensão efetiva (Pollard & Muller, 1976). Para Daniels et al. (2012), que estudaram os diques assimétricos de Swartruggens na África do Sul e Rum na Escócia, cuidados devem ser tomados ao extrapolar dados de diques. A média de espessura observada nos diques foi inferior a 1 m, não devendo a análise ser automaticamente

aplicada a diques maiores. A aplicação destes resultados com diques mais espessos exige uma investigação mais aprofundada.

Observações de campo de diques e soleiras são importantes para a sua interpretação e para o entendimento do problema do mecanismo de intrusão destes. O modelo tradicional de preenchimento de fraturas assume que uma fraqueza linear, como uma falha ou junta é contínua ao longo do dique (Figura 13A). No entanto, há poucos trabalhos de campo atuais de descrições de diques. Motoki (1986) mostra alguns exemplos de diques traquíticos e fonolíticos do Cretáceo inferior intrudidos no corpo sienítico de Ilha Vitória, Estado de São Paulo. Segundo estes autores, observa-se um arredondamento na forma do dique, principalmente e sua porção frontal, não sendo constatada nenhuma fratura contínua na rocha hospedeira ou ao longo da extensão do dique. Não são encontradas falhas ou articulações ao longo da extensão dos diques, sugerindo que a intrusão ocorreu por pressão de magma, sem qualquer influência de zonas de fraqueza pré-existentes na rocha encaixante (Figura 13B).

Modelamentos teóricos e experimentais demonstram que, sob pressões relativamente baixas, menores do que quatro vezes a resistência à tração da rocha encaixante, fraturas hidráulicas de tração são formadas perpendicularmente à direção do eixo de menor esforço, σ3, ou seja, paralelo ao plano σ1-σ2, quando a pressão do magma excede σ3 mais a resistência à tração da rocha encaixante. Este processo é denominado "fraturamento hidráulico de tração" (Figura 14) e, quando as fraturas são imediatamente preenchidas pelo magma, o resultado seriam as intrusões tabulares, tais como diques e soleiras. É interessante notar que a fratura de tração atravessa obliquamente a fratura de cisalhamento. A menos que o sistema de fraturas pré-existente na rocha hospedeira seja sub-paralela ao plano σ1-σ2, o magma não irá preenchê-lo. Na crosta superior, o eixo σ1 é geralmente vertical. Portanto, corpos intrusivos tabulares verticais ou diques são facilmente formados mesmo em corpos massivos, como batólitos graníticos. O presente modelo explica a predominância de diques em relação às soleiras, mesmo em rochas sedimentares bastante estratificadas (Nakamura, 1977; Nakamura et al.,1977; Phillips,1974; Hills, 1975; Haimson, 1975; Bosworth et al., 2000). A partir de

relações observadas entre diques e fraturas no Platô Colorado, Delaney et al. (1986) concluem que ambas situações descritas acima podem ocorrer. No entanto, os autores demonstram que dependendo do ângulo entre a fratura e a direção do esforço principal mínimo (σ3), diques podem preencher fraturas pré-existentes em direções favoráveis à abertura em condições onde a diferença entre o esforço horizontal máximo é pequena quando comparada a pressão dirigida exercida pelo magma.

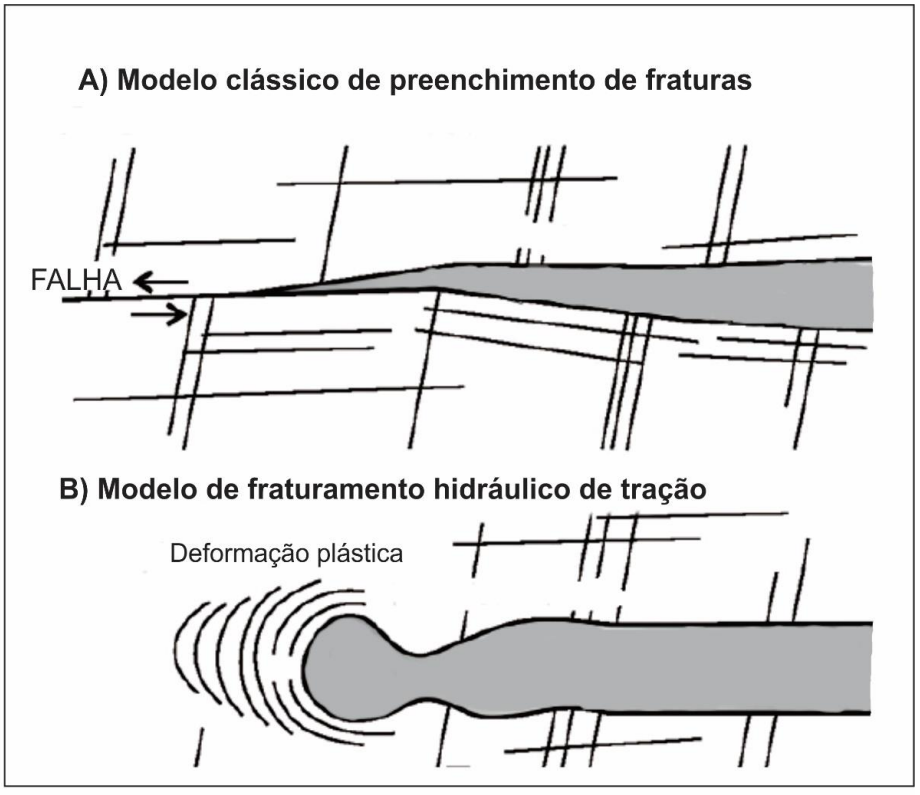

Figura 13. Modelos de corpos tabulares intrusivos de acordo com: (A) Modelo clássico de preenchimento de fraturas pré-existentes; (B) Modelo de fraturamento hidráulico de tração (Modificado de Motoki & Sichel, 2008).

A maioria das soleiras intrudem os corpos rochosos sedimentares sub-horizontais em profundidades rasas. Existem corpos intrusivos concordantes sub-verticais, mas raramente são observadas em campo. Normalmente, eram originalmente intrusões sub-horizontais inclinadas por algum evento tectônico

posterior, mas a ocorrência de soleiras em alguns ambientes geológicos específicos não concorda com o modelo tradicional de preenchimento de fraturas.

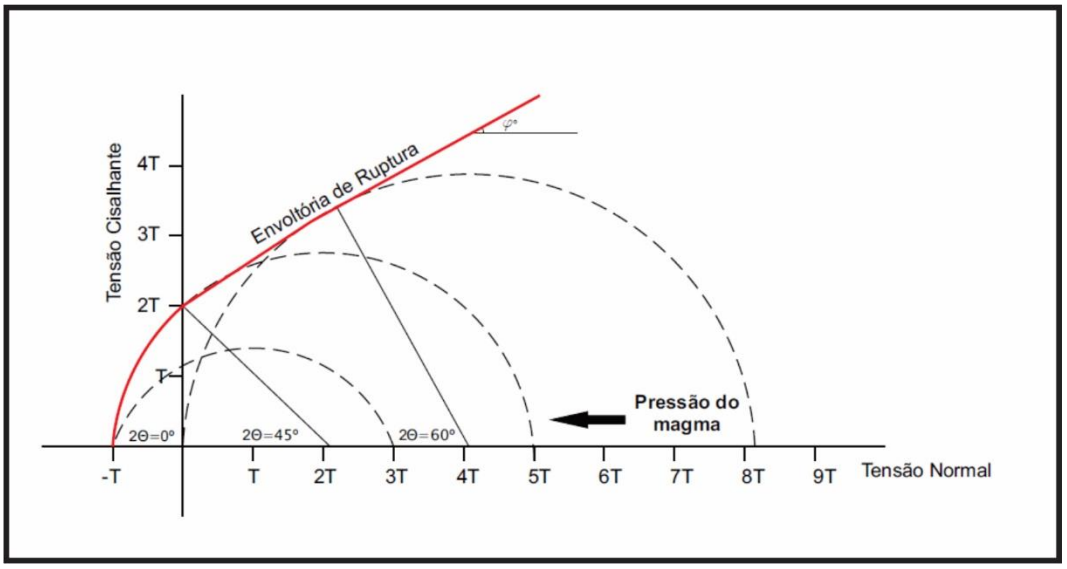

Figura 14. Representação mecânica no Diagrama de Mohr das condições de ruptura e do efeito do magma na resistência das rochas (Modificado de Motoki & Sichel, 2008).

Valentine & Krogh (2006) propuseram os seguintes mecanismos de transição dique-soleira em rochas hospedeiras frágeis: (1) ascensão do magma por flutuabilidade de locais mais profundos para um nível de flutuabilidade neutra, onde se acumularia (e.g. Lister & Keer, 1991; Goulty, 2005); (2) uma mudança de orientação do σ3 de vertical em locais mais profundos para horizontal em locais mais rasos (e.g. Parsons & Thompson, 1992; Galerne et al., 2008; Galerne et al., 2011).

O primeiro mecanismo é baseado na teoria de preenchimento de fratura tradicional, uma vez que assume que o magma basáltico mais denso intrude as formações encaixantes menos densas. O segundo mecanismo é baseado na teoria da fratura hidráulica por tração. Phillips (1974) e Hills (1975) explicaram o mecanismo de intrusão de soleiras (Figura 14), e salientaram a importância dos esforços de compressão lateral e a colocação superficial do corpo rochoso. Em ambientes profundos, a tensão vertical é maior por causa do grande número de

obstáculos e por causa do stress σ1 vertical. Em tais condições, a pressão do magma pode abrir uma fratura elástica sub-vertical. Em locais rasos, tensão vertical é pequena. Quando o esforço horizontal é suficientemente elevado, o σ3 torna vertical e a intrusão tabular ocorre horizontalmente. O stress horizontal se deve principalmente à pressão de magma nas paredes dos diques. Neste nível, a intrusão muda da direção vertical para a horizontal, fazendo a transição dique-soleira (Parsons & Thompson, 1992). Essa transição pode ocorrer também em rochas plutônicas homogêneas, como o granito. Hall (1987) apontou que as grandes soleiras podem transgredir a estratificação da rocha hospedeira quando ocupam uma grande área, mostrando passos abruptos, em vez de discordâncias angulares.

3. APRESENTAÇÃO DOS ARTIGOS CIENTÍFICOS

3.1. ARTIGO 1

TÍTULO: Mafic subvolcanic intrusions and their petrologic relation with the volcanism in the south hinge Torres Syncline, Paraná-Etendeka Igneous Province, southern Brazil.

AUTORES: Carla Cecília Treib Sarmento

Carlos Augusto Sommer

Evandro Fernandes de Lima

PUBLICADO: Maio de 2017, v. 77, p. 70-91.

PERIÓDICO: Journal of South American Earth Sciences

Journal of South American Earth Sciences 77 (2017) 70-91

Contents lists available at ScienceDirect

Journal of South American Earth Sciences

journal homepage: www.elsevier.com/locate/jsames

Mafic subvolcanic intrusions and their petrologic relation with the volcanism in the south hinge Torres Syncline, Paraná-Etendeka Igneous Province, southern Brazil

Carla Cecília Treib Sarmento*, Carlos Augusto Sommer, Evandro Fernandes Lima

Universidade Federal Do Rio Grande Do Sul, Endereço: Av. Bento Gonçalves nº. 9500, Prédio 43136, Sala 107, Bairro Agronomia, cep.91501.970, Porto Alegre, RS, Brazil

a r t i c l e i n f o

Article history:
Received 26 September 2016
Received in revised form
12 January 2017
Accepted 29 April 2017
Available online 3 May 2017

Keywords:
Continental basaltic provinces
Hypabyssal basic intrusions
Lithochemistry
Basic to intermediate volcanism

a b s t r a c t

The hypabyssal intrusions investigated in this study are located in the east-central region of the state of Rio Grande do Sul, in the south hinge of the Torres Syncline. The intrusions comprise twenty-four dikes and ten sills, intruding in ponded pahoehoe, compound pahoehoe, rubbly and acidic lava flows of the south sub-Province of the Paraná Igneous Province and the sedimentary rocks of the Botucatu, Pirambóia, Santa Maria and Rio do Rasto Formations, on the edge of the ParanáBasin. The intrusive dikes in the flows have preferred NNW-SSE direction and the intrusive dikes in the sedimentary rocks have preferred NE-SW direction. Regarding the morphology, the dikes were separated into two different groups: symmetrical and asymmetrical. The small variation in facies is characterized by fine to aphanitic equigranular rocks. The rocks were divided into two types: Silica Supersaturated Tholeiite (SST) e dikes and sills consisting of plagioclase and clinopyroxene as essential minerals, with some olivine and felsic mesostasis, predominant intergranular texture and subordinate subophitic texture; and Silica Saturated Olivine Tholeiite (SSOT) e dikes consisting mainly of plagioclase, clinopyroxene and olivine, and predominant ophitic texture. The major and trace element geochemistry allows classifying these hypabyssal bodies as basalts (SSOT), basaltic andesites and trachyandesites (TSS) of tholeiitic affinity. The mineral chemistry data and the REE behavior, combined with the LILE and HFSE patterns, similar to the flows and low-Ti basic intrusions of southern Brazil and northwestern Namibia allow suggesting that these dikes and sills were part of a feeder system of the magmatism in the Paraná-Etendeka Igneous Province. The preferred direction of the intrusive dikes in the sedimentary rocks of the ParanáBasin coincides with tectonic-magmatic lineaments related to extensional processes and faulting systems that served as vents for dike swarms parallel to the Brazilian coast, with the same direction as the Namibia coast dike swarm. This suggests that these dikes were part of the triple junction system related to the opening of the South Atlantic Ocean. The preferred directions of the intrusive dikes in the lava flows are similar to the directions of the Ponta Grossa and Rio Grande Arcs and the Torres Syncline. They may have been a part of, or been caused by one or more geotectonic cycles that originated these structures. The emplacement process of the asymmetric dikes suggests they were enclosed under the hydraulic fracture model, since they do not follow a pre-existing fracture filling pattern. The emplacement of the sills conforms to the weakness zones of the sedimentary units. Regarding the intrusive dikes in the flows, divided by lithofacies associations, also taking into account the geochemical and petrographic similarities, it is observed that these dikes are part of a supply system of the basic lava flows, stratigraphically positioned above the host lava flows.

1. Introduction

The Paraná-Etendeka Igneous Province (PEIP) is interpreted as a *Large Igneous Province,* and one of the main Continental Basaltic Provinces (CBPs) in the world (Coffin and Eldholm, 1992; Self et al.,

* Corresponding author.
E-mail addresses: carla.treibs@gmail.com (C.C.T. Sarmento), carlos.sommer@ ufrgs.br (C.A. Sommer), evandro.lima@ufrgs.br (E.F. Lima).

http://dx.doi.org/10.1016/j.jsames.2017.04.017
0895-9811/

2006; Bryan and Ernst, 2008). Its magmatism is 90% located in the central-east portion of the South American Plate and the remainder is located in Africa, more precisely in Namibia.

The intrusions of basic tholeiitic rocks are very common phenomena associated with the Paraná-Etendeka Province and studies suggest that the volume of these intrusive bodies in the Paraná Basin is approximately 112,000 km³ (Frank et al., 2009). Although the sills mostly occur in the eastern edge of the Paraná Basin, they are also relatively abundant throughout its extension, usually intruding in the Paleozoic sediments (Almeida, 1986; Zalán et al., 1985) in the states of São Paulo (Machado et al., 2007) and Paraná (Maniesi and Oliveira, 1997; Petersohn et al., 2007; Petersohn and Gouvea, 2009). In the state of Rio Grande do Sul, the hypabyssal bodies related to the PEIP are located in the south edge of the Paraná Basin, with emphasis on the Lomba Grande Basic Complex (Viero and Roisenberg, 1992), the Manoel Viana and Agudo region sills (Renner, 2010) and the Cerro do Coronel region sills (Sarmento et al., 2014). The occurrence of dikes are also common forms of intrusions, often grouped into swarms, more frequently occurring in the states of Paraná (Ponta Grossa dike swarm), Santa Catarina (Florianópolis dike swarm) (Raposo et al., 1998; Deckart et al., 1998; Marques and Ernesto, 2004; Tomazzoli and Lima, 2006; Florisbal et al., 2014; Tomazzoli and Pellerin, 2015), São Paulo and Rio de Janeiro (Serra do Mar dike swarm). These dike swarms are found to have the same geochemical trends among themselves and of the basaltic flows (Turner et al., 1994; Stewart et al., 1996; Corval et al., 2008) of the Paraná Igneous Province, with high-TiO_2 and low-TiO_2 suites (Valente et al., 2007; Corval, 2009).

In the African portion of the province, the dikes and sills associated with the rifting process and magmatism that formed the South Atlantic Ocean are abundant at about 150 km along the coast of Namibia (Siedner and Mitchell, 1976; Ewart et al., 1984; Hunter and Reid, 1987; Marsh et al., 1991). These bodies primarily intrude the basement units of the Damara Mobile Belt and the Karoo basin sediments (Marsh et al., 1991; Lord et al., 1996). They occur as dike swarms, such as the Henties Bay-Outjo (Duncan et al., 1990; Lord et al., 1996; Trumbull et al., 2004), where the picritic to rhyolitic tholeiite dikes are located around Spitzkoppe, western Namibia (Thompson et al., 2007). The Regional, Tafelberge and Horingbaai dolerites are also noteworthy, in addition to the Huab sill complex (Ewart et al., 1984; Duncan et al., 1989) and the Doros Complex (Gibb and Henderson, 1996; Marsh, 2013; Owen-Smith and Ashwal, 2015a). In the Huab basin area both Tafelkop (picritic) and Tafelberg type dikes can be seen cutting up through, and in some cases feeding, the basal volcanic units and are often margin parallel (Jerram et al., 1999; Wanke et al., 2000).

The importance of basic intrusions in the evolution of CBPs has been shown in some studies, notably Raposo et al., 1998; Deckart et al. (1998); Marques and Ernesto (2004).

In the case of the Paraná Igneous Province, although some studies discuss basic intrusions, few investigations have been carried out with the purpose of presenting a statistical overview of the basic/intermediate intrusions and their relationship with the associated volcanic deposits. In addition, there are hardly any studies that consider the flow stratigraphy and typology, in the structural context of the Paraná Basin (e.g. volcanism and sedimentation filling the Torres Syncline).

In this sense, this study aims to characterize the geology and petrology of several intrusive bodies (24 dikes and 10 sills) located in central-eastern Rio Grande do Sul and their relationship with the flows of part of the Serra Geral south sub-province, in the south hinge of the Torres Syncline (Fig. 1).

2. Materials and methods

A set of 42 samples was selected, from the hypabyssal bodies of the studied region, in order to analyze the chemical compositions of the major, minor, and trace elements and rare earth elements (REE). The samples were prepared with an agate ball mill, which allows to obtain less than 200 mesh fractions. The analyzes were carried out at *Acme Laboratories Ltda* (Canada) using the ICP-ES (*Inductively Coupled Plasma Emission Spectrometry*) method for major elements and ICP-MS (*Inductively Coupled Plasma Mass Spectrometry*) method for trace elements and rare earth elements. The detection limits for most of the major elements were on the order of 0.1% and 0.1 ppm for the trace elements. The analytical errors are less than 0.01% for oxides (except FeO 0.04%) and less than 1 ppm for trace and rare-earth elements.

The mineral chemistry data were acquired with the analysis of nine samples. The CAMECA SX-5 electron microprobe used to obtain quantitative and qualitative data is equipped with five WDS spectrometers and one EDS spectrometer, and is located in the Electron Microprobe Laboratory of the CPGq e IGEO e UFRGS. The analytical conditions for the analysis of silicates includes an electron beam of 1 mm, Faraday current of 15 nA with accelerating voltage of 15 kV, and SP1-TAP (Na and Mg), SP2-LLIF (Fe, Ni and V), SP3 e LPET (Ti, Cr and Mn), SP4 e TAP (Na and Mg) and SP5 e PET (K and Ca) spectrometers.

The litho-chemical data were processed in binary and ternary phase diagrams, developed in the GCDkit software (*Geo Chemical Data ToolKIT*), prepared by Janoušek et al. (2006) and MINPET version 2.02 (Richard, 1995), which consists of manipulation and recalculation systems of geochemical data for whole rock analysis of igneous and metamorphic rocks.

3. Geological setting

The Paraná Basin is defined as an intracratonic basin, with an area of approximately 1,500,000 km² in east-central South America (Fig. 1). Formed by a volcano-sedimentary sequence from the Upper Ordovician to the Upper Cretaceous periods, this basin can be divided into six supersequences separated by the regional unconformities (Milani, 1997): Rio Ivaí (Upper Ordovician e Lower Silurian), Paraná (Devonian), Gondwana I (Upper Carboniferous e Lower Triassic), Gondwana II (Middle to Upper Triassic), Gondwana III (Upper Jurassic e Lower Cretaceous) and Bauru (Upper Cretaceous). The Gondwana III supersequence is characterized by a basal sedimentary sequence related to aeolian environments (Botucatu Formation), overlaid by a thick volcanic succession named Serra Geral Formation (Formação Serra Geral - FSG). This unit covers an area of more than 917,000 km² in Brazil, Paraguay, Uruguay and Argentina, with an approximate volume of 450,000 km³ (Frank et al., 2009).

These sequences also occur in the well-exposed sections of the Huab Basin in northwestern Namibia (Jerram et al., 2000), further expanding the coverage area of the deposits before the Gondwana rupture.

Major tectonic structures are found in the Paraná Basin, notably the Ponta Grossa and Rio Grande Arcs and the Torres Syncline. During the syn-volcanic subsidence process, these structures induced the formation of sub-basins, thus playing a major role in the structural evolution of the basin and influencing its current boundaries.

The FSG is characterized by a sequence of lava flows with maximum thickness of 1700 m, with predominant basalts and basaltic andesites of tholeiitic affinity. Acidic flows (rhyolites,

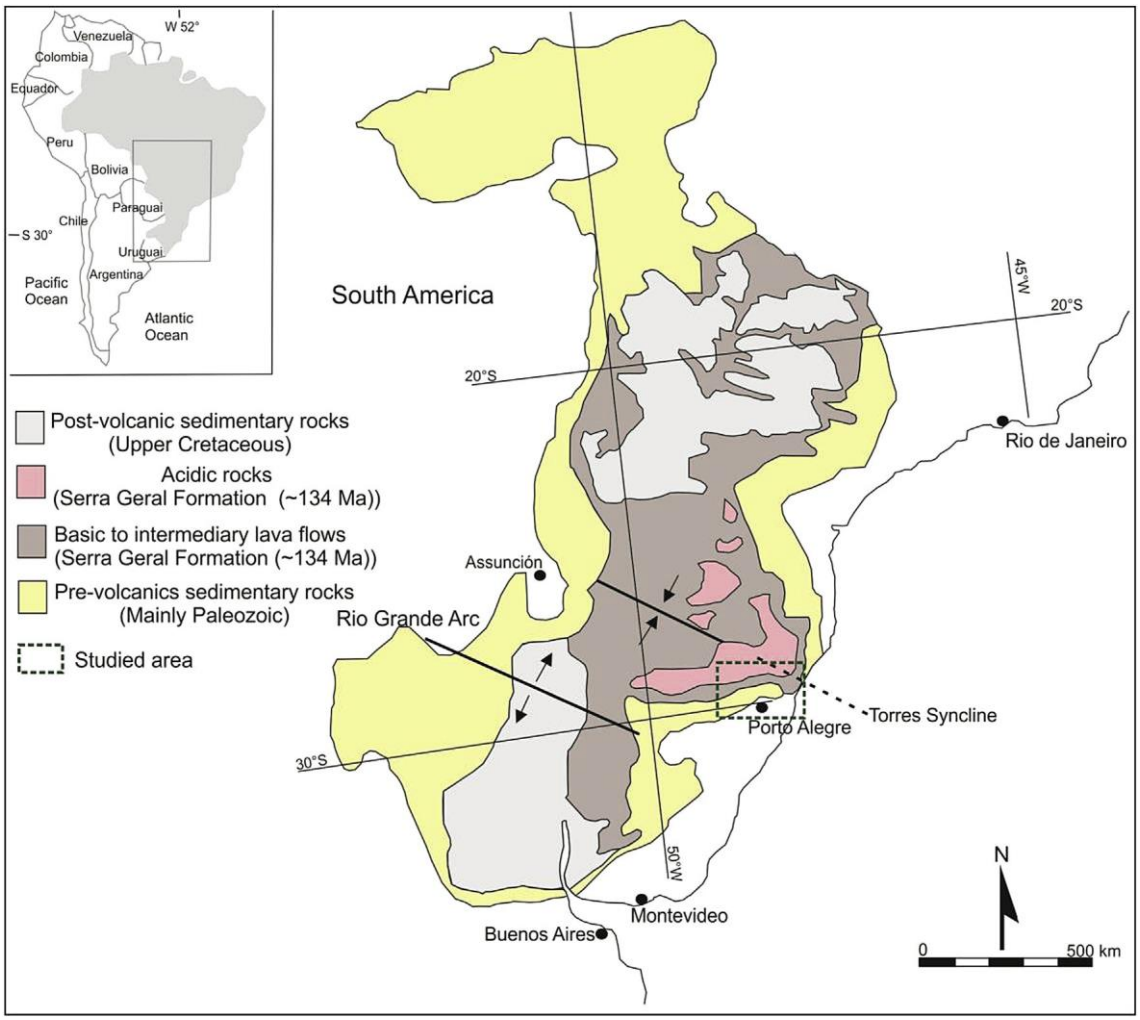

Fig. 1. Simplified geological map of Paraná Basin including Torres Syncline structure. Studied area highlighted. Source: modified from Waichel et al., 2012; Barreto et al., 2014.

rhyodacites) occur subordinately, interspersed with basic flows on top of the volcanic sequence, especially in southernmost Brazil. The occurrence of a large amount of basic to intermediate intrusive bodies (sills and dikes) is common, usually associated with structural discontinuities of the Paraná Basin.

In the southern part of the basin, the flows were deposited mainly over the sandstones of the Botucatu Formation, locally preserving the original morphologies of dunes and sedimentary features. These features suggest contemporaneity among the first volcanic episodes and the active aeolian system of this unit (Scherer, 2002; Waichel et al., 2008).

A new stratigraphic model, based on facies architecture, was recently proposed for the Torres Syncline region (Waichel et al., 2012). It is based on the morphology of the basic and acidic lava flows, paleo-topography and effusion rates, complementing a similar studies on the volcanic and basin stratigraphy on the Etendeka side (e.g. Mountney et al., 1998; Jerram et al., 1999, 2000) for the Huab Basin in Namibia.

Barreto et al. (2014) and Rossetti et al. (2014) conducted a detailed analysis of the emplacement conditions of these basic volcanic rocks in the Santa Cruz do Sul/Herveiras and Estância Velha/Caxias do Sul regions, south hinge of the Torres Syncline, by applying the facies analysis method combined with petrographic and geochemistry data. The flows were divided into lithofacies associations: ponded pahoehoe lava (interdune confined flows), compound pahoehoe lava (small pahoehoe lava lobes stacked in a complex pattern), simple (sheet) pahoehoe lava (tabular lobes with internal structure consisting of basal zone, massive core and vesicular zone) and rubbly lava (thick flows with tabular geometry, massive core and top with auto-breccias).

Several studies (Bellieni et al., 1984; Mantovani et al., 1985) have divided the basic rocks into two major groups: high-Ti basalts, with TiO_2 contents above 2%, and low-Ti basalts, with TiO_2 contents lower than 2%. Subdivisions of these groups into magma-types were proposed by Peate et al. (1992) and Peate (1997), mainly based on the amount of trace elements and the ratios between them. The magma-types with $Ti/Y > 300$ that predominantly occur in the northern portion of the province were named Pitanga, Paranapanema and Ribeira. The Gramado, Esmeralda and Urubici magma-types have $Ti/Y < 300$ and predominantly occur in the south of the province. The acidic volcanic rocks were subdivided into the Palmas (Caxias do Sul and Santa Maria) and Chapecó (Guarapuava and Ourinhos) facies. The acidic rocks of the Chapecó type are mostly in the center of the Paraná Basin and are represented by dacites, rhyodacites, quartz latites and hypohyaline, porphyritic to strongly porphyritic rhyolites. The Palmas type acidic rocks correspond to rhyolites and rhyodacites, typically aphyric, holohyaline to hypocrystalline. In general, the acidic composition rocks are mostly present in the states of Rio Grande do Sul, Santa Catarina and Paraná (Bellieni et al., 1986; Piccirillo and Melfi, 1988;

Piccirillo et al., 1989; Nardy, 1995). The main distinguishing factors of these groups is the abundance of incompatible elements. The Chapecó facies has values of Zr > 500 ppm, Ba > 900 ppm and Sr > 250 ppm, while the Palmas facies has values of Zr < 400 ppm, Ba < 800 ppm and Sr < 170 ppm (Peate et al., 1992).

Renne et al. (1992) suggest that the ages of the basic and acidic rocks of the southern portion of the Paraná Basin are between 131.4 ± 1.6 and 132.9 Ma, and the youngest ones are in the north and central regions (129.9 ± 0.1 and 131.9 ± 0.9 Ma). Thiede and Vasconcelos (2010) obtained results that confirm the ages found by Renne et al. (1992) by the $^{40}Ar/^{39}Ar$ geochronology method (134.7 ± 1 Ma) for the basalts in the south part of the basin. The values obtained in the northern portion of the Paraná Basin are similar to those found in Etendeka by Renne et al. (1996b), recal- culated following Renne et al. (2010) to 134.2 ± 0.4 Ma (Goboboseb I), 134 ± 0.5 Ma (Goboboseb II) and 134.1 ± 0.7 (Springbok) by Dodd et al. (2015).

Recently, Janasi et al. (2011) obtained the age of 134.3 ± 0.8 Ma for a dacite of the Chapecó Group (Ourinhos type) with the U-Pb baddeleyite-zircon system. According to these authors, the dacite is slightly older than the overlying high-Ti basalts (133.6e131.5 Ma) and the obtained data suggest a time period of ~3 Ma for the development of the high-Ti sequence of the Paraná basin. These authors also point out that the values found in the dacite coincide with the $^{40}Ar/^{39}Ar$ values (134.8e134.1 Ma) obtained in the low-Ti basalts (Gramado and Esmeralda) and in the Palmas-type dacites and rhyolites in southern Brazil. The dataset is therefore consistent with the short volcanism and the rapid succession by the high-Ti sequence.

Petrogenetic models obtained from the investigation of hypabyssal bodies show its importance for the understanding of the Paraná Magmatic Province. According to Marques and Ernesto (2004), geochemical and isotopic data from the Ponta Grossa Dike Swarm reveal that asthenospheric components were not significant in the genesis of these dikes and that they may have been little affected by crustal contamination processes. For Renne et al. (1996a), the ages of the Ponta Grossa Dike Swarm are between 133.1 and 130.8 Ma ($^{40}Ar/^{39}Ar$), temporally correlated to the Paraná-Etendeka Province basaltic lava flows. These authors also observed ages close to 120 Ma in dikes near the continental margin, confirming the hypothesis proposed by Piccirillo et al. (1990) who suggest that these dikes were younger feeders of the north subprovince flows, of which there are no remaining outcrops due to subsequent weathering.

The swarms of basic dikes of tholeiitic affinity of the Serra do Mar in São Paulo and Rio de Janeiro (134-130 Ma; $^{40}Ar/^{39}Ar$), could be separated into two different high-Ti and low-Ti suites, similar to the Ponta Grossa dikes and the basalt flows of the Paraná Igneous Province (Turner et al., 1994; Stewart et al., 1996; Corval et al., 2008). Models developed from the Serra do Mar Dike Swarm investigation suggest delamination of the subcontinental lithospheric mantle, encompassed by convective cells rising from the underlying sublithospheric mantle at shallow asthenospheric levels. These phenomena occur during an advanced stage of the Gondwana Supercontinent rifting (Valente et al., 2007; Corval, 2009). The Florianópolis Dike Swarm consists predominantly of high-Ti dolerites. The lowɛTi terms are represented by basalts and basaltic trachyandesites and the dacites are geochemically similar to the Chapecó type acidic volcanic rocks from the Paraná Igneous Province (Tomazzoli and Lima, 2006; Tomazzoli and Pellerin, 2015). Composite dikes occur in southern Florianópolis, with basaltic andesite edges and trachyandesite core, containing swarms of magmatic mafic enclaves. The Florianópolis Dike Swarm was formed between 128.3 ± 0.5 and 119.0 ± 0.9 Ma ($^{40}Ar/^{39}Ar$), and the magmatic peak occurred between 128 to 126 Ma and 122 to 119 Ma (Raposo et al., 1998; Deckart et al., 1998). Thus, these dikes are probably associated with the crustal strain in the final stages leading to the formation of the oceanic crust in this latitude (Marques and Ernesto, 2004). However, Florisbal et al. (2014), in a recent publication, found U-Pb baddeleyite ages from 134.7 ± 0.3 to 133.9 ± 0.7 Ma, older ages than those indicated by $^{40}Ar/^{39}Ar$ and incompatible with a direct link with the syn-rift magmatism associated with the south opening of the Atlantic Ocean. Coutinho (2008), based on petrological and geochronological data, indicates the coastal dike swarm as a component of the north and south arms of a triple junction system centered at the Paraná coast and related to the initial opening of the South Atlantic Ocean.

The Henties Bay-Outjo Dike Swarm in the Damara belt, Namibia, is interpreted as an aborted arm of a triple junction centered on the edge of Walvis Bay. It has a compositional range from basalt to rhyolite with predominantly basaltic low-Ti composition (Duncan et al., 1990; Trumbull et al., 2004). Picritic to rhyolitic dikes are part of this swarm, surrounding the Spitzkoppe, western Namibia, with up to 20% MgO, suggesting that the magma probably originated from the melting of a *mid-ocean ridge basalt* (MORB) mantle source, followed by the limiting reaction of the subcontinental lithospheric mantle, metasomatized just before the formation of these magmas (Thompson et al., 2001, 2007). The Horingbaai dolerites have an affinity for the MORB magmas, with flat REE patterns and isotopic data that plot within the depleted mantle quadrant in the εSr vs. εNd diagram (Erlank et al., 1984; Hawkesworth *et al.*, 1984; Duncan et al., 1989). The Huab River Valley sill complex and associated dikes are separated into four types of doleritic magmas distinguished from one another by different abundance ratios of incompatible elements (Duncan et al., 1989). The Doros Complex is a mafic intrusion stratified into the Damaraland Intrusive Suite, northeastern Namibia, and part of the Paraná-Etendeka Igneous Province with ages of 134-132 Ma ($^{40}Ar/^{39}Ar$) (Marsh and Duncan, 2008). Feeder dikes have been mapped out from the Doros Complex, which highlights this mafic center as being important to the development of the early stratigraphy in the Huab Basin (e.g. Jerram et al., 1999), and highlights the significance of the link between intrusions and the volcanic pile (e.g. Jerram and Bryan, 2015). Based on field, petrological and geophysics data, Owen-Smith and Ashwal (2015a) proposed the origin of the Doros Complex as a result of at least seven spaced magmatic pulses. The authors suggest a large and complex system of interconnected channels and chambers that hosted a range of magmas of different compositions.

4. Results

4.1. Geology of intrusive bodies

The mapped hypabyssal intrusions are located in the Serra Geral Formation lava flows, south hinge of the Torres Syncline and in the sedimentary rocks of the south edge of the Paraná Basin.

The host basal volcanic flows are ponded-type pahoehoe, occupying interdune spaces of the Botucatu Formation, compound pahoehoe, simple (sheet) pahoehoe and subordinately rubbly and acidic lava flows on the top of the volcanic sequence.

The enclosing sedimentary rocks of the studied igneous bodies belong to the Botucatu Formation (fine to coarse sandstones), Pirambóia Formation (fine to medium sandstones), Rio do Rasto Formation (pelites and sandstones), Santa Maria Formation (sandstone and conglomeratic sandstone with subordinate pelites), in addition to bodies intruded into the Rio Bonito and Irati Formations (shales, siltstones and mudstones).

The twenty-four investigated dikes generally have a preferred NW-SE direction, and secondarily a NE-SW direction. The thirteen

dikes that intrude into basic flows have a preferred NNW-SSE and much subordinately, NW-SE and NE-SW directions. The 11 dikes that intrude into the sedimentary rocks have a preferred NE-SW direction (Fig. 2A, B and C).

The rocks have fine to medium-grained equigranular texture in the central portions of the thicker dikes and aphanitic edges. Regarding the morphology, the dikes were divided into two groups: symmetrical and asymmetrical. In this study, these terms are used to denote the thicker dikes with rectilinear forms and dikes with anastomosing geometry and very irregular contact with host-rock respectively.

The symmetrical dikes are the most common ones, intruding the pahoehoe ponded and (Fig. 3A), compound and simple pahoehoe (Fig. 3B and C), rubbly, and acidic flows, in addition to the sedimentary rocks. They show tabular geometry, regular and straight contacts, and thicknesses ranging from 1.0 m to 10 m. The presence of complex dike systems is common, with small secondary dikes, perpendicular and parallel to the main igneous body (Fig. 3C, D and E). When intruding into sedimentary rocks, it may be possible to observe the presence of small sills (5e10 cm), parallel to the main intrusion (Fig. 3G). The presence of centimetric joints is common in these bodies (Fig. 3A). The formation of complex dikes is also found in sedimentary rocks with behavior sometimes discordant, sometimes concordant in relation to the host rock (Fig. 3H).

The asymmetrical dikes occur in a restricted area in the eastern portion of the area, intruding ponded pahoehoe flows. They have reduced thicknesses (15.0 cme1.0 m) and usually show aphanitic texture. Dike systems with massive, centimetric to decimetric structures were observed, with no continuity in thickness. They are usually aphanitic rocks with cooled, sometimes glassy edges. The possible presence of vesicles and xenoliths from the host rock is observed in these dikes (Fig. 4).

The investigated sills have an average of 30 m in thickness, but can reach minimum thicknesses of 5 m and maximum thicknesses of up to 180 m. Fine to aphanitic equigranular texture is observed at the basal and top portions, and the cores of the thicker bodies have predominant fine to medium-grained equigranular texture. In some sills, the top-base relationships with the host rocks are exposed (Fig. 5A, B and C). Columnar joints show a dense and continuous pattern on these sills, but there are some zones with flat and sometimes curve joints (Fig. 5E and F). These variations are compatible with a faster cooling at the body's extremities. The interaction with the host rock includes the development of millimeter-sized glassy layers (Fig. 5D), thermally induced columnar joints in the host sediment, and contact metamorphism (Fig. 5G).

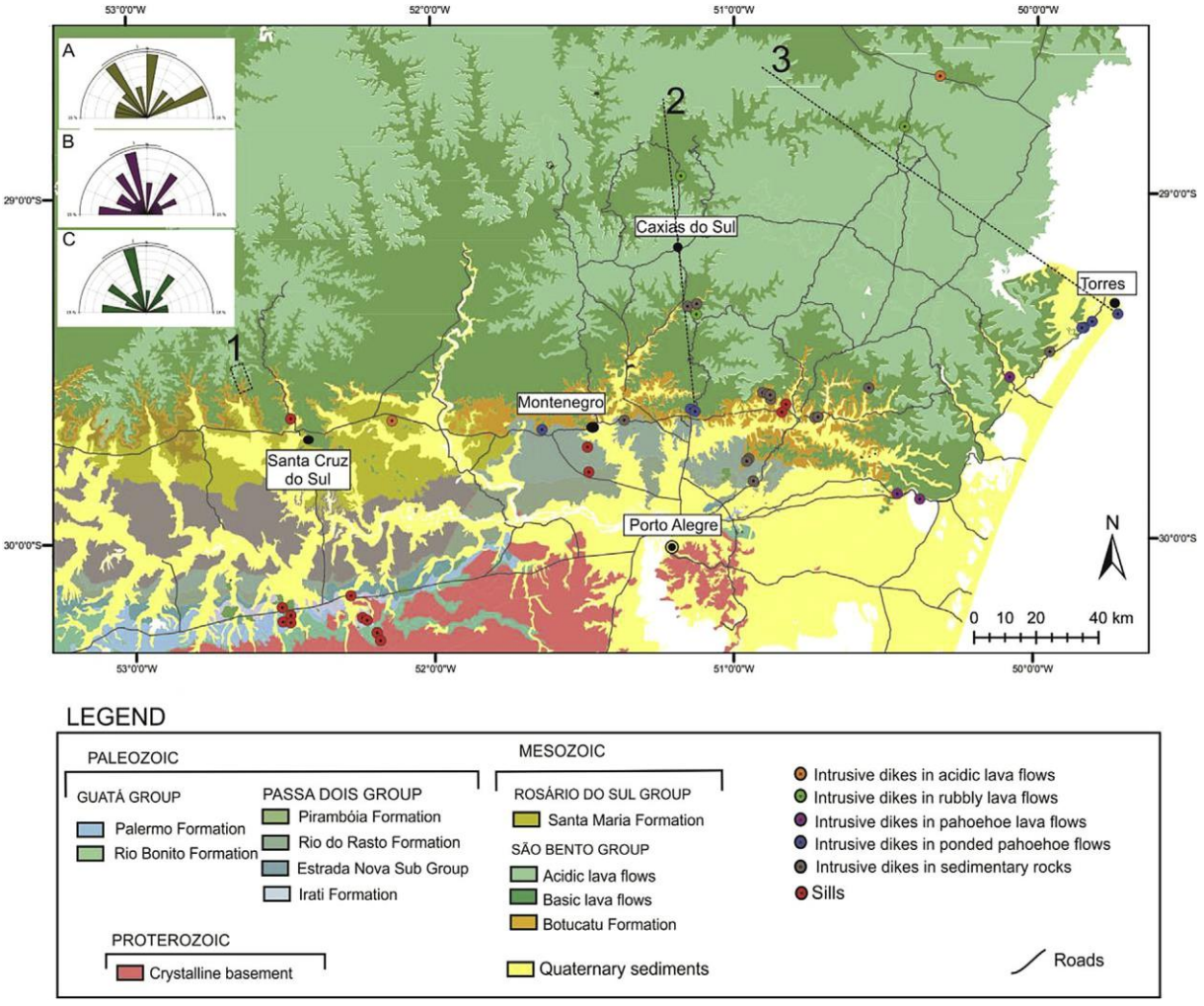

Fig. 2. Geological map of the study area showing the sampling sites. Modified of CPRM (2010). Rosette diagrams with directions of the investigated dikes. (A) Rosette diagram of dikes embedded in sedimentary rocks, (B) embedded in flows and (C) the total diagram of the directions of the investigated dikes. The 1, 2 and 3 profiles are of Fig. 17.

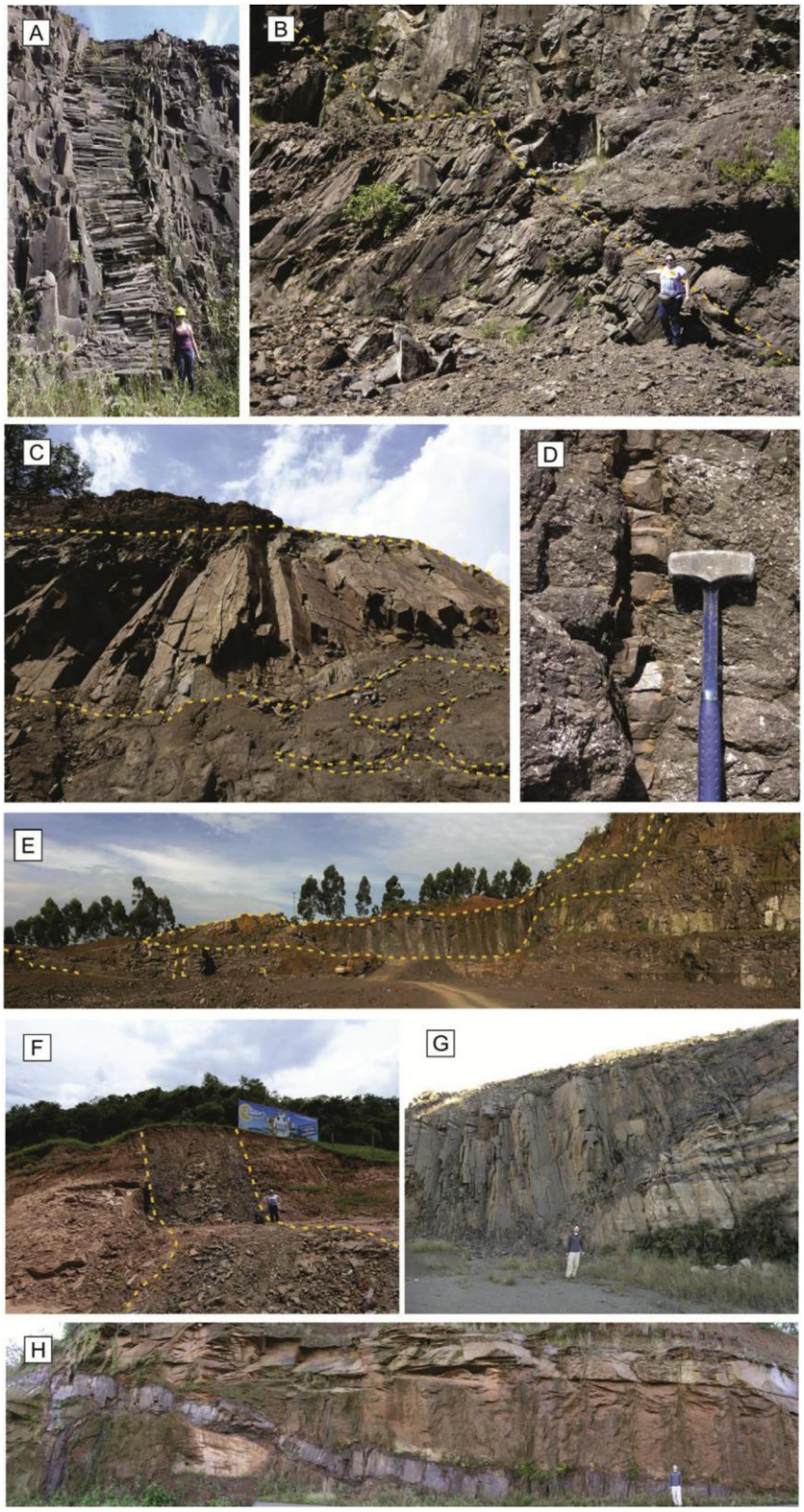

Fig. 3. Macroscopic aspects of representative symmetrical dikes. (A) Symmetrical dike with well marked joints cutting ponded pahoehoe lava flow; (B) large dike cutting simple pahoehoe lava flow; (C) system of dikes with secondary dikes (D) cutting compound pahoehoe lava flow; (E) dike complex systems cutting pahoehoe lava flow; (F) thick dike cutting the Botucatu sandstone; (G) feeder dike with secondary sills below; (H) complex dike with behavior sometimes discordant, sometimes concordant in relation to the host rock.

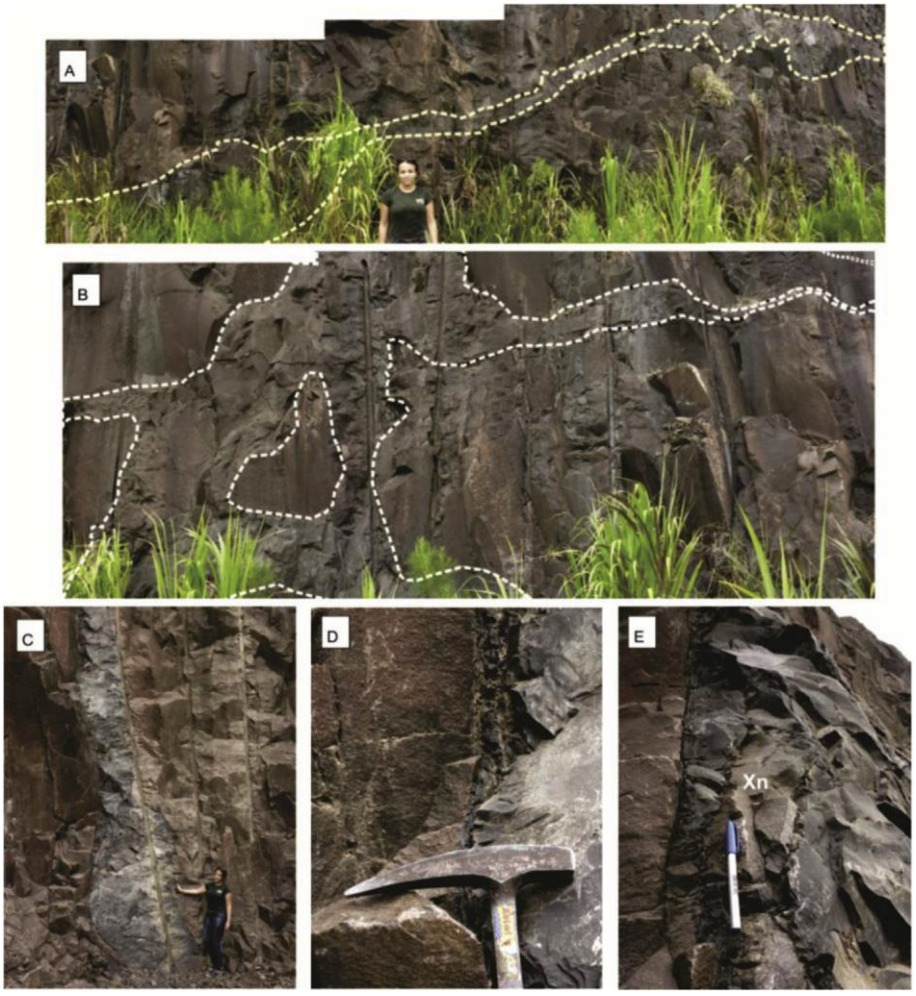

Fig. 4. Macroscopic aspects of asymmetrical dikes. Intrusive complex cutting ponded pahoehoe lava flow (A and B). (C) asymmetrical dikes in ponded pahoehoe lava flow; (D) contact the chilled margin with the host rock; (E) dike of host rock xenolith.

4.2. *Petrography*

4.2.1. *Dikes*

A total of 36 samples of dikes were described. The investigated a total of samples dikes are gray to dark-gray mesocratic diabases, sometimes brownish, due to alterations. They show holocrystalline to hypocrystalline texture (Fig. 6D). They are relatively homogeneous, fine-grained to aphanitic, predominantly equigranular. A slight texture variation can be seen, with grain size fining towards the edges, relative to the cores (Fig. 6).

The percentages of the minerals were obtained by visual estimation, resulting in the following data: plagioclase (45%); pyroxene (35%), olivine (7%), opaque minerals (5e10%) and felsic mesostasis (5 to 7The dikes were divided into two types: (i) Silica Supersaturated Tholeiite (SST) (which comprises the asymmetric dikes and most symmetrical dikes) consisting of plagioclase and clinopyroxene as essential minerals, opaques, apatite and eventual olivine. It has predominant intergranular texture and subordinate subophitic texture, and the presence of felsic mesostasis is common (zeolite);
(ii) Olivine Silica Saturated Olivine Tholeiite (SSOT) (comprising three symmetrical dikes embedded into ponded pahoehoe flows), consisting mainly of plagioclase, clinopyroxene and olivine. Opaque minerals and apatite are common accessories. The ophitic texture is predominant in this rock (Fig. 6).

The plagioclase in the dikes occurs as subhedral to euhedral crystals, usually elongated, with 0.05e1.3 mm in size at the finer grained portions (Fig. 6A). Some microphenocrysts are observed, sometimes forming glomeroporphyritic aggregates, with sizes ranging from 0.8 to 2.0 mm. The plagioclase acicular habit is observed in the SSOT dikes and in irregular TSS dikes (Fig. 6C and D). In the portions with coarser texture, the plagioclase is subhedral to euhedral, 2.0e3.0 mm in size, sometimes showing well-developed normal zoning (Fig. 6 B).

The clinopyroxenes are anhedral to subhedral in the finer grained portions, and are 0.03e0.5 mm in size (Fig. 6A). They generally occur as fine-grained granular aggregates. In the coarser grained portions, the clinopyroxenes are anhedral to subhedral, and 0.5e3.0 mm in size. They show irregular contacts and/or plagioclase inclusions (Fig. 6D). Iron hydroxide sometimes occurs as a weathering product, associated with the clinopyroxene grains.

Olivine is abundant on the SSOT dikes. The crystals are euhedral to subhedral, about 0.3e0.6 mm in size and scattered in the sample (Fig. 6C). It also sometimes occurs in TSS dikes as crystals fully replaced by saponite or serpentinized (Fig. 6E).

Quartz is rare and intergranular, sometimes forming sub-grains (0.2 mm).

The opaque minerals usually show straight faces, often with inclusions of plagioclase and pyroxene. The habit suggests they belong to the Fe and Ti oxides group. They make up about 6e10% of the studied rocks.

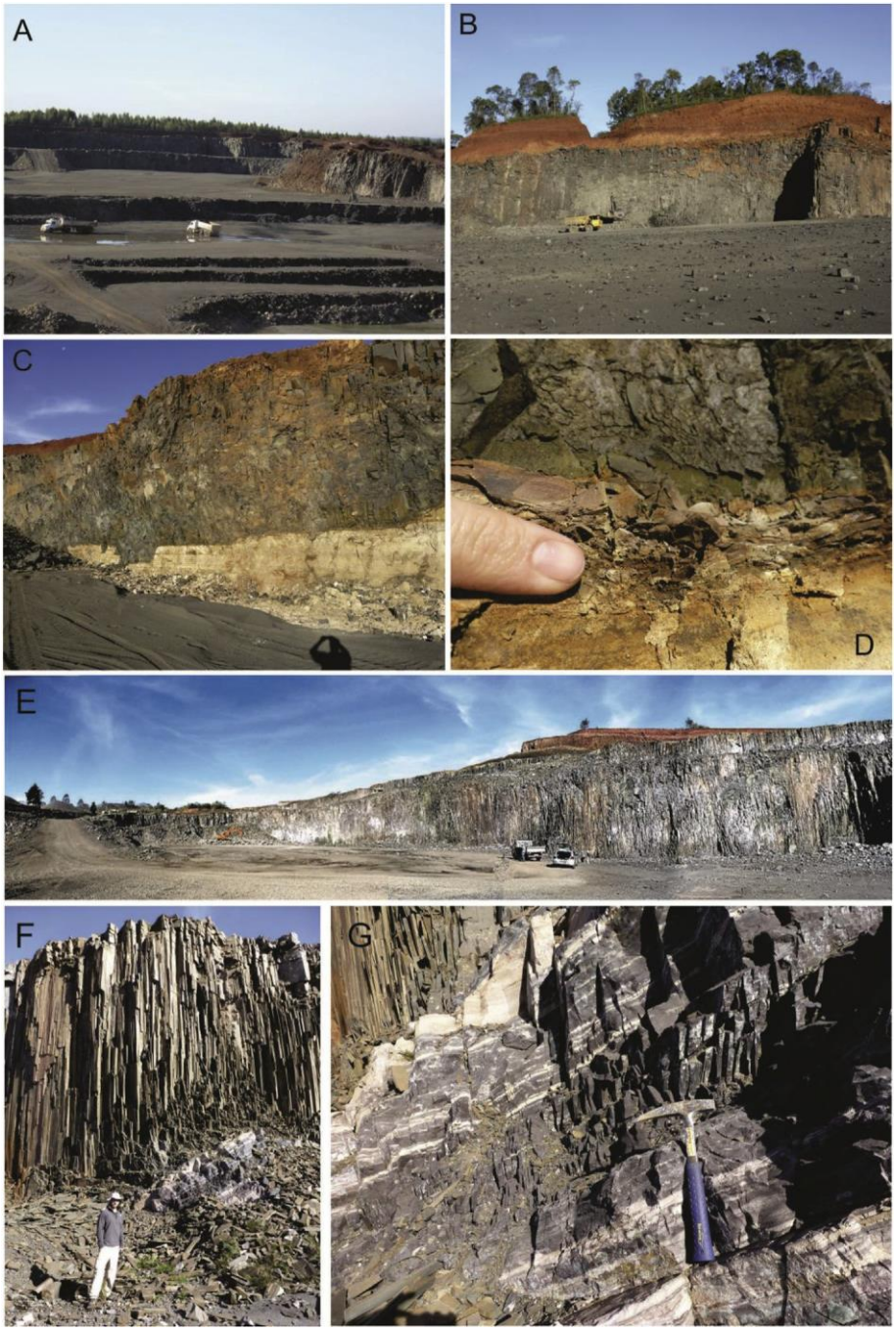

Fig. 5. Macroscopic aspects of representative sills. (A) View of dolerite sill (Vila Rica Mine); (B) relation with the top Pirambóia sandstone; (C) Base relationship with pelites and Rio do Rasto Formation sandstones; (D) glass layer formation in interaction with the host rock. (E) Panoramic view of the dolerite sill (Carollo Mine); (F) Columnar joints dense pattern; (G) Interaction with the surrounding sandstones forming columnar joints thermally induced and contact metamorphism.

Apatite is a common accessory phase, of up to 3% of the total sample. It usually occurs as euhedral and acicular crystals, mainly present in the microgranular material.

Felsic mesostasis is present in most of the SST dikes. It is formed by a homogeneous, low relief material, with low birefringence (gray) and wavy extinction. It ranges from 5 to 7% of the sample volume and can be interpreted as a late zeolite aggregate (Fig. 6F).

4.2.2. *Sills*

A total of 26 samples of sills were described. The sills are also mesocratic dolerites, with holocrystalline texture, fine to medium grained. There is slight grain fining towards the base and top of the sills in the thicker bodies (Fig. 7). The predominant texture is equigranular, although the presence of a few microphenocrysts of plagioclase and clinopyroxene is observed in the finer grained portions.

According to the mineralogy, they are characterized as SST e consisting of plagioclase and clinopyroxene as essential minerals, opaques, and apatite. Orthopyroxene and olivine are occasional. The predominant texture is intergranular and the subordinate texture is subophitic, and the presence of felsic mesostasis is common (zeolite) (Fig. 7).

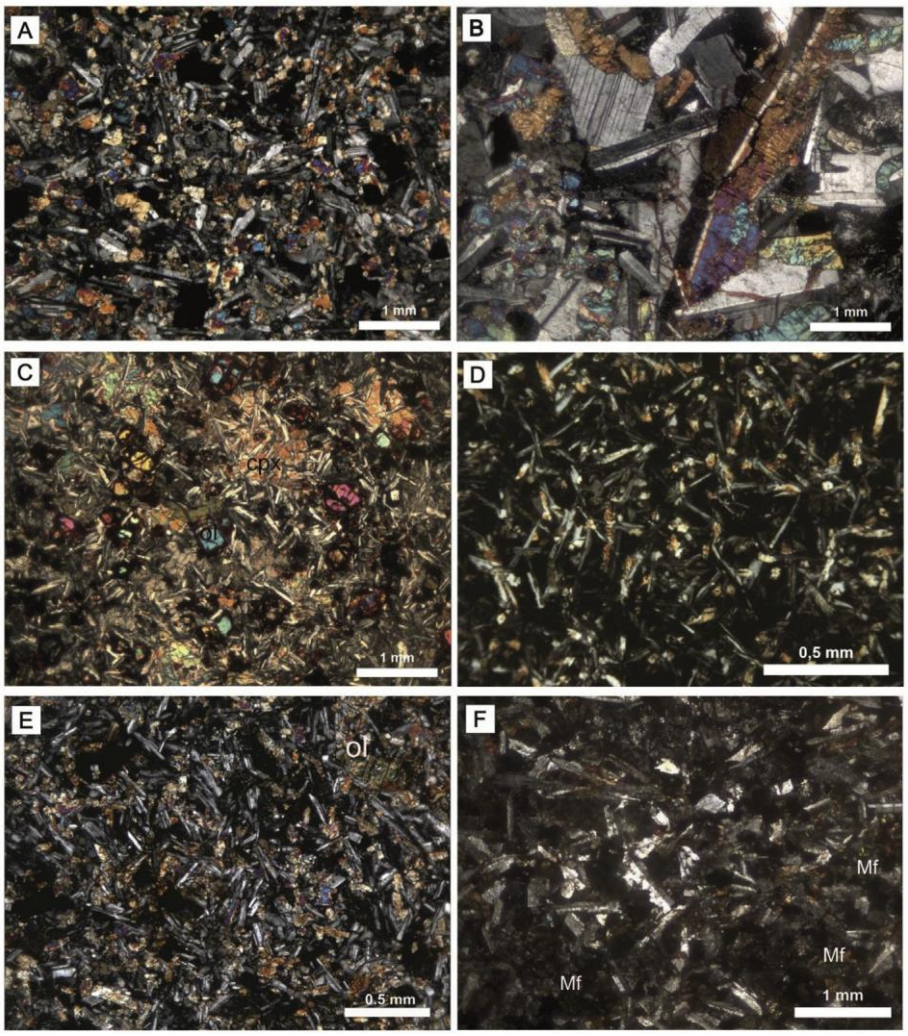

Fig. 6. Microscopic aspects of representative dikes. (A) Fine-grained edge and (B) dike core embedded in the compound pahoehoe flow types with medium-grained intergranular texture between crystals of plagioclase and clinopyroxene; (C) olivine crystals disseminated in the sample of the SSOT type and ofític texture on the clinopyroxene dike embedded in the ponded pahoehoe lava flows; (D) assymetrical dike with acicular habit of plagioclase and glass matrix; (E) dike sample embedded in rubbly lava flow with intergranular texture and serpentinized olivine (F) Zeolitic aggregate in the interstices of plagioclase and clinopyroxene grains in dike embedded in sedimentary rocks (Botucatu Fm.). Clinopyroxene (cpx), olivine (ol), felsic mesostasis (fm). Crossed nicols.

The volume percentages of the minerals in the sills are similar to the dikes: plagioclase (45%); pyroxene (35%), olivine (5%), orthopyroxene (7%), opaque minerals (5e10%) and felsic mesostasis (5e10%).

Plagioclase occurs as subhedral to euhedral prisms, with 0.05e1.7 mm in size in the finer grained portions (Fig. 7A). Microphenocrysts forming glomeroporphyritic aggregates are occasionally observed, and 0.5e2.0 mm in size. In the coarser portions, the plagioclase crystals are subhedral to euhedral, and 2.0e3.0 mm in size (Fig. 7B).

Clinopyroxenes are anhedral to subhedral and 0.03e0.5 mm in size in the finer grained portions (Fig. 7A), 0.5 and 3.0 mm in the coarser grained portions. They generally appear as fine-grained granular aggregates. Rare prismatic microphenocrysts of up to 3,0 mm can be seen, especially in the edges of the intrusive bodies. They show irregular contacts and/or plagioclase inclusions (Fig. 7C). Iron hydroxide sometimes occurs as a weathering product, associated with the clinopyroxene grains.

Orthopyroxene is an early phase, occurring in only one of the analyzed sills, showing subhedral crystals, 0.5e1.0 mm in size, usually with signs of alteration. It is often associated with the clinopyroxene crystals (Fig. 6 D).

Olivine occurs in crystals fully replaced by saponite or serpentinized (Fig. 7E). The crystals are euhedral to subhedral, about 0.3e0.6 mm in size and scattered in the sample (Fig. 7C). A common feature throughout the samples is the presence of crystals with edges and fractures filled by iddingsite.

Interstitial quartz is rare and sometimes forms sub-grains (0.2 mm).

The opaque minerals usually show straight faces, often with inclusions of plagioclase and pyroxene. The habit suggests they belong to the Fe and Ti oxides group.

Apatite is a common accessory phase, of up to 3% of the total sample. It usually occurs as acicular crystals.

Felsic mesostasis is present in most of the sills, ranging from 5 to 10% of the total sample volume (Fig. 7F).

4.2.3. *Mineral chemistry*

The analysis of the dike and sill samples, their chemical composition and variations of each mineral phase of the studied basic and intermediate hypabyssal rocks are shown and discussed in this topic. The samples are: PDY- 06 (Intrusive dike in rubbly lava

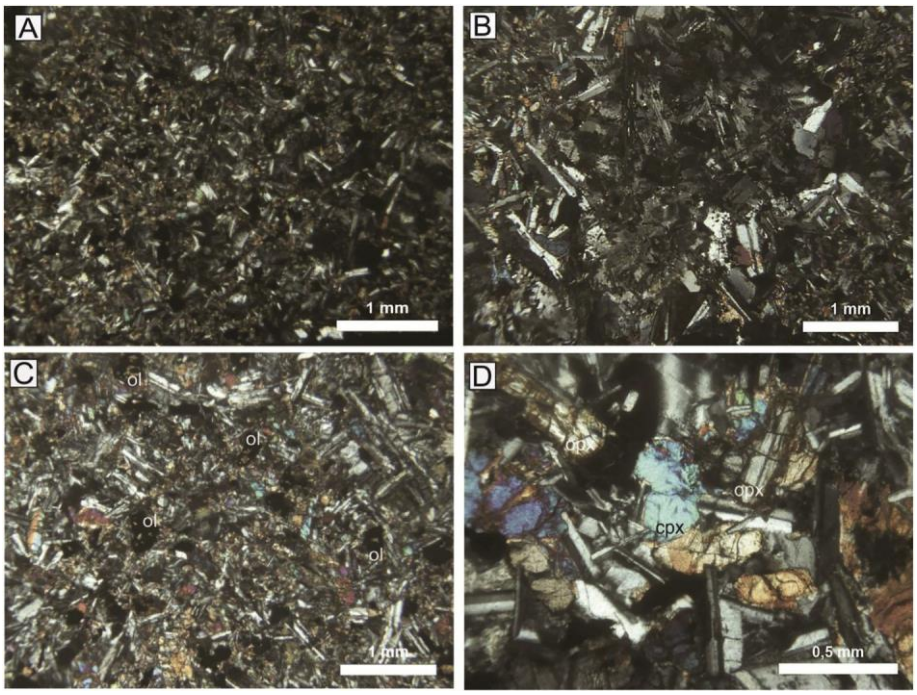

Fig. 7. Microscopic aspects of representative sills. (A) Fine-grained feature edges of igneous bodies and predominantly intergranular texture in most samples; (B) fine-grained average core bodies and felsic mesostasis; (C) orthopyroxene associated with clinopyroxene with subofític texture; (D) olivine crystals replaced by clay minerals (saponite) and iddingsite. Clinopyroxene (cpx), olivine (ol), orthopyroxene (opx). Crossed Nicols.

flows); PDY- 9B and PDY-9D (Intrusive dikes in ponded pahoehoe lava flows); PDY- 12 (Intrusive dike in compound pahoehoe lava flows); PDY- 19 (Intrusive dike in compound pahoehoe lava flows); CCO-005A (Intrusive sill in sedimentary rocks of the Rio Bonito and Irati Formation); PDY-23 (Intrusive dike in sedimentary rocks of the Rio do Rastro Formation); PDY- 44B (Intrusive sill in sedimentary rock of the Santa Maria Formation) and PDY- 47 (Intrusive dike into intrusive sill in sedimentary rocks of the Pirambóia Formation).

The core and edge of the grains of plagioclase, pyroxene and olivine were analyzed.

4.2.3.1. Plagioclases. The plagioclases were classified according to the Or-Ab-Na diagram (Deer et al., 2003), as labradorite, with anorthite (An), albite (Ab) and orthoclase (Or) contents between $An_{67}Ab_{32}Or_1$ and $An_{46}Ab_{51}Or_3$, with little variation between the studied dikes and sills.

The plagioclase is characterized by compositional zoning, where there is depletion of An and enrichment of Ab from the core to the edges of the crystals. This condition can also be confirmed in the variation diagrams, where a depletion of CaO and enrichment of Na_2O is seen with the evolution of differentiation (Fig. 8).

The lowest concentrations of An were found in sample CCO-005A, averaging 47.5% where the plagioclase composition ranges from labradorite in the crystal cores, and labradorite to oligoclase at the crystal edges ($An_{63}Ab_{37}Or_1$ to $An_5Ab_{80}Or_{15}$). The highest contents of anorthite (average of 67%) are found in samples PDY-9B and PDY-9D, with composition ranging from bytownite to andesine ($An_{75}Ab_{24}Or_1$ to $An_{42}Ab_{55}Or_3$). In all studied igneous bodies, the Or component is less than 7%.

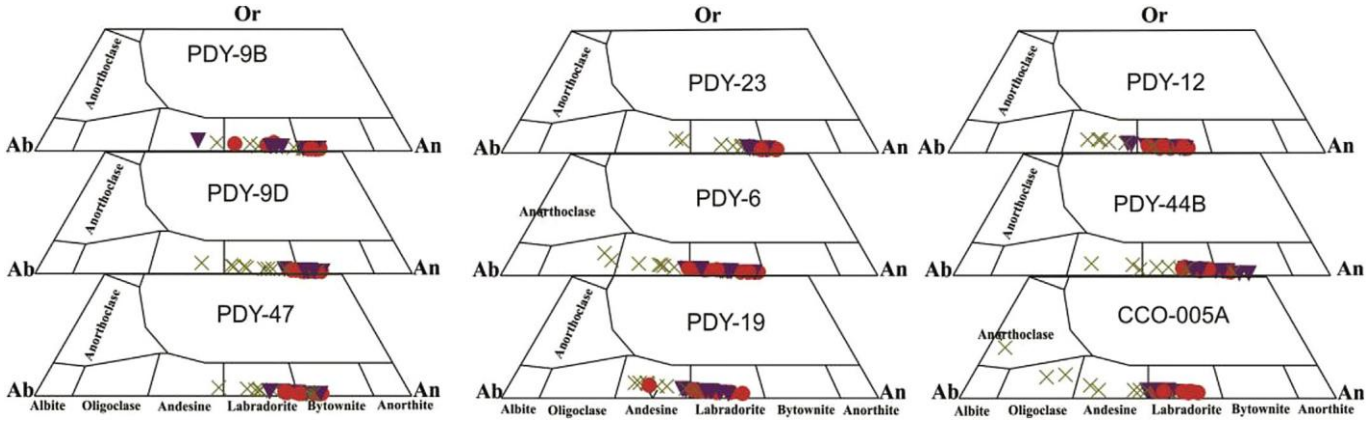

Fig. 8. Compositional Variation of plagioclase of the hypabyssal bodies studied according Or-Ab-In diagram Deer et al. (2003). Circle - center; inverted triangle - the intermediate region; crossed lines - edge of the grains analyzed.

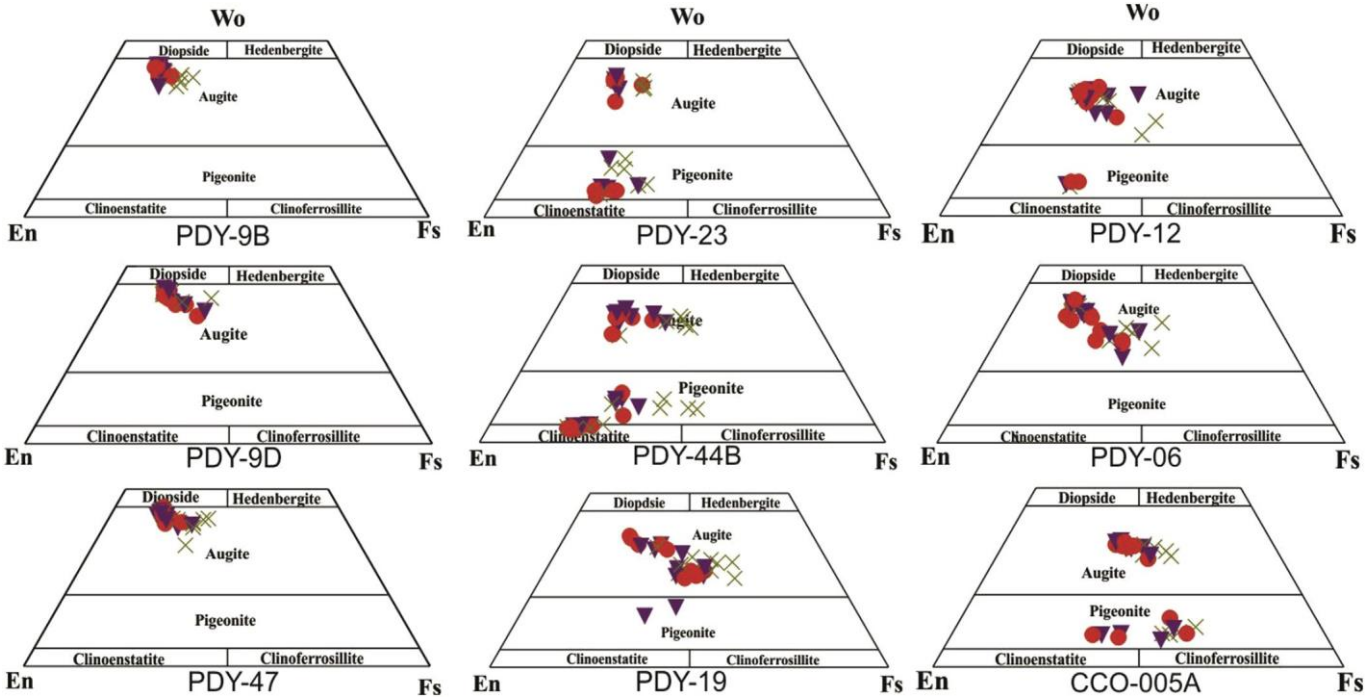

Fig. 9. Compositional variation of pyroxenes for hypabyssal bodies studied according to the ternary diagram (Wo-En-Fs) Morimoto (1988). Circle - center; inverted triangle - the intermediate region; crossed lines - edge of the grains analyzed.

4.2.3.2. *Clinopyroxenes*. The clinopyroxenes are classified as calcium pyroxenes, according to the QUAD diagram (Ca Mg Fe2þ) e J (2Na) of Morinoto (1988). Based on this separation, the Quad field clinopyroxenes were plotted in the Wo-En-Fs diagram (wollastonite e enstatite e ferrossilite) (Fig. 9). The pyroxenes are predominantly augite, both in the core and the edges of the crystals, ranging from $Wo_{39.65}En_{47.10}Fs_{13.25}$ to $Wo_{26.57}En_{34.19}Fs_{39.33}$ in sample PDY-6; $Wo_{42.72}En_{46.29}Fs_{10.99}$ to $Wo_{39.77}En_{38.51}Fs_{21.72}$ in sample PDY-9B; $Wo_{43.59}En_{44.17}Fs_{12.24}$ to $Wo_{37.39}En_{37.20}$ $Fs_{25.41}$ in sample PDY-9D; $Wo_{35.21}En_{48.03}Fs_{16.76}$ to $Wo_{27.11}En_{32.92}Fs_{39.96}$ in sample PDY-12; $Wo_{37.75}En_{45.99}Fs_{16.25}$ to $Wo_{25.52}En_{25.69}Fs_{48.80}$ in sample PDY-19; $Wo_{39.46}En_{48.13}Fs_{12.40}$ to $Wo_{36.32}En_{42.02}Fs_{21.06}$ in sample PDY-23; $Wo_{36.57}En_{48.43}Fs_{14.99}$ to $Wo_{32.50}En_{31.61}Fs_{35.89}$ in sample PDY-44B; $Wo_{44.29}En_{44.51}Fs_{11.20}$ to $Wo_{41.91}En_{33.54}Fs_{24.55}$ in sample PDY-47 and $Wo_{35.10}En_{38.03}Fs_{26.87}$ to $Wo_{30.86}En_{26.68}Fs_{42.46}$ in sample CCO-005A. Zoning is unremarkable and defined by the depletion of MgO, mainly followed by enrichment in FeO and subordinately in CaO from the crystal core to the edges.

Pigeonite occurs in samples PDY-12 ($Wo_{9.63}En_{64.29}Fs_{26.86}$ to $Wo_{8.30}En_{64.29}Fs_{29.61}$), PDY-19 ($Wo_{17.08}En_{44.81}Fs_{31.49}$ to $Wo_{14.65}En_{53.85}Fs_{38.10}$), PDY-23 ($Wo_{16.64}En_{60.97}Fs_{22.40}$ to $Wo_{9.27}En_{55.24}Fs_{35.49}$), PDY-44B ($Wo_{10.72}En_{61.98}Fs_{27.29}$ to $Wo_{9.13}En_{41.95}Fs_{48.92}$) and CCO-005A ($Wo_{13.56}En_{56.54}Fs_{34.47}$ to $Wo_{11.26}En_{30.37}Fs_{58.41}$), more abundant in the last three.

4.2.3.3. *Orthopyroxene*. Orthopyroxene is abundantly found in only one sample (PDY-44B). It is classified as clinoenstatite, with values ranging from $Wo_{4.06}En_{76.43}Fs_{19.51}$ to $Wo_{4.81}$ $En_{67.33}Fs$ $_{19.51.}$

4.2.3.4. *Olivine*. Olivine is an essential phase, exclusively in samples PDY-9B, PDY-9D, PDY-47 and PDY-23, SSOT, with average contents of Fo84, Fo82, Fo85 and Fo75 respectively, with no significant zonation (Fig. 10).

4.3. *Lithochemistry and relation to chemostratigraphic units*

The analyzed samples were divided according to the type of host rocks. The intrusive dikes in the effusive volcanic units of the FSG were separated according to the lithofacies associations used to hierarchize the flows in the south hinge of the Torres Syncline

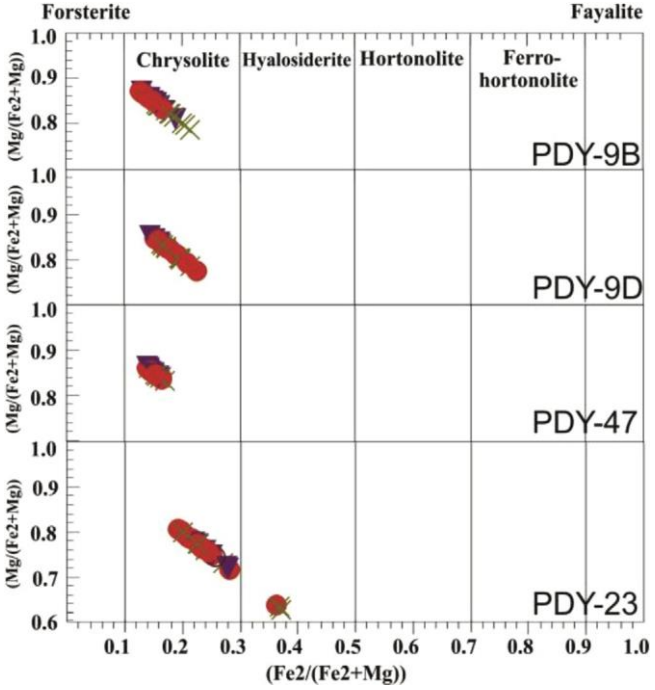

Fig. 10. Compositional Variation of olivine of SSOT type. Circle - center; inverted triangle - the intermediate region; crossed lines - edge of the grains analyzed.

Table 1
Lithochemical results of representative samples of dikes for major elements (wt.%), trace and REE (ppm). *SSOT.

Samples	PDY-9B*	PDY-9D*	PDY-47*	PDY15	PDY-16	PDY-18	PDY-20C	PDY-12B	PDY-19C	PDY-22C
Host rocks	Pahoehoe ponded	Pahoehoe ponded	Pahoehoe ponded	Pahoehoe ponded	Pahoehoe ponded	Pahoehoe ponded	Pahoehoe ponded	Compound pahoehoe	Compound pahoehoe	Compound pahoehoe
SiO_2	47.76	48.12	47.30	50.92	52.96	51.74	50.74	51.33	52.55	55.51
Al_2O_3	14.12	14.94	15.23	13.54	13.41	13.65	13.71	13.64	13.23	13.45
FeOtot	9.71	9.66	9.58	11.16	10.93	11.56	11.56	12.33	12.71	10.28
MnO	0.17	0.17	0.16	0.28	0.23	0.25	0.17	0.21	0.2	0.15
MgO	10.66	8.58	7.75	5.89	5.4	5.12	5.64	5.79	4.84	6.90
CaO	10.4	10.9	11.11	8.58	8.44	9.07	6.47	10.04	8.73	7.15
Na_2O	1.96	2.15	2.14	2.26	2.2	2.39	3.22	2.62	2.71	2.04
K_2O	0.4	0.48	0.56	1.78	1.3	0.96	1.83	0.95	1.34	1.76
TiO_2	1.28	1.31	1.31	1.38	1.38	1.41	1.45	1.39	1.52	1.00
P_2O_5	0.19	0.18	0.18	0.16	0.16	0.17	0.17	0.15	0.16	0.12
LOI	1.8	2.1	3.2	2.5	2.1	2.1	3.4	0.1	0.3	1.3
Total	99.69	99.71	99.69	99.74	99.72	99.71	99.69	99.74	99.75	99.76
Rb	6.9	7.8	8.5	42.3	20.2	16.1	54.6	22.1	34.4	55.2
Ba	264	310	325	260	537	383	724	269	339	322
Sr	321	350	357.9	208	244	401	234	212	225	152.5
Ga	14	14.2	15.8	19	19.2	19.3	18.2	17.5	18.8	15.9
Zr	82.5	97.6	116.4	138.9	141.1	148.1	148.2	122.7	151.7	142.9
Y	18.5	18.5	19.1	26.6	27.8	30.2	27.8	28	31.9	23.1
Nb	3.4	4.1	5.9	10.1	9.6	10.9	10.7	7.2	8.6	9.4
Sc	35	36	37	33	34	34	35	40	36	33
V	261	270	287	359	355	363	378	373	387	238
Co	51.2	47.3	50.3	37.6	37.2	41.3	39.8	45.1	43.3	39.5
Ni	250	139	151.2	33	35	28	35	39	21	39.5
Cu	95	95	85.5	157	149	156	166	165	106	106
Zn	45	48	49	57	55	52	73	43	59	33
La	10.1	10,6	12.3	21.3	19.8	22.6	22.7	15.8	21.5	23.6
Ce	23.6	26.5	27.2	45.2	42	47.1	48.1	34.3	44.2	48.3
Pr	3.1	3.4	3.60	5.3	4.9	5.6	5.7	4.2	5.4	5.56
Nd	14.1	15.2	15.4	21.1	20.2	22.7	23	18.3	22.2	22.5
Sm	3.4	3.7	3.77	5.1	4.8	5.5	5.3	4.2	5.4	4.64
Eu	1.22	1.25	1.43	1.34	1.3	1.48	1.5	1.35	1.56	1.20
Gd	3.75	4.0	4.31	5.38	5.55	5.81	5.8	4.98	6.12	4.81
Tb	0.62	0.64	0.67	0.9	0.89	0.96	0.96	0.88	1.02	0.75
Dy	3.59	3.71	3.80	5.35	5.17	5.66	5.8	5.22	5.89	4.20
Ho	0.67	0.71	0.78	1.13	1.09	1.2	1.27	1,1	1.24	0.90
Er	2.02	1.88	2.14	2.98	2.88	3.22	3.32	3.19	3.48	2.64
Tm	0.28	0.29	0.29	0.46	0.45	0.50	0.51	0.48	0.54	0.40
Yb	1.6	1.71	1.93	2.83	2.96	3.05	3.31	2.93	3.5	2.41
Lu	0.25	0.26	0.29	0.43	0.43	0.46	0.49	0,44	0.52	0.38
Hf	2.2	2.5	3.1	4.0	3.7	4.3	4.1	3.4	4.1	4.1
Ta	0.3	0.3	0.3	0.7	0.7	0.7	0.6	0.4	0.6	0.5
Pb	0.6	0.9	1.4	7.6	5.2	7.6	8.7	1.1	2.1	3.2
Th	0.6	0.7	0.8	5.1	4.9	5.0	5.4	2.7	4.2	7.1
U	<0.1	0.1	<0.1	1.5	1.5	1.4	1.7	0.6	0.7	0.8
Q	0.00	0.00	0.00	0.00	5.03	3.07	0.00	0.00	1.31	11.7
Or	2.36	2.84	3.31	10.52	7.68	5.67	10.81	5.61	7.92	15.13
Ab	16.58	18.19	18.11	19.12	18.62	20.22	27.25	22.17	22.93	21.92
An	28.55	29.7	30.3	21.54	22.88	23.68	17.55	22.65	19.98	14.92
Di	17.88	19.15	19.58	16.76	15.16	17.13	11.42	22.03	18.91	8.90
Hy	13.85	12.47	9.49	25.01	24.09	23.51	17.16	19.86	23.71	19.87
Ol	14.61	11.28	11.68	0.02	0.00	0.00	7.66	3.16	1.31	0.00

Samples	PDY-6	PDY-38A	PSJ-023B	PDY-43A	PDY-7	PDY-10	PDY-13A	PDY-25	PDY-50A	PDY-51B
Host rocks	Rubbly	Rubbly	Acidic flows	Acidic flows	Sedimentary rocks	Sedimentary rocks	Sedimentary rocks	Sedimentary rocks	Sedimentary rocks	Sedimentary rocks
SiO_2	52.22	52.55	53.60	53.97	51.69	52.53	53.17	52.87	53.90	51.50
Al_2O_3	13.13	13.07	12.62	13.14	13.26	14.52	13.09	14.7	12.33	13.63
FeOtot	12.05	12.75	13.30	11.70	12.46	10.64	13.37	9.77	14.13	12.23
MnO	0.2	0.24	0.31	0.19	0.17	0.18	0.18	0.16	0.22	0.19
MgO	5.26	4.96	4.01	4.76	5.37	5.71	3.24	5.82	3.26	4.71
CaO	9.32	9.26	7.45	8.07	9.45	9.08	4.61	8.58	7.11	7.77
Na_2O	2.46	2.62	2.74	2.46	2.66	2.43	2.8	2.69	2.90	2.66
K2O	1.25	1.05	1.39	1.60	0.97	1.33	2.61	1.55	1.73	1.51
TiO_2	1.37	1.45	1.84	1.24	1.41	1.15	1.83	1.3	1.88	1.47
P_2O_5	0.19	0.13	0.22	0.14	0.16	0.15	0.25	0.18	0.27	0.19
LOI	0.9	0.2	0.70	1.2	0.7	0.7	3.0	1.0	0.4	2.5
Total	99.74	99.76	99.72	99.77	99.74	99.64	99.66	99.74	99.72	99.71
Rb	46.5	40.4	48.5	49.6	28.9	34.5	91.4	47.3	66.1	46.2

(*continued on next page*)

Table 1 (*continued*)

Samples	PDY-6	PDY-38A	PSJ-023B	PDY-43A	PDY-7	PDY-10	PDY-13A	PDY-25	PDY-50A	PDY-51B
Host rocks	Rubbly	Rubbly	Acidic flows	Acidic flows	Sedimentary rocks	Sedimentary rocks	Sedimentary rocks	Sedimentary rocks	Sedimentary rocks	Sedimentary rocks
Ba	340	178	328	284	361	1310	1025	380	320	456
Sr	211	174	195.8	187.7	225	292	238	294	178	232.2
Ga	20.1	17	19.0	18.6	18.3	17.9	21.6	17.2	20.3	19.3
Zr	147.9	114.3	185.3	124.1	134.4	136.2	187.8	161.7	174.3	155.0
Y	32.1	32.6	42.6	23.1	32.2	26.1	54.5	25.7	38.4	32.1
Nb	9.7	5.2	10.5	8.5	8.7	8.3	13.3	13.2	11.4	12.4
Sc	38	40	37	41	41	36	33	34	39	36
V	381	362	491	336	398	288	436	275	501	364
Co	46.2	47.8	44.0	43.2	44.3	41.5	38.1	39.3	40.7	42.1
Ni	39	20	37	15.1	17	48	<20	17	7.2	24.2
Cu	97	192	208.5	52.3	160	63	166	35	202.1	135.5
Zn	62	48	68	48	66	43	116	40	73	80
La	21.6	10.7	21.5	17.9	18.7	21.5	38.4	24.1	22.6	22.8
Ce	43.4	24.7	44.7	35.6	37.6	44.6	62.9	48.3	46.0	44.8
Pr	5.6	3.5	5.93	4.71	4.8	5.4	9.9	6.1	6.10	5.85
Nd	24.9	16.3	24.6	18.1	20.5	22	42.1	23.7	26.1	23.5
Sm	5.5	4.2	6.5	4.6	4.9	4.6	10.1	5.0	6.4	5.5
Eu	1.55	1.39	1.81	1.26	1.53	1.38	2,78	1.39	1.65	1.54
Gd	5.78	5.22	7.08	4.57	5.58	4.86	11.14	5.22	7.09	5.91
Tb	0.98	0.97	1.22	0.77	0.99	0.78	1.86	0.85	1.17	0.97
Dy	6.14	6.11	7.43	4.58	5.6	4.6	10.92	4.81	6.93	5.52
Ho	1.2	1.27	1.46	0.91	1.2	0.98	2.2	0.96	1.49	1.09
Er	3.58	3.49	4.12	2.64	3.65	2.86	6.46	2.78	4.26	3.31
Tm	0.5	0.52	0.61	0.39	0.51	0.42	0.96	0.44	0.64	0.47
Yb	3.27	3.18	3.69	2.44	3.48	2.55	6.19	2.53	4.06	3.22
Lu	0.48	0.48	0.62	0.38	0.48	0.38	0.86	0.42	0.60	0.48
Hf	3.8	3.4	5.1	3.1	4.1	3.8	5.0	4.4	4.7	4.1
Ta	0.7	0.4	0.6	0.7	0.5	0.4	0.9	0.7	1.0	0.7
Pb	2.3	0.9	1.9	2.4	1.4	1.8	3	2.6	1.6	2.2
Th	4.2	1.7	4.6	4.6	3.3	4.3	7.1	4.5	6.4	5.6
U	1.0	<0.1	0.3	1.2	0.6	0.7	2.0	<0.1	1.8	1.1
Q	1.76	1.86	4.76	4.61	0.44	1.65	4.11	1.23	4.34	1.35
Or	7.39	6.2	8.21	9.46	5.73	7.86	15.42	9.16	10.22	8.92
Ab	20.82	22.17	23.18	20.82	22.51	20.56	23.69	22.76	24.54	22.51
An	21.09	18.03	20.09	15.52	21.38	24.78	15.44	27.69	15.52	20.79
Di	20.18	20.55	14.97	16.12	20.67	16.38	5.20	15.03	15.51	14.06
Hy	23.20	23.45	24.34	23.52	23.85	24.02	27.27	23.12	23.43	25.02
Ol	0.00	0.00	0.00	0.00	0.00	0.00	0.00	0.00	0.00	0.00

(Barreto et al., 2014; Rossetti et al., 2014; Waichel et al., 2012). The concentrations of major, trace and REE is shown in Tables 1 and 2. The intrusive dikes and sills in sedimentary rocks in the south edge of the Paraná Basin were identified with a single symbol.

The investigated sills are chemically equivalent to basaltic andesites, with SiO_2 concentrations between 50.84 and 55.39% and alkali concentrations between 5.10 and 3.04% (Fig. 11A). The dikes are classified as basalts, basaltic andesites and trachyandesites in the TAS diagram (Le Bas et al., 1986), with SiO_2 concentrations of 47.30e55.51% and alkali concentrations of 5.41%e2.36%. The tholeiitic affinity is shown in the SiO_2 versus FeO_{tot}/MgO diagram (Miyashiro, 1978). In low-mobility trace element diagrams (Winchester and Floyd, 1977), the samples are located in the basalt and basaltic andesite fields (Fig. 11C).

In general, it is found that the less differentiated compositions tend to be intrusive in the ponded pahoehoe volcanic units, while the more evolved ones occur mainly in compound pahoehoe lava flows. The behavior of the intrusive dikes in the sedimentary rocks is similar to that observed in the distribution of sills.

The subalkaline/tholeiitic affinity of the magmatism is confirmed in the AFM diagram, combined with low Al_2O_3 values (Middlemost, 1975; Wilson, 1989). The Fe enrichment of these rocks explains their position in the field of basalts and high-Fe tholeiitic andesites in Jensen's diagram (1976), despite several samples plotting in the high-Mg tholeiitic basalt field (Fig. 12).

With the use of MgO as the differentiation index to establish the behavior of major and trace elements with the magmatism evolution of the hypabyssal rocks (Figs. 13 and 14), the Al_2O_3 and CaO contents tend to decrease with the fall in MgO contents combined with the increase of SiO_2, Na_2O, K_2O, P_2O_5, FeO_t and TiO_2. These patterns suggest that the magmatism evolution was primarily controlled by the fractionation of plagioclase, augite and titanomagnetite. The olivine fractionation must have occurred only in the less evolved rocks. These findings are consistent with the petrogenetic interpretations suggested by Bellieni et al. (1984) and Piccirillo et al. (1989).

An increase in the contents of Ba, Rb, Zr, Y, Nb and Th is observed with the decrease in Mg contents. Nickel, by contrast, has a positive correlation with MgO, suggesting the extraction of this element in mafic phases. This behavior can be explained by magmatic differentiation processes. The low contents of Ni and MgO values < 6% indicate a relatively evolved condition of these magmas. Unlike the samples with Ni contents of 139e250 ppm and MgO values of 8.6e10.7%, which correspond to SSOT, showing a less evolved source of the magma.

The samples, when normalized to primitive mantle standard (McDonough and Sun, 1995), show enrichment in incompatible elements, with negative Nb and Ta anomalies (Fig. 16A). According to some authors, this pattern may suggest the presence of some residual phase rich in Nb and Ta, during the partial melting

Table 2
Lithochemical results of representative samples of sills for major elements (wt.%), trace and REE (ppm).

Samples	PDY-26	PDY-28	PDY-41	PDY-44A	PDY-46A	PDY-48A	PDY-49C	CCO-005B	CCO-029B	CCO-011-1B
SiO_2	50.96	50.84	53.42	53.63	55.39	54.16	54.00	54.49	53.92	52.79
Al_2O_3	15.1	15.35	13.40	14.83	14.68	12.37	12.37	12.47	13.09	13.66
FeOtot	9.73	9.56	11.78	9.37	8.87	14.02	14.00	13.20	14.11	11.60
MnO	0.15	0.16	0.21	0.18	0.15	0.22	0.22	0.18	0.21	0.22
MgO	6.9	7.07	5.33	5.88	4.70	3.29	3.35	2.83	3.72	5.55
CaO	9.98	10.01	9.03	8.12	7.66	7.11	7.20	6.45	7.37	9.12
Na_2O	1.95	1.96	2.33	2.37	2.44	2.78	2.75	2.84	2.70	2.21
K_2O	1.11	1.08	0.95	1.74	2.09	1.59	1.64	2.26	1.91	1.34
TiO_2	1.19	1.21	1.33	1.31	1.21	1.87	1.86	1.92	1.64	1.31
P_2O_5	0.16	0.16	0.13	0.16	0.23	0.26	0.26	0.21	0.19	0.14
LOI	1.3	1.2	0.5	1.1	1.3	0.5	0.5	1.5	0.9	0.5
Total	99.70	99.71	99.72	99.74	99.75	99.72	99.72	98.31	98.86	98.48
Rb	32.0	31.4	35.9	48.0	65.8	57.4	63.1	81.9	70.7	44.2
Ba	323	332	312	410	481	310	330	516	433	284
Sr	283	281	198.8	228.6	266.5	163.4	162.5	238	217	196
Ga	16,8	16.7	18.2	18.3	19.0	19.7	20.9	21.1	20.1	17.6
Zr	147.8	247.6	126.6	178.2	187.5	175.4	177.0	184.5	160.4	117.8
Y	22.5	25	23.5	27.6	23.5	38.9	37.5	34.9	34.4	23.1
Nb	11.9	12.4	7.7	14.1	16.4	11.9	11.9	12.9	11.4	8.5
Sc	34	34	41	32	30	39	38	39	40	43
V	274	273	415	253	239	498	494	553	433	373
Co	46.6	44,3	42.3	37.8	35.0	41.5	41.8	43.1	48.0	45.9
Ni	31	32	8.2	25.0	10.1	7.0	9.1	20	28	52
Cu	240	88	139.2	32.7	15.9	208.7	202.0	142	176.2	138
Zn	28	30	39	23	30	60	71	51	53	42
La	19.3	23.4	17.8	26.3	30.0	23.0	22.7	27.8	25.5	16
Ce	39,9	46.6	36.8	51.1	57.2	46.3	45.7	59.7	52.1	36.3
Pr	5.1	5.9	4.80	6.63	7.33	5.94	5.96	7.3	6.84	4.4
Nd	20	24.5	18.8	25.3	26.8	24.7	24.5	31.2	27.8	18.4
Sm	4.5	5.2	4.28	5.48	5.91	5.83	6.27	6.3	6.12	4.2
Eu	1.29	1.35	1.23	1.50	1.47	1.68	1.67	1.62	1.53	1.17
Gd	4.53	4.74	4.74	5.71	5.46	6.87	6.94	6.38	6.20	4.32
Tb	0.76	0.79	0.77	0.88	0.86	1.18	1.17	1.08	1.05	0.74
Dy	4.47	4.69	4.51	4.89	4.80	7.00	6.97	6.27	5.73	4.31
Ho	0.8	0.88	0.91	1.05	0.96	1.53	1.48	1.27	1.17	0.89
Er	2.48	2.43	2,63	2.95	2.69	4.26	4.23	3.71	3.45	2.54
Tm	0.35	0.38	0.39	0.45	0.40	0.62	0.59	0.8	0.52	0.32
Yb	2.25	2.36	2.49	2.98	2.47	4.04	3.98	3.35	3.20	2.3
Lu	0.37	0.36	0.38	0.40	0.37	0.62	0.60	0.52	0.48	0.35
Hf	3.9	6.8	3.4	4.6	4.6	4.4	4.5	5.0	4.7	3.3
Ta	0.6	0.7	0.5	0.7	1.1	0.9	0.8	0.9	0.8	0.5
Pb	2.2	2.1	1.2	2.6	2.5	2.2	1.7	2.6	1.1	2.2
Th	3.4	4.4	4.5	6.4	6.7	6.3	6.1	8.9	7.2	5.0
U	<0.1	<0.1	1.1	0.8	1.3	1.7	2.1	1.8	1.3	1.1
Q	0.9	0.54	4.7	3.56	6.67	5.63	5.28	5.54	3.07	2.97
Or	6.56	6.38	5.61	10.28	12.35	9.40	9.69	13.36	11.29	7.92
Ab	16.50	16.58	19.72	20.05	20.65	23.52	23.27	24.03	22.85	18.70
An	29.17	29.90	23.30	24.69	22.93	16.58	16.57	14.60	17.96	23.40
Di	16.06	15.56	17.42	12.19	11.46	14.64	15.03	13.90	14.95	17.63
Hy	25.43	25.79	24.35	23.98	20.55	23.76	23.70	21.32	25.22	24.53
Ol	0.00	0.00	0.00	0.00	0.00	0.00	0.00	0.00	0.00	0.00

processes, or even be the result of crustal contamination (Wilson, 1989; Piccirillo et al., 1989; Hawkesworth, 1984). The negative Sr anomaly indicates the plagioclase fractionation in the evolution of the intrusive bodies. The patterns observed in these multi-element diagrams and the LILE behavior (*Large Ion Lithophile Elements*) (K, Rb, Ba, Sr, Pb), combined with low levels of HFSE (*High Field Strength Elements)* (Nb, Ta, Zr, Hf, Ti, P) are very similar to those of intraplate tholeiitic basalts. A slight increase in the fractionation of some elements is observed, especially heavy rare earth elements (REE) with the increase in differentiation.

The SSOT dikes, when normalized to the C1 chondrite standard (McDonough and Sun, 1995), show relatively low REE patterns (S_{REE} ¼ 82e78) and slight enrichment in LREE relative to HREE (La_N/Yb_N ¼ 3.7e3.9). There is very little fractionation between light REEs (La_N/Sm_N ¼ 1.6e1.8) and heavy REEs (Tb_N/Yb_N ¼ 1.5e1.6) and they are devoid of negative Eu anomaly (Eu/Eu^*_N ¼ 1.04) (Fig. 16B).

The SST dikes show moderate patterns of these elements (S_{REE} ¼ 82e207) and they are characterized by a slight enrichment in light REEs relative to heavy REEs (La_N/Yb_N ¼ 2.0e6.6). They have a slight fractionation between light REEs (La_N/Sm_N ¼ 1.4e2.8) and heavy REEs (Tb_N/Yb_N ¼ 1.2e1.5) (Fig. 16B). Mild negative Eu anomalies are observed (Eu/Eu^*_N¼ 0.83), suggesting plagioclase fractionation (Wilson, 1989; Rollinson, 1993). The patterns shown by the intrusions are similar to those shown by Peate et al. (1992, 1997, 1999) and Marques et al. (1989) for tholeiitic basalts of large continental provinces such as the Paraná Igneous Province. The sills follow the same trend, with moderate REE patterns (S_{REE} ¼ 90e157), light REE fractionation (La_N/Sm_N ¼ 2.2e3.1), heavy REE fractionation (Tb_N/Yb_N ¼ 1.4e1.6), enrichment of light REE relative to heavy REE (La_N/Yb_N ¼ 3.8e6.6) and negative Eu anomaly (Eu/Eu^*_N¼0.81).

The most SST dikes and sills exhibit CIPW normative quartz

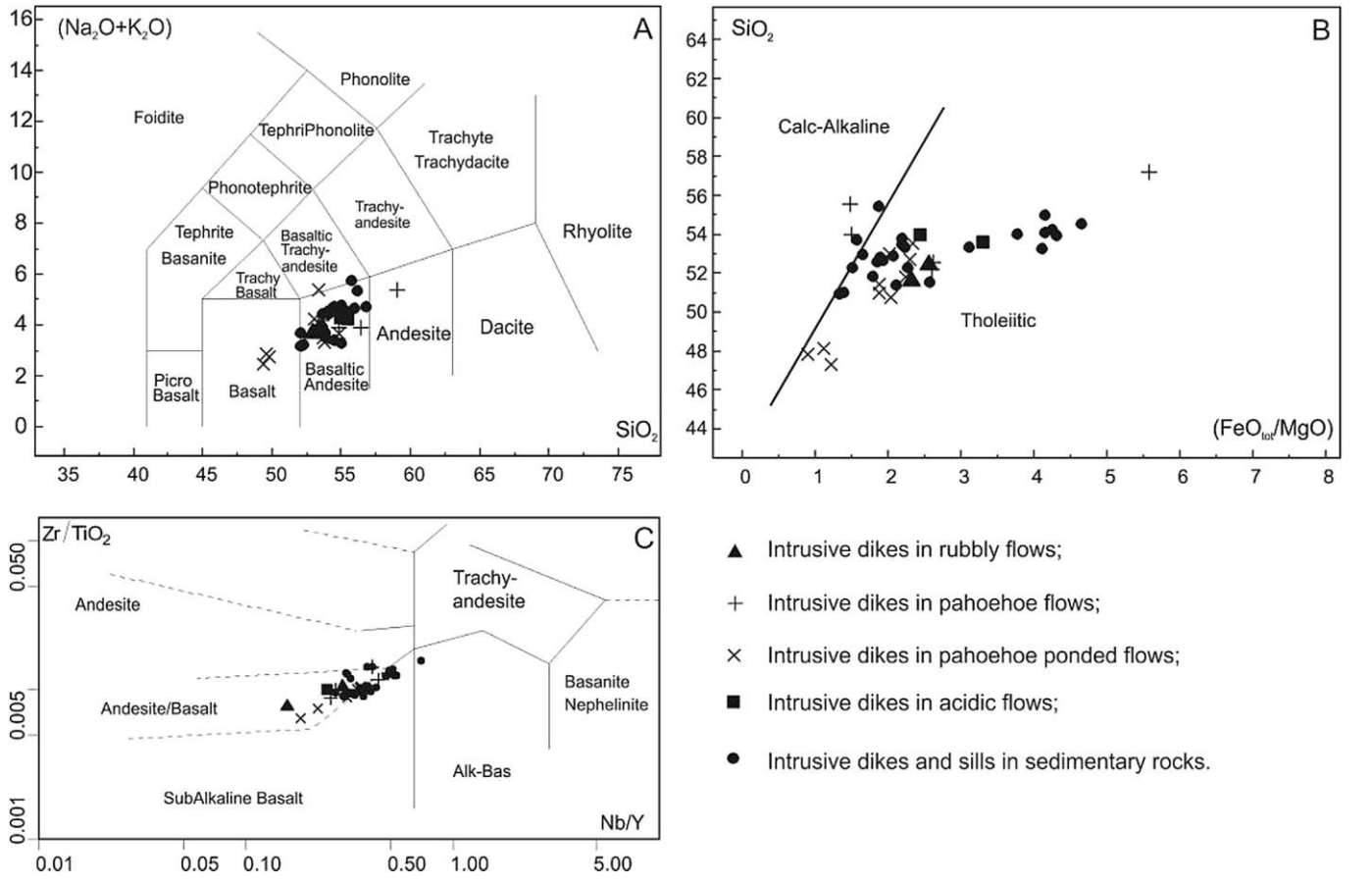

Fig. 11. Classification Diagrams of dikes and sills studied. A) TAS (Le Bas et al., 1986); B) Diagram SiO_2 versus FeO_{tot}/MgO (Miyashiro, 1978); C) Zr/TiO2 versus Nb/Y (Winchester and Floyd., 1977).

from 0.54 to 11.7 wt.%, diopside from 8.9 to 17.63% and hypersthene from 19.87 to 27.27 wt.%. These rocks are classified as quartz tholeiites. Some SST dikes exhibit CIPW normative olivine from 0.02 to 7.66, diopside from 11.42 to 16.76 wt.% and hypersthene from 17.16 to 25.01 wt.%, classified as olivine tholeiites. All SSOT dikes display CIPW normative olivine from 11.28 to 14.61 wt.%, diopside from 17.88 to 19.58 wt.% and hypersthene from 9.49 to 13.85 wt.% and are classified as olivine tholeiites.

All studied samples have TiO_2 concentrations lower than 2%, allowing to relate them to the low-Ti magmas, characteristic of the southern sub-province of the Paraná Igneous Province. According to several authors (Mantovani et al., 1985; Marques et al., 1989; Peate et al., 1992), the low-Ti group can be subdivided into three different subgroups, or magma-types, called Ribeira, Esmeralda and Gramado, according to criteria based on TiO_2 and SiO_2 concentrations, and other incompatible trace elements.

The intrusive body samples show Sr contents between 152 and 321 ppm, Zr/Y between 4.1 and 5.9, Ti/Zr from 61 to 94, and Ti/Y between 258 and 486, suggesting a correlation with the Gramado magma. By comparing the trace elements and REE data of the low-TiO_2 magma types of the Serra Geral Formation (Peate et al., 1992, 1997) in Rio Grande do Sul, much similarity can be seen with the geochemical signatures of the dolerites in the region. When compared to the low-Ti magma-types of Etendeka Province, the SST dikes and sills are geochemically equivalent to the Tafelberg-type basalts (Ewart et al., 1984; Milner et al., 1994) and the SSOT dikes are geochemically similar to Tafelkop-type basalts (Fig. 15).

5. Discussion

The magma emplacement mechanism conditioned by stratigraphic and tectonic factors, along preexisting fractures (Billings, 1972) is widely accepted in Brazil. For some authors, the presence of ancient fault systems in the Pre-Cambrian basement is considered a primary factor for the occurrence of magmatic Phanerozoic events (Almeida, 1986; Ricommini, 1997; Ricommini et al., 2004). These authors assume that the upper crust is highly fractured and the magma pressure is not enough to fracture the host rock. Some authors consider the fracture-filling model an important mechanism for dike intrusions (Delaney et al., 1986; Bear et al., 1994; Delaney and Gartner, 1997; Valentine and Krogh, 2006).

The preferred direction of the investigated symmetrical dikes enclosed in the sedimentary rocks of the Paraná Basin (NE-SW) coincides with the direction of large tectonic structures transverse to the main axis of the Paraná Basin, such as the Leão and Bento Gonçalves tectonic-magmatic lineaments (Zalán et al., 1985). Deckart et al. (1998) suggest that the most important lineaments are linked to triple junction systems, related to extensional processes and intracratonic rifting. The fault systems are deep structures that served as ducts for the Florianópolis and Serra do Mar dike swarms (Almeida, 1986.; Heilbron et al., 2004), parallel to the Brazilian coast (NE-SW) e and the Henties Bay-Outjo dike swarm, Namibian coast, coinciding with the direction of the South Atlantic Ocean opening (Ewart et al., 1984; Trumbull et al., 2004). The intrusive symmetrical dikes in the Serra Geral Formation have NW-

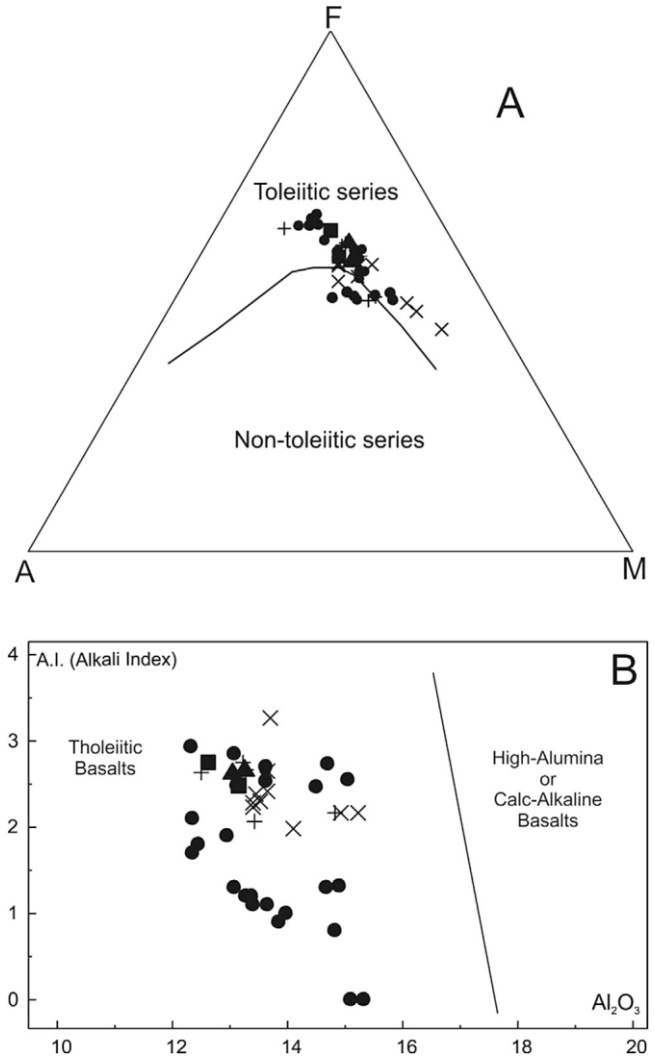

Fig. 12. (A) Diagram of AFM type (Na2O þ K2O) - F (FeOt) - M (MgO), with the dividing line between the fields second Irvine and Baraguar (1971) and (B) Middlemost classification diagram (1975) of dikes and sills studied. For symbol legend see Fig. 11.

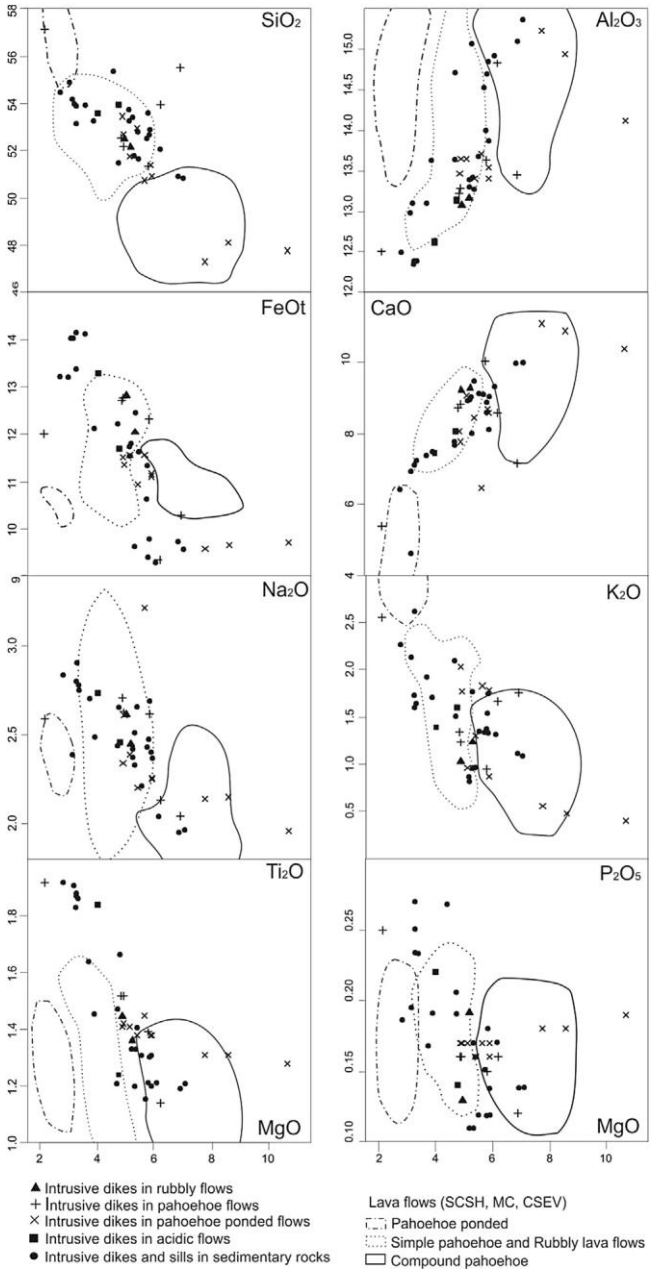

Fig. 13. Binary diagrams displaying major elements variation (wt.%) relative to MgO of the studied rocks. Delimited fields refer to the lavas of the south hinge Torres Syncline (Barreto et al., 2014; Rossetti et al., 2014) of Santa Cruz do Sul/Herveiras (SCSH), Morro da Cruz (MC) and Caxias do Sul/Estancia Velha (CSEV) areas.

SE preferred directions, similar to the directions of Ponta Grossa Arc, Rio Grande Arc and Torres Syncline (Zalán et al., 1985). The arcs are structures that can be recognized by an inflection in the crystalline basement which are associated with staggered faults that downgraded the basin sediments, with some blocks located below the sea level, in the current continental shelf (Fúlfaro et al., 1982). The morphology of asymmetrical dikes and secondary dikes and sills associated with the main intrusions has been attributed to a hydraulic fracture model, with gradients of magmatic depression or regional stress and the magnitude of asymmetry controlled by the fracture length (under pressure) and an effective stress gradient (Pollard and Muller, 1976). For Daniels et al. (2012), who studied the asymmetrical dikes of Swartruggens in South Africa and Rum in Scotland, the extrapolation of data from dikes should be done carefully. The average thickness observed in the dikes was lower than 1 m, and this analysis should not be automatically applied to larger dikes. The application of these results to thicker dikes requires further investigation.

The studied sills intrude the sedimentary rocks on the southern edge of the Paraná Basin, including the Rio Bonito, Irati, Rio do Rastro, Santa Maria and Pirambóia Formations. These formations are stratigraphically older than the Botucatu Formation, which is contemporaneous to the magmatic event that originated the Paraná Igneous Province. For this reason, it is safe to say they cannot be confused with thick flows, despite having all the characteristics of sills.

The intrusive bodies show little diversity characterized by the equigranular fine to very fine texture. The small facies and textural variation may be linked to the shallow depths where the magma crystallized and also the thinness of the magmatic bodies. In general, these rocks are characterized by intergranular and subophitic texture in SST, as evidenced by the fabric formed by plagioclase, clinopyroxene and orthopyroxene, its main mineral components. The ophitic texture is characteristic of SSOT rocks, whose main

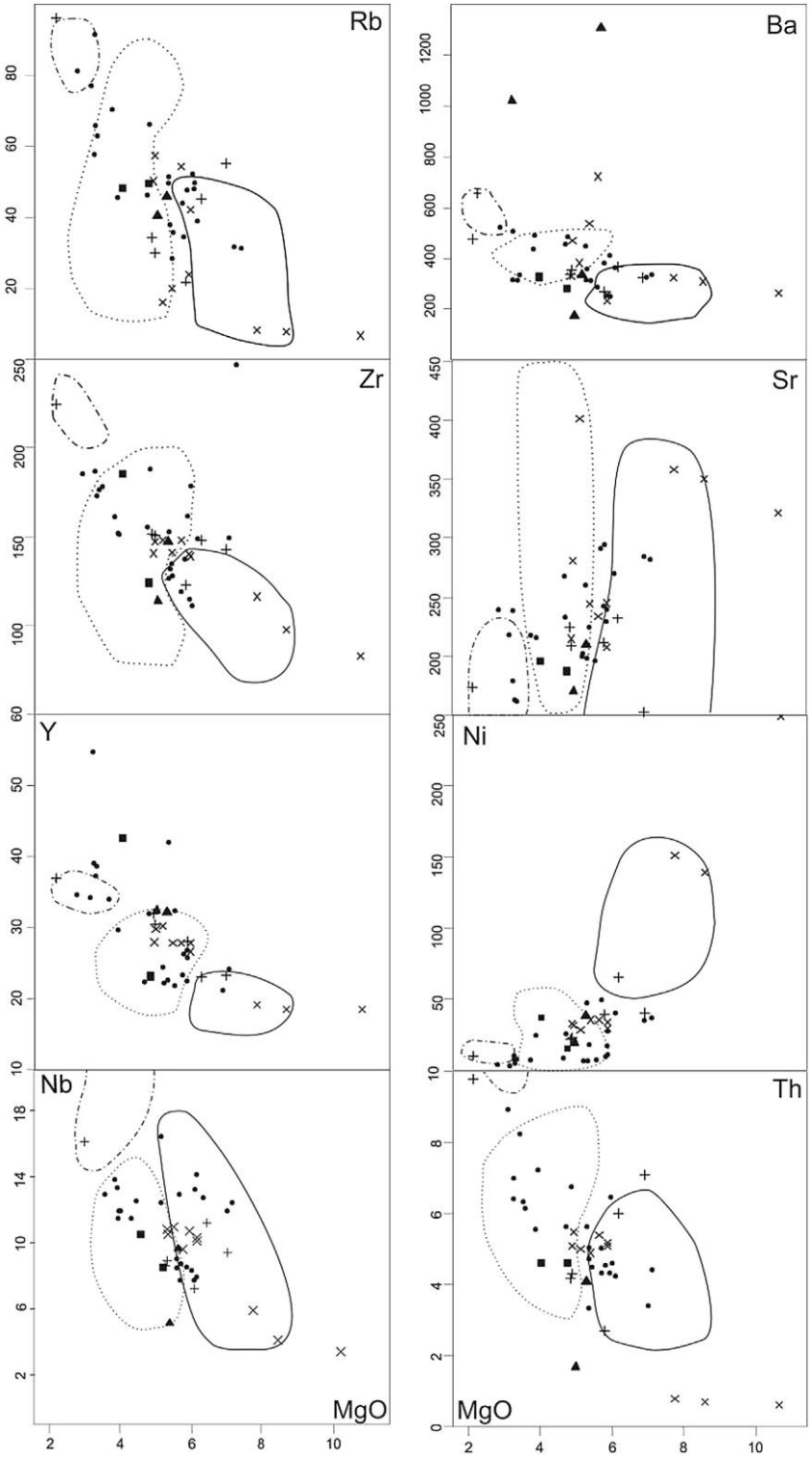

Fig. 14. Binary diagrams displaying trace elements variation (ppm) relative to MgO (wt.%) of the studied rocks. Delimited fields refer to the lavas of the south hinge Torres Syncline (Barreto et al., 2014; Rossetti et al., 2014) of Santa Cruz do Sul/Herveiras (SCSH), Morro da Cruz (MC) and Caxias do Sul/Estancia Velha (CSEV) areas. For symbol legend see Fig. 13.

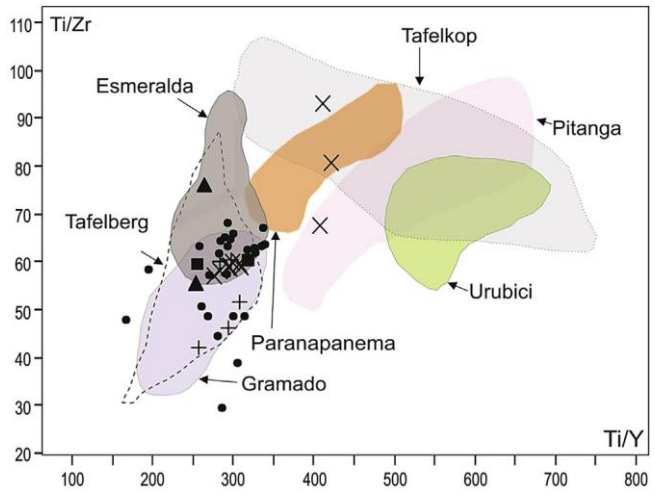

Fig. 15. Binary Diagram displaying Ti/Zr vs. Ti/Y of the studied rocks.shown fields of low-Ti and high-Ti of the Paraná magma-types (Peate et al., 1992, 1997; Turner et al., 1999) and fields of low-Ti of the Etendeka magma-types Ewart et al., 1984; Milner et al., 1994). Legend like Fig. 13.

components are plagioclase, clinopyroxene and olivine. The SSOT mineral chemistry indicates similarity with the central portion of the Lomba Grande Basic Complex with average values of An64-81, $Wo_{42}En_{49}Fs_9$ and Fo74 (Viero and Roisenberg, 1992). It is also similar to the diabase dikes cutting the Doros gabbros, northwestern Namibia, with values of An71-86, $Wo_{37-43}En_{45-50}Fs_{9-14}$ and Fo81-84 (Owen-Smith and Ashwal, 2015b).

The geochemical data show the sub-alkaline nature of the magmatism related to the intrusive bodies, whose tholeiitic affinity may be ascertained by the relationship between alkalis, FeO_t and MgO and the low contents of Al_2O_3.

The SST rocks show low contents of MgO, Cr and Ni, suggesting these rocks were formed by an evolved magma that underwent previous fractionation processes, probably involving olivine and pyroxene. The behavior of major elements in relation to the differentiation index suggests magmatic differentiation processes, involving fractional crystallization mechanisms mainly controlled by the plagioclase and pyroxene fractionation. The patterns observed in multi-element diagrams and the behavior of LILEs, combined with low HFSE contents, show the similar signature of the Continental Basalt Provinces. The positive Pb anomaly observed in the asymmetrical dikes (Fig. 16) is also seen in many samples from the low-Ti Henties Bay-Outjio, False Bay, Garies and Saldahna Bay dike swarms in northwestern Namibia (Trumbull et al., 2007). The rare earth element patterns show moderate values, when normalized to C1 chondrite, and are characterized by a moderate enrichment in light REEs relative to heavy REEs and a weak Eu anomaly, very similar to those of continental tholeiitic basalts, such as the Paraná-Etendeka Igneous Province.

The SSOT rocks exhibit relatively high levels of MgO, Cr and Ni and slightly positive Eu anomaly. They exhibit relatively low REE patterns and weak enrichment of LREEs relative to HREEs. They are similar to some samples from the coarse facies of the Lomba Grande Basic Complex (Viero and Roisenberg, 1992), in addition to having a chemical signature similar to that of intrusions related to the Etendeka Formation in northwestern Namibia, such as the Henties Bay-Outjo and False Bay low-Ti dike swarms with MgO >6% (La_N/Yb_N 2e4) (Duncan et al., 1990; Trumbull et al., 2004; Thompson et al., 2001, 2007), and the Huab River Valley sills (Duncan et al., 1989).

When geochemically compared with the flows according to the lithofacies associations of the south hinge of the Torres Syncline, a similarity is seen between the basal compound pahoehoe lava flows of the SCSH, MC, CSEV areas in SiO_2 contents (46.70e50.56%), alkalis (2.74e4.93%) and MgO (4.38e8.77%) and the SSOT dikes. The simple (sheet) pahoehoe and rubbly lava flows have a geochemical signature similar to the studied TSS bodies with SiO_2 contents between 50.30 and 56.84%, alkali contents of 2.64e5.59% and MgO contents between 2.92 and 5.69% (Figs. 11 and 12). The same similarity can be observed when comparing the major and trace elements between the studied sills and dikes and the types of flows (Figs. 13 and 14).

The stratigraphy of the Gondwana III supersequence in the Torres Syncline is composed by: 1 - Botucatu Paleoerg; 2 e Basic volcanic episode I, composed by compound pahoehoe and interdune ponded pahoehoe lava; 3 e Basic volcanic episode II, mainly composed of simple (sheet) pahoehoe lava; 4 e Acidic volcanic episode I, composed by acidic lava domes; 5 e Basic volcanic episode III, mainly consisting of rubbly lava flows and 6 e Acidic volcanic episode II, consisting of tabular acidic lava flows (Waichel et al., 2012).

In the correlation of the investigated intrusives with these units the SSOT dikes only dissect the ponded pahoehoe lava flows near the Santa Cruz do Sul/Herveiras (SCSH), Morro da Cruz (MC), Caxias do Sul/Estância Velha (CSEV) (Barreto et al., 2014; Rossetti et al., 2014) and Rota do Sol (RTS) areas (Waichel et al., 2012) (Fig. 17). These flows are stratigraphically below the compound pahoehoe lava flows, the only ones rich in olivine and the geochemical signature shows a rock less differentiated than the other flows. The TSS dikes are found dissecting the Botucatu sandstone and the ponded pahoehoe lava flows (asymmetrical dikes) compound pahoehoe, rubbly and acidic episode II flows near the RTS region.

6. Conclusions

The dikes in the south hinge of the Torres Syncline, located in the central-eastern region of the state of Rio Grande do Sulhave preferred NE-SW direction when intruding the sedimentary rocks of the Paraná Basin. This direction coincides with the tectonic-magmatic lineaments related to extensional processes and fault systems that served as ducts for dike swarms parallel to the Brazilian and Namíbia coast. This suggests that these dikes are part of the triple junction system related to the opening of the South Atlantic Ocean. The intrusive dikes in the flows of the Serra Geral Formation have preferred NW-SE directions, similar to the Ponta Grossa and Rio Grande Arcs and the Torres Syncline. This condition suggests that these dikes may have been part of or be caused by one or more geotectonic cycles that originated these structures.

The emplacement process of the asymmetrical dikes, as well as the secondary dikes and sills associated with the main intrusions suggest that they were enclosed under a hydraulic fracture model, since they do not follow a pattern of pre-existing fracture filling.

The emplacement of the sills is concordant with the weakness zones of the sedimentary rocks of the Rio Bonito, Iratí, Rio do Rastro, Pirambóia and Santa Maria Formations, in the south edge of the Paraná Basin.

The whole rock geochemical signature of the SSOT dikes shows similarity with the composition of the Lomba Grande Basic Complex, RS, Brazil and with the basic intrusions of P-MORB affinity with MgO >6% related to the Paraná-Etendeka Igneous Province, in Namibia. It shows the possibility of these dikes being part of a feeder system of this province. The geochemistry of the SST dikes

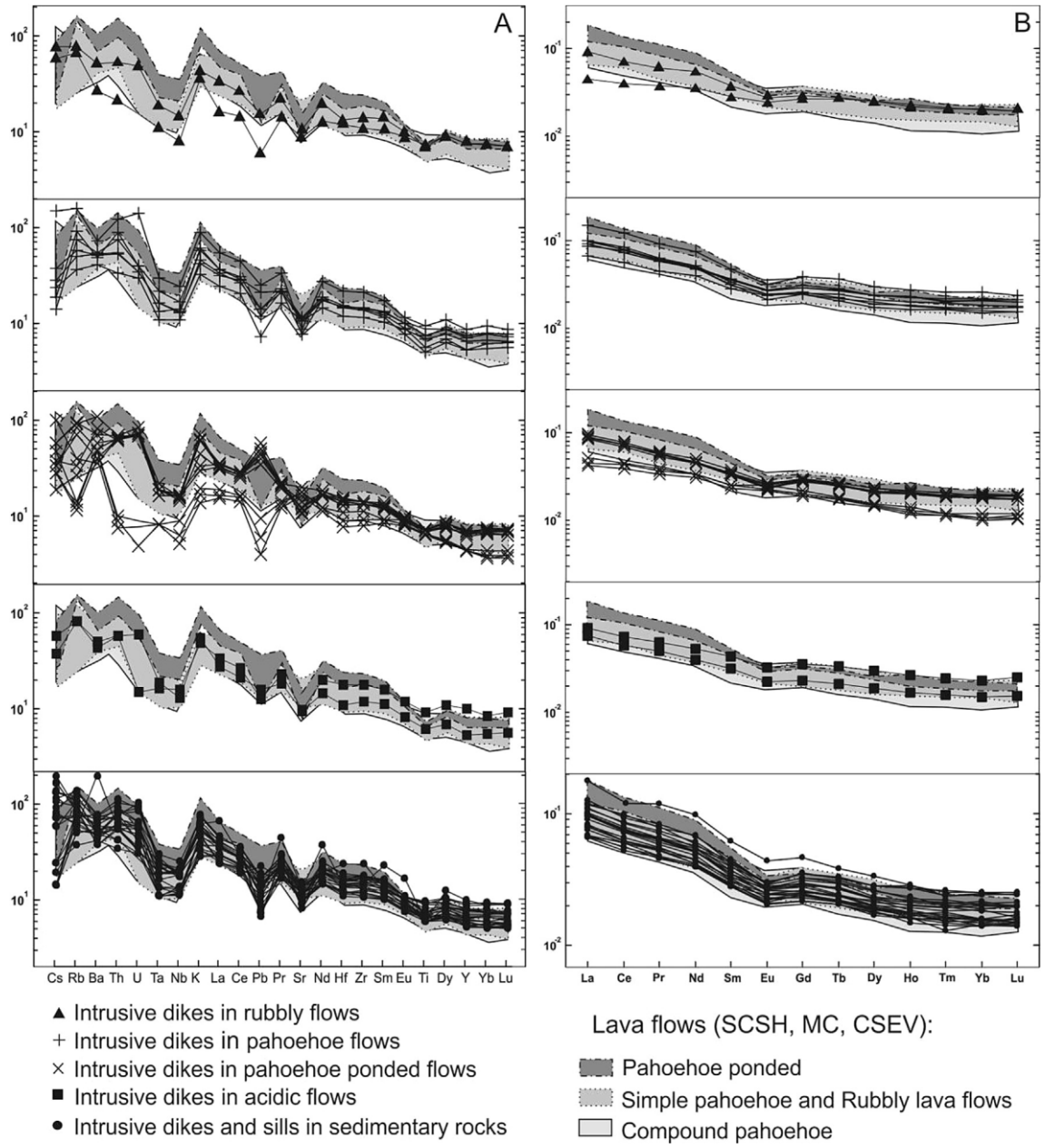

Fig. 16. Trace element abundance (A) and REE patterns (B) normalized to the primitive mantle (McDonough and Sun, 1995) and chondrite C1 of the studied rocks. Delimited fields refer to the lavas of the south hinge Torres Syncline (Barreto et al., 2014; Rossetti et al., 2014) of Santa Cruz do Sul/Herveiras (SCSH), Morro da Cruz (MC) and Caxias do Sul/Estancia Velha (CSEV) areas.

and sills indicates typical characteristics of basaltic andesites and LILE, HFSE and REE patterns similar to the magmatism of low-Ti suites of great continental basaltic provinces, such as the volcanic rocks of the Paraná-Etendeka Igneous Province.

In the correlation of the dikes with the lava flow stratigraphy, the SST dikes intrude in the simple pahoehoe, compound pahoehoe and rubbly lava flows, suggesting that these dikes are part of a feeder system of the basic lava flows stratigraphically positioned above the host lava flows. Also taking into account the geochemical and petrographic similarities, SST dikes were also observed in acidic lava flows at higher altitudes of the south sub-province lava flow package, which may mean that these dikes served as feeders of the basic flows, from which there are no remaining outcrops in the region due to subsequent erosion. The SSOT dikes were found intruding only in ponded pahoehoe lava flows. This aspect suggests that these dikes could be part of a feeder system or a component of the dikes that effectively fed the less differentiated basaltic compound pahoehoe lava flows, stratigraphically found above the host flows.

The study of the intrusions associated with the Continental Basaltic Provinces as feeder systems and contribution for the lithostratigraphic heterogeneity between the lava flows is of utmost importance to understand the evolution of the south sub-province of the Paraná-Etendeka Igneous Province.

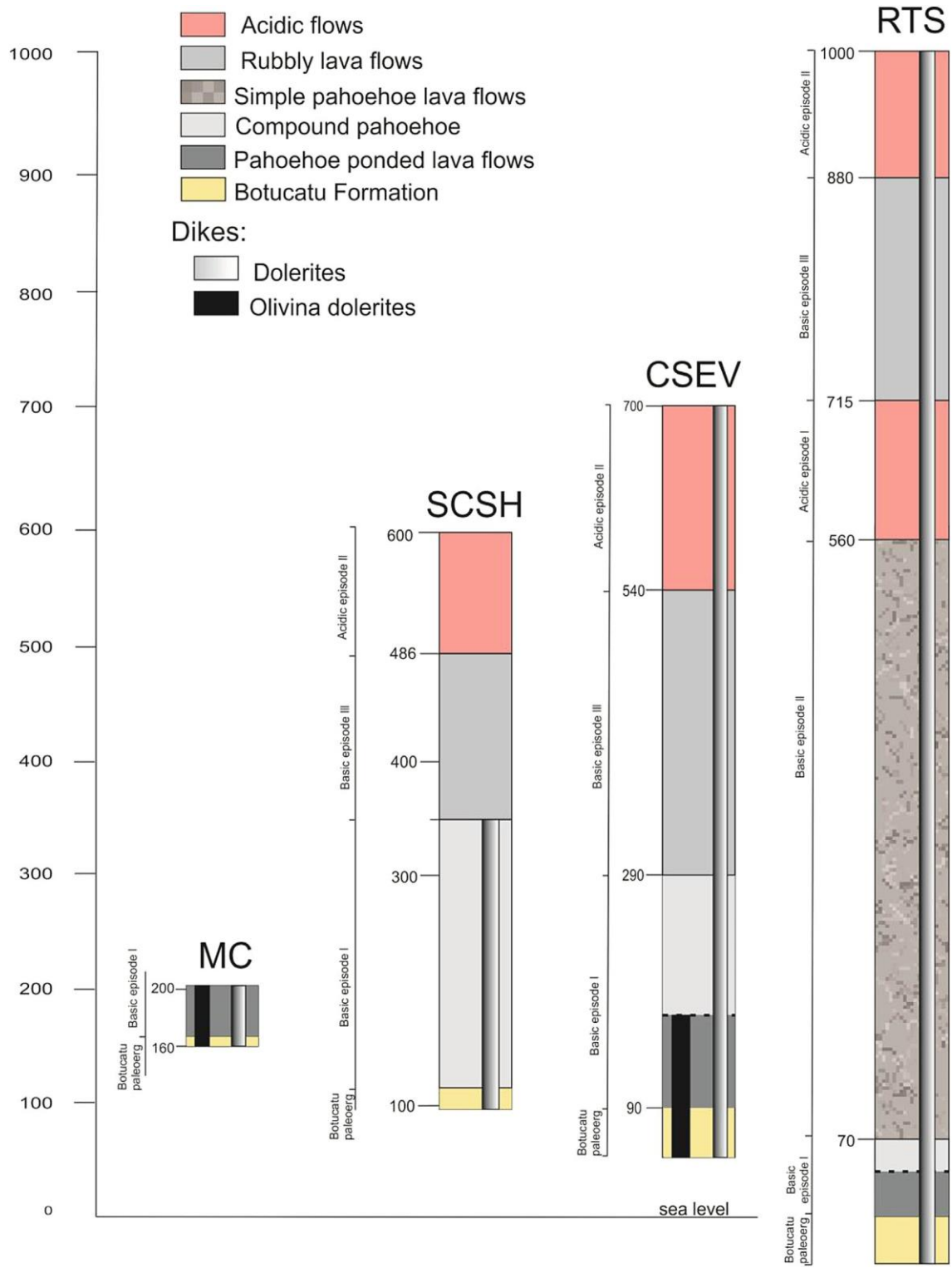

Fig. 17. Stratigraphic profiles of Santa Cruz do Sul/Herveiras (SCSH), Morro da Cruz (MC), Caxias do Sul/Estância Velha (CSEV) and Rota do Sol (RTS) areas with the types of flows and dikes represented in legend.

Acknowledgments

C. C. T. Sarmento would like to thank D. S. Oliveira, S. Benites, R. Noll Filho and H. Ligabue for helping with the collecting of the samples. Thanks to CAPES for the PhD research grant. This work had partial financial support to C.A. Sommer and E.F. Lima from CNPq (400724/2014-6, 441766/2014-5, 302213/2012-0, 303584/2009-2, 473683/2007, 5470641/2008-8, 470203/2007-2, 471402/2012-5, 303038/2009-8 and 470505/2010-9), and from the Rio Grande do Sul State Research Foundation (FAPERGS) 1180/12-8, and PRONEX 10/0045-6. We also thank the laboratory support from the IGEO/UFRGS.

References

Almeida, F.F.M., 1986. Distribuição regional e relações tectônicas do magmatismo pós-paleozóico no Brasil. Rev. Bras. Geociências 16 (4), 325e349.

Barreto, C.J.S., Lima, E.F., Scherer, C.M., Rossetti, L.M.M., 2014. Lithofacies analysis of basic lava flows of the Paranáigneous province in the south hinge of Torres Syncline, Southern Brazil. J. Volcanol. Geotherm. Res. 285, 81e99.

Le Bas, M.J., LeMaitre, R.W., Streckeisen, A., Zannetin, B.A., 1986. Chemical classification of volcanic rocks based on the total alkali-silica diagram. J. Pet. 27 (3), 745e750.

Bear, G., Beyth, M., Reches, Z., 1994. Dikes emplaced into fractured basement, timna igneous complex, Israel. J. Geophys. Res. 99, 24039e24050.

Bellieni, G., Comin-Chiaramonti, P., Marques, L.S., Melfi, A.J., Stolf, A.D., 1984. Low-pressure evolution of basalt sills from bore-holes in the ParanáBasin, Brazil. TMPM 33, 25e47.

Bellieni, G., Comin-Chiaramonti, P., Marques, L.S., Melfi, A.J., Nardy, A.J.R., Roisemberg, A., 1986. High-and-low-TiO2 flood basalt from the ParanáPlateau (Brazil): petrology and geochemical aspects bearing on their mantle origin. Neues Jahrb. fur Mineral. Stuttg. 150 (3), 273e306.

Billings, M.P., 1972. Structural Geology. Prentice-Hall Inc, Englewood Cliffs, New Jersey, USA, 606 pp.

Bryan, S.E., Ernst, R.E., 2008. Revised definition of large igneous provinces (LIPs). Earth Sci. Rev. 86, 175e202.

Coffin, M.F., Eldholm, O., 1992. Volcanism and continental break-up: a global compilation of large igneous provinces. In: Geological Society of London Special Publication, vol. 68, pp. 17e30.

Corval, A.V., 2009. Petrogênese e Contexto Geodinâmico das Suítes Basálticas Toleíticas (de alto -TiO2 e baixo - TiO2) do Cretáceo Inferior da Formação Centro-oriental do Enxame de Diques da Serra do Mar. Tese (Doutorado) - Centro de Tecnologia e Ciências. Faculdade de Geologia. Universidade do Estado do Rio de Janeiro, Rio de Janeiro, RJ.

Corval, A., Valente, S., Duarte, B.P., Famelli, N., Zanon, M., 2008. Dados petrológicos preliminares dos diabásios dos setores centro-norte e nordeste do Enxame de Diques da Serra do Mar. Geochim. Bras. 22, 159e177.

Coutinho, J.M.V., 2008. Dyke swarms of the Paranátriple junction, southern Brazil. Geol. Usp. Série Científica 8 (2), 29e52.

CPRM, 2010. Geologia Recursos Minerais do Estado de Rio Grande do Sul - Escala, 1, p. 750, 000.

Daniels, K.A., Kavanagh, J.L., Menand, T., Sparks, R.S.J., 2012. The Shapes of Dikes: Evidence for the Influence of Cooling and Inelastic Deformation. GSA Bulletin, 124; no. 7/8, pp. 1102e1112. http://dx.doi.org/10.1130/B30537.1.

Deckart, K., Féraud, G., Marques, L.S., Bertrand, H., 1998. New time constraints on dyke swarms related to the Paranáe Etendeka magmatic province, and subsequent South Atlantic opening, southeastern Brazil. J. Volcanol. Geotherm. Res. 80, 67e83.

Deer, W.A., Howie, R.A., Zussman, J., 2003. An Introduction to the Rock-Forming Minerals. Longman Scientific and Technical, New York.

Delaney, P.T., Gartner, A.E., 1997. Physical processes of shallow mafic dike emplacement near the San Rafael Swell, Utha. Geol. Soc. Am. Bull. 109, 1117e1192.

Delaney, P.T., Pollard, D.D., Ziony, J.I., Mckee, E.H., 1986. Field relations between dikes and joints: emplacement processes and paleostress analyses. J. Geophys. Res. 91, 4920e4983.

Dodd, S.C., Mac Niocaill, C., Muxworthy, A.R., 2015. Long duration (>4 Ma) and steady-state volcanic activity in the early cretaceous ParanáeEtendeka large igneous province: new palaeomagnetic data from Namibia. Earth Planet. Sci. Lett. 414 (15), 16e29.

Duncan, A.R., Newton, S.R., van den Berg, C., Reid, D.L., 1989. Geochemistry and petrology of dolerite sills in the Huab River valley, Damaraland, north-western Namibia. Communs Geol. Surv. Namib. 5, 5e18.

Duncan, A.R., Armstrong, R.A., Erlank, A.J., Marsh, J.S., Watkins, R.T., 1990. MORB-related dolerites associated with the final phases of Karoo flood basalt volcanism in southern Africa. In: Parker, J.A.J., Rickwood, P.C., Tucker, D.H. (Eds.), Mafic Dikes and Emplacement Mechanisms. A.A. Balkema, Rotterdam, The Netherlands, pp. 119e129.

Erlank, A.J., Marsh, J.S., Duncan, A.R., Miller, R.M., Hawkesworth, C.J., Betton, P.J., Rex, D.C., 1984. Geochemistry and petrogenesis of the Etendeka volcanic rocks from SWA/Namibia. In: Erlank, A.J. (Ed.), Petrogenesis of Volcanic Rocks of the Karoo Province, vol. 13. Special Publication of the Geological Society of South Africa, pp. 195e245.

Ewart, A.J., Marsh, J.S., Duncan, A.R., Miller, R.M., Hawkesworth, C.J., Betton, P.J., Rex, D.C., 1984. Geochemistry and petrogenesis of the Etendeka volcanic rocks from SWA/Namibia. In: Erlank, A.J. (Ed.), Petrogenesis of Volcanic Rocks of the Karoo Province. Geological Society of South Africa Special Publication 13, Johannesburg, pp. 195e245.

Florisbal, L.M., Heaman, L.M., Janasi, V.A., Bitencourt, M.F., 2014. Tectonic significance of the Florianópolis dyke swarm, ParanáeEtendeka magmatic province: a reappraisal based on precise UePb dating. J. Volcanol. Geotherm. Res. 289, 140e150.

Frank, H.T., Gomes, M.E.B., Formoso, M.L.L., 2009. Review of the areal extent and the volume of the Serra Geral Formation, ParanáBasin, south America. Pesqui. em Geociências 36 (1), 49e57.

Fúlfaro, V.J., Saad, A.R., Santos, M.V., Vianna, R.B., 1982. Compartimentação e evolução tectônica da bacia do Paraná Rev. Bras. Geociências 12, 590e611.

Gibb, F.G.F., Henderson, C.M.B., 1996. The Shiant Isles Main Sill: structure and mineral fractionation trends. Mineral. Mag. 60, 67e98.

Hawkesworth, C.J., Marsh, J.S., Duncan, A.R., Erlank, A.J., Norry, M.J., 1984. The role of continental lithosphere in the generation of the Karoo volcanic rocks: evidence from combined Nd- and Sr-isotope studies. Spec. Publ. Geol. Soc. S. Afr. 13, 341e354.

Heilbron, M., Pedrosa-Soares, A.C., Campos Neto, M.C., Silva, L.C., Trow, R.A.J., Janasi, V.A., 2004. Província mantiqueira. In: Mantesso-Neto, V., Bartorelli, A., Carneiro, C.D.R., Brito-Neves, B.B. (Eds.), Livro Geologia do Continente Sul_Americano: Evolução da obra de Fernando Flávio Marques de Almeida. Editora Beca, Sao Paulo, p. 647.

Hunter, D.R., Reid, D.L., 1987. Mafic dike swarms in southern Africa. In: Halls, H.C., Fahrig, W.F. (Eds.), Mafic Dike Swarms, vol. 34, pp. 445e456. Geological Association of Canada Special Paper.

Irvine, T.N., Baraguar, W.R.A., 1971. A guide to the chemical classification of the common volcanic rocks. Can. J. Earth Sci. 8 (5), 523e548.

Janasi, V.A., Freitas, V.A., Heaman, L.H., 2011. The onset of flood basalt volcanism, Northern ParanáBasin, Brazil: a precise U-Pb baddeleyite/zircon age for a Chapecó-type dacite. Earth Planet. Sci. Lett. 302 (1e2), 147e153.

Janoušek, V., Farrow, C.M., Erban, V., Šmíd, J., 2006. Technical note interpretation of whole-rock geochemical data in igneous geochemistry: introducing geochemical data toolkit (GCDkit). J. Pet. 47 (6), 1255e1259.

Jerram, D.A., Bryan, S.E., 2015. Plumbing systems of shallow level intrusive complexes. In: Breitkreuz, C.H., Rocchi, S. (Eds.), Physical Geology of Shallow Magmatic Systems. Advances in Volcanology. Springer, Berlin, pp. 1-22. http://dx.doi.org/10.1007/11157_2015_8.

Jerram, D.A., Mountney, N., Holzforster, F., Stollhofen, H., 1999. Internal stratigraphic relationships in the Etendeka Group in the Huab Basin, NW Namibia: understanding the onset of flood volcanism. J. Geodyn. 28, 393e418.

Jerram, D.A., Mountney, N., Howell, J., Long, D., Stollhofen, H., 2000. Death of a sand sea: an active aeolian erg systematically buried by the Etendeka flood basalts of NW Namibia. J. Geol. Soc. Lond. 157 (3), 513-516.

Lord, J., Oliver, G., Soulsby, J., 1996. Landsat MSS imagery of a Lower Cretaceous regional dyke swarm, Damaraland, Namibia: a precursor to the splitting of Western Gondwana. Int. J. Remote Sens. 17, 2945e2954.

Machado, F.B., Nardy, A.J.R., Oliveira, M.A.F., 2007. Geologia e aspectos petrológicos das rochas intrusivas e efusivas mesozóicas de parte da borda leste da bacia do Paranáno estado de Sao Paulo. Rev. Bras. Geociências 37 (1), 64e80.

Maniesi, V., Oliveira, M.A.F., 1997. Petrologia das soleiras de diabásio de Reserva e Salto do Itararé PR. Geochim. Bras. 11 (2), 153e169.

Mantovani, M.S.M., Marques, L.S., Souza, M.A., Atalla, L., Civeta, L., Inonocenti, F., 1985. Trace element and strontium isotope constrains of the origin and evo- lution of Paraná continental flood basalts of Santa Catarina state (southern Brazil). J. Pet. 26, 187e209.

Marques, L.S., Ernesto, M., 2004. O Magmatismo Toleítico da Bacia do Paraná. In: Mantesso-Neto, V., Bartorelli, A., Carneiro, C.D.R., Brito-Neves, B.B. (Eds.), Livro Geologia do Continente Sul-Americano: Evolução da obra de Fernando Flávio Marques de Almeida. Editora Beca, Sao Paulo.

Marques, L.S., Figueiredo, A.M.G., Saiki, M., Vasconcellos, M.B.A., 1989. Geoquímica analítica dos elementos terras raras - aplicação da técnica de análise por ativação neutrônica. In: Formoso, M.L.L., Nardy, L.V.S., Hartmann, L.A. (Eds.), Geoquímica Dos Elementos Terras Raras No Brasil (15-20), CPRM/DNPM. Sociedade Brasileira de Geoquímica, Rio de Janeiro.

Marsh, B.D., 2013. On some fundamentals of igneous petrology. Contrib. Miner. Pet. 166, 665e690.

Marsh, J.S., Duncan, A.R., 2008. Doros gabbroic complex. In: Miller, R.M. (Ed.), The Geology of Namibia, vol. 3. Geological Survey of Namibia, Windhoek, pp. 18e75.

Marsh, J.S., Erlank, A.J., Duncan, A.R., 1991. Report: preliminary geochemical data for dolerite dykes and sills of the southern part of the Etendeka Igneous Province.Communs Geol. Surv. Namib. 7, 77e80.

McDonough, W.S., Sun, S., 1995. The composition of the Earth. Chem. Geol. 120, 223e253.

Middlemost, E.A.K., 1975. The basalt clan. Earth Sci. Rev. 11, 337e364.

Milani, E.J., 1997. Evolução tectono-estratigráfica da Bacia do Paraná e seu relacionamento com a geodinâmica fanerozóica do Gondwana Sul-Ocidental. 2 v. Tese (Doutorado). Instituto de Geociências e UFRGS, Porto Alegre.

Milner, S.C., Duncan, A.R., Ewart, A., Marsh, J.S., 1994. Promotion of the Etendeka Formation to group status: a new integrated stratigraphy. Commun. Geol. Surv. Namib. 9, 5e11.

Miyashiro, A., 1978. Nature of alkalic volcanic rock series. Contrib. Mineral. Pet. 66, 91e104.

Morimoto, N., 1988. Mineralogy and Petrology 39, 55e76.

Mountney, N., Howell, J., Flint, S., Jerram, D., 1998. Aeolian and alluvial deposition within the mesozoic Etjo sandstone formation, northwest Namibia. J. Afr. Earth Sci. 27 (2), 175e192.

Nardy, A.J.R., 1995. Geologia e petrologia do vulcanismo mesozóico da região central da Bacia do Paraná Tese (Doutorado). Instituto de Geociências e Ciências Exatas, Universidade Estadual Paulista, Rio Claro, Sao Paulo.

Owen-Smith, T.M., Ashwal, L.D., 2015a. Evidence for multiple pulses of crystal-bearing magma during emplacement of the Doros layered intrusion, Namibia. Lithos 238, 120e139.

Owen-Smith, T.M., Ashwal, L.D., 2015b. Geology of the early cretaceous Doros layeredmafic intrusion, Namibia: complexity on a small scale. South Afr. J. Geol. 118 (2), 185e211.

Peate, D.W., 1997. The Paranáeetendeka Province. In: Mahoney, J.J., Coffin, M.F. (Eds.), *Large* Igneous Provinces: Continental, Oceanic and Planetary Flood Volcanism. American Geophysical Union, Washington, DC, pp. 217e245.

Peate, D.W., Hawkesworth, C.J., Mantovani, M.S.M., 1992. Chemical stratigraphy of the Paraná Lavas (South América): classification of magma types and their spatial distribution. Bulletin of Volcanol. 55 (1), 119e139. Berlin.

Peate, D.W., Hawkesworth, C.J., Mantovani, M.S.M., Rogers, N.W., Turner, S.P., 1999. Petrogenesis and stratigraphy of the high-Ti/Y Urubici magma type in the Paraná flood basalt province and implications for the nature of 'Dupal'- type mantle in the South Atlantic region. J. Petrol. 40, 451e473.

Petersohn, E., Gouvea, E.M., 2009. Geologia e geoquímica da soleira de Reserva, Estado do Paraná Rev. Bras. Geociências 39 (4), 740e750.

Petersohn, E., Vasconcellos, E.M.G., Lopes, K., 2007. Petrologia de sills encaixados nas Formações Irati e Ponta Grossa (Bacia do Paraná) no Estado do Paraná Geochim. Bras. 21, 58e70.

Piccirillo, E.M., Melfi, A.J., 1988. The Mesozoic Flood Volcanism of the Paraná Basin - Petrogenetic and Geophysical Aspects. USP, São Paulo.

Piccirillo, E.M., Civetta, L., Petrini, R., Longinelli, A., Bellieni, G., Comin-Chiaramonti, P., Marques, L.S., Melfi, A.J., 1989. Regional variations within the Paraná Flood Basalts (Southern Brazil): evidence for subcontinental mantle heterogeneity and crustal contamination. Chem. Geol. 75, 103e122.

Piccirillo, E.M., Bellieni, G., Cavazzini, G., Comin-Chiaramonti, P., Petrini, R., Melfi, A.J., Pinesi, J.P.P., Zantadeschi, P., Demin, A., 1990. Lower Cretaceous Tholeiitic Dyke Swarms from the Ponta Grossa (Southeast Brazil): Petrology, Sr- Nd Isotopes and Genetic Relationships Whith the Paraná Flood Volcanic. Chemical Geology, Netherlands, vol. 89, pp. 19e48.

Pollard, D.D., Muller, O.H., 1976. The effect of gradients in regional stress and magma pressure on the form of sheet intrusions in cross section. J. Geophys. Res. 81, 975e984. http://dx.doi.org/10.1029/JB081i005p00975.

Raposo, M.I.B., Ernesto, M., Renne, P.R., 1998. Paleomagnetism and $^{40}Ar/^{39}Ar$ dating of the early cretaceous Florianópolis dike swarm (Santa Catarina island), southern Brazil. Phys. Earth Planet. Inter. 108, 275e290.

Renne, P.R., Ernesto, M., Pacca, I.G., Coe, R.S., Glen, J.M., Prévot, M., Perrin, M., 1992. The age of Paraná flood volcanism, rifting of Gondwana land, and the jurassic-cretaceous boundary. Science 258, 975e979.

Renne, P.R., Glen, J.M., Milner, S.C., Duncan, A.R., 1996b. Age of Etendeka flood volcanism and associated intrusions in southwestern Africa: Geology, 24, pp. 659e662. http://dx.doi.org/10.1130/0091-7613(1996)0242.3.CO;2.

Renne, P.R., Deckart, K., Ernesto, M., Féraud, G., Piccirillo, E.M., 1996a. Age of the Ponta Grossa dike swarm (Brazil), and implications to Paraná flood volcanism.
Earth Planet. Sci. Lett. 144, 199e211. http://dx.doi.org/10.1016/0012-821X(96) 00155-0.

Renne, P.R., Mundil, R., Balco, G., Min, K., Ludwig, K.R., 2010. Joint determination of
^{40}K decay constants and $^{40}Are^{40}K$ for the Fish Canyon sanidine standard, and improved accuracy for $^{40}Are^{39}Ar$ geochronology. Geochim. Cosmochim. Acta 74, 5349.

Renner, L.C. 2010. Geoquímica de sills basálticos da Formaçao Serra Geral, sul do Brasil, com base em rocha total e micro-análise de minerais. Tese (Doutorado) e Instituto de Geociências. Programa de Pós-Graduaçao em Geociências, Uni- versidade Federal do Rio Grande do Sul, Porto Alegre, RS

Richard, L.R., 1995. Minpet for Windows e Version 2.02. Minpet Geological Soft- ware, Quebec.

Ricommini, C., 1997. Arcabouço estrutural e aspectos do tectonismo gerador e deformador da bacia Bauru no estado de Sao Paulo. Rev. Bras. Geociências 27 (2), 153e162.

Ricommini, C., Sant'anna, L.G., Ferrari, A.L., 2004. Evoluçao geológica do rift conti- nental do Sudeste do Brasil. In: Mantesso-Neto, V., Bartorelli, A., Carneiro, C.D.R., Brito-Neves, B.B. (Eds.), Geologia do Continente Sul-Americno: Evoluçao da obra de Fernando Flávio Marques de Almeida. Editora Beca, Sao Paulo, pp. 385e405.

Rollinson, H., 1993. Using Geochemical Data: Evaluation, Presentation, Interpreta- tion. Longman, Harlow, 352 pp.

Rossetti, L.M., Lima, E.F., Waichel, B.L., Scherer, C.M., Barreto, C.J., 2014. Stratigraphical framework of basaltic lavas in Torres Syncline main valley, southern Parana-Etendeka Volcanic Province. J. S. Am. Earth Sci. 56, 409e421.

Sarmento, C.C.T., Sommer, C.A., Lima, E.F., Oliveira, D.S., 2014. Corpos hipabissais correlacionados à Formaçao Serra Geral na regiao do Cerro do Coronel, RS: geologia e petrologia. Geol. Usp. Série Científica 14 (2), 23e44.

Scherer, C.M.S., 2002. Preservation of aeolian genetic units by lava flows in the lower cretaceous of the Paraná Basin, southern Brazil.
Sedimentology 49, 97e116.

Self, S., Widdowson, M., Thordarson, T., Jay, A.E., 2006. Volatile fluxes during flood basalt eruptions and potential effects on global environment: a Deccan perspective. Earth Planet. Sci. Lett. 248, 518e532.

Siedner, G., Mitchell, J.G., 1976. Episodic Mesozoic volcanism in Namibia and Brazil; KeAr isochron study bearing on the opening of the South Atlantic. Earth Planet. Sci. Lett. 30, 292e302.

Stewart, K., Turner, S., Kelley, S., Hawkesworth, C.J., Kirstein, L., Mantovani, M., 1996. 3-D, Ar/Ar geochronology in the Paranácontinental flood basalt province. Earth Planet. Sci. Lett. 143, 95e109.

Thiede, D.S., Vasconcelos, P.M., 2010. Paraná flood basalts: rapid extrusion hypothesis confirmed by new $^{40}Ar/^{39}Ar$ results. Geology 38 (8), 747e750.

Thompson, R.N., Gibson, S.A., Dickin, A.P., Smith, P.M., 2001. Early Cretaceous basalt and picrite dykes of the southern Etendeka region, NW Namibia: windows into the role of the Tristan mantle plume in Parana-Etendeka magmatism. J. Pet. 42, 2049e2081.

Thompson, R.N., Riches, A.J.V., Antoshechkina, P.M., Pearson, D.G., Nowell, G.M., Ottley, C.J., Dickin, A.P., Hards, V.L., Nguno, A.-K., Niku-Paavola, V., 2007. Origin of CFB magmatism: multi-tiered intracrustal picriterhyolite magmatic plumbing at Spitzkoppe, western Namibia, during Early Cretaceous Etendeka magmatism. J. Pet. 48, 1119e1154.

Tomazzoli, E.R., Lima, E.F., 2006. Magmatismo ácido-básico na ilha do Arvoredo-SC. Rev. Bras. Geociências 36, 57e76.

Tomazzoli, E.E., Pellerin, J.M., 2015. Unidades do mapa geológico da ilha de Santa Catarina: as Rochas. Geosul, Florianóp. 30 (60), 225e247.

Trumbull, R.B., Vietor, T., Hahne, K., Wackerle, R., Ledru, P., 2004. Aeromagnetic mapping and reconnaissance geochemistry of the early cretaceous Henties bay-Outjo mafic dike swarm, Etendeka igneous province, Namibia. J. Afr. Earth Sci. 40, 17e29.

Trumbull, R.B., Reid, D.L., Beer, C., Acken, D., Romer, R.L., 2007. Magmatism and continental breakup at the west margin of southern Africa: a geochemical comparison of dolerite dikes from northwestern Namibia and the Western Cape. South Afr. J. Geol. 110, 477e502.

Turner, S., Regelous, M., Kelley, S., Hawkesworth, C., Mantovani, M., 1994. Magmatism and continental break-up in the South Atlantic: high precision $^{40}Ar/^{39}Ar$ geochronology. Earth Planet. Sci. Lett. 121, 333e348.

Turner, S., Peate, D., Hawkesworth, C., Mantovani, M., 1999. Chemical stratigraphy of the Paraná basalt succession in western Uruguay: further evidence for the diachronous nature of the Paraná magma types. J. Geodyn. 28 (4), 459e469.

Valente, S.C., Corval, A., Duarte, B.P., Ellam, R.L., Fallick, A.E., Dutra, T., 2007. Tectonic boundaries, crustal weakness zones and plume-subcontinental lithospheric mantle interactions in the Serra do Mar Dyke Swarm, SE Brazil. Rev. Bras. Geociências 37, 194e201.

Valentine, A.G., Krogh, K.E.C., 2006. Emplacement of shallow dikes and sills beneath a small basaltic volcanic center - the role of pre-existing structure (Paiute Ridge, southern Nevada, USA). Earth Planet. Sci. Lett. 246, 217e230.

Viero, A.P., Roisenberg, A., 1992. Petrologia e geoquímica do Complexo Básico Lomba Grande. Pesqui. em Geociências 19 (1), 41e54.

Waichel, B.L., Scherer, C.M.S., Frank, H.T., 2008. Basaltic lava flows covering active Aeolian dunes in the Paraná Basin in Southern Brazil: features and emplacement aspects. J. Volcanol. Geotherm. Res. 171 (1), 59e72.

Waichel, B.L., Lima, E.F., Viana, A., Scherer, C.M.S., Bueno, G., Dutra, G., 2012. Stratigraphy and volcanic facies architecture of the Torres Syncline, southern Brazil, and its role in understanding the Paraná-Etendeka continental flood basalt province. J. Volcanol. Geotherm. Res. 215, 74e82.

Wanke, A., Stollhofen, H., Stanistreet, I.G., Lorenz, V., 2000. Karoo unconformities in NW-Namibia and their tectonic implications. Communs Geol. Surv. Namib. 12, 291e301.

Wilson, M., 1989. Igneous Petrogenesis a Global Tectonic Approach. Springer, Berlin. Winchester, J.A., Floyd, P.A., 1977. Geochemical discrimination of different magma series and their differentiation products using immobile elements. Chem. Geol. 20, 325e343.

Zalán, P.V., Conceiçao, J.C.J., Astolfi, M.A.M., Appi, V.T., Wolff, S., Vieira, I.S., Marques, A., 1985. Estilos Estruturais Relacionado Às Intruses Magmáticas Básicas Em Rochas Sedimentares. Boletim Técnico da Petrobras 28 (4), 221e230. Rio de Janeiro, RJ.

3.2. ARTIGO 2

TÍTULO: Sr-Nd-Pb isotopic insights of the mafic subvolcanic intrusions from Paraná-Etendeka Igneous Province: Petrologic and isotopic relationship with the volcanism of the southern Brazil

AUTORES: Carla Cecília Treib Sarmento; Carlos Augusto Sommer; Evandro Fernandes de Lima; Carla Joana Santos Barreto; Jean Michael Lafon.

SUBMETIDO: Em novembro de 2017.

PERIÓDICO: Journal of Volcanology and Geothermal Research

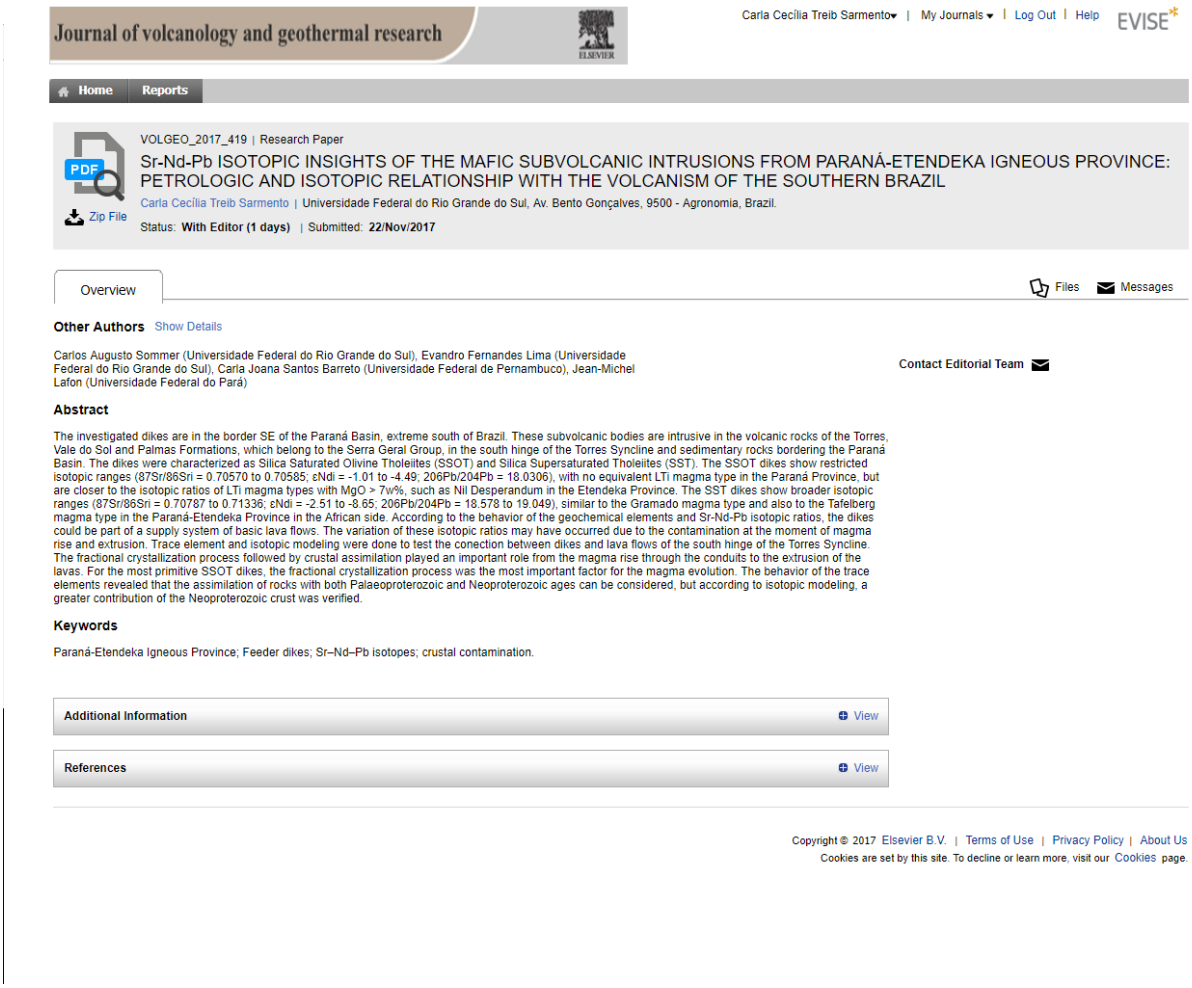

Journal of volcanology and geothermal research

Carla Cecília Treib Sarmento | My Journals | Log Out | Help EVISE

Home Reports

VOLGEO_2017_419 | Research Paper

Sr-Nd-Pb ISOTOPIC INSIGHTS OF THE MAFIC SUBVOLCANIC INTRUSIONS FROM PARANÁ-ETENDEKA IGNEOUS PROVINCE: PETROLOGIC AND ISOTOPIC RELATIONSHIP WITH THE VOLCANISM OF THE SOUTHERN BRAZIL

Carla Cecília Treib Sarmento | Universidade Federal do Rio Grande do Sul, Av. Bento Gonçalves, 9500 - Agronomia, Brazil.

Status: **With Editor (1 days)** | Submitted: **22/Nov/2017**

Zip File

Overview

Files Messages

Other Authors Show Details

Carlos Augusto Sommer (Universidade Federal do Rio Grande do Sul), Evandro Fernandes Lima (Universidade Federal do Rio Grande do Sul), Carla Joana Santos Barreto (Universidade Federal de Pernambuco), Jean-Michel Lafon (Universidade Federal do Pará)

Contact Editorial Team

Abstract

The investigated dikes are in the border SE of the Paraná Basin, extreme south of Brazil. These subvolcanic bodies are intrusive in the volcanic rocks of the Torres, Vale do Sol and Palmas Formations, which belong to the Serra Geral Group, in the south hinge of the Torres Syncline and sedimentary rocks bordering the Paraná Basin. The dikes were characterized as Silica Saturated Olivine Tholeiites (SSOT) and Silica Supersaturated Tholeiites (SST). The SSOT dikes show restricted isotopic ranges (87Sr/86Sri = 0.70570 to 0.70585; εNdi = -1.01 to -4.49; 206Pb/204Pb = 18.0306), with no equivalent LTi magma type in the Paraná Province, but are closer to the isotopic ratios of LTi magma types with MgO > 7w%, such as Nil Desperandum in the Etendeka Province. The SST dikes show broader isotopic ranges (87Sr/86Sri = 0.70787 to 0.71336; εNdi = -2.51 to -8.65; 206Pb/204Pb = 18.578 to 19.049), similar to the Gramado magma type and also to the Tafelberg magma type in the Paraná-Etendeka Province in the African side. According to the behavior of the geochemical elements and Sr-Nd-Pb isotopic ratios, the dikes could be part of a supply system of basic lava flows. The variation of these isotopic ratios may have occurred due to the contamination at the moment of magma rise and extrusion. Trace element and isotopic modeling were done to test the conection between dikes and lava flows of the south hinge of the Torres Syncline. The fractional crystallization process followed by crustal assimilation played an important role from the magma rise through the conduits to the extrusion of the lavas. For the most primitive SSOT dikes, the fractional crystallization process was the most important factor for the magma evolution. The behavior of the trace elements revealed that the assimilation of rocks with both Palaeoproterozoic and Neoproterozoic ages can be considered, but according to isotopic modeling, a greater contribution of the Neoproterozoic crust was verified.

Keywords

Paraná-Etendeka Igneous Province; Feeder dikes; Sr–Nd–Pb isotopes; crustal contamination.

Additional Information View

References View

Copyright © 2017 Elsevier B.V. | Terms of Use | Privacy Policy | About Us

Cookies are set by this site. To decline or learn more, visit our Cookies page.

Comprovante de submissão do artigo 2.

Sr-Nd-Pb ISOTOPIC INSIGHTS OF THE MAFIC SUBVOLCANIC INTRUSIONS FROM PARANÁ-ETENDEKA IGNEOUS PROVINCE: PETROLOGIC AND ISOTOPIC RELATIONSHIP WITH THE VOLCANISM OF THE SOUTHERN BRAZIL

Carla Cecília Treib Sarmento[1]; Carlos Augusto Sommer[1]; Evandro Fernandes de Lima[1]; Carla Joana Santos Barreto[2]; Jean Michel Lafon[3]

Instituição: (1) UNIVERSIDADE FEDERAL DO RIO GRANDE DO SUL

(2) UNIVERSIDADE FEDERAL DE PERNAMBUCO

(3) UNIVERSIDADE FEDERAL DO PARÁ

Endereço: Av. Bento Gonçalves nº. 9500 – Prédio 43136 - sala 107

Bairro Agronomia – cep.91501.970, Porto Alegre, RS - Brasil

Telefone de contato: (51) 33087398

E-mail: carla.treibs@gmail.com; carlos.sommer@ufrgs.br; evandro.lima@ufrgs.br; carlabarreto@hotmail.com; lafonjm@ufpa.br

ABSTRACT

The investigated dikes are located in the southeast of the Paraná Basin, extreme south of Brazil. These subvolcanic bodies are intrusive in the volcanic rocks of the Torres, Vale do Sol and Palmas Formations, which belong to the Serra Geral Group, in the south hinge of the Torres Syncline and sedimentary rocks bordering the Paraná Basin. The dikes were characterized as Silica Saturated Olivine Tholeiites (SSOT) and Silica Supersaturated Tholeiites (SST). The SSOT dikes show restricted isotopic ranges ($^{87}Sr/^{86}Sr_i$ = 0.70570 to 0.70585; εNd_i = -1.01 to -4.49; $^{206}Pb/^{204}Pb$ = 18.0306), with no equivalent LTi magma type in the Paraná Province, but are closer to the isotopic ratios of LTi magma types with MgO > 7w%, such as Nil Desperandum in the Etendeka Province. The SST dikes show broader isotopic ranges ($^{87}Sr/^{86}Sr_i$ = 0.70787 to 0.71336; εNd_i = -2.51 to -8.65; $^{206}Pb/^{204}Pb$ = 18.578 to 19.049), similar to the Gramado magma type and also to the Tafelberg magma type in the Paraná-Etendeka Province in the African side. According to the behavior of the geochemical elements and Sr-Nd-Pb isotopic ratios, the dikes could be part of a supply system of basic lava flows. The variation of these isotopic ratios may have occurred due to the contamination at the moment of magma rise and extrusion. Trace element and isotopic modeling were done to test the conection between dikes and lava flows of the south hinge of the Torres Syncline. The fractional crystallization process followed by crustal assimilation played an important role from the magma rise through the conduits to the extrusion of the lavas. For the most primitive SSOT dikes, the fractional crystallization process was the most important factor for the magma evolution. The behavior of the trace elements revealed that the assimilation of rocks with both Palaeoproterozoic and Neoproterozoic ages can be considered, but according to isotopic modeling, a greater contribution of the Neoproterozoic crust was verified.

Keywords: Paraná-Etendeka Igneous Province; Feeder dikes; Sr–Nd–Pb isotopes; crustal contamination.

1. INTRODUCTION

The Continental Basaltic Provinces (CBPs) are one of the types of Large Igneous Provinces (LIPs) that are characterized by having been developed in a relatively short time period (~ 10^6 years), in which large volumes of lavas and associated intrusions (10^5 - 10^7 km^3)

were generated and accumulated (Coffin & Eldholm, 1992, Self et al., 2006; Bryan & Ernst, 2008).

The Paraná-Etendeka Igneous Province (PEIP) is a predominantly basic tholeiitic volcanic sequence of lower Cretaceous age, in addition to associated acidic and intrusive rocks. It is located mostly in the center-eastern portion of the South American Plate and a small part is in Namibia.

Intrusions of basic tholeiitic rocks are very common in this province and studies suggest that the volume of these intrusive bodies in the Paraná Basin is approximately 112,000 km^3 (Frank et al., 2009). The dikes often occur clustered in the form of swarms, with more concentrated occurrences in the states of Paraná (Ponta Grossa dike swarm), Santa Catarina (Florianópolis dike swarm) (Raposo et al., 1998; Deckart et al., 1998; Marques & Ernesto, 2004; Tomazzoli & Lima, 2006; Florisbal et al., 2014, 2017; Tomazzoli & Pellerin, 2015), São Paulo and Rio de Janeiro (Serra do Mar dike swarm) (Turner et al., 1994; Stewart et al., 1996; Corval et al., 2008; Valente et al., 2007; Corval, 2009).

The dikes identified in the sothernmost Brazil (Rio Grande do Sul State) do not occur as swarms, but the investigated intrusives have a preferred NE-SW orientation where they cut the sedimentary rocks of the southern border of the Paraná Basin and NW-SE as they cut the successions of lavas of the Serra Geral Group (Sarmento *et al.,* 2017). The sills are more concentrated in the eastern boundary of the Paraná Basin and occur throughout its extension, usually intruding the Paleozoic sediments (Almeida, 1986; Zalán et al., 1985) in the states of São Paulo (Machado et al., 2007) and Paraná (Maniesi & Oliveira, 1997; Petersohn et al., 2007; Petersohn & Gouvea, 2009). In Rio Grande do Sul State, the sills related to the PEIP are found in the southern boundary of the Paraná Basin, namely the Lomba Grande Basic Complex (Viero & Roisenberg, 1992), in the region of Manoel Viana and Agudo (Renner, 2010), the sills of the Cerro do Coronel region (Sarmento et al., 2014) and sills on the southern edge of the Paraná Basin (Sarmento et al., 2017).

In the Etendeka Province, on the African side, the dikes and sills associated with the rifting and magmatism processes that formed the South Atlantic are abundant in about 150 km along the coast of Namibia (Siedner & Mitchell, 1976; Ewart et al., 1998, 2004; Hunter & Reid, 1987; Marsh et al., 1991). These bodies intruded mainly the Damara basement and the sedimentary rocks of the Karoo basin (Marsh et al., 1991; Lord et al., 1996). They occur as dike swarms, such as the Henties Bay-Outjo (Duncan et al., 1990; Lord et al., 1996; Trumbull et al., 2004, 2007), which includes the picritic to rhyolitic tholeiitic dikes near Spitzkoppe, western Namibia (Thompson et al., 2001, 2007). The Regional, Tafelberg and Horingbaai dolerites (Erlank et al., 1984), in addition to the Huab sills complex (Ewart et al., 1984;

Duncan et al., 1989) and Doros Complex (Gibb & Henderson, 1996; Marsh, 2013; Owen-Smith & Ashwal, 2015) are also noteworthy. In the Huab Basin both Tafelkop (picritic) and Tafelberg type dikes can be seen cutting and, in some cases, feeding the basal volcanic units (Jerram et al., 1999; Wanke et al., 2000).

Studies on the evolution of CBPs have highlighted the great importance of basic intrusions (Deckart et al., 1998; Marques & Ernesto, 2004; Bryan, 2007; Bryan & Ernst, 2006; 2008; Valente et al., 2007; Corval, 2009; Vanderkluysen et al., 2011; Florisbal et al., 2014, 2017).

In the studies about the Serra Geral Group basic intrusions, few investigations link these occurrences with volcanic successions (e.g. Piccirillo et al., 1990). In the structural context of the Paraná Basin, such as the volcanism and sedimentation filling up the Torres Syncline, there are no studies with integrated approaches of geochemistry, modeling and isotopic studies that consider the stratigraphy and typology of the flow.

For this reason, the main goals of this study are: (1) Petrologic and isotopic studies (Sr, Nd and Pb) of several intrusive bodies located in the central-eastern region of Rio Grande do Sul State; (2) to discuss the petrogenesis of the magmas of these hypabyssal bodies and their correlation with the associated flow types of the south hinge of the Torres Syncline through geochemical and isotopic modeling; (3) to investigate the relationship of the studied dikes of the Paraná Province with intrusive bodies of the Etendeka Province.

The geological, geochemical and isotopic data are integrated with the lithostratigraphy nomenclature proposed by Rossetti et al. (2017) for the Serra Geral Group in southern Brazil. The volcanic successions were divided into Torres Formation, Vale do Sol Formation, Palmas Formation and Esmeralda Formation. The Torres Formation is composed of: (i) compound pahoehoe basaltic lithofacies and (ii) ponded pahoehoe interdune andesitic lithofacies. To identify them in this work, the denominations Torres Formation (*compound pahoehoe*) and Torres Formation (*ponded pahoehoe*) are respectively used.

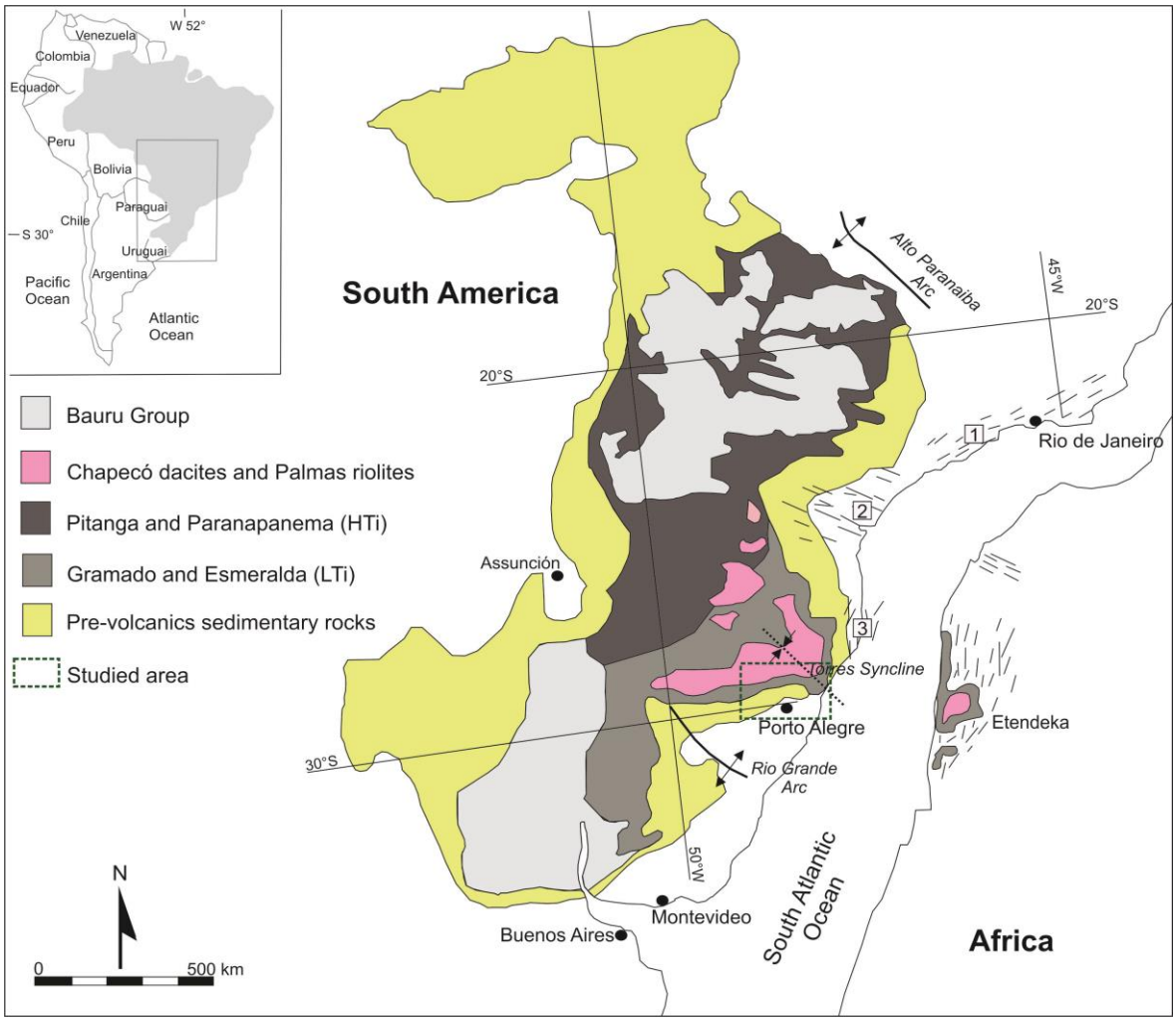

Figure 1. Distribution of the Paraná-Etendeka Igneous Province and main tectonic structures in a pre-drift reconstruction (modified after Peate et al., 1992; Stewart et al., 1996; Hawkesworth et al., 2000). Dike swarms: 1 - Ponta Grossa; 2 – Serra do Mar; 3 – Florianópolis.

2. ANALYTICAL TECHNIQUES

2.1. Geochemistry

A set of 42 samples was selected, from the hypabyssal bodies of the studied region, in order to analyze the chemical compositions of the major, minor, and trace elements and rare earth elements (REE). The samples were prepared with an agate ball mill, which allows to obtain less than 200 mesh fractions. The analyzes were carried out at *Acme Laboratories Ltda* (Canada) using the ICP-ES (*Inductively Coupled Plasma Emission Spectrometry*) method for major elements and ICP-MS (*Inductively Coupled Plasma Mass Spectrometry*) method for trace elements and rare earth elements (REE). The detection limits for most of the major elements were on the order of 0.1% and 0.1 ppm for the trace elements.

2.2. Sr, Nd, and Pb isotopes

The Sr, Nd, Sm, and Pb isotope analyses in the Isotope Geology Laboratory at Universidade Federal do Pará (Pará–Iso–UFPA), Belém–Brazil. For the sample digestion procedure, ~100 mg of the rock sample was first mixed with a ^{149}Sm–^{150}Nd spike and was then dissolved with HNO_3, HCl, and HF in Teflon Savillex® bombs in a microwave oven. A two-step ion-exchange chromatography procedure was used for Pb, Sr, Nd, and Sm purification. The first step consisted of loading the sample solution in Teflon columns filled with cationic resin (Biorad Dowex AG 50 W-X8) using 2 N HCl and 3 N HNO_3 to separately collect Pb, Sr, and REEs. In the following stage, the Nd and Sm were separated from each other and from other REEs in Teflon columns filled with Eichron® Ln resin using 0.2 N and 0.3 N HCl. For multi-collector ICP-MS (MC-ICP-MS) isotopic analysis of Sr, a second stage of separation with Eichron® Sr resin and 3.5 N HNO3 was applied to obtain a high-purity Sr fraction and to avoid isobaric interference of heavy REEs (HREEs; Yang et al., 2012). For the purification of Pb, a second step of chromatographic separation with Eichron® Sr resin and HCl (2 N and 6 N) was also required. The Pb was collected after elution with 3 ml of 6 N HCl. The isotopic analyses were conducted in a Thermo-Finnigan Neptune MC-ICP-MS equipped with nine Faraday collectors. Sr, Sm, and Nd fractions were previously dissolved in 2 ml of 3 HNO_3 3 wt.%. The uncertainty calculations for the Sm/Nd and $^{143}Nd/^{144}Nd$ ratios are based on repeated analyses of BCR-1 and La Jolla reference materials, respectively (Oliveira et al., 2008). The Sr isotopic ratios were normalized to $^{86}Sr/^{88}Sr = 0.1194$. The Nd isotopic compositions were normalized to $^{146}Nd/^{144}Nd = 0.7219$, and the decay constant used was that revised by Lugmair & Marti (1978), $6{,}54 \times 10^{-12}$ $year^{-1}$. The Pb fraction was dissolved in HNO_3 3 wt.% and mixed with a solution of 50 ppb Tl for the correction of mass discrimination. More details on the experimental procedures are available in Krymsky et al. (2007), Oliveira et al. (2008), and Romero et al. (2013).

3. GEOLOGICAL BACKGROUND

The Paraná Basin is defined as an intracratonic basin, with an area of approximately 1,500,000 km^2 in east-central South America (Figure 1). Formed by a volcano-sedimentary sequence from the Upper Ordovician to the Upper Cretaceous periods, this basin can be divided into six supersequences separated by the regional unconformities: Rio Ivaí (Upper Ordovician – Lower Silurian), Paraná (Devonian), Gondwana I (Upper Carboniferous –

Lower Triassic), Gondwana II (Middle to Upper Triassic), Gondwana III (Upper Jurassic – Lower Cretaceous) and Bauru (Upper Cretaceous) (Milani, 1997). The Gondwana III supersequence is characterized by a basal sedimentary sequence related to aeolian environments (Botucatu Formation), overlaid by a thick volcanic succession named Serra Geral Group. This unit covers an area of more than 917,000 km^2 in Brazil, Paraguay, Uruguay and Argentina, with an approximate volume of 450,000 km^3 (Frank et al., 2009).

These sequences also occur in the well-exposed sections of the Huab Basin in northwestern Namibia (Jerram et al., 2000), further expanding the coverage area of the deposits before the Gondwana rupture.

Major tectonic structures are found in the Paraná Basin, notably the Ponta Grossa and Rio Grande Arcs and the Torres Syncline. During the syn-volcanic subsidence process, these structures induced the formation of sub-basins, thus playing a major role in the structural evolution of the basin and influencing its current boundaries.

The Serra Geral Group is a sequence of lava flows with maximum thickness of 1,700 meters at the centre of the basin (São Paulo state–Brazil; Almeida, 1986), with predominant basalts and basaltic andesites of tholeiitic affinity. Acidic lava flows (rhyolites, rhyodacites) occur, interspersed with basic flows on top of the volcanic sequence, especially in southernmost Brazil (Melfi et al., 1988). The occurrence of a large amount of basic to intermediate intrusive bodies (sills and dikes) is common, usually associated with structural discontinuities of the Paraná Basin.

In the southern part of the basin, the basic lava flows were deposited mainly over the aeolian sandstones of the Botucatu Formation, locally preserving the original morphologies of dunes and sedimentary features. These features suggest contemporaneity among the first volcanic episodes and the active aeolian system of this unit (Scherer, 2002; Waichel et al., 2008).

The basic rocks of Serra Geral Group have been divided into two major groups: high-Ti basalts, with TiO_2 contents above 2%, and low-Ti basalts, with TiO_2 contents lower than 2% (Bellieni et al., 1984; Mantovani et al., 1985). Subdivisions of these groups into magma-types were proposed on basis in the amount of trace elements and the ratios between them (Peate et al., 1992; Peate, 1997). The magma-types with $Ti/Y > 300$ that predominantly occur in the northern portion of the province were named Pitanga, Paranapanema and Ribeira. The Gramado, Esmeralda and Urubici magma-types have $Ti/Y < 300$ and predominantly occur in the south of the province.

The acidic volcanic rocks were subdivided into Palmas (Caxias do Sul and Santa Maria) and Chapecó (Guarapuava and Ourinhos) facies. The acidic rocks of the Chapecó type

are mostly in the center of the Paraná Basin and are represented by dacites, rhyodacites, quartz latites and rhyolites. The Palmas-type acidic rocks correspond to rhyolites and rhyodacites. In general, the acidic composition rocks are mostly present in the states of Rio Grande do Sul, Santa Catarina and Paraná (Bellieni et al., 1986; Piccirillo et al., 1988, 1989; Nardy, 1995). The main distinguishing factors of these groups is the abundance of incompatible elements. The Chapecó facies has values of Zr> 500 ppm, Ba > 900 ppm and Sr> 250 ppm, while the Palmas facies has values of Zr< 400 ppm, Ba < 800 ppm and Sr < 170 ppm (Peate et al., 1992).

A stratigraphic model, based on facies architecture, was proposed for the Torres Syncline region (Waichel et al., 2012). It is based on the morphology of the basic and acidic lava flows, paleo-topography and effusion rates. This model is similar to those proposed for the Huab Basin, Namibia, on the the Etendeka side (e.g. Mountney et al., 1998; Jerram et al., 1999, 2000).

Barreto et al. (2014) and Rossetti et al. (2014) suggest te use of the facies analysis method combined with petrographic and geochemistry data to investigate the emplacement conditions of the basic volcanic rocks in these Santa Cruz do Sul/Herveiras and EstânciaVelha/Caxias do Sul regions, south hinge of the Torres Syncline. The lava flows were divided into lithofacies associations: ponded pahoehoe lava (interdune confined flows), compound pahoehoe lava (small pahoehoe lava lobes stacked in a complex pattern), simple (sheet) pahoehoe lava (tabular lobes with internal structure consisting of basal zone, massive core and vesicular zone) and rubbly lava (thick flows with tabular geometry, massive core and top with scoriaceous breccias).

A formal nomenclature was proposed to the lithostratigraphy and volcanology of the Serra Geral Formation (Rossetti et al., 2017), further this designation of formation was replaced by Serra Geral Group (SGG). They divided this unit in four lava formation because of the heterogeneity of the lava packages: (i) Torres Formation - characterized by chemically more primitive basaltic compound pahoehoe (>5 wt% MgO), andesi-basaltic and andesitic ponded pahoehoe flow fields; (ii) Vale do Sol Formation - characterized by groups vertically stacked sheet-like rubbly pahoehoe basaltic andesites (SiO_2 > 51 wt%; MgO < 5 wt%); (iii) Dacites and rhyolites of Palmas Formation overlay Vale do Sol Formation flows in the central and eastern area and rest directly upon Torres Formation lavas in the west and (iv) Esmeralda Formation - is the upper stratigraphic unit and it is formed by a basaltic pahoehoe flow field emplaced during the waning phase of volcanic activity of the low-TiO_2 lava sequence.

Barreto et al., (2016) conducted a study of the geochemical and Sr–Pb–Nd isotopic variations of the basaltic lava flows (with initial (132Ma) Sr isotopic ratios at 0.707798 –

0.715751, εNd at −8.36 to −5.41 and Pb isotopic variations $^{206}Pb/^{204}Pb$ = 18.42 – 18.86) belonging to low Ti Gramado magmatism using the local-scale stratigraphy as guidelines. They discussed the petrogenesis of these lava flows within a single magma type and evaluated qualitatively and quantitatively the role of crustal contamination in the lava flows and the potential contaminants involved in lava flows of the Santa Cruz do Sul /Herveiras, Lajeado and Morro da Cruz regions.

Petrogenetic models obtained from the investigation of hypabyssal bodies show its importance for the understanding of the Paraná Magmatic Province. According to Marques & Ernesto (2004), geochemical and isotopic data from the Ponta Grossa Dike Swarm reveal that asthenospheric components were not significant in the genesis of these dikes and that they may have been little affected by crustal contamination processes. For Renne et al. (1996), the ages of the Ponta Grossa Dike Swarm are between 133.1 and 130.8 Ma ($^{40}Ar/^{39}Ar$), temporally correlated to the Paraná-Etendeka Province basaltic lava flows. These authors also observed ages close to 120 Ma in dikes near the continental margin, confirming the hypothesis proposed by Piccirillo et al. (1990) who suggest that these dikes were younger feeders of the north sub-province flows, of which there are no remaining outcrops due to subsequent weathering. Almeida et al. (2017) report the first high-precision ID-TIMS U-Pb baddeleyite/zircon and $^{40}Ar/^{39}Ar$ step-heating phlogopite age data for dolerite and lamprophyre dikes and a mafic intrusion (José Fernandes Gabbro), Ponta Grossa Arch, Brazil. U-Pb zircon data yielded the best estimate for the emplacement ages of a high Ti-P-Sr basaltic dike (133.9±0.2 Ma), a dike with basaltic andesite composition (133.4±0.2 Ma) and the José Fernandes Gabbro (134.5±0.1 Ma). An $^{40}Ar/^{39}Ar$ phlogopite age of 133.7±0.1 Ma from a lamprophyre dike is identical within error to the U-Pb age of the dolerite dikes, indicating that tholeiitic and alkaline magmatism were coeval in the Ponta Grossa Arch.

The swarms of basic dikes of tholeiitic affinity of the Serra do Mar in São Paulo and Rio de Janeiro (134-130 Ma; $^{40}Ar/^{39}Ar$), could be separated into two different high-Ti and low-Ti suites, similar to the Ponta Grossa dikes and the basalt flows of the Paraná Igneous Province (Turner et al., 1994; Stewart et al., 1996; Corval et al., 2008). Models developed from the Serra do Mar Dike Swarm investigation suggest delamination of the subcontinental lithospheric mantle, encompassed by convective cells rising from the underlying sublithospheric mantle at shallow asthenospheric levels. These phenomena occur during an advanced stage of the Gondwana Supercontinent rifting (Valente et al., 2007; Corval, 2009).

The Florianópolis Dike Swarm consists predominantly of high-Ti diabases. The low–Ti terms are represented by basalts and basaltic trachyandesites and the dacites are geochemically similar to the Chapecó type acidic volcanic rocks from the Paraná Igneous

Province (Tomazzoli & Lima, 2006; Tomazzoli & Pellerin, 2015). Composite dikes occur in southern Florianópolis, with basaltic andesite edges and trachyandesite core, containing swarms of magmatic mafic enclaves. The Florianópolis Dike Swarm was formed between 128.3 $\pm$ 0.5 and 119.0 $\pm$ 0.9 Ma ($^{40}Ar/^{39}Ar$), and the magmatic peak occurred between 128 to 126 Ma and 122 to 119 Ma (Raposo et al., 1998; Deckart et al., 1998). Thus, these dikes are probably associated with the crustal strain in the final stages leading to the formation of the oceanic crust in this latitude (Marques & Ernesto, 2004). However, Florisbal et al. (2014) obtained U-Pb baddeleyite ages from 134.7 ± 0.3 to 133.9 ± 0.7 Ma, older ages than those indicated by $^{40}Ar/^{39}Ar$ and incompatible with a direct link with the syn-rift magmatism associated with the south opening of the Atlantic Ocean.

The Henties Bay-Outjo Dike Swarm in the Damara belt, Namibia, is interpreted as an aborted arm of a triple junction centered on the edge of Walvis Bay. It has a compositional range from basalt to rhyolite with predominantly basaltic low-Ti composition (Duncan et al., 1990; Trumbull et al., 2004, 2007). Picritic to rhyolitic dikes are part of this swarm, surrounding the Spitzkoppe, western Namibia, with up to 20% MgO, suggesting that the magma probably originated from the melting of a *mid-ocean ridge basalt* (MORB) mantle source, followed by the limiting reaction of the subcontinental lithospheric mantle, metasomatized just before the formation of these magmas (Thompson et al., 2001; 2007).

The Horingbaai dolerites have an affinity for the MORB magmas, with flat REE patterns and isotopic data that plot within the depleted mantle quadrant in the εSr vs. εNd diagram (Erlank et al., 1984; Hawkesworth et al., 1984; Duncan et al., 1989; Trumbull., et al 2007). The Huab River Valley sill complex and associated dikes are separated into four types of doleritic magmas distinguished from one another by different abundance ratios of incompatible elements (Duncan et al., 1989).

The Doros Complex is a layered mafic intrusion into the Damaraland Intrusive Suite, northeastern Namibia, and part of the Paraná-Etendeka Igneous Province with ages of 134-132 Ma ($^{40}Ar/^{39}Ar$) (Marsh & Duncan, 2008). Based on field, petrological and geophysics data, Owen-Smith & Ashwal (2015) proposed the origin of the Doros Complex as a result of at least seven spaced magmatic pulses. The authors suggest a large and complex system of interconnected channels and chambers that hosted a range of magmas of different compositions. Feeder dikes have been mapped out from the Doros Complex, which highlights this mafic center as being important to the development of the early stratigraphy in the Huab Basin (e.g. Jerram et al., 1999), and highlights the significance of the link between intrusions and the volcanic pile (e.g. Jerram & Bryan 2015).

4. LOCAL GEOLOGY

The investigated dikes are intruded in the basal volcanic flows of the Torres Formation (*ponded pahoehoe*), occupying interdune spaces of the Botucatu Formation, Torres Formation (*compound pahoehoe*) and subordinately the flows of the Vale do Sol Formation and acidic flows of the Palmas Formation at the top of the SGG volcanic sequence, southern Brazil. The sedimentary host rocks belong to the Botucatu Formation, Pirambóia Formation and Rio do Rasto Formation (Figure 2) (Sarmento et al., 2017).

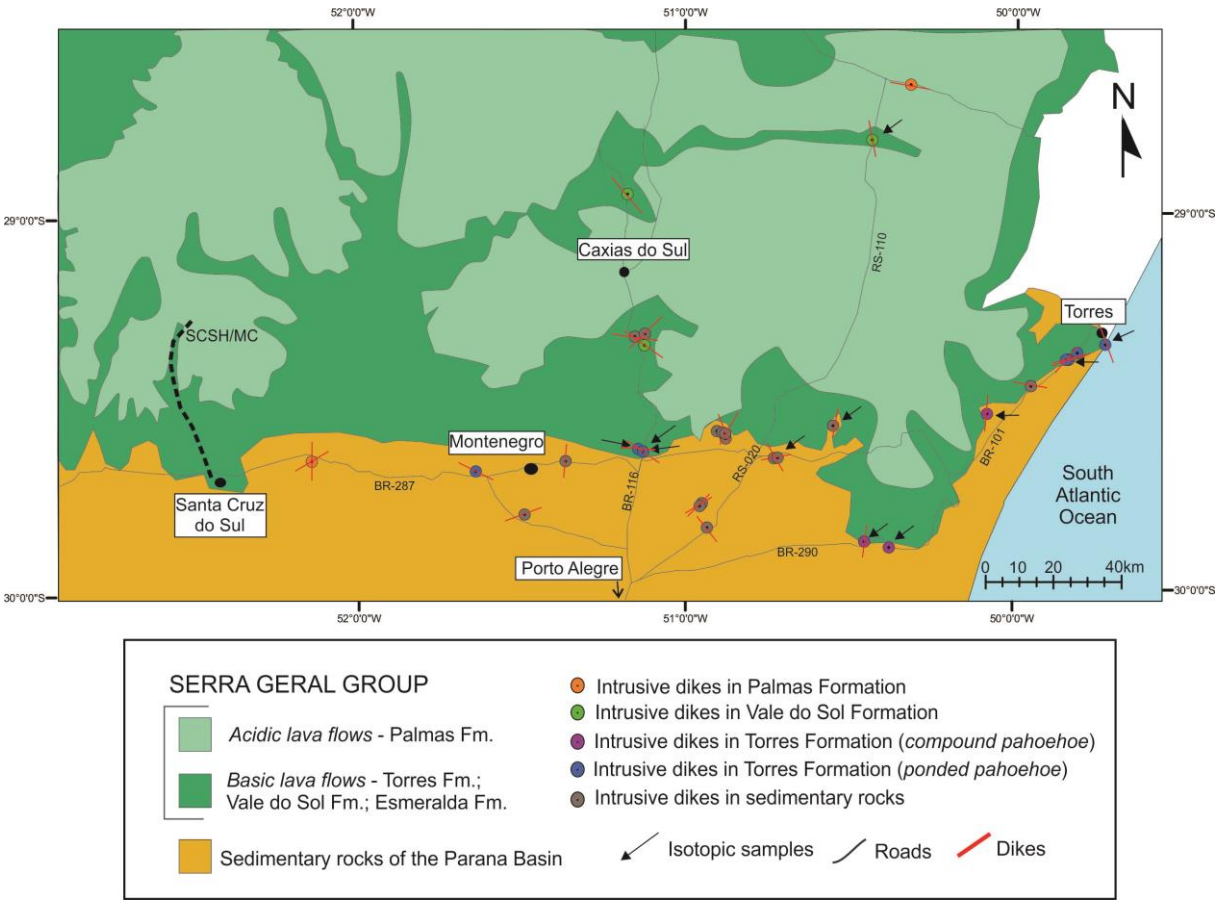

Figure 2. Geological map of the study area showing the sampling sites. Modified of CPRM (2010). (SCSH) = Santa Cruz do Sul / Herveiras region; (MC) = Morro da Cruz region.

The rocks are characterized by fine to medium equigranular texture in the central portions and aphanitic edges in thicker dikes. Regarding morphology, the dikes were separated into two distinct groups: symmetrical and asymmetrical.

The symmetrical dikes are the most common ones and intruding the Torres (Figure 3A and B), Vale do Sol and Palmas Formations flows, as well as the sedimentary rocks. They show tabular geometry, regular and straight contacts and thicknesses ranging from 1.0 m to 10 m. The presence of complex dike systems (Figure 3C) sometimes with small orthogonal secondary dikes parallel to the main igneous body are common. When they are intrusive in

sedimentary rocks, it is possible to observe the presence of small sills (5 to 10 cm) parallel to the main intrusion (Figure 3D). The asymmetric dikes occur in a restricted area in the eastern portion of the region, cutting of the Torres Formations flows (*ponded pahoehoe*). They are characterized by having reduced thicknesses (15.0 cm to 1.0 m) and usually show aphanitic texture. Dike systems with massive structure, centimetric to decimetric were observed, with no continuity in thickness. The possible presence of vesicles and xenoliths from the host rock is observed in these dikes (Figure 3 E).

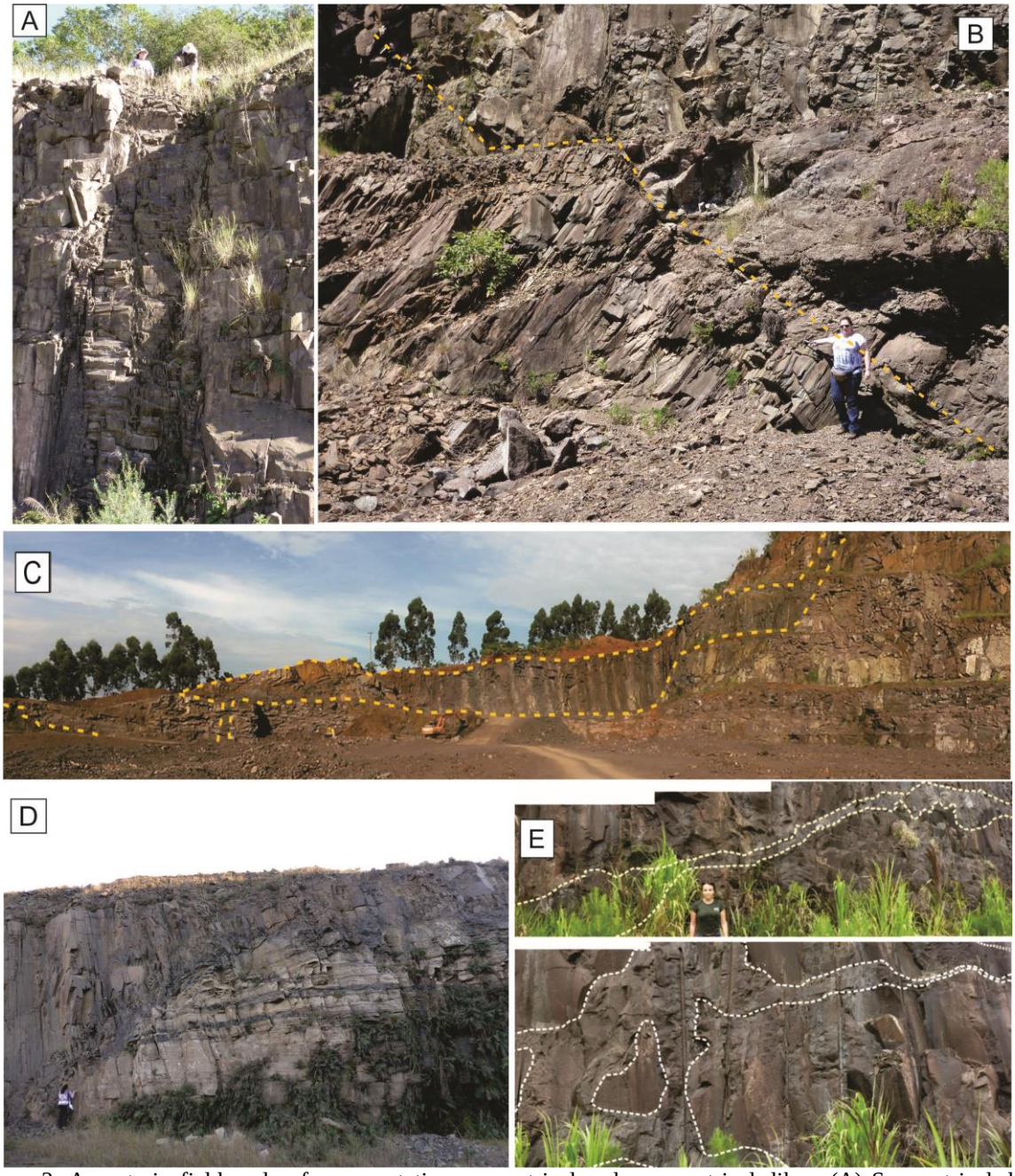

Figure 3. Aspects in field scale of representative symmetrical and asymmetrical dikes. (A) Symmetrical dike with well marked joints cutting Torres Formation (*ponded pahoehoe*) lava flow; (B) large dike cutting simple Torres Formation (*compound pahoehoe*) lava flow; (C) dike complex systems cutting Torres Formation (*compound pahoehoe*) lava flow; (D) dike cutting sedimentary rock; (E) Main aspects of asymmetrical dikes: In the photo above, the intrusive complex cut Torres Formation (*ponded pahoehoe*) lava flow; the photo below shows dikes within Torres Formation lava flow (From Sarmento et al. 2017).

5. PETROGRAPHY

The investigated dikes correspond to mesocratic dolerites and show holocrystalline to hypocrystalline texture. They are relatively homogeneous with fine-grained to aphanitic and predominantly equigranular texture. A slight textural variation can be identified, with grain size fining towards the edges, relative to the cores of the dikes (Figure 4).

The dikes were separated into two types: (i) Silica Supersaturated Tholeiite (SST) (comprising the asymmetric and most symmetrical dikes) with plagioclase (An~60), augite (~ $En_{38-47}Wo_{28-34}Fs_{22-33}$) and pigeonite (~ $En_{48}Wo_7Fs_{48}$) as essential minerals, opaques, apatite and sometimes olivine replaced by secondary minerals such as bowlingite and iddingsite (Figure 4). The predominant textures are intergranular and subordinate subophitic and the presence of felsic mesostasis (zeolite) is common; (ii) Silica Saturated Olivine Tholeiite (SSOT) (consisting of three symmetrical dikes embedded in the Torres Formation flows (*ponded pahoehoe*)) - mainly comprised by plagioclase (An>70), augite (~ $En_{40-43}Wo_{37-47}Fs_{13-22}$), and olivine (Fo~85). Opaque minerals and apatite are frequent accessory phases. The ophitic texture is predominant in this type (Figure 4C) (Sarmento et al., 2017).

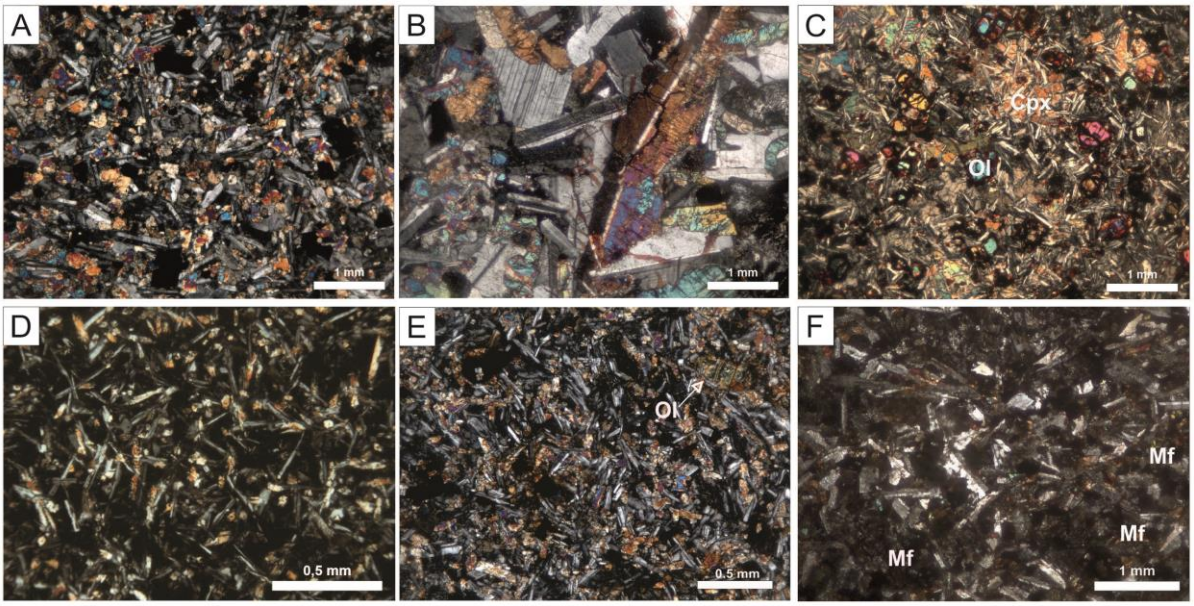

Figure 4. Microscopic aspects of representative dikes. (A) Fine-grained edge and (B) dike core embedded in the Torres Formation (*compound pahoehoe*) with medium-grained intergranular texture between crystals of plagioclase and clinopyroxene; (C) olivine crystals disseminated in the sample of the SSOT type and ofític texture on the clinopyroxene dike embedded in the Torres Formation (*ponded pahoehoe*); (D) assymetrical dike with acicular habit of plagioclase and glass matrix; (E) dike sample embedded in Vale do Sol Formation with intergranular texture and serpentinized olivine (F) Zeolitic aggregate in the interstices of plagioclase and clinopyroxene grains in dike embedded in sedimentary rocks (Botucatu Formation). Clinopyroxene (cpx), olivine (ol), felsic mesostasis (fm). Crossed nicols. (From Sarmento et al. 2017)

6. WHOLE-ROCK GEOCHEMISTRY

The chemical and mineralogical studies of the investigated dikes are detailed in Sarmento et al., 2017.

The analyzed samples were divided according to the type of host rocks. The intrusive dikes in the volcanic units were separated according of the SGG formations, following the proposal of Rossetti et al., (2017), used to hierarchize the south hinge flows of the Torres Syncline. On the other hand, intrusive dikes in sedimentary rocks, located on the south border of the Paraná basin, were all identified with a single symbol. The concentrations of major, trace and REE is shown in Table 1. The dikes are classified as basalts, basaltic andesites and trachyandesites in the TAS diagram (Le Bas et al., 1986) with of SiO_2 concentrations between 47.30 and 55.51% and alkalis between 5.41% and 2.36%. The subalkaline/tholeiitic affinity of the dikes is confirmed in the AFM diagram (Irvine & Baragar, 1971), combined with low Al_2O_3 values (Middlemost, 1975; Wilson, 1989) (Figure 5).

By using MgO as the differentiation index to establish the behavior of major and trace elements with the magmatism evolution of the hypabyssal rocks, the of Al_2O_3 and CaO contents tend to decrease with the decrease in MgO contents combined with the increase of SiO_2, Na_2O, K_2O, P_2O_5, FeO_t and TiO_2 (Figure 6). These patterns suggest that the magmatism evolution was basically controlled by the fractionation of plagioclase, augite, and titanomagnetite. The olivine fractionation must have occurred only in the least evolved rocks.

Regarding the behavior of the trace elements (Figure 7), there is an increase in the contents of Ba, Rb, Zr, Y, Nb and Th with the decrease of Mg contents. Nickel, on the other hand, has a positive correlation with MgO, suggesting the extraction of this element in mafic phases. This behavior can be explained by magmatic differentiation processes. SST dikes show low Ni content and MgO < 6%, indicating a relatively evolved condition of these magmas. SSOT dikes show less differentiated signatures, with Ni levels of 139 to 250 ppm and MgO values of 8.6 to 10.7%.

The CIPW normative compositions (Figure 8) highlight the differences between the major elements in the SSOT olivine tholeiite dikes and the SST quartz tholeiite dikes. The latter plot just below the composition of the experimental cotectic melting at 1 atm pressure (dashed line, based on Thompson et al., 1983; 2001). This condition suggests that the differentiation of these magmas occurred at relatively low pressures within the crust, as presented in previous studies on basaltic LTi magmas of MgO ~ 5% of the PEIP (Peate, 1997; Ewart et al., 1998).

The samples, when normalized to the primitive mantle standard (McDonough & Sun, 1995), show enrichment in incompatible elements, with negative Nb and Ta anomalies (Figure 9A and B). According to some authors, this pattern may suggest the presence of some residual phase rich in Nb and Ta, during the partial melting processes, or even be a consequence of crustal contamination (Wilson, 1989; Piccirillo et al., 1989; Hawkesworth, 1984). The negative Sr anomaly indicates the fractionation of plagioclase in the evolution of the intrusive bodies. The patterns observed in these multi-element diagrams and the LILE behavior (Large Ion Lithophile Elements) (K, Rb, Ba, Sr, Pb), combined with low levels of HFSE (High Field Strength Elements) (Nb, Ta, Zr, Hf; Ti, P) are very similar to those of intraplate tholeiitic basalts (Piccirillo et al., 1989). A slight increase in the fractionation is observed, mainly heavy rare earth elements (HREE), with increased differentiation (Figure 9C and D).

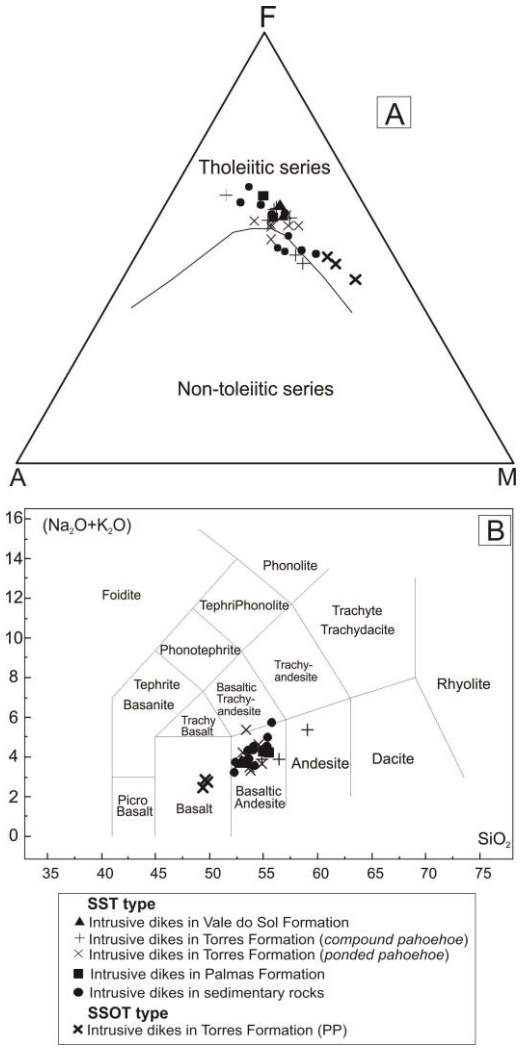

Figure 5. Classification Diagrams: (A) Diagram of AFM type (Na_2O + K_2O) - F (FeOt) - M (MgO), with the dividing line between the fields second Irvine &Baragar (1971) and (B) TAS (Le Bas et al., 1986).

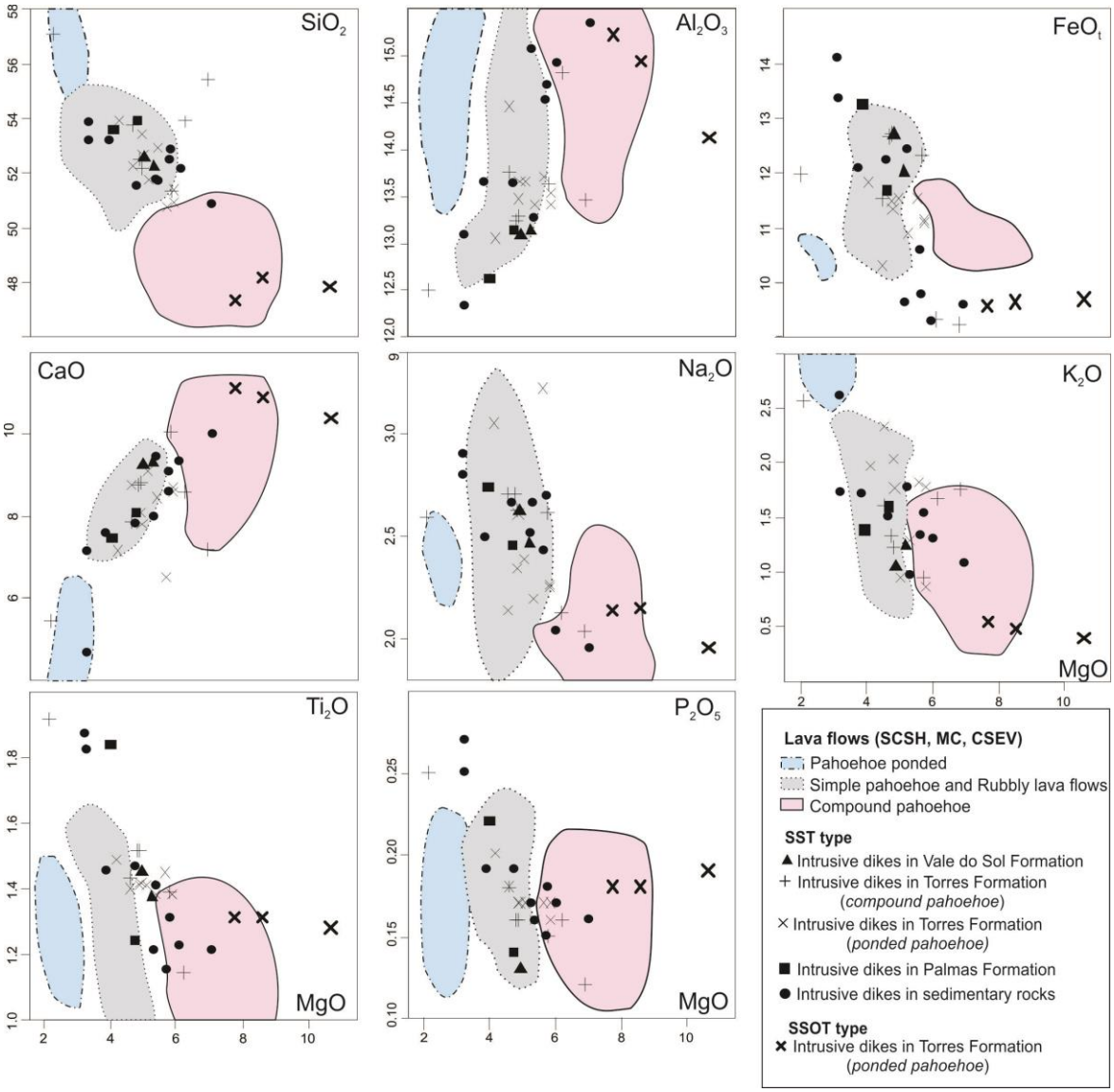

Figure 6. Binary diagrams displaying major elements variation (wt.%) relative to MgO of the studied rocks. Fields refer to lavas of the south hinge of theTorres Syncline (Barreto et al., 2014; Rossetti et al., 2014) of Santa Cruz do Sul / Herveiras (SCSH), Morro da Cruz (MC) and Caxias do Sul / Estancia Velha (CSEV) areas. (From Sarmento et al., 2017).

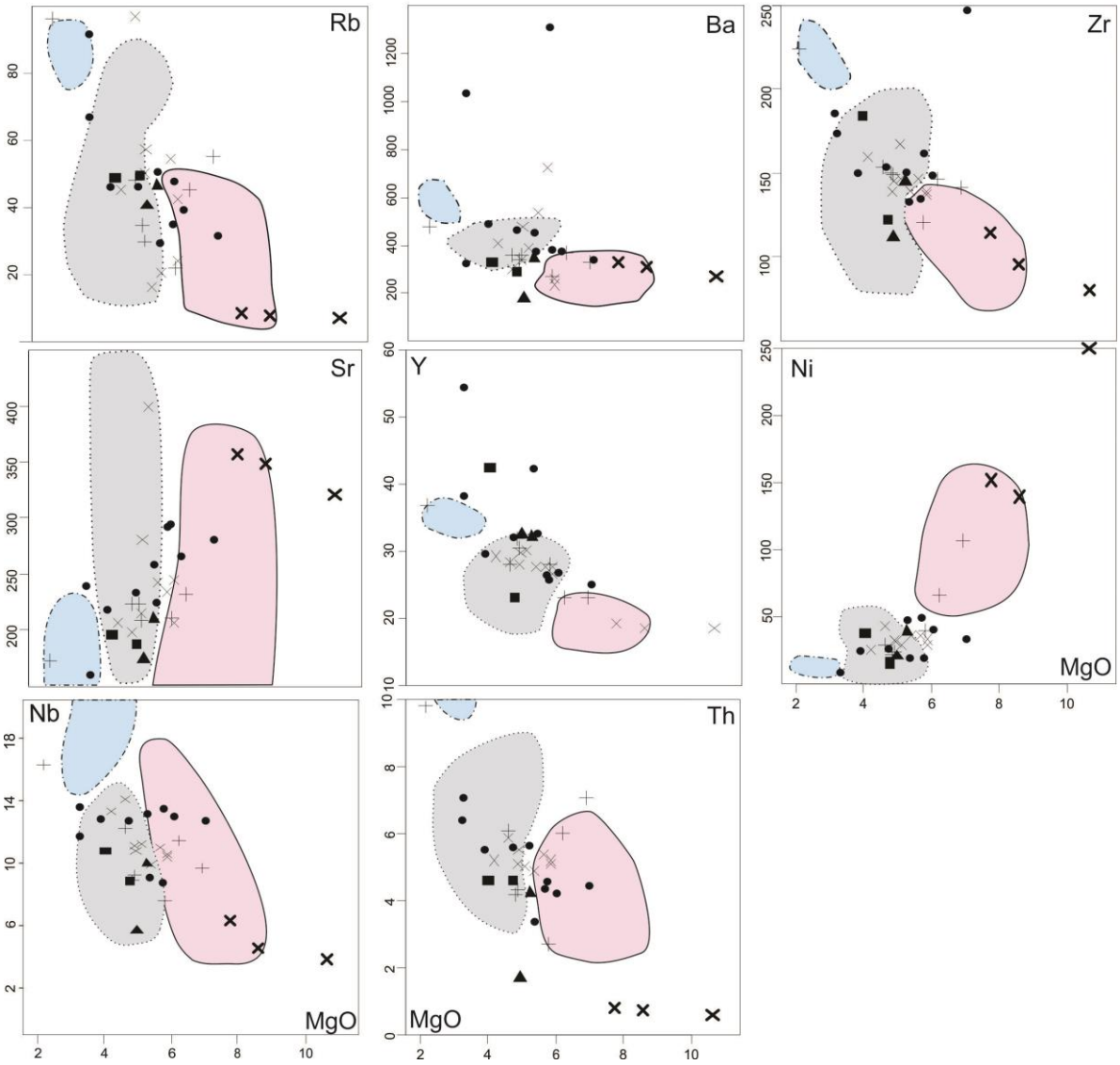

Figure 7. Binary diagrams displaying trace elements variation (ppm) relative to MgO (wt.%) of the studied rocks. Delimited fields refer to the lavas of the south hinge Torres Syncline (Barreto et al., 2014; Rossetti et al., 2014). Caption as in the figure 6 (From Sarmento et al., 2017).

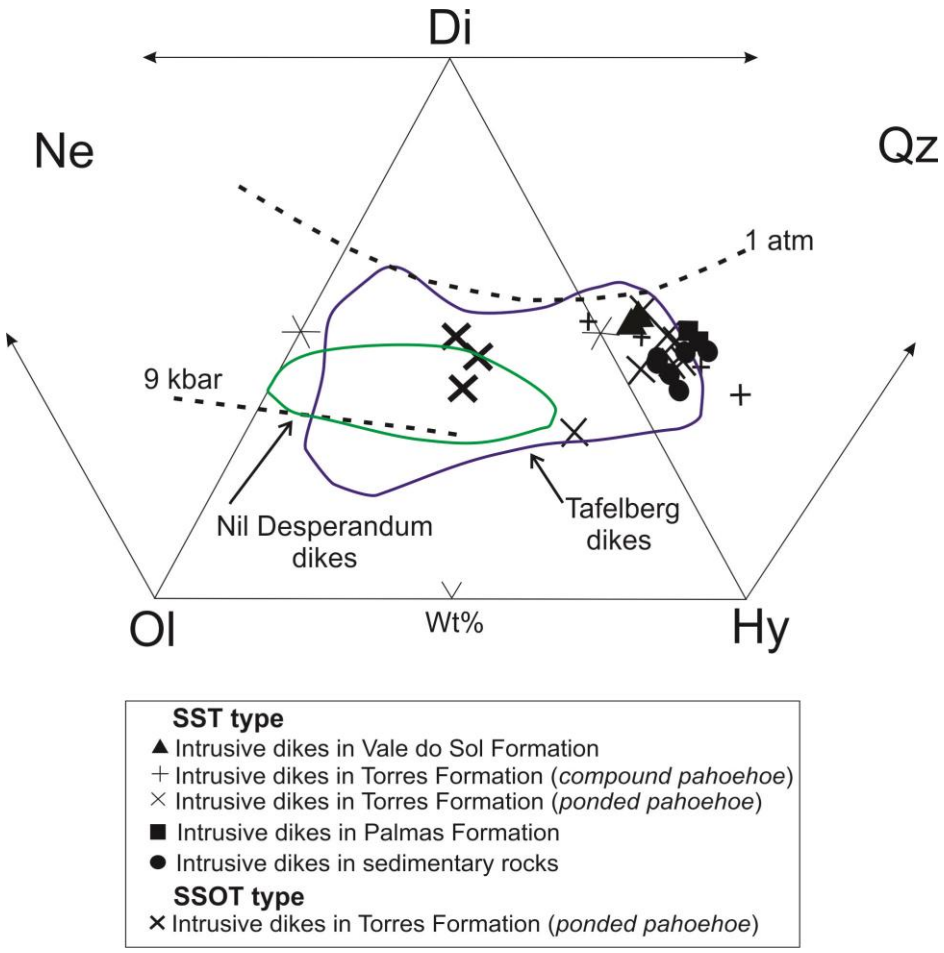

Figure 8. CIPW normative diopside, olivine, hyperstene, nepheline and quartz in investigated dikes. The norms assume a ratio of Fe_2O_3/FeO = 0,15. Cotectics at 1 atm and 9kbar for the equilibrium (ol + plag + cpx + basaltic liquid) are from Thompson et al. (1983; 2001). Field of Tafelberg and Nil Desperandum dikes are taken from Thompson et al. (2001) and Trumbull et al. (2007).

The SSOT dikes, when normalized to the C1 chondrite standard (McDonough & Sun, 1995), show relatively low REE patterns (ΣREE = 82 - 78) and slight enrichment in LREE relative to HREE (LaN/YbN = 3.7 - 3.9). They exhibit very little fractionation between light REEs (LaN/SmN = 1.6 – 1.8) and heavy REEs (TbN/YbN =1.5 – 1.6) and are devoid of negative Eu anomalies (Eu/Eu*N = 1.04) (Figure 9C).

The SST dikes show moderate patterns of these elements (Σ_{REE} = 82 - 207) and they are characterized by a slight enrichment in light REEs compared to heavy REEs (La_N/Yb_N = 2.0 – 6.6). They show a slight fractionation in light REEs (La_N/Sm_N = 1.4 – 2.8) and in heavy REEs (Tb_N/Yb_N = 1.2 – 1.5) (Figure 9C and D). Slight negative Eu anomalies are observed (Eu/Eu^*_N = 0.83), which suggests plagioclase fractionation.

The pattern presented by the intrusions are similar to those presented by Peate et al. (1992, 1997, 1999) and Marques et al. (1989) for tholeiitic basalts of large continental provinces such as those of the Paraná Province. All the studied samples show TiO_2 concentrations lower than 2%, which allows them to be related to low-Ti magmas,

characteristic of the south sub-province of the Paraná Magmatic Province. According to several authors (Mantovani et al., 1985; Marques et al., 1989; Peate et al., 1992), the low-Ti group can be subdivided into three subgroups, or different magma types, called Ribeira, Esmeralda, and Gramado, according to criteria based on the concentrations of TiO_2, SiO_2 and other incompatible trace elements.

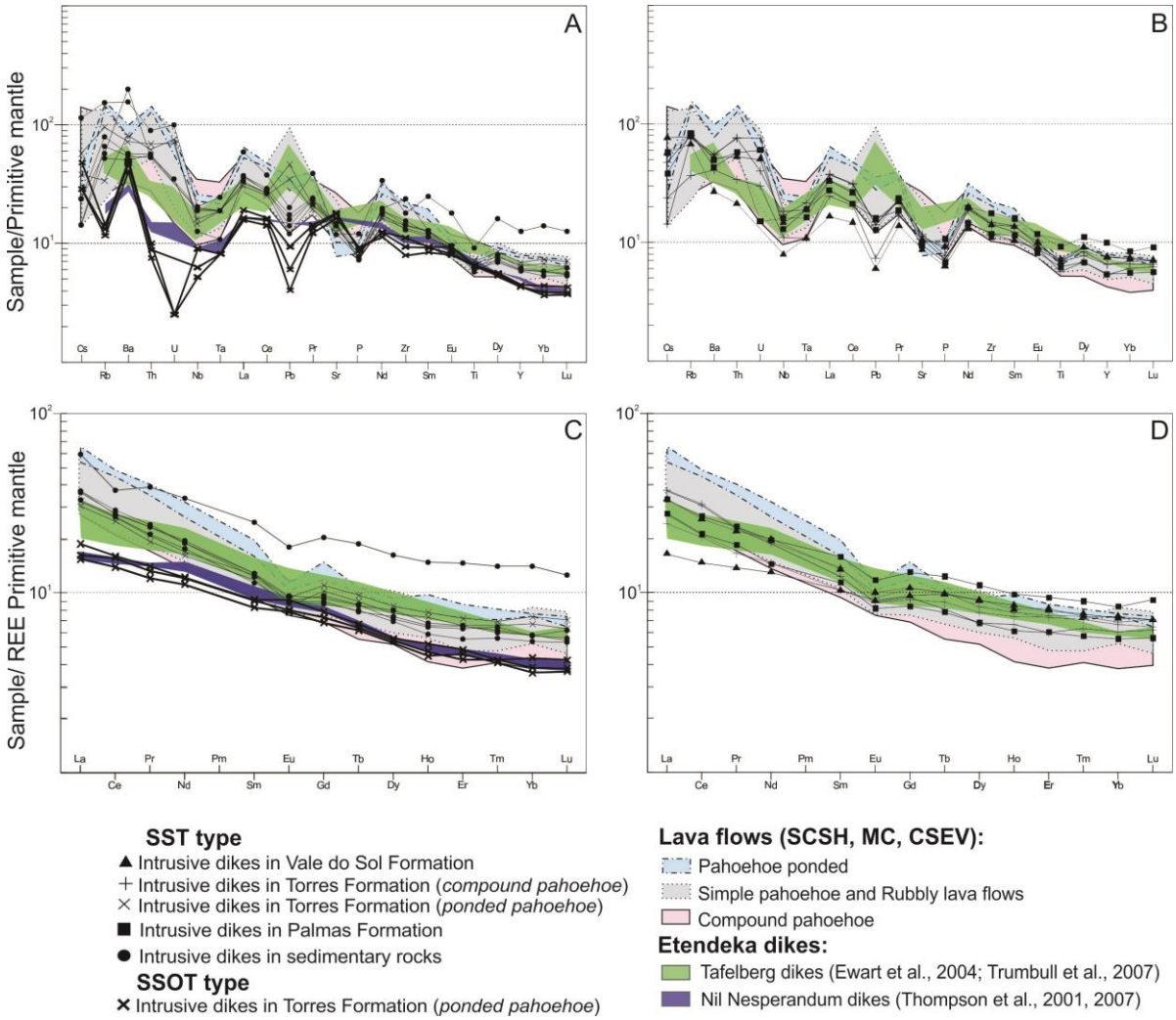

Figure 9. Trace element abundance (A and B) and REE patterns (C and D) normalized to the primitive mantle (McDonough & Sun, 1995) and chondrite C1 of the studied rocks. Delimited fields refer to the lavas of the south hinge Torres Syncline (Barreto et al., 2014; Rossetti et al., 2014).

*Table 1. Lithochemical results of representative samples of dikes and lava flows for major elements (wt.%), trace and REE (ppm). *SSOT; # Barreto et al., (2016).*

Samples	PDY-9B*	PDY-9D*	PDY-47*	PDY-36	PDY-16	PDY-20C	PDY-12B	PDY-21	PDY-22A
Host rocks	*Pahoehoe pounded*	*Pahoehoe pounded*	*Pahoehoe pounded*	*Pahoehoe pounded*	*Pahoehoe pounded*	*Pahoehoe pounded*	*Compound pahoehoe*	*Compound pahoehoe*	*Compound pahoehoe*
SiO_2	47.76	48.12	47.30	52.25	52.96	50.74	51.33	53.93	57.16
Al_2O_3	14.12	14.94	15.23	14.46	13.41	13.71	13.64	14.83	12.5
FeOtot	9.71	9.66	9.58	10.32	10.93	11.56	12.33	9.35	12
MnO	0.17	0.17	0.16	0.15	0.23	0.17	0.21	0.16	0.13
MgO	10.66	8.58	7.75	4.63	5.4	5.64	5.79	6.2	2.15
CaO	10.4	10.9	11.11	8.74	8.44	6.47	10.04	8.59	5.39
Na_2O	1.96	2.15	2.14	2.14	2.2	3.22	2.62	2.13	2.59
K_2O	0.4	0.48	0.56	2.34	1.3	1.83	0.95	1.67	2.56
TiO_2	1.28	1.31	1.31	1.4	1.38	1.45	1.39	1.14	1.92
P_2O_5	0.19	0.18	0.18	0.18	0.16	0.17	0.15	0.16	0.25
LOI	1.8	2.1	3.2	1.9	2.1	3.4	0.1	0.5	1.7
Total	99.69	99.71	99.69	99.74	99.72	99.69	99.74	99.75	99.75
Rb	6.9	7.8	8.5	96.8	20.2	54.6	22.1	45.4	96.1
Ba	264	310	325	296	537	724	269	365	479
Sr	321	350	357.9	199	244	234	212	232	174
Ga	14	14.2	15.8	20.4	19.2	18.2	17.5	17.7	20.1
Zr	82.5	97.6	116.4	358.5	141.1	148.2	122.7	147.9	224.6
Y	18.5	18.5	19.1	28.3	27.8	27.8	28	23	37
Nb	3.4	4.1	5.9	13.9	9.6	10.7	7.2	11.2	16.1
Sc	35	36	37	34	34	35	40	31	31
V	261	270	287	300	355	378	373	239	440
Co	51.2	47.3	50.3	41.7	37.2	39.8	45.1	40.5	30.7
Ni	250	139	151.2	42	35	35	39	65	20
Cu	95	95	85.5	121	149	166	165	35	132
Zn	45	48	49	60	55	73	43	34	85
La	10.1	10.6	12.3	26.2	19.8	22.7	15.8	23.9	35.1
Ce	23.6	26.5	27.2	53.7	42	48.1	34.3	51.6	74.3
Pr	3.1	3.4	3.60	6.8	4.9	5.7	4.2	5.8	8.5
Nd	14.1	15.2	15.4	27.1	20.2	23	18.3	23.5	34.7
Sm	3.4	3.7	3.77	5.5	4.8	5.3	4.2	5	7.1
Eu	1.22	1.25	1.43	1.42	1.3	1.5	1.35	1.37	1.79
Gd	3.75	4	4.31	5.79	5.55	5.8	4.98	5.12	7.74
Tb	0.62	0.64	0.67	0.96	0.89	0.96	0.88	0.8	1.32
Dy	3.59	3.71	3.80	5.56	5.17	5.8	5.22	4.57	7.45
Ho	0.67	0.71	0.78	1.04	1.09	1.27	1.1	0.99	1.49
Er	2.02	1.88	2.14	2.93	2.88	3.32	3.19	2.63	4.08
Tm	0.28	0.29	0.29	0.45	0.45	0.51	0.48	0.43	0.63
Yb	1.6	1.71	1.93	3.09	2.96	3.31	2.93	2.67	4.17
Lu	0.25	0.26	0.29	0.46	0.43	0.49	0.44	0.42	0.59
Hf	2.2	2.5	3.1	9.4	3.7	4.1	3.4	4.3	6.1
Ta	0.3	0.3	0.3	1.2	0.7	0.6	0.4	0.8	1.1
Pb	0.6	0.9	1.4	7.9	5.2	8.7	1.1	2.1	3.8
Th	0.6	0.7	0.8	5.9	4.9	5.4	2.7	6	9.8
U	<0.1	0.1	<0.1	0.5	1.5	1.7	0.6	0.8	2.9

Table 1. (continued)

Samples of dikes	PDY-38A	PDY-10	PDY-25	PDY-31B	Samples of Lava flows	PDY-35D	PSC2C#	PSC26#	PSC4B#	PSC20#
Country rocks	*rubbly*	*Sedimentary rocks*	*Sedimentary rocks*	*Sedimentary rocks*		*Ponded pahoehoe*	*Compond pahoehoe*	*Simple pahoehoe*	*rubbly*	*rubbly*
SiO_2	52.55	52.53	52.87	52.18	SiO_2	60.87	49.45	53.20	55.46	52.22
Al_2O_3	13.07	14.52	14.7	14.92	Al_2O_3	12.49	15.39	14.88	12.97	14.24
FeOtot	12.75	10.64	9.77	9.28	FeOtot	9.92	10.56	9.62	13.69	13.09
MnO	0.24	0.18	0.16	0.15	MnO	0.16	0.16	0.17	0.19	0.2
MgO	4.96	5.71	5.82	6.1	MgO	1.54	5.96	5.45	3.11	4.77
CaO	9.26	9.08	8.58	9.3	CaO	4.54	10.42	8.91	6.57	8.63
Na_2O	2.62	2.43	2.69	2.04	Na_2O	2.88	2.09	2.21	2.57	2.53
K_2O	1.05	1.33	1.55	1.31	K2O	3..28	0.85	1.92	2.19	1.17
TiO_2	1.45	1.15	1.3	1.21	TiO_2	1.55	0.15	1.14	1.56	1.47
P_2O_5	0.13	0.15	0.18	0.17	P_2O_5	0.25	2.5	0.17	0.2	0.2
LOI	0.2	0.7	1	2	LOI	1.2	0.16	1.1	1.3	1.2
Total	99.76	99.64	99.74	99.74	Total	99.76	99.79	99.80	99.76	99.77
Rb	40.4	34.5	47.3	39.2	Rb	121.7	49.3	73.2	81.3	41.5
Ba	178	1310	380	361	Ba	596	350	358	404	330
Sr	174	292	294	269	Sr	186	258.2	211	214.6	225.7
Ga	17	17.9	17.2	15.9	Ga	17.7	18	16.8	23.2	20
Zr	114.3	136.2	161.7	150.4	Zr	422.3	115	144.3	168.5	147.7
Y	32.6	26.1	25.7	26.7	Y	39.6	30.8	24.3	31.1	29
Nb	5.2	8.3	13.2	12.7	Nb	18.3	6.6	8.7	12.9	9.4
Sc	40	36	34	33	Sc	24	35	32	33	34
V	362	288	275	266	V	157				
Co	47.8	41.5	39.3	40.6	Co	23.8	40.9	38.1	39.1	36.7
Ni	20	48	17	39	Ni	<20				
Cu	192	63	35	15	Cu	29				
Zn	48	43	40	41	Zn	89				
La	10.7	21.5	24.1	23.9	La	41.9	24.7	22	26.7	23.1
Ce	24.7	44.6	48.3	46	Ce	83	41.4	46.2	54.7	46
Pr	3.5	5.4	6.1	5.9	Pr	10.4	6.24	5.84	6.8	5.69
Nd	16.3	22	23.7	23.7	Nd	41.4	27.8	25.4	27.9	22
Sm	4.2	4.6	5	5.2	Sm	8.5	5.53	4.82	5.88	4.96
Eu	1.39	1.38	1.39	1.48	Eu	2	1.61	1.33	1.53	1.49
Gd	5.22	4.86	5.22	5.07	Gd	8.56	6.32	5.41	6.05	5.61
Tb	0.97	0.78	0.85	0.84	Tb	1.35	0.91	0.77	1	0.84
Dy	6.11	4.96	4.81	5.38	Dy	8.03	5.94	4.45	5.34	5.68
Ho	1.27	0.98	0.96	1.01	Ho	1.47	1.13	0.92	1.22	1.07
Er	3.49	2.86	2.78	2.88	Er	4.5	3.17	2.55	3.19	2.73
Tm	0.52	0.42	0.44	0.41	Tm	0.64	0.44	0.38	0.44	0.43
Yb	3.18	2.55	2.53	2.56	Yb	4.09	2.78	2.45	2.75	2.92
Lu	0.48	0.38	0.42	0.37	Lu	0.66	0.43	0.39	0.44	0.41
Hf	3.4	3.8	4.4	3.9	Hf	11.6	3.8	4.1	4.8	4.1
Ta	0.4	0.4	0.7	0.7	Ta	1.3	0.5	0.6	0.8	0.5
Pb	0.9	1.8	2.6	2.4	Pb	4.8	2.6	1.9	2.9	3.1
Th	1.7	4.3	4.5	4.2	Th	11.7	3.6	5.9	7.1	5.7
U	<0.1	0.7	<0.1	<0.1	U	1.9	0.6	1.1	1.4	1.5

7. GEOCHEMISTRY OF THE Sr-Nd-Pb ISOTOPES

The isotope analyzes of Sr, Nd, and Pb are shown in table 2 and in Figures 10 and 11. These figures include the fields of Pitanga, Paranapanema, and Urubici (HTi) magma types and Gramado and Esmeralda (LTi) magma types (Mantovani et al., 1985; Hawkesworth et al., 1986; Petrini et al., 1987; Piccirillo et al., 1989; Peate et al., 1992, 1999; Peate & Hawkesworth, 1996; Rocha-Júnior et al., 2013). In addition, these figures include the fields of the SGG basic flows, of ponded pahoehoe, compound and simple pahoehoe, and rubbly flows, belonging to the south hinge of the Torres Syncline (Barreto et al., 2016). The initial $^{87}Sr/^{86}Sr$ and $^{143}Nd/^{144}Nd$ ratios were recalculated for the mean age of 132 Ma, based on published Ar-Ar ages for Paraná basalts (e.g. Renne et al., 1992; Thiede & Vasconcelos, 2010) and the U-Pb ages obtained in felsic rocks of this province (Janasi et al., 2011).

The SSOT dikes show relatively low initial $^{87}Sr/^{86}Sr_i$ ratios, between 0.70570 and 0.70585, and εNd_i values between -1.01 and -4.49 ($^{143}Nd/^{144}Nd$ = 0.51242 and 0.51224). Samples of SST dikes show a higher variation, with $^{87}Sr/^{86}Sr$ ratios ranging from 0.70786 to 0.71637, with corresponding values of εNd_i ranging from -2.51 to -7.05 ($^{143}Nd/^{144}Nd$ = 0.51234 to 0.51211).

In the of $^{143}Nd/^{144}Nd_i$ versus $^{87}Sr/^{86}Sr_i$ diagram (Figure 10), the SSOT dike samples are plotted within the Urubici, Paranapanema and Pitanga magma fields, with one of the samples plotting in the slightly enriched mantle reservoir (EM-I).

The SST dikes that cut the Torres Formation exhibit a greater range of $^{87}Sr/^{86}Sr_i$, without showing a direct isotope correlation between the host rocks and the dikes. The intrusive dike sample in the Vale do Sol Formation has more radiogenic Nd and less radiogenic Sr, similar to the most primitive LTi flows of the Gramado magma-type.

The analyzed SSOT dike sample shows present-day Pb isotope composition of 18.0306 for $^{206}Pb/^{204}Pb$, 15.6192 for $^{207}Pb/^{204}Pb$ and 38.9327 for $^{208}Pb/^{204}Pb$. The SST dikes have ratios of 18.5785 - 19.0490 for $^{206}Pb/^{204}Pb$, 15.6542 - 15.7139 for $^{207}Pb/^{204}Pb$ and 38.8315 - 39.1370 for $^{208}Pb/^{204}Pb$. In the of $^{207}Pb/^{204}Pb$ versus $^{206}Pb/^{204}Pb$ and $^{208}Pb/^{204}Pb$ versus $^{206}Pb/^{204}Pb$ diagrams (Figure 11), samples of the analyzed dikes plot above the Northern Hemisphere Reference Line (NHRL) (Allegre et al., 1988). The SST dikes show present-day Pb ratios close to the Gramado magma-type field, although some samples are more radiogenic, like the present-day Pb ratios of the more radiogenic lavas of the Torres Formation.

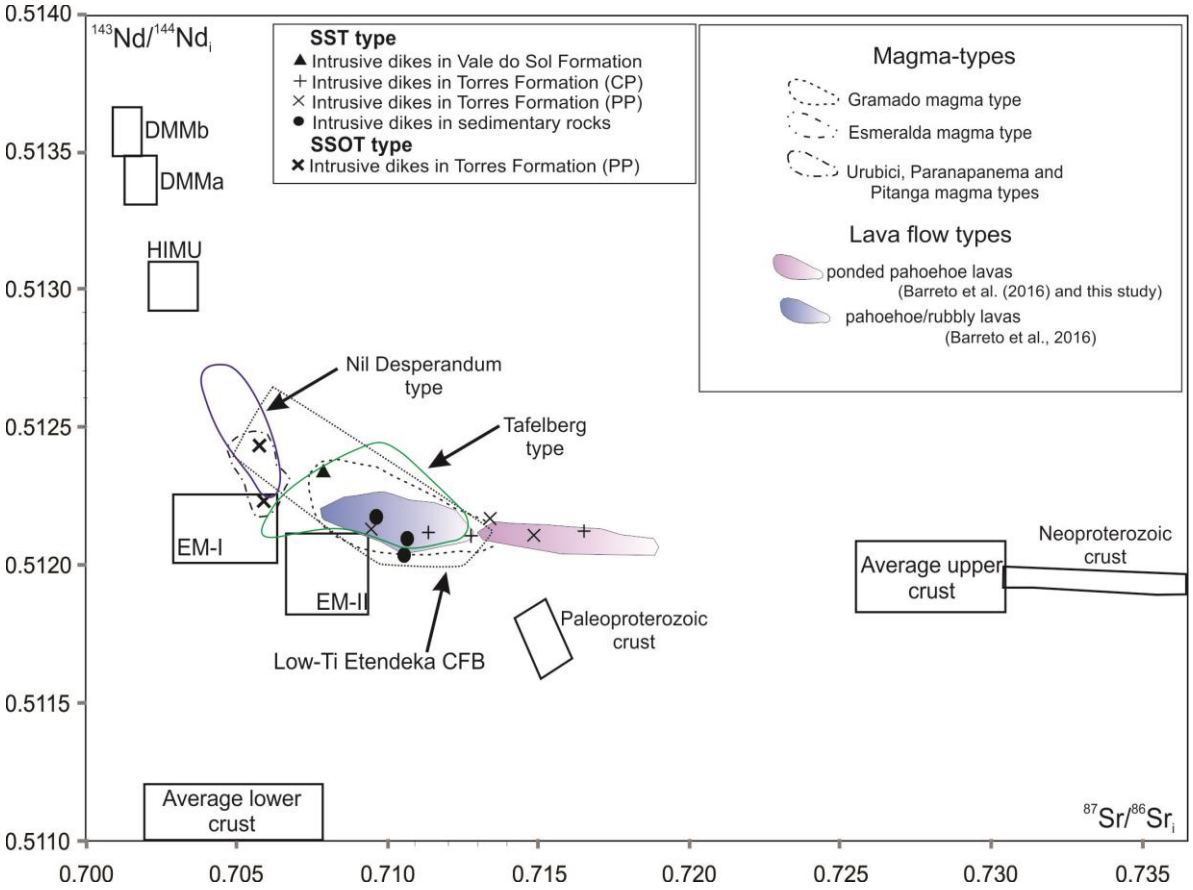

Figure 10. $^{143}Nd/^{144}Ndi$ versus $^{87}Sr/^{86}Sri$ variation diagram for the studied intrusions. Dotted fields ascribed some magma types of the Paraná-Etendeka CFBs (Mantovani et al., 1985; Petrini et al., 1987; Piccirillo et al., 1989; Peate et al., 1992, 1999; Peate and Hawkesworth, 1996; Ewart et al., 1998, 2004; Rocha-Júnior et al., 2013). Fields of the Tafelberg type and Nil Desperandum type of the Etendeka dikes are taken from Ewart et al. (2004), Trumbull et al. (2007) and Thompson et al. (2001; 2007). The lava flows of the SCSH and MC (Barreto et al. 2016) were inserted for comparison. The mantle components DMMa, DMMb, HIMU, EM-I, and EM-II are taken from Zindler and Hart (1986). The boxes for average upper and lower crusts are taken from Taylor and McLennan (1985). The Palaeoproterozoic (Gregory 2014) and Neoproterozoic crusts (Florisbal et al. 2009) of the basement are also represented.

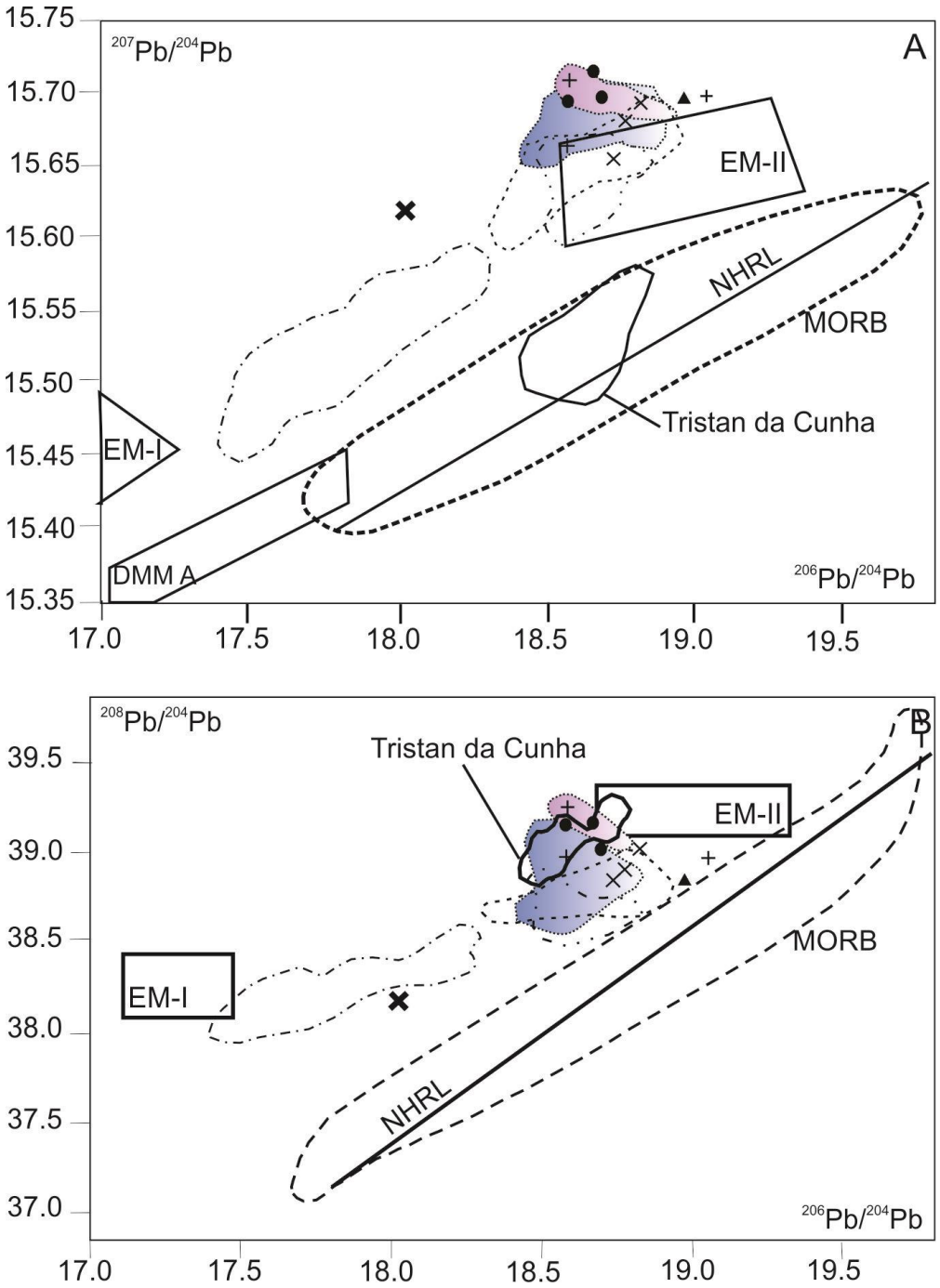

Figure 11. Lead isotope compositions for dikes in comparison to the fields for Tristan da Cunha volcanics (Rohde et al., 2013), and the mantle components EM-I, EM-II, and DMMA (Zindler & Hart, 1986). Neoproterozoic crust (Florisbal et al. 2009) of the basement is also represented. NHRL, Northern Hemisphere Reference Line (Hart, 1984). Symbols and fields of magma types are as in Figure 10 caption.

Table 2. Isotopic compositions of Sr, Nd, and Pb in studied dikes and representative samples of the lava flows studied

Samples (dikes)	$^{87}Sr/^{86}Sr$	$^{87}Sr/^{86}Sr_{(i)}$	$^{143}Nd/^{144}Nd$	$^{143}Nd/^{144}Nd_{(i)}$	$eNd_{(i)}$	T_{DM} (Ga)	$^{206}Pb/^{204}Pb$	$^{207}Pb/^{204}Pb$	$^{208}Pb/^{204}Pb$
PDY-9B*	0.70592(12)	0.70570	0.512552(20)	0.512419	-1.01	1.24	n.d.	n.d.	n.d.
PDY-9D*	0.70607(27)	0.70585	0.512328(24)	0.512241	-4.49	0.97	18.0306(84)	15.6192(72)	38.1288(175)
PDY-10	0.71081(20)	0.71059	0.512144(16)	0.512028	-8.65	1.74	n.d.	n.d.	n.d.
PDY-12A	0.71155(14)	0.71133	0.512245(13)	0.512122	-6.82	1.71	18.583 (62)	15.663 (51)	38.933(127)
PDY-16A	0.70964(32)	0.70942	0.512249(27)	0.512127	-6.72	1.68	18.737 (29)	15.654 (26)	38.8343(66)
PDY-20B	0.71502(16)	0.71479	0.512242(20)	0.512117	-6.91	1.77	18.775 (55)	15.680 (46)	38.8763(115)
PDY-21	0.71295(16)	0.71273	0.512216(9)	0.512105	-7.14	1.48	18.584 (80)	15.707 (66)	39.232(166)
PDY-22A	0.71660(25)	0.71637	0.512233(15)	0.512127	-6.70	1.35	19.049 (39)	15.697(32)	38.953 (84)
PDY-25	0.71081(22)	0.71058	n.d.	n.d.	n.d.	n.d.	18.668 (30)	15.714(25)	39.144 (65)
PDY-28	0.70991(15)	0.70969	0.512293(13)	0.512177	-5.73	1.43	18.696 (43)	15.696 (37)	39.001(92)
PDY-31B	0.71075(28)	0.71053	0.512214(52)	0.512099	-7.25	1.56	18.578 (13)	15.694(12)	39.137 (29)
PDY-36	0.71358(28)	0.71336	0.512270(17)	0.512164	-5.98	1.29	18.826 (54)	15.693(45)	39.001 (109)
PDY-38B	0.70809(42)	0.70787	0.512491(20)	0.512342	-2.51	2.02	18.973 (29)	15.696 (24)	38.831 (58)
Host Samples (lava flows)									
PDY-35D	0.71883 (19)	0.71861	0.512174(20)	0.512060	-8.01	1.61	18.939(08)	15.688(7)	38.946(17)
PSC-2C[#]	0.71128(117)	0.71024	0.512159(12)	0.512045	-8.31	1.65	18.499(16)	15.678(14)	38.909(36)
PSC-26[#]	0.71430(15)	0.71242	0.512220(4)	0.512108	-7.09	1.50	18.742(2)	15.698(2)	39.082(6)
PSC-4B[#]	0.71502(35)	0.71296	0.512232(12)	0.512118	-6.89	1.52	18.795(6)	15.669(5)	38.913(14)
PSC-20[#]	0.711125(22)	0.71012	0.512295(8)	0.512180	-5.68	1.42	18.781(3)	15.669(2)	38.847(6)

Initial ratios for Sr and Nd and epsilon values corrected to 132 Ma; Pb ratios are measured; Measurement errors for Sr and Nd isotope ratios in parenthesis refer to last digits (2σ); n.d. = not determined; [#] Barreto et al. (2016); *SSOT dike types.

8. DISCUSSIONS

8.1. *Relationship between the dikes of the Paraná and Etendeka Provinces*.

Based on comparative studies of the geochemical and isotopic signatures of the studied dikes with lower Cretaceous mafic LTi dikes in northwestern Namibia, a similarity was observed of the SST dikes with the quartz-tholeiitic Tafelberg magma dikes of the Henties Bay-Outjo dike swarm (Figure 10), with initial isotopic ratios consistent with a lithospheric source and lower crustal source input ($^{87}Sr/^{86}Sr$ = 0.7101 to 0.7122; εNd= -2 to -7 and $^{206}Pb/^{204}Pb$ = 18.74 to 19.10 (Erlank et al., 1984 ; Duncan et al., 1990; Thompson et al., 2001, 2007; Trumbull et al., 2004, 2007). The LTi Tafelberg magma type (Erlank et al., 1984), which includes flows and intrusive bodies of the Etendeka Province, have geochemical and isotopic signatures similar to that of the LTi Gramado magma-type of the Paraná Province (Milner et al., 1995). These two magma-types are very heterogeneous with respect to their Nd and Sr isotopic compositions, which is consistent with their variable trace element characteristics (Ewart et al., 2004).

The SSOT type dike samples are isotopically similar to the HTi Paranapanema and Pitanga magma types (Figure 10). This condition is also observed when incompatible trace element Ti/Zr vs. Ti/Y ratios are compared (Figure 15; Sarmento *et al.*, 2017), which are similar to those of the LTi Tafelkopf magma type of the Etendeka Province. The LTi SSOT

dikes show a geochemical signature of major and trace elements similar to the low-Ti intrusions related to the Etendeka Province in the northwest and southeast of Namibia, such as the Henties Bay-Outjo dike swarms and False Bay with MgO > 6 % (La_N/Yb_N 2-4) (Duncan et al., 1990; Trumbull et al., 2007; Thompson et al., 2001, 2007), and the Huab River Valley sills (Duncan et al., 1989). When compared with the isotopic ratio variations of the African intrusions, they show greater similarity with the olivine-tholeiitic dolerites of the LTi Nil Desperandum magma type proposed by Thompson et al. (2001) (La/Nb_n = ~ 2.0 – 2.5; $^{87}Sr/^{86}Sr$ = 0.7036 to 0.7077, εNd = - 1.42 to +3.63 and $^{206}Pb/^{204}Pb$ = 17.56 to 19.71), although the SSOT dikes have higher ratios of La/Nb_n = ~ 2.5 – 3.0. These dikes belong to the Nil Desperandum-Twyfelfontei dike swarm. According to Trumbull et al. (2007), the Nil Desperandum dolerites have element patterns normalized to the Primitive Mantle similar, but somewhat more uniform, such as the Tafelberg type (low Pb, Rb, U, Th) and less radiogenic isotopic ratios.

This finding confirms the hypothesis of Sarmento et al., (2017) that shows the geochemical similarity to the intrusions related to the Etendeka Province in Namibia, such as the low-Ti dike swarms (Duncan et al., 1990; Trumbull et al., 2007; Thompson et al., 2001; 2007) and the Huab River Valley sills (Duncan et al., 1989).

8.2. *Torres Syncline dikes and flow associations.*

There are several studies on the geochemical correlation and Sr-Nd-Pb isotope compositions of dikes with lava flows related to continental basaltic provinces such as Deccan (Bondre et al., 2006; Seth et al., 2009, 2013; Vanderkluysen et al., 2011), Columbia River (e.g. Brueseke et al., 2007, Wolff et al., 2008) and the Paraná-Etendeka Province (Hawkesworth et al., 1984; Duncan et al., 1989; Piccirillo et al., 1990). These studies were mostly based on the geochemical and isotopic characterization of the flow types.

The SST dikes samples, when compared to the flows according to the lithofacies associations of the Santa Cruz/Herveiras and Morro da Cruz regions in southern Brazil, with $^{87}Sr/^{86}Sr_i$ = 0.707798 to 0.712962, $\varepsilon Nd_{(132)}$ = -8.36 to -5.41 and $^{143}Nd/^{144}Nd_i$ = 0.512045 - 0.512194 (Barreto et al., 2016) (Figure 11), show the similarity of the pahoehoe and rubbly flows, with all the samples of intrusive dikes in sedimentary rocks, two samples of intrusive dikes in the Torres Formation (*compound pahoehoe*) flows and one sample of intrusive dikes in the Torres Formation (*ponded pahoehoe*) flows. These dikes show high initial isotopic Sr

ratios, very low εNd and high $^{207}Pb/^{204}Pb$ ratios, along with low Ni and Mg contents, supporting the hypothesis that these magmas must have undergone significant crustal contamination in the magma chamber. In the field of ponded pahoehoe flows, with high initial $^{87}Sr/^{86}Sr_i$ ratios of 0.715629 to 0.715751, εNd_i ranging from -8.20 to -8.08 and $^{143}Nd/^{144}Nd_i$ = 0.512051 - 0.512057 (Barreto et al., 2016), three samples are plotted, with two samples of intrusive dikes in the Torres Formation (*ponded pahoehoe*) flows and one sample of intrusive dikes in the Torres Formation (*compound pahoehoe*) flows, the latter exhibiting the most radiogenic Sr signature. The intrusive dike sample in the Vale do Sol Formation flows is not found in any of the previously mentioned types of flows, but it has an isotopic signature similar to the more primitive terms of the Gramado magma-type.

The SSOT dikes are positioned near the field of slightly enriched mantle reservoir (EM-I). They have less radiogenic isotopic ratios than all the other studied samples of dikes and lavas flows. This suggests the possible sources of these magmas are: (a) recycling of the sub-continental delaminated lithosphere; b) recycling of old subducted pelagic sediments and also low U and Th rates (Zindler & Hart, 1986; Wilson, 1989; Rollinson, 1993).

The Pb content of some of these flows and dikes is greater than those of the previously analyzed Gramado magma, reinforcing the role of the crustal contamination process, due to the Pb increase in the crust. In addition, high Rb/Sr ratios show that these magmas probably persisted for a long time in the upper crust, allowing these signatures to be generated (Hawkesworth et al., 1983; Mantovani et al., 1985).

In the $^{207}Pb/^{204}Pb$ *versus* $^{206}Pb/^{204}Pb$ and $^{208}Pb/^{204}Pb$ *versus* $^{206}Pb/^{204}Pb$ diagrams (Figure 9), the Pb isotopic signatures of the SST dikes fall above and within the field of the Gramado magma-type. Some samples of intrusive dikes in the Torres Formation (*ponded pahoehoe* and *compound pahoehoe*) plot in and near the EM-II enriched mantle field. This indicates a possible oceanic and/or sub-continental upper lithospheric source (Rollinson, 1993). This is a characteristic that, combined with negative anomalies of Nb and Ta in relation to La, enrichment of LREEs in relation to HREEs along with enrichment of LILEs, as well as negative ε_{Nd} signatures, supports the model that explains part of the CBPs, which involves contributions from sources enriched in incompatible elements (sources in the sub-continental lithospheric mantle - SCLM) (Hergt *et al.*, 1991; Lightfoot *et al.*, 1993; Peate & Hawkesworth, 1996; Marques *et al.*, 1999; Jourdan *et al.*, 2007; Rocha-Júnior *et al.*, 2013).

8.3. *Petrogenesis of flows and dikes*

Comparing the geochemical characterists of the investigated dikes with the SGG lava formations of the south hinge of the Torres Syncline, we can observe the similarity of the Torres Formation (*compound pahoehoe*) basal flows in the Santa Cruz do Sul/Herveiras, Morro da Cruz, and Caxias do Sul / Estância Velha regions, in contents of SiO_2 (46.70 to 50.56%), alkalis (2.74 to 4.93%) and MgO (4.38 to 8.77%) with the SSOT type dikes. These dikes have relatively high levels of MgO, Cr and Ni, and a slightly positive Eu anomaly. The SST dikes, with low MgO, Cr, and Ni contents, have a geochemical signature similar to the Vale do Sol Formation flows, with levels ranging from 50.30 to 56.84%, alkalis from 2.64 to 5.59%, and MgO from 2.92 to 5.69%.

The hypothesis of fractional crystallization using mass balance (Stormer & Nicholls, 1978) was tested to calculate the percentage of fractionated minerals and total fractionated magma. The data were based on mineral chemistry results of olivine, pyroxene and plagioclase crystals of the studied dikes (Sarmento et al., 2017) according to tables 3, 4 and 5. The titanomagnetite results were extracted from Renner (2010).

Table 3. Selected representative microprobe analyses of olivines of SSOT bodies.

Mineral	**Olivina**			
	Mean	**Mean**	**Mean**	**Mean**
Samples	**PDY-9B (n=4)**	**PDY-9D(n=3)**	**PDY-23(n=3)**	**PDY-47(n=4)**
SiO2	39.81	40.17	38.79	40.50
Al2O3	0.06	0.04	0.03	0.08
FeO	13.55	14.69	22.05	13.61
MnO	0.21	0.23	0.32	0.21
MgO	46.50	44.84	38.50	44.25
CaO	0.26	0.29	0.21	0.26
NiO	0.29	0.28	0.28	0.28
TiO2	0.03	0.03	0.05	0.01
Cr2O3	0.07	0.07	0.05	0.05
Total	100.77	100.63	100.26	99.24
Mg#	86	84	80	85
Name	*Chrysolite*	*Chrysolite*	*Chrysolite*	*Chrysolite*

Mg # = 100x [Mg/(Mg+Fe)]; n= number of analyses.

Table 4. Selected representative microprobe analyses of pyroxenes in SSOT and SST dikes.

Mineral	**Piroxenes**						
	Mean	**Mean**	**Mean**	**Mean**	**Mean**	**Mean**	**Mean**
Samples	**PDY-9B (n=5)**	**PDY-9D(n=5)**	**PDY-23(n=4)**	**PDY-47(n=5)**	**PDY-6(n=4)**	**PDY-12(n=3)**	**PDY-19(n=4)**
SiO_2	50.52	51.06	54.68	50.71	51.18	50.54	49.84
Al_2O_3	3.44	3.56	0.79	3.77	2.03	1.66	1.39
FeO	7.78	8.38	15.75	8.27	13.63	14.68	19.83
MnO	0.17	0.21	0.34	0.20	0.33	0.41	0.47
MgO	15.55	15.21	24.68	14.63	15.65	17.65	13.11
CaO	15.04	20.05	3.71	20.09	16.06	15.33	13.56
Na_2O	0.26	0.28	0.03	0.30	0.23	0.16	0.18
TiO_2	1.13	1.08	0.28	1.38	0.58	0.57	0.70
Cr_2O_3	0.44	0.32	0.13	0.30	0.04	0.04	0.02
Total	99.05	100.14	100.40	99.58	99.85	98.60	99.10
Wo(%)	35.07	41.84	7.33	42.69	32.95	29.67	28.46
En (%)	50.45	44.16	67.85	43.26	44.68	47.53	33.26
Fs (%)	14.47	13.99	24.82	14.05	22.36	22.80	38.28
Name	*Augite*	*Augite*	*Pigeonite*	*Augite*	*Augite*	*Augite*	*Augite*

Wo= Wollastinote; En= Enstatite; Fs= Ferrosilite; n= number of analyses.

Table 5. Selected representative microprobe analyses of plagioclase in SSOT and SST dikes.

Mineral	**Plagioclase**						
	Mean	**Mean**	**Mean**	**Mean**	**Mean**	**Mean**	**Mean**
Samples	**PDY-9B (n=5)**	**PDY-9D(n=5)**	**PDY-23(n=5)**	**PDY-47(n=5)**	**PDY-6(n=5)**	**PDY-12(n=4)**	**PDY-19(n=5**
SiO_2	50.58	50.29	51.24	50.73	52.97	52.08	53.86
Al_2O_3	30.09	31.10	30.46	30.48	28.86	28.74	27.77
FeO	0.66	0.45	0.42	0.60	0.80	0.03	0.81
MnO	0.03	0.01	0.01	0.01	0.02	0.03	0.03
MgO	0.47	0.23	0.26	0.29	0.16	0.15	0.10
CaO	13.49	14.96	14.21	14.56	12.37	12.26	11.24
Na_2O	3.46	3.00	3.26	3.17	4.50	4.39	4.97
K_2O	0.18	0.12	0.19	0.14	0.24	0.27	0.33
TiO_2	0.08	0.06	0.05	0.07	0.07	0.06	0.07
Total	99.11	100.24	100.28	100.03	100.20	98.77	99.18
An #	68	73	70	71	60	60	54
Name	*Bytownite*	*Bytownite*	*Bytownite*	*Bytownite*	*Labradorite*	*Labradorite*	*Labradorite*

An# = 100xCa/(Ca+Na); n = number of analyses.

In the first test, the obtained results show the evolution of the least differentiated basalts of the SSOT dikes (initial liquid: PDY-9D) for the Torres Formation (*compound pahoehoe*) basalt flows (final liquid: PSC2C (Barreto *et al.*, 2016)). The modeling was conducted with 40.68% fractional modeling, in the proportions of 46.51% of plagioclase, 31.10% of clinopyroxene, 18.21% of olivine and 4.18% of titanomagnetite, with a low sum of squared differences between the observed values and calculated compositions (Σres^2 = 0.1172) (Table 6). In the second test, the mass balance was calculated using sample PDY-9D as the initial liquid that showed the transition from basalt to the Vale do Sol Formation basaltic andesite (sample PSC20) with 64.48% fractional modeling in the proportions of 49.84% of plagioclase, 31.24% of clinopyroxene, 13.93% of olivine and 4.99% of titanomagnetite, with a sum of squared residuals of Σres^2 = 0.2281 (Table 7). The third modeling started from the same initial basalt of the previous tests (PDY-9D) to a more differentiated basaltic andesite composition of the Vale do Sol Formation flows (sample PSC4B). The results indicate partial compatibility with fractional crystallization processes, with 76.42% fractional modeling in the proportions of 50.44% of plagioclase, 31.09% of clinopyroxene, 12.93% olivine and 5.54% of titanomagnetite (Table 8). These fractional crystallization models provide a good fit to the major elements considering the reasonable required proportions and the low sum of square of residuals.

Table 6. Major element modeling between SSOT dikes and lava flows of the SCSH section.

Test 1	**L_o (PDY-9D)**	**L_f (PSC2C)**	**Plag**	**Ti-mag**	**Cpx**	**Ol**	**XL-frac**	**Δ_0**	**Δ_f**	**residual (Δ_0-Δ_f)**
SiO_2	49.87	51.46	52.48	0	51.55	39.53	47.636	1.586	1.554	0.032
TiO_2	1.35	1.11	0.1	16.58	1.26	0.03	1.136	-0.244	-0.009	-0.235
Al_2O_3	15.48	16.01	29.67	1	3.5	0.06	14.94	0.531	0.437	0.094
FeOtot	10.01	10.99	0.57	81.91	7.2	16.09	8.861	0.977	0.866	0.112
MnO	0.17	0.17	0.05	0.29	0.22	0.25	0.148	-0.01	0.008	-0.017
MgO	8.89	6.20	0.16	0.21	15.78	43.67	12.943	-2.69	-2.742	0.052
CaO	11.29	10.84	12.62	0.02	20.21	0.29	12.209	-0.454	-0.556	0.102
Na_2O	2.23	2.17	4.15	0	0.27	0	2.017	-0.053	0.064	-0.118
K_2O	0.49	0.88	0.2	0	0.01	0	0.098	0.387	0.32	0.067
P_2O_5	0.18	0.16	0	0	0	0.07	0.013	-0.03	0.058	-0.089
TOT	100	100	100	100	100	100				
Σres^2										0.1172
subtracted phases (100%)			46.51	4.18	31.1	18.21				
fractionated total (%)										40.68

Ol= olivine; Plag= plagioclase; cpx= clinopyroxene; Ti-mag= titano magnetite; Lo= initial liquid; Lf= final liquid; XL-frac = crystallized fraction in the parental magma; $\Delta 0$ = observed difference between the magmas ; Δf = calculated difference between the magmas; Σres^2 = sum of the squares of residuals.

Table 7. Major element modeling between SSOT dikes and lava flows of the SCSH section.

Test 2	**L_o (PDY-9D)**	**L_f (PSC20)**	**Plag**	**Ti-mag**	**Cpx**	**Ol**	**XL-frac**	**Δ_0**	**Δ_f**	**residual (Δ_0-Δ_f)**
SiO_2	49.87	53.71	52.48	0	51.55	39.53	47.77	3.843	3.835	0.008
TiO_2	1.35	1.51	0.1	16.58	1.26	0.03	1.27	0.154	0.153	0.001
Al_2O_3	15.48	14.65	29.67	1	3.5	0.06	15.94	-0.836	-0.834	-0.002
FeOtot	10.01	12.13	0.57	81.91	7.2	16.09	8.86	2.116	2.106	0.01
MnO	0.17	0.21	0.05	0.29	0.22	0.25	0.14	0.03	0.042	-0.012
MgO	8.89	4.91	0.16	0.21	15.78	43.67	11.10	-3.986	-3.994	0.009
CaO	11.29	8.88	12.62	0.02	20.21	0.29	12.65	-2.42	-2.431	0.011
Na_2O	2.23	2.60	4.15	0	0.27	0	2.16	0.374	0.288	0.086
K_2O	0.49	1.20	0.2	0	0.01	0	0.10	0.706	0.709	-0.003
P_2O_5	0.18	0.21	0	0	0	0.07	0.01	0.019	0.126	-0.107
TOT	100	100	100	100	100	100				
Σres^2										0.2281
subtracted phases (100%)			49.84	4.99	31.24	13.93				
fractionated total (%)										64.48

Ol= olivine; Plag= plagioclase; cpx= clinopyroxene; Ti-mag= titano magnetite; L_o= initial liquid; L_f= final liquid; XL-frac = crystallized fraction in the parental magma; Δ_0 = observed difference between the magmas ; Δ_f = calculated difference between the magmas; Σres^2 = sum of the squares of residuals.

Table 8. Major element modeling between SSOT dikes and lava flows of the SCSH section.

Test 3	**L_o (PDY-9D)**	**L_f (PSC4B)**	**Plag**	**Ti-mag**	**Cpx**	**Ol**	**XL-frac**	**Δ_0**	**Δ_f**	**residual (Δ_0-Δ_f)**
SiO_2	49.87	57.09	52.48	0	51.55	39.53	47.61	7.217	7.242	-0.026
TiO_2	1.35	1.61	0.1	16.58	1.26	0.03	1.363	0.248	0.186	0.063
Al_2O_3	15.48	13.35	29.67	1	3.5	0.06	16.118	-2.133	-2.115	-0.018
FeOtot	10.01	12.69	0.57	81.91	7.2	16.09	9.141	2.68	2.713	-0.033
MnO	0.17	0.20	0.05	0.29	0.22	0.25	0.14	0.019	0.042	-0.023
MgO	8.89	3.20	0.16	0.21	15.78	43.67	10.644	-5.691	-5.688	-0.003
CaO	11.29	6.76	12.62	0.02	20.21	0.29	12.689	-4.534	-4.529	-0.005
Na_2O	2.23	2.65	4.15	0	0.27	0	2.18	0.417	0.356	0.062
K_2O	0.49	2.25	0.2	0	0.01	0	0.106	1.757	1.642	0.115
P_2O_5	0.18	0.21	0	0	0	0.07	0.009	0.019	0.151	-0.131
TOT	100	100	100	100	100	100				
Σres^2										0.0407
subtracted phases (100%)			50.44	5.54	31.09	12.93				
fractionated total (%)										76.42

Ol= olivine; Plag= plagioclase; cpx= clinopyroxene; Ti-mag= titano magnetite; L_o= initial liquid; L_f= final liquid; XL-frac = crystallized fraction in the parental magma; Δ_0 = observed difference between the magmas ; Δ_f = calculated difference between the magmas; Σres^2 = sum of the squares of residuals.

Although the major elements reproduce the fractional crystallization model, the relative variation of the isotopic signatures with the enrichment of the incompatible trace elements suggests an additional contribution of contamination from the upper and/or lower crust. The high $^{87}Sr/^{86}Sr_i$ ratio, combined with geochemical variations in the SGG lava flows on the south hinge of the Torres Syncline (Barreto et al., 2016) imply that assimilation and fractional crystallization (AFC, De Paolo, 1981) were simultaneous processes in the magma residence inside the magma chamber or during the ascent of the magmas through the crust. In order to test the crustal contamination effect on the behavior of trace elements during the magma ascent, the AFC trends were calculated with the initial magma composition of those of the SSOT dikes (samples PDY-9B and PDY -9D).

The selected contaminants were Neoproterozoic and Palaeoproterozoic rocks of basement units geographically close to the studied area, with geochemical information and Sr-Nd data available in the literature.

The contaminants selected for the development of AFC curves are the Neoproterozoic Ponta Grossa Granite (sample 630 from Philipp et al., 2007) and Capão do Leão Granite (sample 443C from Philipp *et al.*, 2007 and samples GCL-03 and GCL- 05 from Silva, 2016) units. The chosen Palaeoproterozoic units are tonalites of the Arroyo dos Ratos Complex (samples TG-02O and TG-02G of Gregory, 2014). The AFC modeling was conducted using the software Petrograph (version 2.0 beta) in which the AFC curves with the r-value variables were superimposed on the Ba-Zr, Rb-Zr and Zr-Th diagrams (Figure 12). These incompatible trace elements were selected because they are good indicators of both fractional crystallization processes and crustal contamination. For the Neoproterozoic contaminants, the AFC curve results from all diagrams suggest that it is possible to obtain basaltic andesite magmas in the final liquid. In the Ba *versus* Zr and Zr *versus* Th diagrams, the AFC curves reach about 10% to 55% of differentiation (contaminant sample GCL-03 - Capão do Leão Granite), with 2% to 11% assimilation (Figure 12A and B). In the Rb *versus* Zr diagram, the AFC curves reach the samples at about 10% to 45% differentiation (sample 630 - Ponta Grossa Granite), with 4% to 9% assimilation (Figure 12C). For the Palaeoproterozoic contaminants, in the Ba *versus* Zr diagram, the AFM curve reaches 10% to 55% crystallization (sample TG-02G - Arroio dos Ratos Tonalite), with an assimilation rate of 2% to 11% (Figure 12D). As to the Rb *versus* Zr diagram, the AFM curve reaches 8% to 50% crystallization (TG-02O - Arroio dos Ratos Tonalite) with an assimilation rate of approximately 2% to 10% (Figure 11E). Finally, with the same sample, it is observed that the AFM curve reaches 20% to 60% crystallization in the Zr *versus* Th diagram, with assimilation of 4% to 12% (Figure 12F).

According to the trace element modeling results, it was observed that there was fractionation among the SSOT dikes and that fractional crystallization (FC) alone can explain its petrogenesis. For the fractionation of these dikes for the flows, the importance of the crustal assimilation is clear for the evolution of these rocks.

Based on the results, it was not possible to identify a single crustal contaminant to explain the AFC trends because the two contaminants used were assumed as composition of the assimilated material. In this case, these data reinforce the hypothesis of Barreto et al. (2016), who state that both Palaeoproterozoic and Neoproterozoic crustal materials associated with distinct degrees of assimilation are required.

Isotopic ratios were inserted into binary $^{87}Sr/^{86}Sr_i$ *versus* Sr diagrams for the considered units (Figure 13). The best results show the parental magma as the olivine tholeiitic SSTO dikes and the Neoproterozoic units such as the Capão do Leão Granite (sample 443C) as contaminants. Assimilation rates are 8% to 12% (crystallization from 40% to 60%). If Palaeoproterozoic units such as the Arroio dos Ratos Complex Tonalite are used, the results are not satisfactory.

The AFC models based on trace elements and Sr isotopes suggest an important role of the crustal contamination process in the petrogenesis of these rocks. Although in the AFC models the trace elements show an assimilation of both Palaeoproterozoic and Neoproterozoic contaminants in varying degrees (r values), a greater contribution of the Neoproterozoic crust is considered. This condition is supported by the behavior of the AFC curve in the Sr isotope modeling (Figure 13), when using the Dom Feliciano Suite units as a contaminant.

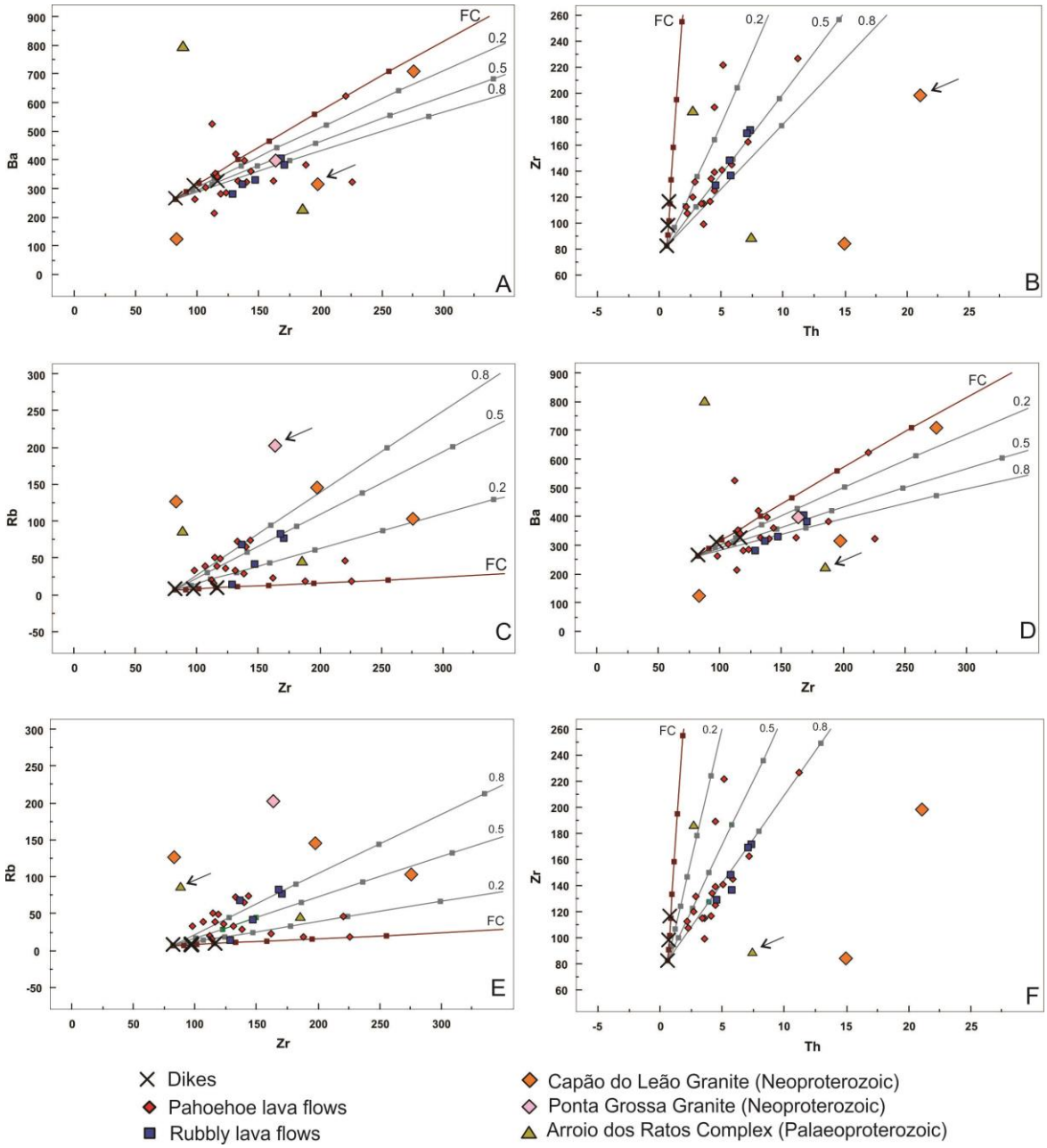

Figure 12. Variation diagrams of selected trace elements, illustrating the results of modelling of assimilation-fractional crystallization (AFC) and fractional crystallization (FC) for the generation of basaltic and basaltic andesite magmas in Santa Cruz do Sul / Herveiras (SCSH) areas (Barreto et al., 2016) from SSOT basic dikes magmas (Sarmento et al., 2017). Variations in r (degree of assimilation/degree of crystallization), depending on the magma starting composition are placed on the evolution curves of AFC process. The squares represent increases of 10% in the crystallization degree. Bulk distribution coefficient to Ba = 0.1813, Rb = 0.0899, Zr = 0.0618, Th = 0.0596.

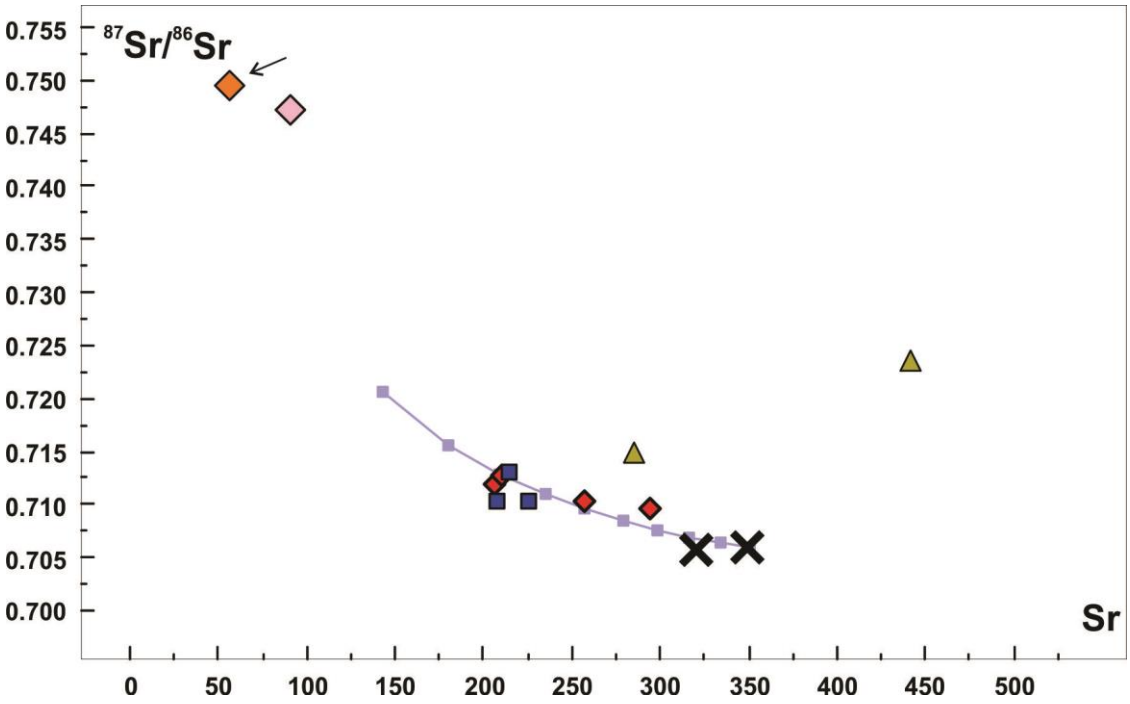

Figure 13. Modelling of assimilation-fractional crystallization (AFC) for the generation of basaltic and e basaltic andesite magmas in Santa Cruz do Sul / Herveiras (SCSH) areas (Barreto et al., 2016) and SST dikes from SSOT basic dikes magmas (Sarmento et al., 2017). The line represents AFC trajectory - The squares represent increases of 10% in the crystallization degree. Degree of assimilation/degree of crystallization ("r") used = 0,4. Sr bulk distribution coefficient used = 0,941. Legend like figure 9 to dikes and figure 11 to the others.

9. CONCLUSIONS

Dikes associated to PEIP occur in the southeastern part of the Paraná Basin, southernmost Brazil. Thue are intrusive in both sedimentary rocks and basal lavas flows of the Paraná Group. The dikes were characterized as Silica Saturated Olivine Tholeiites (SSOT) and Silica Supersaturated Tholeiites (SST). Geochemical data SST dikes have geochemical and Sr-Nd isotopic similarities with the lavas of the Gramado magma-type and, consequently, with the Tafelberg magma-type of the Paraná-Etendeka Igneous Province. These magmas would be derived largely from a lithospheric mantle source enriched with some crustal assimilation. On the other hand, the SSTO dikes would be derived from a lithospheric mantle source enriched with less crustal contribution and have isotopic compositions similar to the Nil Desperandum magma type, with MgO > 7%, and without corresponding in the Paraná Magmatic Province. However, more data and studies are needed to obtain more robust models about the comparison of these intrusions.

The SST dikes cut the Torres and Vale do Sol Formations lava flows. The behavior of the geochemical elements and the Sr-Nd-Pb isotopic ratios suggest that these dikes may have contributed as part of a feeder dikes system which supply basic lavas to flows

stratigraphically positioned above the basal and host flows. The SST dikes intrusive in ponded pahoehoe and pahoehoe lava flows of the Torres Formation, with higher $^{87}Sr/^{86}Sr_i$ ratios have undergone a higher degree of crustal assimilation or are part of the refeeding system of the same lava flows unit. The dike intrusive in the Vale do Sol Formation lava flows, at the top of the volcanic sequence, may have been part of a conduit system for the Esmeralda magma-type lava flows (Esmeralda Formation) as it shows less contaminated isotopic signatures and similar trace elements.

The SSOT dikes were found intruding only in the Torres Formation (*ponded pahoehoe*) flows. Although they have lower Sr and Pb isotopic ratios, could be part of a feeding system or a component of the dikes that effectively fed the olivine-basalte flows of the Torres Formation (*compound pahoehoe*), found stratigraphically above the host lava flows. The variation of these ratios may have occurred due to the assimilation at the time of magma rise and extrusion.

Observations of the AFC and FC modeling based on trace elements and isotope ratios suggest that, for the SSOT dikes, the FC process was the most important one for their differatiation. Modeling for the SSOT dikes and lava flows show that crustal assimilation played a major role in the petrogenesis of these rocks in the south hinge of the Torres Syncline. Both Palaeoproterozoic and Neoproterozoic assimilations are considered, but a greater contribution of the Neoproterozoic crust was observed in this study.

Thus, the continuous fractional crystallization followed by crustal assimilation is indicated to explain the rise of these magmas from the conduits to the emplacement of the lava flows.

ACKNOWLEDGMENTS

Thanks to CAPES for the PhD research grant. This work had partial financial support to C.A. Sommer and E.F. Lima from CNPq (400724/2014-6, 441766/2014-5, 302213/2012-0, 303584/2009-2, 473683/2007, 5470641/2008-8, 470203/2007-2, 471402/2012-5, 303038/2009-8 and 470505/2010-9), and from the Rio Grande do Sul State Research Foundation (FAPERGS) 1180/12-8, and PRONEX 10/0045-6. We also thank the laboratory support from the IGEO/UFRGS.

REFERENCES

Allegre, C. J., Lewin, E., Dupre, B., 1988. A coherent crust-mantle model for the uranium-thorium-lead isotopic system. Chem. Geol. 70, 211-234.

Almeida, F.F.M., 1986. Distribuição regional e relações tectônicas do magmatismo pós-paleozóico no Brasil. Revista Brasileira Geciências 16(4), 325-349.

Almeida, V. V., Janasi, L. M., Heaman, L. M., Shaulis, Hollanda, M. H. B.M., Renne, P. R., 2017. Contemporaneous alkaline and tholeiitic magmatism in the Ponta Grossa Arch, Paraná-Etendeka Magmatic Province: Constraints from U-Pb zircon/baddeleyite and 40Ar/39Ar phlogopite dating of the José Fernandes Gabbro and mafic dykes. Journal of Volcanology and Geothermal Research. (Accepted Manuscript) doi: 10.1016/j.jvolgeores.2017.01.018

Barreto, C. J. S., Lima, E. F., Scherer, C. M., Rossetti, L. M. M., 2014. Lithofacies analysis of basic lava flows of the Paraná igneous province in the south hinge of Torres Syncline, Southern Brazil. Journal of Volcanology and Geothermal Research 285, 81–99.

Barreto, C. J. S., Lafon, J. M., Lima, E. F., Sommer, C. A., 2016. Geochemical and Sr–Nd–Pb isotopic insight into the low-Ti basalts from southern Paraná Igneous Province, Brazil: the role of crustal contamination. International Geology Review 59(1):1 DOI: 10.1080/00206814.2016.1147988

Bellieni, G., Comin-Chiaramonti, P., Marques, L.S., Melfi, A.J., Nardy, A.J.R., Papatrechas, C., Piccirillo, E.M., Roisenberg, A., and Stolfa, D., 1986. Petrogenetic aspects of acid and basaltic lavas from the Paraná Plateau (Brazil): Geological,
mineralogical and petrochemical relationships: Journal of Petrology 27, 915–944. doi:10.1093/petrology/27.4.915

Bellieni, G., Comin-Chiaramonti, P., Marques, L. S.,Melfi, A. J.,Stolf A, D., 1984. Low-pressure evolution of basalt sills from bore-holes in the Paraná Basin, Brazil. TMPM 33, 25-47.

Bondre, N.R., Hart, W.K., Sheth, H.C., 2006. Geology and geochemistry of the Sangamner mafic dyke swarm, western Deccan volcanic province, India: implications for regional stratigraphy. Journal of Geology 114, 155–170.

Brueseke, M. E., Heizler, M. T., Hart,W. K. & Mertzman, S. A., 2007. Distribution and geochronology of Oregon Plateau (U.S.A.) flood basalt volcanism: The Steens Basalt revisited. J. Volcanol. Geotherm. Res. 161 187–214

Bryan, S.E., 2007. Silicic Large Igneous Provinces. Episodes 30, 20-31.

Bryan, S.E. & Ernst, R.E., 2006. Proposed Revision to Large Igneous Province Classification. http://www.mantleplumes.org/LIPClass2.html.

Bryan, S.E.; Ernst, R.E., 2008. Revised definition of Large Igneous Provinces (LIPs). Earth Sciences Review 86, 175-202.

Coffin, M. F. & Eldholm, O., 1992. Volcanism and continental break-up: A global compilation of large igneous provinces. In: Geological Society of London Special Publication 68, 17-30.

Corval, A., Valente, S., Duarte, B. P., Famelli, N., Zanon, M., 2008. Dados petrológicos preliminares dos diabásios dos setores centro-norte e nordeste do Enxame de Diques da Serra do Mar. Geochimica Brasiliensis 22, 159-177.

Corval, A. V., 2009. Petrogênese e Contexto Geodinâmico das Suítes Basálticas Toleíticas (de alto -TiO_2 e baixo - TiO_2) do Cretáceo Inferior da Formação Centro-oriental do Enxame de Diques da Serra do Mar. Tese (Doutorado) - Centro de Tecnologia e Ciências. Faculdade de Geologia. Universidade do Estado do Rio de Janeiro, Rio de Janeiro, RJ.

CPRM, 2010. Geologia Recursos Minerais do Estado de Rio Grande do Sul - Escala, 1, p. 750, 000.

Deckart, K., Féraud, G., Marques, L.S., Bertrand, H., 1998. New time constraints on dyke swarms related to the Paraná – Etendeka magmatic province, and subsequent South Atlantic opening, southeastern Brazil. Journal of Volcanology and Geothermal Research 80, 67-83.

De Paolo, D.J., 1981, Nd isotopic studies: Some new perspectives on Earth Structure and Evolution: EOS, Transactions American Geophysical Union 62, 137–145. doi:10.1029/EO062i014p00137-01

Duncan, A.R., Newton, S. R., van den Berg, C., Reid, D. L., 1989. Geochemistry and petrology of dolerite sills in the Huab River Valley, Damaraland, north-western Namibia, Communs geol. Surv. Namibia 5, 5-18

Duncan, A.R., Armstrong, R.A., Erlank, A.J., Marsh, J.S. and Watkins, R.T., 1990. MORB-related dolerites associated with the final phases of Karoo flood basalt volcanism in southern Africa. In: J.A.J. Parker, P. C. Rickwood and D.H. Tucker (Editors), Mafic Dikes and Emplacement Mechanisms, A.A. Balkema, Rotterdam, The Netherlands, 119-129.

Erlank, A.J., Marsh, J.S., Duncan, A.R., Miller, R.M., Hawkesworth, C.J., Betton, P.J. and Rex, D.C., 1984. Geochemistry and petrogenesis of the Etendeka volcanic rocks from SWA/ Namibia. In: A.J. Erlank (Editor), Petrogenesis of Volcanic Rocks of the Karoo Province. Special Publication of the Geological Society of South Africa 13, 195-245.

Ewart, A.J., Marsh, J.S., Duncan, A.R., Miller, R.M., Hawkesworth, C.J., Betton, P.J., Rex, D.C., 1984. Geochemistry and petrogenesis of the Etendeka volcanic rocks from SWA/ Namibia. In: Erlank, A.J. (Ed.), Petrogenesis of Volcanic Rocks of the Karoo Province, Geological Society of South Africa Special Publication 13, 195–245.

Ewart A., Milner, S.C., Armstrong, R.A., Duncan, A.R., 1998. Etendeka volcanism of the Goboboseb Mountains and Messum Igneous Complex, Namibia. Part I: Geochemical evidence of early Cretaceous Tristan plume melts and the role of crustal contamination in the Parana-Etendeka CFB. Journal of Petrology 39, 191-225.

Ewart, A., Marsh, J.S., Milner, S.C., Duncan, A.R., Kamber, B.S., Armstrong, R.A., 2004. Petrology and geochemistry of Early Cretaceous bimodal continental flood volcanism of the

northwest Etendeka, Namibia. Part 1: Introduction, mafic lavas and re-evaluation of mantle source components. Journal of Petrology 45, 59-105.

Florisbal, L.M., Bitencourt, M.F., Nardi, L.V.S., and Conceição, R. V., 2009, Early post-collisional granitic and coeval mafic magmatism of medium- to high-K tholeiitic affinity within the Neoproterozoic Southern Brazilian Shear Belt: Precambrian Research 175, 135–148. doi:10.1016/j.precamres.2009.09.003

Florisbal, L. M., Heaman, L. M., Janasi, V. A., Bitencourt, M. F., 2014. Tectonic significance of the Florianópolis Dyke Swarm, Paraná–Etendeka Magmatic Province: A reappraisal based on precise U–Pb dating. Journal of Volcanology and Geothermal Research 289, 140-150.

Florisbal, L. M., Janasi, V. A., Bitencourt, M. F., Nardi, L. V. S., Marteleto, N. S., 2017. Geological, geochemical and isotope diversity of ~ 134 Ma dykes from the Florianópolis Dyke Swarm, Paraná Magmatic Province: Geodynamic controls on petrogenesis. Journal of Volcanology and Geothermal Research. (Accepted Manuscript)

Frank, H. T., Gomes, M. E. B., Formoso, M. L. L., 2009. Review of the areal extent and the volume of the Serra Geral Formation, Paraná Basin, South America. Pesquisas em Geociências 36 (1), 49-57.

Gibb, F.G.F., Henderson, C.M.B., 1996. The Shiant Isles Main Sill: structure and mineral fractionation trends. Mineralogical Magazine 60, 67–98.

Gregory, T.R., 2014, Evolução Petrológica do magmatismo TTG Paleoproterozóico do Complexo Arroio dos Ratos, distrito de Quitéria, São Jerônimo/RS [PhD Thesis]: Porto Alegre, Universidade Federal do Rio Grande do Sul, 100 p.

Hart, S.R., 1984, A large-scale isotope anomaly in the southern hemisphere mantle: Nature 309, 753–757. doi:10.1038/309753a0

Hawkesworth, C.J., Erlank, A.J., Marsh, J.S., Menzies, M.A., and Van Calsteren, P., 1983, Evolution of the continental lithosphere: Evidence from volcanics and xenoliths in Southern Africa, in: Hawkesworth, C.J., and Norry, M.J., eds., Continental basalts and mantle xenoliths: Nantwich, Shiva, 111–138.

Hawkesworth, C.J., Marsh, J.S., Duncan, A.R., Erlank, A.J. and Norry, M.J., 1984. The role of continental lithosphere in the generation of the Karoo volcanic rocks: evidence from combined Nd- and Sr-isotope studies. Spec. Publ. geol. Soc. S. Afr. 13, 341-354.

Hawkesworth, C.J., Mantovani, M.S.M., Taylor, P.N., and Palacz, Z., 1986, Evidence from the Parana of south Brazil for a continental contribution to Dupal basalts: Nature 322, 356–359. doi:10.1038/322356a0

Hawkesworth, C., Gallagher, K., Kirstein, L., Mantovani, M.S.M., Peate, D.W., Turner, S.P., 2000. Tectonic controls on magmatism associated with continental break-up: an example from the Paraná–Etendeka Province. Earth Planet. Sci. Lett. 179, 335–349. http://dx.doi.org/10.1016/S0012-821X(00)00114-X.

Hergt, J., Peate, D.W., and Hawkesworth, C.J., 1991, The petrogenesis of Mesozoic Gondwana low-Ti flood basalts: Earth and Planetary Science Letters 105, 134–148. doi:10.1016/0012-821X(91)90126-3

Hunter, D.R. & Reid, D.L., 1987. Mafic dike swarms in Southern Africa. In: H. C. Halls and W. F. Fahrig (Editors), Mafic Dike Swarms. Geological Association of Canada Special Paper 34, 445-456.

Irvine, T.N., Baraguar, W.R.A., 1971. A guide to the chemical classification of the common volcanic rocks. Can. J. Earth Sci. 8 (5), 523-548.

Janasi, V. A., Freitas, V. A., Heaman, L. H., 2011. The onset of flood basalt volcanism, Northern Paraná Basin, Brazil: A precise U-Pb baddeleyite/zircon age for a Chapecó-type dacite. Earth and Planetary Science Letters 302(1-2), 147-153.

Jerram, D.A., Bryan, S.E., 2015. Plumbing systems of shallow level intrusive complexes. In: Breitkreuz, C.H., Rocchi, S. (Eds.), Physical Geology of Shallow Magmatic Systems. Advances in Volcanology. Springer, Berlin, pp. 1-22. http://dx.doi.org/10.1007/11157_2015_8.

Jerram, D.A., Mountney, N., Holzforster, F., Stollhofen, H., 1999. Internal stratigraphic relationships in the Etendeka Group in the Huab Basin, NW Namibia: understanding the onset of flood volcanism. J. Geodyn. 28, 393-418.

Jerram, D. A., Mountney, N., Howell, J., Long, D., Stollhofen, H., 2000. Death of a sand sea: an active aeolian erg systematically buried by the Etendeka flood basalts of NW Namibia. Journal of the Geological Society of London 157(3), 513–516.

Jourdan, F., Bertrand, H., Scharer, U., Blichert-Toft, J., Feraud, G., and Kampunzu, B., 2007, Major and Trace Element and Sr, Nd, Hf, and Pb Isotope Compositions of the Karoo Large Igneous Province, Botswana-Zimbabwe: Lithosphere vs Mantle Plume Contribution: Journal of Petrology 48(6), 1043–1077. doi:10.1093/petrology/egm010

Krymsky, R.S., Macambira, M.J.B., Lafon, J.M., and Estumano, G.S., 2007, Uranium-lead dating method at the Pará-Iso Isotope Geology laboratory, UFPA, Belém – Brazil: Anais Da Academia Brasileira De Ciências 79, 115–128. doi:10.1590/S0001-37652007000100014

Le Bas, M. J., LeMaitre, R. W., Streckeisen, A., Zannetin, B. A., 1986. Chemical classification of volcanic rocks based on the total alkali-silica diagram. Journal of Petrology 27(3), 745-750.

Lightfoot, P.C., Hawkesworth, C.J., Hergt, J., Naldrett, A.J., Gorbachev, N.S., Fedorenko, V.A., and Doherty, W., 1993, Remobilisation of the major, trace-element, and from picritic and tholeiitic Siberian Trap, Russia continental lithosphere by a mantle plume: Sr-, Nd-, and Pb-isotope evidence from picritic and tholeiitic lavas of the Noril'sk District: Contributions to Mineralogy and Petrology 114, 171–188. doi:10.1007/BF00307754

Lord, J., Oliver, G., Soulsby, J., 1996. Landsat MSS imagery of a Lower Cretaceous regional dyke swarm, Damaraland, Namibia: a precursor to the splitting of Western Gondwana. International Journal of Remote Sensing 17, 2945–2954.

Lugmair, G.W., Marti, K., 1978. Lunar initial $^{143}Nd/^{144}Nd$: Differential evolution of the lunar crust and mantle: Earth and Planetary Science Letters 39, 349–357. doi:10.1016/0012-821X(78)90021-3

Machado, F. B., Nardy, A. J. R. & Oliveira, M. A. F., 2007. Geologia e aspectos petrológicos das rochas intrusivas e efusivas mesozóicas de parte da borda leste da bacia do Paraná no estado de São Paulo. Revista Brasileira de Geociências, 37(1), 64-80.

Maniesi Petersohn, V., Oliveira, M. A. F., 1997. Petrologia das soleiras de diabásio de Reserva e Salto do Itararé, PR. Geochimica Brasiliensis 11(2), 153-169.

Mantovani, M.S.M., Marques, L.S., Souza, M.A., Atalla, L., Civeta, L., Inonocenti, F., 1985.Trace Element and Strontium Isotope Constrains of the Origin and Evolution of Paraná Continental Flood Basalts of Santa Catarina State (Southern Brazil). Journal of Petrology 26, 187-209.

Marques, L.S., Ernesto, M., 2004. O Magmatismo Toleítico da Bacia do Paraná. In: Mantesso-Neto, V., Bartorelli, A., Carneiro, C. D. R., Brito-Neves, B. B. (Eds), Livro Geologia do Continente Sul-Americano: Evolução da obra de Fernando Flávio Marques de Almeida. São Paulo: Editora Beca.

Marques, L.S., Figueiredo, A.M.G., Saiki, M., Vasconcellos, M.B.A., 1989. Geoquímica analítica dos elementos terras raras - Aplicação da técnica de análise por ativação neutrônica. In: Formoso, M.L.L.; Nardy, L.V.S. & L.A. Hartmann (Coords.), Geoquímica dos Elementos Terras Raras no Brasil. CPRM/DNPM, Sociedade Brasileira de Geoquímica, Rio de Janeiro, pp. 15-20.

Marsh, B.D., 2013. On some fundamentals of igneous petrology. Contributions to Mineralogy and Petrology 166, 665–690.

Marsh, J.S., Duncan, A.R., 2008. Doros Gabbroic Complex. In: Miller, R.M. (Ed.) The Geology of Namibia vol. 3. Geological Survey of Namibia, Windhoek, pp. 18-78.

Marsh, J. S., Erlank, A. J., Duncan, A. R. 1991. Report: Preliminary geochemical data for dolerite dykes and sills of the southern part of the Etendeka Igneous Province, Communs geol. Surv., Namibia 7, 77-80.

McDonough, W. S., Sun, S., 1995. The composition of the Earth. Chemical Geology 120, 223-253.

Melfi, A.J., Nardy, A.J.R., and Piccirillo, E.M., 1988, Geological and magmatic aspects of the Paraná Basin: An introduction, In: Piccirillo, E.M., and Melfi, A.J. (Eds.), The Mesozoic flood volcanism of the Paraná Basin: Petrogenetic and geophysical aspects. IAG-USP, p. 1–13.

Middlemost, E. A. K., 1975. The basalt clan. Earth Science Review 11, 337-64.

Milani, E. J., 1997. Evolução tectono-estratigráfica da Bacia do Paraná e seu relacionamento com a geodinâmica fanerozóica do Gondwana Sul-Ocidental. 2 v.
Tese (Doutorado). Porto Alegre: Instituto de Geociências – UFRGS.

Milner, S. C., le Roex, A. P. & O'Connor, J. M., 1995. Age of Mesozoic rocks in northwestern Namibia, and their relationship to continental breakup. Journal of the Geological Society, London 152, 97-104.

Mountney, N., Howell, J., Flint, S., Jerram, D., 1998. Aeolian and alluvial deposition within the mesozoic Etjo sandstone formation, northwest Namibia. J. Afr. Earth Sci. 27 (2), 175-192.

Nardy, A. J. R., 1995. Geologia e petrologia do vulcanismo mesozóico da região central da Bacia do Paraná. Tese (Doutorado). Instituto de Geociências e Ciências Exatas, Universidade Estadual Paulista. Rio Claro, São Paulo.

Oliveira, E.C., Lafon, J.M., Gioia, S.M.C.L., and Pimentel, M.M., 2008, Datação Sm-Nd em rocha total e granada do metamorfismo granulítico da região de Tartarugal Grande: Amapá Central: Revista Brasileira Geociências 38, 116–129.

Owen-Smith, T. M., Ashwal, L. D. 2015., Evidence for multiple pulses of crystal-bearing magma during emplacement of the Doros layered intrusion, Namibia. Lithos 238, 120-139.

Peate, D. W. Hawkesworth, C. J., Mantovani, M. S. M., 1992. Chemical stratigraphy of the Paraná lavas (South América): classification of magma types and their spatial distribution. Bulletin of Volcanology 55 (1), 119-139.

Peate D.W. 1997. The Paraná–Etendeka province. In: Mahoney J.J., Coffin M.F. Large Igneous Provinces: Continental, Oceanic and Planetary Flood Volcanism. American Geophysical Union, Washington, DC, pp. 217-245.

Peate, D.W., Hawkesworth, C.J., Mantovani, M.S.M., Rogers, N.W., Turner, S.P., 1999. Petrogenesis and stratigraphy of the high-Ti/Y Urubici magma type in the Paraná flood basalt province and implications for the nature of 'Dupal'- type mantle in the South Atlantic region. J. Petrol. 40, 451-473.

Peate, P.W., and Hawkesworth, C.J., 1996, Lihospheric to astenospheric transition in Low-Ti flood basalts from southern Paraná: Brazil. Chemical Geology 127, 1–24.

Petersohn, E., Gouvea, E. M., 2009. Geologia e geoquímica da soleira de Reserva, Estado do Paraná. Revista Brasileira de Geociências 39(4), 740-750.

Petersohn, E., Vasconcellos, E. M. G., Lopes, K., 2007. Petrologia de *sills* encaixados nas Formações Irati e Ponta Grossa (Bacia do Paraná) no Estado do Paraná. Geochimica Brasiliensis 21, 58-70.

Petrini, R., Civetta, L., Piccirillo, E.M., Bellieni, G., Comin-Chiaramonti, P., Marques, L.S., and Melfi, A.J., 1987, Mantle heterogeneity and crustal contamination in the genesis of low-Ti continental flood basalts from the Paraná plateau (Brazil): Sr-Nd isotope and geochemical evidence. Journal of Petrology 28, 701–726. doi:10.1093/petrology/28.4.701

Philipp, R.P., Machado, R., and Junior, F.C., 2007, A geração dos granitóides Neoproterozóicos do Batólito Pelotas: Evidências dos isótopos de Sr e Nd e implicações para o crescimento continental da Porção Sul do Brasil. In: Iannuzzi, R., and Frantz, J.C., (Eds.), 50 anos de Geologia: Instituto de Geociências: Contribuicões, Comunicação e Identidade, 399p.

Piccirillo, E. M., Melfi A. J., 1988. The Mesozoic flood volcanism of the Paraná Basin - petrogenetic and geophysical aspects. USP, São Paulo.

Piccirillo, E. M., Civetta, L., Petrini, R., Longinelli, A., Bellieni, G., Comin-Chiaramonti, P., Marques, L. S., Melfi, A. J. 1989. Regional variations within the Paraná Flood Basalts (Southern Brazil): Evidence for subcontinental mantle heterogeneity and crustal contamination. Chemical Geology 75, 103-122.

Piccirillo, E. M., Bellieni, G., Cavazzini, G., Comin-Chiaramonti, P., Petrini, R., Melfi, A. J., Pinesi, J. P. P., Zantadeschi, P., Demin, A., 1990. Lower Cretaceous tholeiitic dyke swarms from the Ponta Grossa (southeast Brazil): Petrology, Sr-Nd isotopes and genetic relationships whith the Paraná flood volcanic. Chemical Geology, Netherlands, 89, 19-48.

Raposo, M. I. B., Ernesto, M., Renne, P. R., 1998. Paleomagnetism and $^{40}Ar/^{39}Ar$ dating of the Early Cretaceous Florianópolis dike swarm (Santa Catarina Island), Southern Brazil. Physics of the Earth and Planetary Interiors 108, 275-290.

Renne, P. R., Ernesto, M., Pacca, I. G., Coe, R. S., Glen, J. M., Prévot, M., Perrin, M. 1992., The age of Paraná Flood Volcanism, rifting of Gondwana land, and the Jurassic-Cretaceous boundary. Science 258, 975-979.

Renne, P.R., Deckart, K., Ernesto, M., Féraud, G., and Piccirillo, E.M., 1996, Age of the Ponta Grossa dike swarm (Brazil), and implications to Paraná flood volcanism. Earth and Planetary Science Letters 144, 199–211. doi: 10.1016/0012-821X(96)00155-0.

Renner, L.C. 2010. Geoquímica de sills basálticos da Formação Serra Geral, sul do Brasil, com base em rocha total e micro-análise de minerais. Tese (Doutorado) – Instituto de Geociências. Programa de Pós-Graduação em Geociências, Universidade Federal do Rio Grande do Sul, Porto Alegre, RS.

Rocha-Júnior, E.R.V., Marques, L.S., Babinski, M., Nardy, A.J.R., Figueiredo, A.M.G., and Machado, F.B., 2013, Sr-Nd-Pb isotopic constraints on the nature of the mantle sources involved in the genesis of the high-Ti tholeiites from northern Paraná Continental Flood Basalts (Brazil). Journal of South American Earth Sciences 46, 9–25. doi:10.1016/j.jsames.2013.04.004

Rohde, J., Hoernle, K., Hauff, F., Werner, R., O'Connor, J., Class, C., Garbe Schonberg, D., and Jokat, W., 2013, 70 Ma chemical zonation of the Tristan-gough hotspot track. Geology 41, 335–338. doi:10.1130/G33790.1

Rollinson, H., 1993. Using Geochemical Data: Evaluation, Presentation, Interpretation. Longman, Harlow, 352 pp.

Romero, J.A.S., Lafon, J.M., Nogueira, A.C.R., and Soares, J.L., 2013, Sr isotope geochemistry and Pb-Pb geochronology of the Neoproterozoic cap carbonates, Tangará da Serra, Brazil. International Geology Review 55, 185–203. doi:10.1080/ 00206814.2012.692517

Rossetti, L. M., Lima, E. F., Waichel, B. L., Scherer, C. M., Barreto, C. J., 2014. Stratigraphical framework of basaltic lavas in Torres Syncline main valley, southern Parana-Etendeka Volcanic Province. Journal of South American Earth Sciences 56, 409-421.

Rossetti, L. M., Lima, E. F., Waichel, B. L., Hole M. J., Scherer, C. M., Simões, M. S., 2017. Lithostratigraphy and volcanology of the Serra Geral Group, Paraná-Etendeka Igneous Province in Southern Brazil: Towards a formal stratigraphical framework. J. Volcanol. Geotherm. Res., In Press, http://dx.doi.org/10.1016/j.jvolgeores.2017.05.008

Sarmento, C.C.T., Sommer, C. A., Lima, E. F., Oliveira, D. S., 2014. Corpos hipabissais correlacionados à Formação Serra Geral naregião do Cerro do Coronel, RS: geologia e petrologia. Geologia USP, Série Científica 14(2), 23-44.

Sarmento, C.C.T., Sommer, C. A., Lima, E. F., 2017. Mafic subvolcanic intrusions and their petrologic relation with the volcanism in the south hinge Torres Syncline, Paraná-Etendeka Igneous Province, southern Brazil. Journal of South American Earth Sciences 77, 70-91.

Scherer, C. M. S., 2002. Preservation of Aeolian genetic units by lava flows in the Lower Cretaceous of the Paraná Basin, southern Brazil. Sedimentology 49, 97-116.

Self, S., Widdowson, M., Thordarson, T., Jay, A. E., 2006. Volatile fluxes during flood basalt eruptions and potential effects on global environment: a Deccan perspective. Earth and Planetary Science Letters 248, 518–532.

Sheth, H.C., Ray, J.S., Ray, R., Vanderkluysen, L., Mahoney, J.J., Kumar, A., Shukla, A.D., Das, P., Adhikari, S., Jana, B., 2009. Geology and geochemistry of Pachmarhi dykes and sills, Satpura Gondwana Basin, central India: problems of dyke-sillflow correlations in the Deccan Traps. Contributions to Mineralogy and Petrology 158, 357–380.

Sheth, H.C., Zellmer, G.F., Kshirsagar, P.V., Cucciniello, C., 2013. Geochemistry of the Palitana flood basalt sequence and the Eastern Saurashtra dykes, Deccan Traps: clues to petrogenesis, dyke-flow relationships, and regional lava stratigraphy. Bulletin of Volcanology 75, 701-723. http://dx.doi.org/10.1007/s00445-013-0701-x.

Siedner, G., Mitchell, J.G., 1976. Episodic Mesozoic volcanism in Namibia and Brazil; K–Ar isochron study bearing on the opening of the South Atlantic. Earth and Planetary Science Letters 30, 292–302.

Silva, R. F., 2016. O granito capão do leão: magmatismo Tipo-I altamente fracionado no sudeste do Cinturão Dom Feliciano, RS. Dissertação (Mestrado) – Instituto de Geociências. Programa de Pós-Graduação em Geociências, Universidade Federal do Rio Grande do Sul, Porto Alegre, RS.

Stewart, K., Turner, S., Kelley, S., Hawkesworth, C. J., Kirstein, L., Mantovani, M., 1996. 3-D, Ar/Ar geochronology in the Paraná continental flood basalt province. Earth and Planetary Science Letters 143, 95-109.

Stormer, J.C., and Nicholls, J., 1978, XLFRAC: A program for the interactive testing of magmatic differentiation models: Computers & Geosciences, v. 4. p. 143–159. doi:10.1016/0098-3004(78)90083-3

Taylor, S.R., and McLennan, S.M., 1985, The Continental Crust: Its Composition and Evolution: Cambridge, MA, Blackwell Scientific, 312 p.

Thiede, D. S., Vasconcelos, P. M., 2010. Paraná flood basalts: Rapid extrusion hypothesis confirmed by new $^{40}Ar/^{39}Ar$ results. Geology 38 (8), 747- 750.

Thompson, R.N., Morrison, M.A., Dickin, A.P. and Hendry, G.L., 1983. Continental flood basalts … Arachnid's rule OK. In: C. J. Hawkesworth and M. J. Norry (Eds.), Continental Flood Basalts and Mantle Xenoliths. Shiva, Nantwich, United Kingdom, pp. 158-185.

Thompson, R. N., Gibson, S. A., Dickin, A. P. & Smith, P. M., 2001. Early Cretaceous basalt and picrite dykes of the southern Etendeka region, NW Namibia: windows into the role of the Tristan mantle plume in Parana-Etendeka magmatism. Journal of Petrology 42, 2049-2081.

Thompson, R.N., Riches, A.J.V., Antoshechkina, P.M., Pearson, D.G., Nowell, G.M., Ottley, C.J., Dickin, A.P., Hards, V.L., Nguno, A.-K. and Niku-Paavola, V., 2007. Origin of CFB magmatism: multi-tiered intracrustal picriterhyolite magmatic plumbing at Spitzkoppe, western Namibia, during Early Cretaceous Etendeka magmatism. Journal of Petrology 48, 1119-1154.

Tomazzoli, E.R. & Lima, E.F., 2006. Magmatismo ácido-básico na ilha do Arvoredo-SC. Revista Brasileira de Geociências 36, 57–76.

Tomazzoli, E. E. & Pellerin, J. M., 2015. Unidades do mapa geológico da ilha de Santa Catarina: as Rochas. Florianópolis. Geosul 60(30), 225-247.

Trumbull, R.B., Vietor, T., Hahne, K., Wackerle, R. and Ledru, P., 2004. Aeromagnetic mapping and reconnaissance geochemistry of the Early Cretaceous Henties Bay-Outjo mafic dike swarm, Etendeka Igneous Province, Namibia. Journal of African Earth Sciences 40, 17-29.

Trumbull, R.B., Reid, D.L., Beer, C., Acken, D., Romer, R.L., 2007. Magmatism and continental breakup at the west margin of southern Africa: a geochemical comparison of dolerite dikes from northwestern Namibia and the Western Cape. South Afr. J. Geol. 110, 477-502.

Turner, S., Regelous, M., Kelley, S., Hawkesworth, C., Mantovani, M., 1994. Magmatism and continental break-up in the South Atlantic: high precision $^{40}Ar/^{39}Ar$ geochronology. Earth and Planetary Science Letters 121, 333-348.

Valente, S.C.; Corval, A.; Duarte, B.P.; Ellam, R. L.; Fallick, A.E.; Dutra, T., 2007. Tectonic boundaries, crustal weakness zones and plume-subcontinental lithospheric mantle interactions in the Serra do Mar Dyke Swarm, SE Brazil. Revista Brasileira de Geociências 37, 194-201.

Vanderkluysen, L., Mahoney, J.J., Hooper, P.R., Sheth, H.C., Ray, R., 2011. The feeder system of the Deccan Traps (India): insights from dyke geochemistry. Journal of Petrology 52, 315–343.

Viero, A. P. & Roisenberg, A., 1992. Petrologia e geoquímica do Complexo Básico Lomba Grande. Pesquisas em Geociências 19 (1), 41 – 54.

Waichel, B. L., Lima, E. F., Viana, A., Scherer, C.M. S., Bueno, G., Dutra, G., 2012. Stratigraphy and volcanic facies architecture of the Torres Syncline, Southern Brazil, and its role in understanding the Paraná-Etendeka Continental Flood Basalt Province.
Journal of Volcanology and Geothermal Research 215, 74-82.

Waichel, B. L., Scherer, C. M. S., Frank, H. T., 2008. Basaltic lava flows covering active Aeolian dunes in the Paraná Basin in Southern Brazil: Features and emplacement aspects. Journal of Volcanology and Geothermal Research 171(1), 59-72.

Wanke, A., Stollhofen, H., Stanistreet, I.G., Lorenz, V., 2000. Karoo unconformities in NW-Namibia and their tectonic implications. Communs Geol. Surv. Namib. 12, 291-301.

Wilson, M., 1989. Igneous Petrogenesis a global tectonic approach. Berlin: Springer.

Wolff, J. A., Ramos, F. C., Hart G. L., Patterson, J. D., Brandon, A. D., 2008. Columbia River flood basalts from a centralized crustal magmatic system. Nature Geoscience 1, 177-180.

Yang, Y.H., Wu, F.Y., Liu, Z.C., Chu, Z.Y., Xie, L.W., and Yang, J.H., 2012, Evaluation of Sr chemical purification technique for natural geological samples using common cation-exchange and Sr-specific extraction chromatographic resin prior to MC-ICP-MS or TIMS measurement: Journal of Analytical Atomic Spectrometry 27, 516–522. doi:10.1039/ c2ja10333h

Zalán, P. V., Conceição, J. C. J., Astolfi, M .A. M., Appi, V. T., Wolff, S., Vieira, I. S., Marques, A., 1985. Estilos estruturais relacionado às intrusões magmáticas básicas em rochas sedimentares. Rio de Janeiro, RJ. Boletim Técnico da PETROBRAS 28 (4): 221 – 230.

Zindler, A., and Hart, S., 1986, Chemical geodynamics: Annual Review of Earth and Planetary Sciences 14, 493–571. doi:10.1146/annurev.ea.14.050186.002425

3.3. ARTIGO 3

TÍTULO: Petrogenesis of mafic sills from Paraná-Etendeka Igneous Province in southernmost Brazil: Trace element and isotope geochemistry

AUTORES: Carla Cecília Treib Sarmento; Carlos Augusto Sommer; Evandro Fernandes de Lima; Edinei Koester.

SUBMETIDO: Em novembro de 2017

PERIÓDICO: Geological Journal

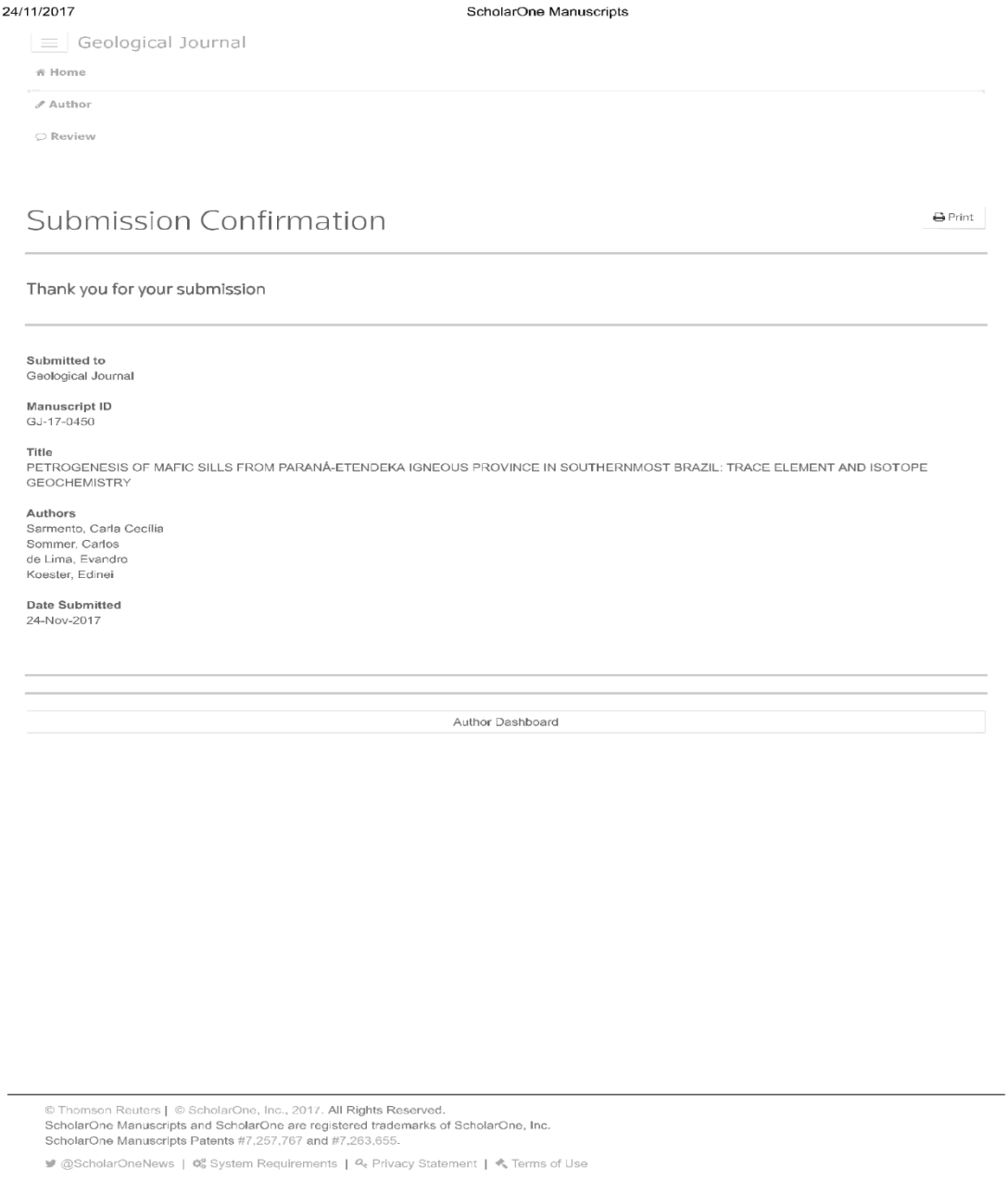

24/11/2017 ScholarOne Manuscripts

Geological Journal

Home

Author

Review

Submission Confirmation

Print

Thank you for your submission

Submitted to
Geological Journal

Manuscript ID
GJ-17-0450

Title
PETROGENESIS OF MAFIC SILLS FROM PARANÁ-ETENDEKA IGNEOUS PROVINCE IN SOUTHERNMOST BRAZIL: TRACE ELEMENT AND ISOTOPE GEOCHEMISTRY

Authors
Sarmento, Carla Cecília
Sommer, Carlos
de Lima, Evandro
Koester, Edinei

Date Submitted
24-Nov-2017

Author Dashboard

PETROGENESIS OF MAFIC SILLS FROM PARANÁ-ETENDEKA IGNEOUS PROVINCE IN SOUTHERNMOST BRAZIL: TRACE ELEMENT AND ISOTOPE GEOCHEMISTRY

Carla Cecília Treib Sarmento[1], Carlos Augusto Sommer[2], Evandro Fernandes de Lima[2], Edinei Koester[2]

[1]Programa de Pós-Graduação em Geociências, UFRGS;

[2]Instituto de Geociências, UFRGS.

Abstract:

This study conducts a petrological investigation of the mafic sills related to Paraná-Etendeka Igneous Province in the Cerro do Coronel region, located in the southern border of the Paraná Basin with the Sul-Rio-Grandense Shield in the extreme south of Brazil. These intrusive bodies form a lineation with NW-SE orientation. The less differentiated lithotypes are located in the basal portions and a slight evolution is observed towards its upper portions. The geochemical data of major elements and trace elements allow classifying the rocks of these sills as basaltic andesites of tholeiitic affinity, and they are compatible with those present in the Paraná Igneous Province magmatism. These sills have limited isotopic variations ($^{87}Sr/^{86}Sr_i$ = 0.71138 to 0.71293; εNd_i = -3.04 to -4.61; $^{206}Pb/^{204}Pb$ = 18.568 to 18.815). The high initial $^{87}Sr/^{86}Sr$ ratios of these rocks indicate a source of intermediate continental crust, but the Pb isotope data suggest a preference for an oceanic lithospheric enriched source or a subcontinental lithospheric source. The $^{144}Nd/^{143}Nd$ ratios appear slightly higher in samples from the southern portion when compared to those from the northern portion, suggesting that these bodies may have undergone fractionation and crust assimilation. Based on the trace element modeling of these sills, fractional crystallization was the main process in the evolution of these rocks on a local scale. However, according to Sr isotopic ratio modeling, the fractional crystallization followed by crustal assimilation, with Palaeoproterozoic crust as an assimilant, had an important role in the genesis of sills on a regional scale.

KEYWORDS: Paraná-Etendeka Igneous Province; mafic sills; Sr–Nd–Pb isotopes; crustal contamination;

1 INTRODUCTION

The Paraná-Etendeka Igneous Province (PIPE), located mostly in the central-eastern portion of the South American Plate and a smaller part in Namibia, is a dominantly basic tholeiitic volcanic sequence of lower Cretaceous age, in addition to associated acidic and intrusive rocks. It is considered a LIP (*Large Igneous Province*) of the Basalt Continental Province (CBP) type, characterized by being developed in a relatively short period of time (~10^6 years), in which large volumes of lava and associated intrusions (10^5 -10^7 km^3) were generated and accumulated (Coffin & Eldholm, 1992, Self *et al*., 2006; Bryan & Ernst, 2008).

Intrusions of basic tholeiitic rocks are an expressive component of the PIPE. In the South American portion of the province, the sills have a higher concentration in the eastern border of the Paraná Basin and occur throughout its extension, usually intrusive in the Paleozoic sediments (Almeida, 1986; Zalán *et al*., 1985) in the states of São Paulo (Machado *et al*., 2007), and Paraná (Maniesi & Oliveira, 1997; Petersohn *et al*., 2007; Petersohn & Gouvea, 2009). In Rio Grande do Sul, these hypabyssal bodies are found on the south border of the Paraná Basin, notably the *sills* of the Manoel Viana and Agudo region (Renner, 2010), the *sills* of the Cerro do Coronel region (Sarmento *et al*., 2014) and the *sills* on the southern edge of the Paraná Basin (Sarmento *et al.,* 2017). In the African portion of the province, these intrusions mainly cut the Damara basement and the sedimentary rocks of the Karoo basin (Marsh *et al*., 1991; Lord et al., 1996). They are represented mainly by the Huab *sill* Complex (Ewart *et al*., 1984; Duncan *et al*., 1989) and Doros Complex (Gibb & Henderson, 1996; Marsh, 2013; Owen-Smith & Ashwal, 2015).

This study aims to investigate the petrogenesis and isotopic variation of Sr-Pb-Nd ratios on a local scale of three andesite-basaltic sills in the Cerro do Coronel region and contribute to the understanding of the processes related to the origin and evolution of magmas related to Paraná-Etendeka Magmatic Province in southernmost Brazil.

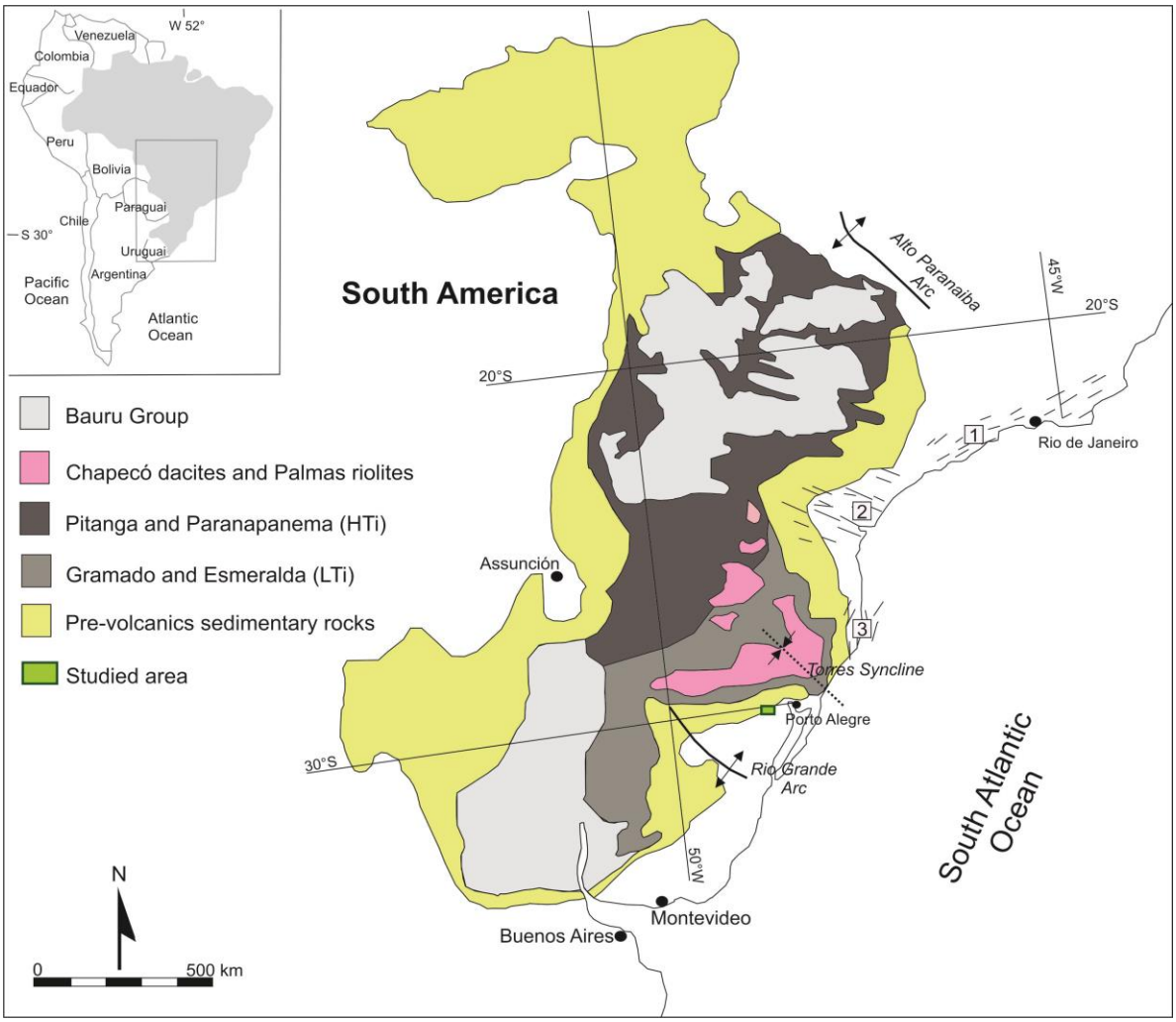

Figure 1. Simplified geological map of Parana Basin including Torres Syncline structure. Studied area highlighted (Fig. 2). Source: modified from Waichel et al., 2012; Barreto et al., 2014. Dike swarms: 1 – Santos-Rio de Janeiro; 2 - Ponta Grossa; 3 – Florianopolis.

2. ANALYTICAL PROCEDURES

2.1. Geochemistry

A set of 20 samples was selected, from the hypabyssal bodies of the studied region, in order to analyze the chemical compositions of the major, minor, and trace elements and rare earth elements (REE). The samples were prepared with an agate ball mill, which allows to obtain less than 200 mesh fractions. The analyzes were carried out at *Acme Laboratories Ltda* (Canada) using the ICP-ES (*Inductively Coupled Plasma Emission Spectrometry*) method for major elements and ICP-MS (*Inductively Coupled Plasma Mass Spectrometry*) method for trace elements and rare earth elements (REE). The detection limits for most of the major elements were on the order of 0.1% and 0.1 ppm for the trace elements.

2.2. Sr, Nd and Pb Isotopes

The isotopic analyzes of Sr, Nd, Sm, and Pb were performed at the Isotope Geology Laboratory of the Federal University of Rio Grande do Sul using a Thermal Ionization Mass Spectrometer (*TIMS*), model VG Sector 54.

The pulverized samples were weighed, mixed $^{149}Sm/^{150}Nd$ and $^{87}Rb/^{84}Sr$ spikes were added, and dissolved with concentrated HF and HNO_3 mixtures and solutions of 6N HCl in 7 ml Savillex® Teflon vials, where they were heated on a hot plate at 40 °C for seven days, undergoing periodic stirring procedures so that possible dissolution and homogenization problems with samples and spikes were minimized.

When the dissolution was completed, the samples were dried and re-dissolved in 2.5N HCl. Rb, Sr and REE were separated using columns filled with Dowex AG-50-X8 cation exchange resin (200-400 *mesh*) using 2.5N HCl for Rb and Sr and 6N HCl for the REEs. Nd and Sm were separated from the other REEs using HDEHP LN cation exchange resin columns (50-100μm) and 0.18N HCl for Nd and 0.5N HCl for Sm. Pb was separated with Dowex AG-1X8 cation exchange resin columns (200-400 *mesh*), diluted with 0.6N HBr and collected with 6N HCl.

The isotopic ratios were determined in the static multi-collector mode using Faraday collectors. Rb, Sr, Sm and Pb were dried and loaded on single Re filaments, and the Nd isotopes were loaded on triple Ta-Re-Ta filaments. Rb was dried and loaded with HNO_3, while Sr, Sm, Nd, and Pb were loaded with H_3PO_4, and the former was also loaded with silica gel.

The NIST standards measurements were: NBS 987 ($^{87}Sr/^{86}Sr = 0.71026 \pm 0.000011$; 1σ; n = 100) and the isotopic ratios were normalized to $^{86}Sr/^{88}Sr = 0.1194$; La Jolla (0.511848 ± 0.000021; 1σ; n = 100) and normalized to $^{146}Nd/^{144}Nd = 0.7219$. Pb was corrected for fractionation in 0.1% amu-1 based on NBS-981 standard analyzes. Total blank values for Rb and Sm were <500 pg, for Sr <60 pg, for Nd <150 pg and for Pb <100 pg. Typical analytical errors for $^{87}Rb/^{86}Sr$, $^{147}Sm/^{144}Nd$ and the $^{206}Pb/^{204}Pb$ ratio were equal to or better than 0.1%. The Rb-Sr age was calculated according to Ludwig (2001). The Nd model ages were calculated according to De Paolo (1981). The decay constants used were those recommended by Steiger & Jäger (1977) and Wasserburg *et al.* (1981).

3. GEOLOGICAL BACKGROUND

The Paraná Basin is defined as an intracratonic basin that occupies an area of approximately 1,500,000 km^2 in center-eastern South America (Figure 1). Consisting of a volcano-sedimentary succession that covers the Upper Ordovician to the Upper Cretaceous periods, this basin can be divided into six supersequences separated by regional unconformities (Milani, 1997): Rio Ivaí (Upper Ordovician - Lower Silurian), Paraná (Devonian), Gondwana I (Upper Carboniferous - Lower Triassic), Gondwana II (Middle Triassic - Upper Triassic), Gondwana III (Upper Jurassic - Lower Cretaceous) and Bauru (Upper Cretaceous). The Gondwana III Supersequence is characterized by a basal sedimentary sequence related to wind environments (Botucatu Formation), superimposed by a thick volcanic succession stratigraphically denominated Serra Geral Group (GSG). This unit covers an area of over 917,000 km^2 in Brazil, Paraguay, Uruguay and Argentina, with an approximate volume of 450,000 km^3 (Frank *et al*., 2009).

These sequences also occur in well-exposed sections in the Huab Basin in northwestern Namibia (Jerram *et al*., 2000), further expanding the area coverage of the deposits before the Gondwana break.

Petrogenetic models obtained from the investigation of hypabyssal bodies show their importance for the understanding of the PIPE. According to Marques and Ernesto (2004), geomorphic isotope data from the Ponta Grossa Dike Swarm reveal that asthenospheric components were not significant in the genesis of these dikes and that they may have been little affected by crustal contamination processes. For Renne *et al*. (1996), the ages of the Ponta Grossa Dike Swarm are between 133.1 and 130.8 Ma (^{40}Ar/^{39}Ar), temporally correlated to the basaltic flows of the Paraná-Etendeka Province. These authors also observed ages close to 120Ma in dikes near the continental margin, corroborating the hypothesis proposed by Piccirillo *et al*. (1990), who suggest that these dikes fed the younger flows of the northern sub-province, which do not show any remaining outcrops, due to subsequent erosion.

The Serra do Mar basic dike swarms of tholeiitic affinity in São Paulo and Rio de Janeiro (134-130 Ma, ^{40}Ar/^{39}Ar) could be separated into two distinct high-Ti and low-Ti suites, similar to the Ponta Grossa dikes and basaltic flows of the Paraná Magmatic Province (Turner *et al*., 1994; Stewart *et al*., 1996; Corval *et al*., 2008). Models developed from the verification of the Serra do Mar Dike Swarm suggest the delamination of the subcontinental lithospheric mantle, enclosed by ascending convective cells from the underlying sub-lithospheric mantle at shallow asthenospheric levels. These phenomena occurred during an advanced rifting stage of the Gondwana supercontinent (Valente *et al*., 2007; Corval, 2009).

The Florianópolis Dike Swarm is predominantly composed of high-Ti diabases. The low-Ti terms are represented by basalts and basaltic trachyandesites, and the dacites are geochemically similar to the Chapecó type acidic volcanic rocks of the Paraná Magmatic Province (Tomazzoli & Lima, 2006; Tomazzoli & Pellerin, 2015). Compound dikes occur in south Florianópolis, with basaltic andesite edges and a trachyandesite core containing swarms of magmatic mafic enclaves. According to some authors, the Florianópolis Dike Swarm was formed in the range of 128.3 $\pm$ 0.5 to 119.0 $\pm$ 0.9 Ma ($^{40}Ar/^{39}Ar$), with a magmatic peak occurring between the intervals of 128 and 126 Ma and 122 and 119 Ma (Raposo *et al*., 1998; Deckart *et al*., 1998). Thus, these dikes are probably associated with crustal distension in the late stages that preceded the formation of the oceanic crust at this latitude (Marques & Ernesto, 2004). However, in a recent publication by Florisbal *et al.* (2014; 2017), new ages were presented, using the U-Pb method in baddeleyite, with values ranging between 134.7 ± 0.3 and 133.9 ± 0.7 Ma, that is, older than those indicated by the $^{40}Ar/^{39}Ar$ methodology. In this case, they did not have a direct connection with the syn-rift magmatism associated with the south opening of the Atlantic Ocean. Coutinho (2008), based on petrological and geochronological data, suggests that the swarm of coastal dikes are components of the north and south arms of a triple-junction system centered on the coast of the state of Paraná and related to the initial opening of the South Atlantic.

In the African part of the Paraná-Etendeka Province, there are several studies on the petrology of the intrusive systems. The Henties Bay-Outjo Dike Swarm in the Damara belt, Namibia, is interpreted as an aborted arm of a triple junction centered on the edge of Walvis Bay. It has a compositional range from basalt to rhyolite with predominant low-Ti basaltic composition (Duncan *et al*., 1990; Trumbull *et al*., 2004, 2007). This swarm includes dikes with picritic terms around Spitzkoppe, western Namibia, with up to 20% MgO, suggesting that the magma probably originated from the melting of a *mid-ocean ridge basalt* (MORB), followed by the limiting reaction of the metasomatized subcontinental lithospheric mantle just prior to the formation of these magmas. (Thompson *et al*., 2001, 2007). Horingbaai dolerites have an affinity for MORB type magmas, with flat REE patterns and isotopic data plotting within the depleted mantle quadrant in the εSr vs. εNd diagram (Erlank *et al*., 1984; Hawkesworth *et al.*, 1984). The Huab River Valley *sills* complex and associated dikes are separated into four types of dolerite magmas that differ from one another by different ratios of incompatible elements (Duncan *et al*., 1989). The Doros Complex is a mafic intrusion stratified within the Damaraland Intrusive Suite, northeastern Namibia and part of the Paraná-Etendeka Magmatic Province, ages 134-132 Ma ($^{40}Ar/^{39}Ar$) (Marsh, 2013). Based on field, petrological and geophysical data, Owen-Smith & Ashwal (2015) proposed the origin of the

Doros Complex as a result of at least seven spaced magmatic pulses. The authors suggest a large and complex system of interconnected conduits and chambers that housed a range of magmas of different compositions.

4. GEOLOGY OF THE CERRO DO CORONEL REGION

The Cerro do Coronel region is characterized by the presence of dolerite sills arranged in an NW-SE preferred direction, concordantly intrusive in sedimentary units of the Paraná Basin, at the northern boundary of the South-Rio-Grandense Shield (Eick et al., 1984; UFRGS, 2006; Sarmento et al., 2014).

The basement units are granitoids linked to the Cordilheira Intrusive Suite and the Encruzilhada do Sul Intrusive Suite (Philipp et al., 2002). The host rocks of the sills are stratigraphically correlated with two units of the Paraná Basin: Rio Bonito and Irati Formations. The Rio Bonito Formation (Guatá Group) is characterized in the area by lenticular packages of medium to fine sandstone, yellow and cemented, medium to fine arkosean sandstones, with yellow to grayish siltstone lenses and dark gray to carbon black carbonaceous pelites or with remains of organic matter with silicification features due to the concordant intrusion of the diabase. The Irati Formation rocks (Passa Dois Group) make erosive contact with the sub-horizontal sequence of alluvial and colluvial deposits of the Capivari Arroio floodplain and tributaries. In the vicinity of the NE fault that divides the Cerro do Coronel, there are carbonate concretions, brecciated, with veins filled by calcite and occasionally by pyrite. At the base of the sequence, a conglomerate occurs, followed by brittle yellow to gray siltstone with small carbonate concretions, yellow to gray siltstone with fine sandstone lenses and yellow and gray concretions. The sequence is partially covered by the dolerite sill.

The Cerro do Coronel is an inselberg of approximately 12.4 km^2, with a flat top, which stands out in the geological-geomorphological context of the region. The base is comprised of the sedimentary rocks of the Irati and Rio Bonito Formations, which make contact with an N70E fault, and are concordantly intruded by a dolerite body (Figure 2E). This set of units geomorphologically defines a bysmalith, characterized as a feature related to an intrusion concordant to different units of host rocks, which were placed side by side by faulting (Eick et al., 1984; Sarmento et al., 2014). The Cerro do Coronel dolerite sill (sill 2) is also affected by the N70E fault that determined the separation of the intrusion into two portions with different thicknesses. The portion located to the north is about 180 m thick, and the one located to the south is approximately 30 m thick. Sill 1 is northwest (BR-290) of Cerro do Coronel, is

approximately 20 m thick and makes contact with rocks of the Irati Formation (Figure 2B). Sills 3 and 4, located southeast, are about 30 m thick and make contact with rocks of the Rio Bonito Formation (Figures 2A and D). Polygonal and centimetric sub-vertical columnar jointing is observed in the upper and lower portions of the sill. Elongated polygonal jointing is observed locally and is commonly disturbed in regions with intense sub-vertical tabular fracturing (Figures 2C and 2D).

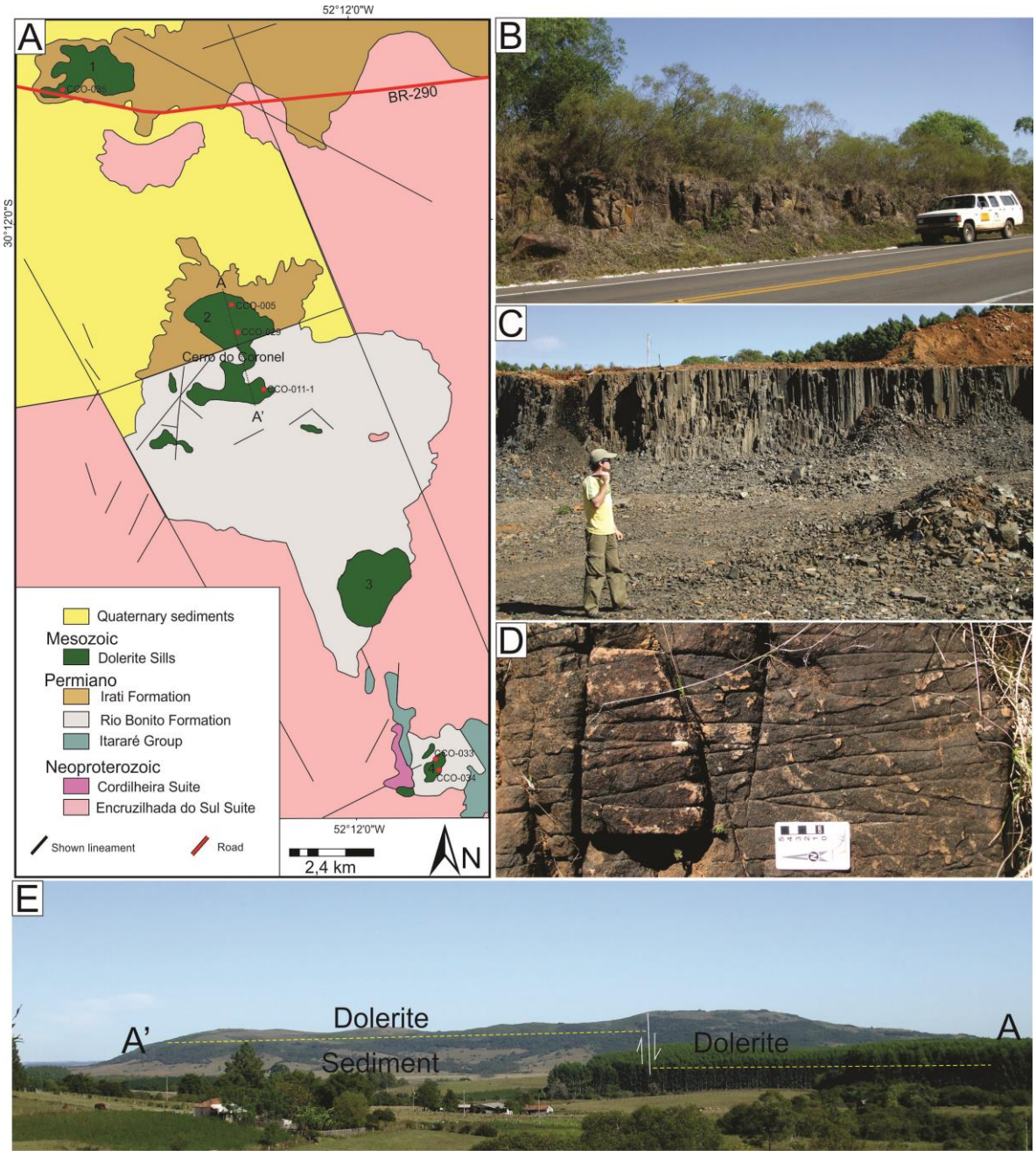

Figure 2. (A) Geological map of the study area; (B) Sill 1 with metric columnar joints (BR-290); (C) Soleira 4: Dolerite sill showing centimetric columnar joints; (D) Intense subvertical fracturing on the Cerro do Coronel (sill 2). (E) Panoramic view of the Cerro do Coronel (sill 2) showing the fault that determined the separation of the intrusion in two parts with different thicknesses.

5. PETROGRAPHY

Holocrystalline rocks correspond to relatively homogeneous mesocratic dolerites, with fine grain sizes. A small textural variation can be identified, with grain-size thinning towards the base and top of the sills (Figures 3A and B). Pockets with gabbro texture of little expression are located at the base of the northern portion of the dolerite body. The predominant texture is equigranular, although the presence of few phenocrysts of plagioclase and pyroxene it is observed.

The mineralogy observed in the intrusive bodies consists mainly of plagioclase (~ Ab_{51} An_{46} Or_3), augite (~ En_{33} Wo_{34} Fs_{33}), pigeonite (~ En_{10} Wo_{42} Fs_{48}) and titanomagnetite. Apatite is a frequent accessory phase (Figure 3). Felsic mesostasis is present in most of the sills (zeolitic aggregates).

Plagioclase occurs as subhedral to euhedral prisms, usually elongated, with sizes ranging from 0.05 to 1.3 mm. Rare phenocrysts are observed, sometimes forming glomeroporphyritic aggregates, ranging in size from 0.8 to 2.0 mm and occasionally with normal, well-developed zonation.

The clinopyroxene crystals are subhedral and range from 0.05 to 0.8 mm in size. They occur in general as granular aggregates of fine grains, usually associated with opaque minerals. Rare prismatic phenocrysts up to 4.0 mm can be observed, especially at the base of the sill. Uralitization occurs only in localized portions of the intrusive body, with the occurrence of iron hydroxides as products of weathering alteration. In the coarser grain size portions, the augite crystals range from 1.0 to 8.0 mm in sizes and develop symplectic and skeletal texture with plagioclase. They are often partially or fully included in the plagioclase.

Olivine is rare. Two grains from a sample of the base of the Cerro do Coronel dolerite were identified. The largest grain is euhedral, approximately 1.2 mm in size, with medium cleavage and edges and fractures filled by iddingsite. Characteristics determined by scanning electron microscopy (SEM/EDS) indicate a composition richer in MgO (Fo > 50%).

Quartz is scarce and occurs as an intergranular product, sometimes forming sub-grains (0.2 to 0.5 mm) or intergrown with feldspar, defining a micrographic texture.

Opaque minerals generally have straight faces and are almost always associated with pyroxenes, often included in them and in plagioclase. The habit suggests that they belong to the group of Fe and Ti oxides.

Apatite is a common accessory phase, up to 3% of the total sample. They usually occur as euhedral and acicular crystals, present mainly in the microgranular material.

The felsic mesostasis is formed by a homogeneous material of light brown color and low relief, low birefringence (gray) and wavy extinction. It ranges from 10 to 12% of the sample volume and can be interpreted as a late zeolitic aggregate. They can also be observed in vermicular or dendritic shapes, forming the micrographic and granophyric texture, identified as quartz-feldspar intergrowths. They occur in the interstices between the crystals of plagioclase and clinopyroxenes.

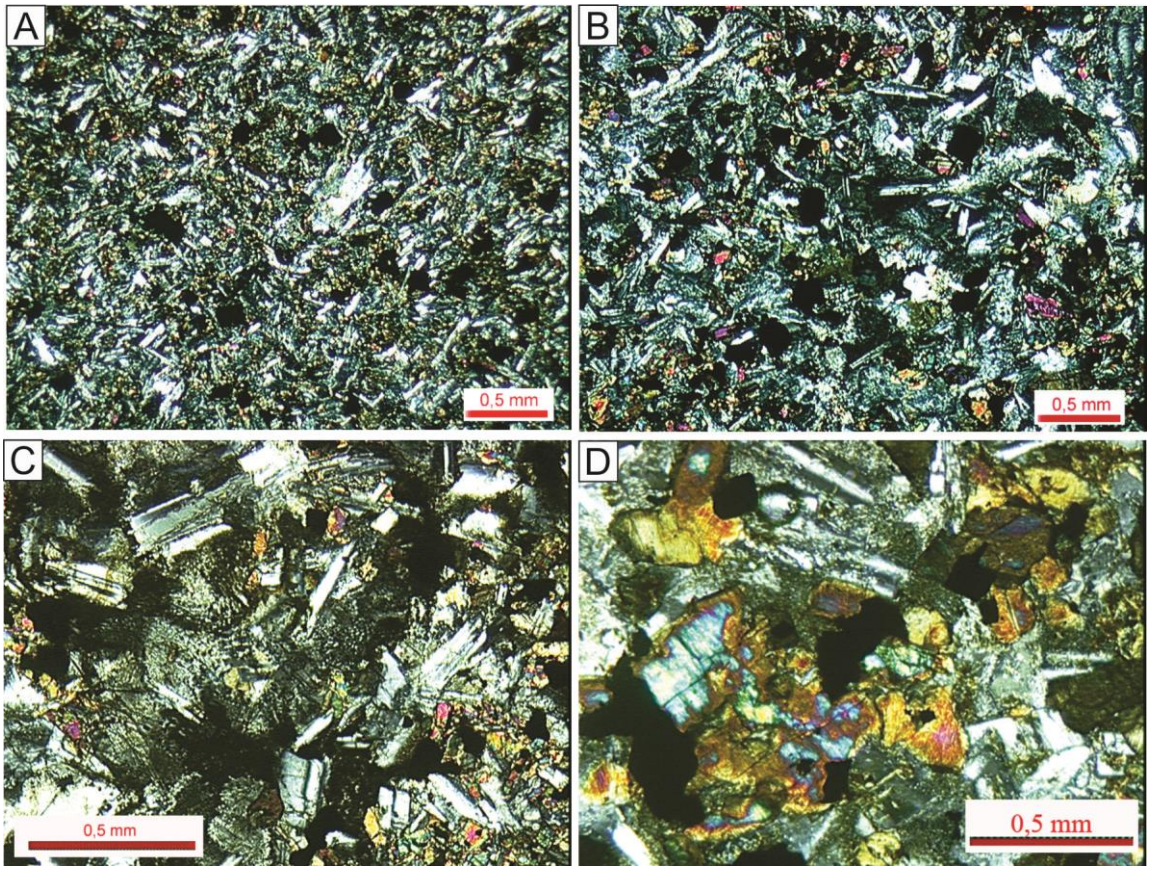

Figure 3. Microscopic aspects of the sills: (A) and (B) grain-size thinning towards the base and top of the sills; (B) intergranular texture formed by plagioclase and clinopyroxenes; (C) Zeolitic aggregate in the interstices of plagioclase and clinopyroxene grains; (D) coronitic texture in the clinopyroxene grains formed by uralitization. Crossed nicols.

6. LITHOCHEMISTRY

6.1. Whole Rock Geochemistry

Chemical data of the dolerites are shown in Table 1. The samples are in the basaltic andesite field in the TAS diagram (Le Bas et al., 1986), with concentrations of SiO_2 between 52.47 and 54.99% and of alkalis between 5.15 and 3.55%. The samples are subalkaline in the Irvine and Baragar diagram (1971) and are in the boundary between basalts and basaltic andesites, defined by the correlation between trace elements of low mobility (Figure 4).

The tholeiitic affinity of the magmatism is marked by FeO_t enrichment relative to MgO, combined with low Al_2O_3 values (Wilson, 1989).

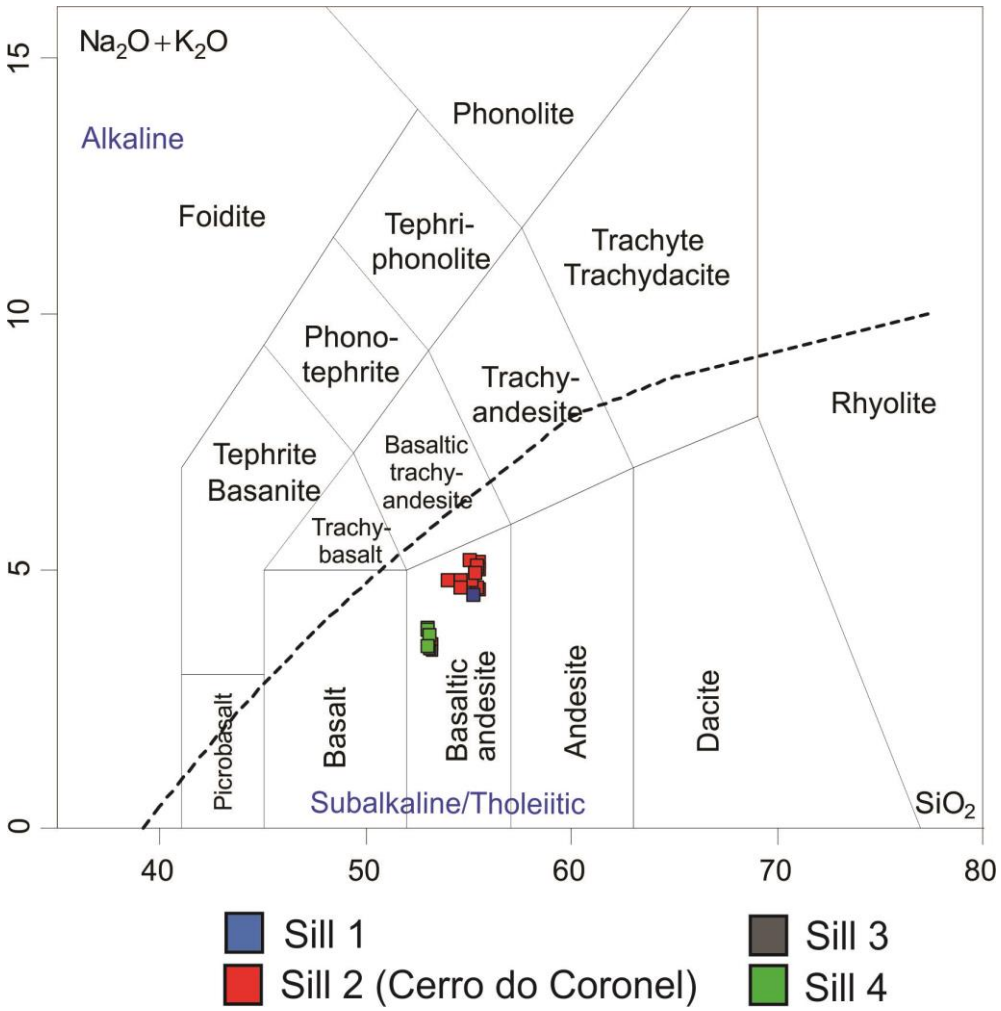

Figure 4. Classification Diagram TAS (Le Bas et al., 1986) of the sills of the Cerro do Coronel region.

All the rocks show normative quartz, hypersthene, and diopside, classifying them as supersaturated tholeiites. Using MgO as the differentiation index to establish the behavior of the major elements and trace elements with the evolution of the magmatism of the hypabyssal rocks of the Cerro do Coronel region (Figures 5 and 6), we observe a trend for the contents of Al_2O_3 and CaO to decrease with the decrease in MgO, in addition to the increase in SiO_2, Na_2O, K_2O, P_2O_5, FeO_t, and TiO_2. The MgO contents are lower than 6%, which, combined with the low values of Cr and Ni, suggests that the magma that gave rise to the intrusion underwent previous fractionation processes, probably involving olivine and augite.

The distribution of the samples from the Cerro do Coronel dolerites shows that the less differentiated terms are in the basal portion of the intrusive body and that a slight evolution is observed towards its upper portions. This same trend is observed among the dolerite sills,

where those located in the Northwest are more differentiated than those located in the Southeast. There is an increase in the contents of Ba, Rb, Sr, Zr, Y, Nb, and Th with the decrease of Mg contents. On the other hand, Ni has a positive correlation with MgO, suggesting the extraction of this element in mafic phases.

In the north part of the dolerite, the Rb, Sr, Ba, Zr, Nb, Th and Y contents are slightly higher than at the base of south Cerro do Coronel, and in the other intrusions to the southeast.

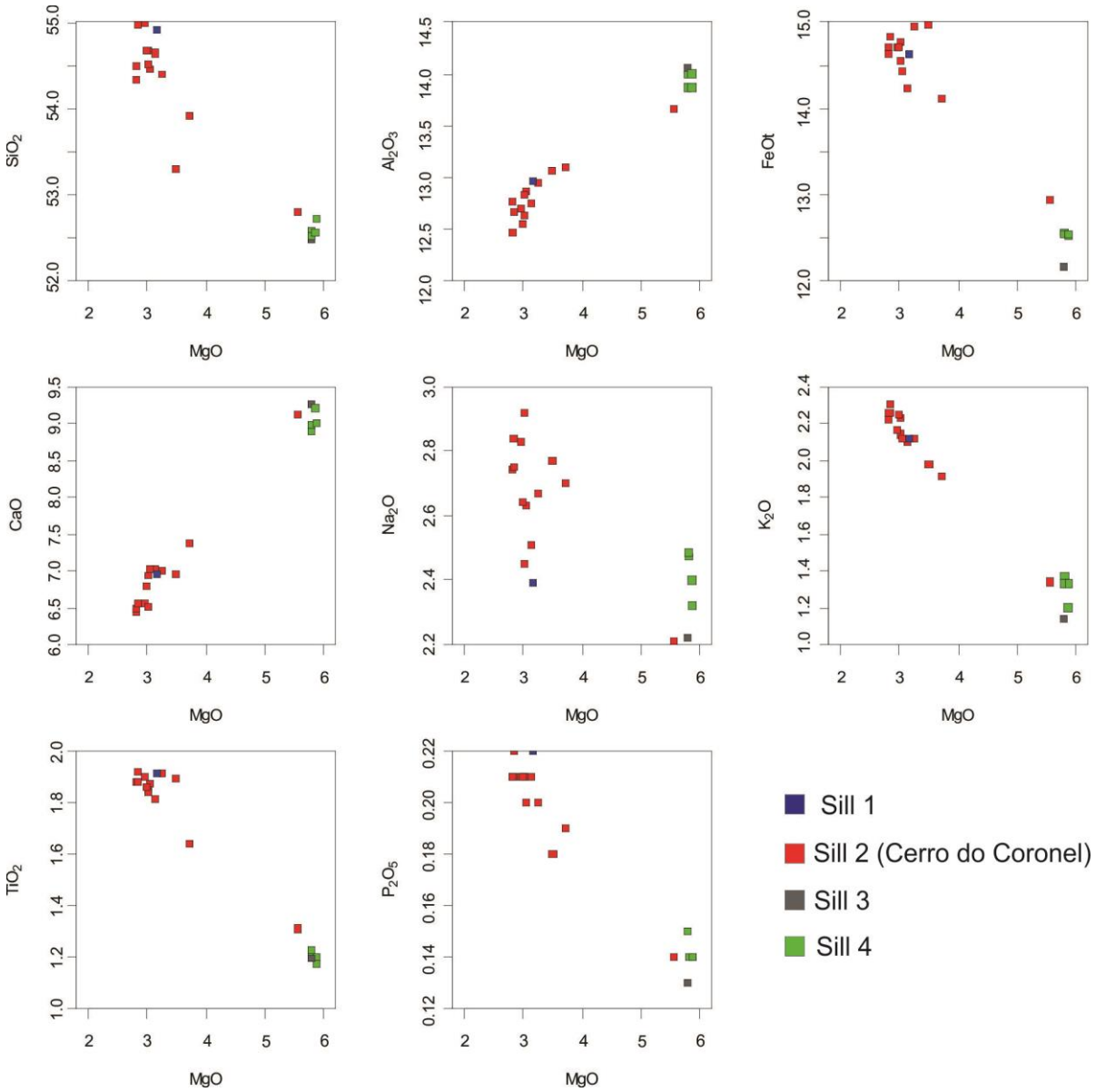

Figure 5. Binary diagrams displaying major elements variation (wt.%) relative to MgO of the studied sills.

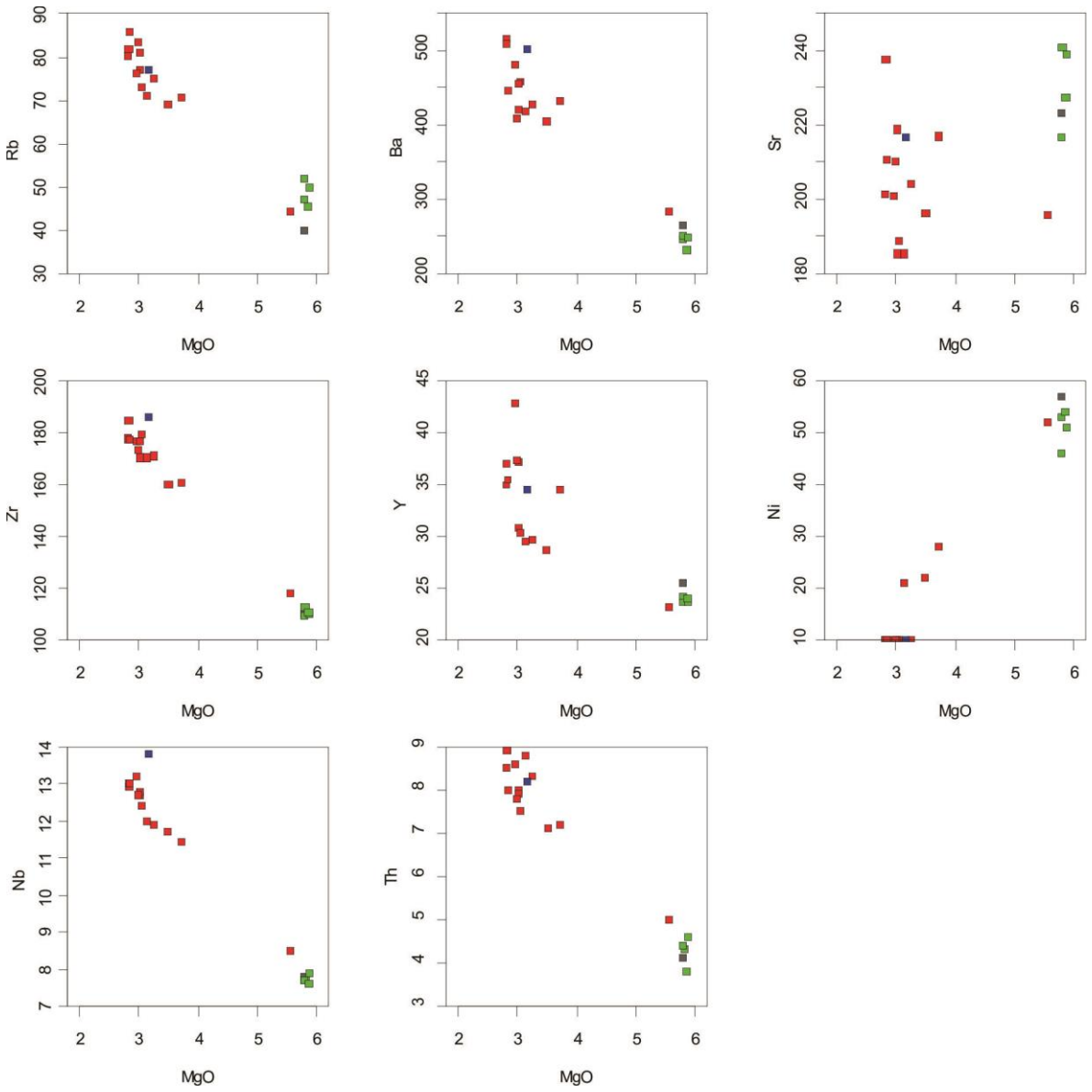

Figure 6. Binary diagrams displaying trace elements variation (ppm) relative to MgO (wt.%) of the studied dolerites. Symbols are the same as in Figure 5.

The dolerite samples, when normalized by the primitive mantle pattern (McDonough & Sun, 1995), shown an enrichment in incompatible elements with negative anomalies in Nb and Ta (Figure 7A). According to some authors, this pattern may suggest the presence of some residual phase rich in Nb and Ta, during the partial melting processes, or even be a consequence of crustal contamination (Wilson, 1989; Piccirillo et al., 1989; Hawkesworth, 1986). The negative Sr anomaly indicates the fractionation of plagioclase in the evolution of the intrusive bodies. The patterns observed in these multielement diagrams and behavior of LILEs (*Large Ion Lithophile Elements*) (K, Rb, Ba, Sr, Pb), combined with the low HFSE levels (*High Field Strength Elements*) (Nb, Ta, Zr, Hf, Ti, P) are very similar to those of intraplate tholeiitic basalts (Piccirillo et al., 1989). There is a slight increase in the fractionation of some elements, mainly heavy REEs, with the increase of differentiation. The

rare earth element patterns, when normalized to the C1 chondrite pattern (McDonough & Sun, 1995), show moderate values of these elements (Σ_{REE} = 90 - 172) and are characterized by a moderate enrichment of the light REEs with respect to the heavy REEs (La_N/Yb_N = 4.7 - 5.8). They present a slight fractionation in light REEs (La_N/Sm_N = 2.4 - 2.8) and in heavy REEs (Eu_N/Yb_N = 1.1 - 1.5) (Figure 7B). Slight Eu anomalies are observed (Eu/Eu^*_N = 0.8), which suggest the fractionation of plagioclase.

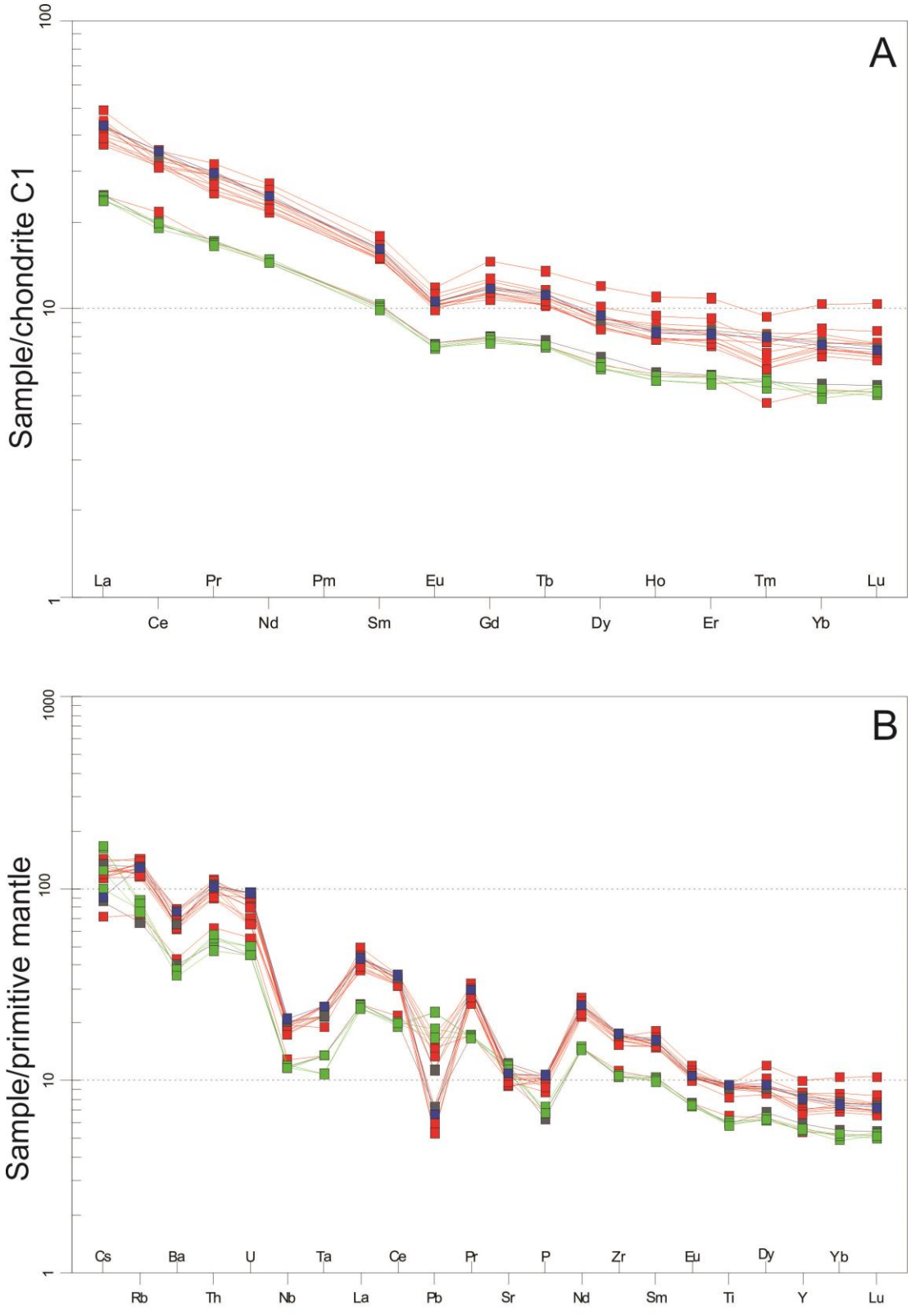

Figure 7. Trace element abundance (A) and REE patterns (B) normalized to the primitive mantle (McDonough and Sun, 1995) and chondrite C1 of the studied rocks of the Cerro do Coronel region. Symbols are the same as in Figure 5.

6.2. Isotopic Geochemistry

The results of Sr, Nd, and Pb radiogenic isotopes of the investigated sills are shown in Table 2. The initial $^{87}Sr/^{86}Sr$ and $^{143}Nd/^{144}Nd$ ratios were recalculated for the mean age of 132 Ma, based on publications about Ar-Ar ages for PIPE basalts (e.g. Renne et al., 1992; Thiede and Vasconcelos, 2010; Almeida et al., 2017) as well as U-Pb ages obtained in felsic rocks of this province (Janasi *et al*., 2011).

The sills have high initial $^{87}Sr/^{86}Sr$ ratios (0.71138 and 0.71293) and low initial $^{143}Nd/^{144}Nd$ ratios (0.512205 and 0.512315), with εNd_i values between - 3.14 and - 5.20. The T_{DM} model ages, calculated for 132 Ma, are between 1.10 and 1.23 Ga. According to the Zindler & Hart diagram (1986), it can be observed that all samples correspond to enriched sources, considering the values of $\mathcal{E}Nd_i$ and $\mathcal{E}Sr_i$ to infer potential reservoirs of these magmas.

The studied rocks are plotted near the boundary between the upper and lower continental crust sources, with low rates of $^{143}Nd/^{144}Nd_i$ and high rates of $^{87}Sr/^{86}Sr_i$ (Figure 8). It is also noted that the initial $^{143}Nd/^{144}Nd$ ratios of the southern portion rocks are slightly higher than the ratios of the northern portion.

The Pb isotopes of the dolerites have $^{206}Pb/^{204}Pb$ values between 18.568 and 18.815, $^{207}Pb/^{204}Pb$ values of 15.549 to 15.702 and $^{208}Pb/^{204}Pb$ of 38.562 to 38.961. In the diagrams of $^{207}Pb/^{204}Pb$ versus $^{206}Pb/^{204}Pb$ and $^{208}Pb/^{204}Pb$ versus $^{206}Pb/^{204}Pb$ (Figure 9) the analyzed dike samples plot above the *Northern Hemisphere Reference Line* (NHRL) (Allegre et al., 1988). In the diagram of $^{207}Pb/^{204}Pb$ versus $^{206}Pb/^{204}Pb$, samples from Cerro do Coronel plot within the enriched mantle reservoir field (EM-II), and the sample of sill 1 is more radiogenic and plots above the EM-II field. The sill 4 sample is in the field of the Tristan da Cunha volcanic rocks. In the $^{208}Pb/^{204}Pb$ versus $^{206}Pb/^{204}Pb$ diagram, all samples plot between the MORB and EM-II fields.

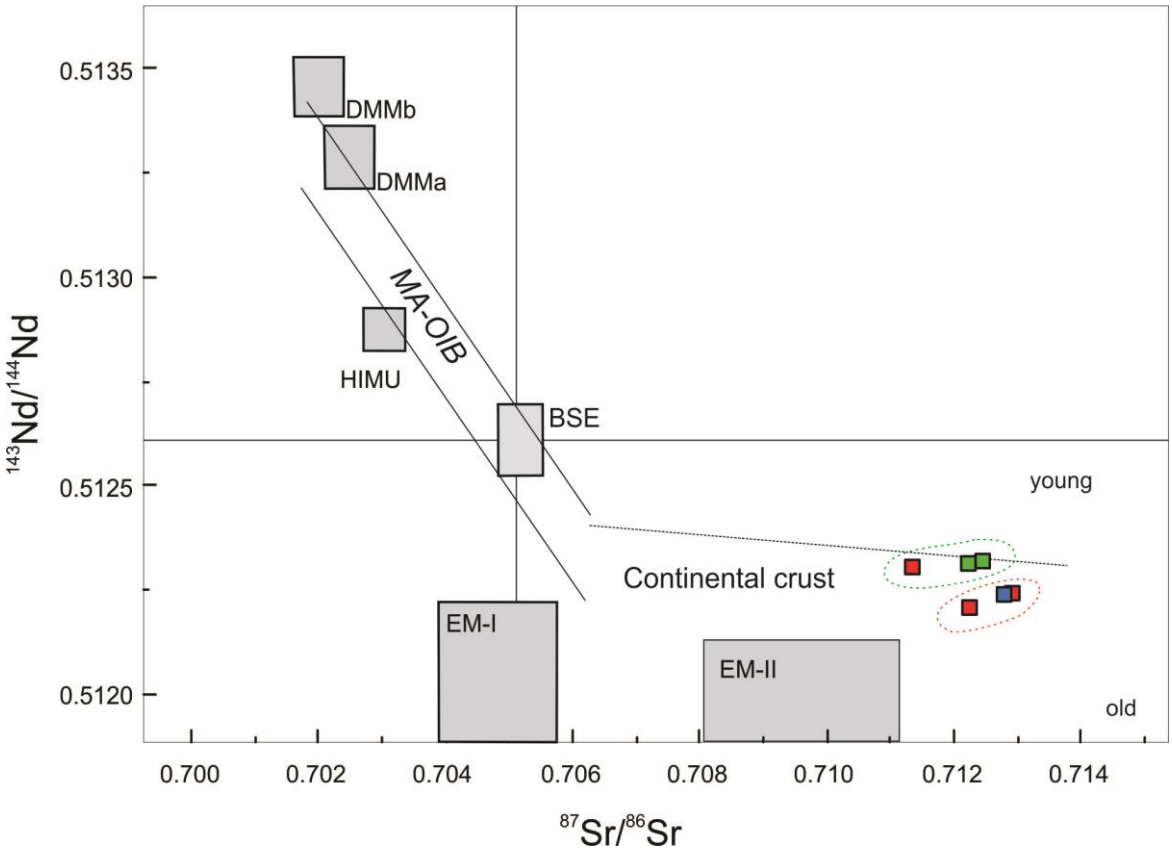

Figure 8. $^{87}Sr/^{86}Sr(i)$ versus $^{143}Nd/^{144}Nd(i)$ diagram, modified after De Paolo and Wasserburg (1979) and Zindler and Hart (1986). Symbols are the same as in Figure 5. dashed lines: Red= northern portion; Green= southern portion.

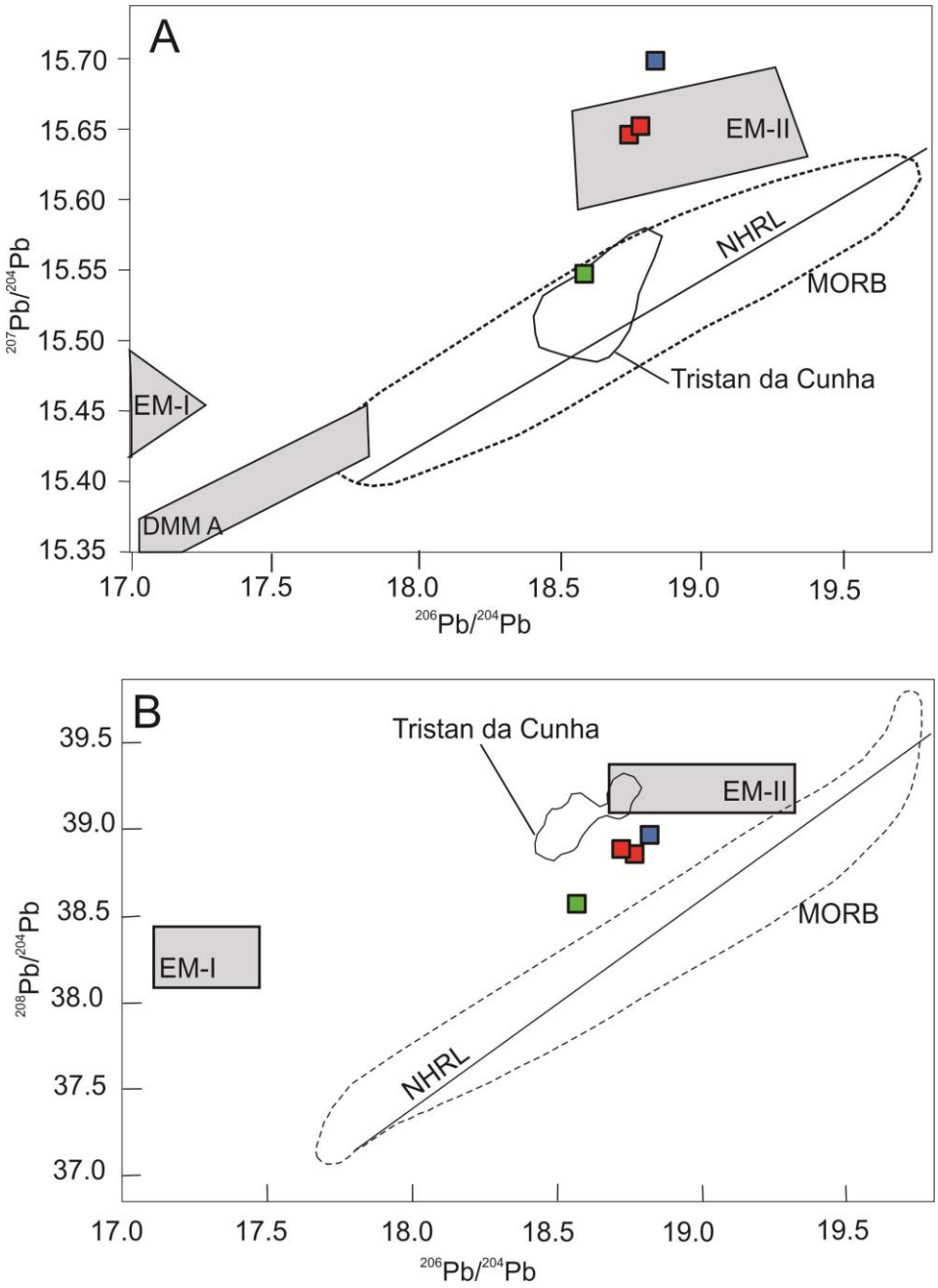

Figure 9. Lead isotope compositions for the lava flows of the SCSH, LJ, and MC sections in comparison to the fields for Tristan da Cunha volcanics (Rohde et al. 2013), and the mantle components EM-I, EM-II, and DMMA (Zindler and Hart 1986). NHRL, Northern Hemisphere Reference Line (Hart 1984). Symbols are the same as in Figure. 5.

7. DISCUSSIONS

7.1. Emplacement and petrogenesis of sills

In the Cerro do Coronel region, the intrusions follow the regional trend, on an NW-SE alignment, and stratigraphic conditioning, evidenced by the existence of preferential intrusion levels, first the Irati and Rio Bonito Formation (throughout the basin), then the Botucatu

Formation (in São Paulo and Rio Grande do Sul) and the Serra Alta and Teresina Formations (Paraná and Santa Catarina).

Among the studied sills, the Cerro do Coronel one stands out, which was placed concordantly in the two formations mentioned above. Due to the erosive processes, the upper contact of the intrusive body with the Irati Formation was not preserved. The sill was also affected by the N70E fault, which determined the separation of the intrusion into two portions with different thicknesses. The southeastern dolerite body is approximately 30 m thick, while in the northwestern portion the sill is about 180 m in thickness. This fact evidences a reactivation of the fault that resulted in the uplifting of the southeast portion and the descent of the northwest portion. The dolerite bodies located to the southeast of Cerro do Coronel also have a concordant contact with the sedimentary rocks of the Rio Bonito Formation, whereas the body located to the northwest concordantly cuts the Irati Formation sedimentary rocks (Eick et al., 1984; Sarmento et al., 2014).

The intrusive bodies present small faciological diversity characterized by fine to very fine equigranular texture and the very localized presence of gabbroic pockets with augite crystals and acicular plagioclase. The small faciological and textural variation may be related to the low depth in which the magma crystallized and also to the little thickness of the magmatic body. In general, the rock is characterized by intergranular texture, evidenced by the plagioclase and augite fabric, the main mineralogical constituents.

The geochemical data show the subalkaline nature of the magmatism related to the Cerro do Coronel intrusive bodies, whose tholeiitic affinity can be verified by the relationships between alkalis, FeO_t and MgO, and the low Al_2O_3 content. The presence of normative quartz, hypersthene, and diopside confirms the characterization and allows to interpret these rocks as supersaturated tholeiites. The dolerites present low levels of MgO, Cr, and Ni, which suggests that these rocks were formed by an evolved magma that underwent previous fractionation processes, probably involving olivine and augite. The behavior of the major elements in relation to the differentiation index suggests magmatic differentiation processes involving fractional crystallization mechanisms mainly controlled by the fractionation of plagioclase and augite. These findings are consistent with the petrogenetic interpretations suggested by Bellieni et al. (1984) and Piccirillo et al. (1988).

The patterns presented by the dolerites in the multi-element diagrams and the behavior of the LILEs, combined with the low levels of HFSE, are very similar to those of continental tholeiitic basalts. The behavior of rare earth elements shows moderate values when

normalized to C1 chondrite. They are characterized by a moderate enrichment of light REEs in relation to heavy REEs and a slight Eu anomaly, similar to those presented by Peate et al. (1992, 1997, 1999), Marques et al. (1989) and Hawkesworth et al. (2000) for tholeiitic basalts of large continental provinces such as those of the Paraná Magmatic Province.

The major and trace elements geochemical signatures of the rocks, such as light REE values higher than those of heavy REEs and negative anomalies of Nb, Ta and Sr (Figure 11A), a slight Eu anomaly the low to moderate values of these elements are similar to other mafic intrusions in the south sub-province of the Paraná Magmatic Province (Renner, 2010; Muzio et al., 2012, 2017; Sarmento et al., 2014; 2017) However, these sills tend to be more differentiated when compared to the sills and mafic intrusions of the Etendeka Province, Namibia (Ewart *et al*., 1984; Duncan *et al*., 1989; Gibb & Henderson, 1996; Marsh, 2013; Owen-Smith & Ashwal, 2015).

The isotope data obtained from the intrusions show signatures similar to the values specified for the low-Ti basic rocks of the south sub-province of the Paraná Magmatic Province (Mantovani et al. 1985; Hawkesworth et al. 1986; Piccirillo et al. 1989; Peate et al. 1992, 1999; Peate & Hawkesworth 1996). The T_{DM} calculated for 132 Ma is indicative of melting of older protoliths (between 1.1 and 1.2 Ga). The initial $^{87}Sr/^{86}Sr$ signatures obtained in this study are substantially superior to any previously reported subcontinental lithospheric mantle sources (Duncan et al., 1984; Hawkesworth et al., 1984; Jourdan et al., 2007). However, the Pb isotopic data suggest that these mafic intrusions originated from a source such as EM-II. This could lead to a possible enriched oceanic source or to a subcontinental lithospheric source, characterized by enrichment of Rb and LREE, resulting in radiogenic Sr and non-radiogenic Nd (Allegre, 2008).

The rocks show an increase in the initial ratios of $^{87}Sr/^{86}Sr$ of the base (sample 011-1), top (sample 029) and intermediate portion of sill 2 (Cerro do Coronel) respectively, as well as the increase of SiO_2. This condition can be explained by faster cooling at the ends and, consequently, the increase of the evolution towards the core of the sill. Samples of sill 4 (samples 033 and 034) have higher $^{87}Sr/^{86}Sr$ ratios compared to the sample from the base of sill 2 (sample 011-1), even as a part of the more primitive rocks of the region. This suggests that the rocks of sill 4 may have undergone greater crust assimilation and also, the sample from the base of sill 2 may have been part of one of the sill conduits and had undergone less crustal assimilation (Figure 8).

7.2. Petrogenetic magmatism modeling

Among the processes of magmatic differentiation, one of the most effective ones is fractional crystallization. In the study of the magmatic evolution of the hypabyssal bodies of the Cerro do Coronel region, a traditional geochemical mass balance model was used (Stormer & Nicholls, 1978) to calculate the percentage of fractionated minerals and fractionated total magma. The data were based on mineral chemistry results from olivine, pyroxenes and plagioclase crystals from the studied dikes (Sarmento et al., 2017b). The titanomagnetite results were extracted from Renner (2010).

The first test was performed for the range of 52.79 to 53.92% SiO_2, corresponding to a less differentiated composition (starting liquid: sample 011-1B - base of the main sill) for a magma of slightly more differentiated composition (final liquid: CCO-029 - top of the main sill) (Table 3). The modeling could be done with 40.00% fractionate in the proportions of 49.10% plagioclase, 41.12% clinopyroxene, 8.41% olivine and 1.36% titanomagnetite, with a low residual sum of squares between the observed values and computed compositions (Σres^2 = 0.2802). In the second test (Table 4), mass balance was calculated using sample 011-1B as an initial liquid that showed the transition from a more differentiated andesite-basaltic one (sample 005) with the modeling of 51.28% fractionate in the proportions of 49.87% plagioclase, 40.16% clinopyroxene, 8.28% olivine and 1.69% titanomagnetite with a residual sum of squares of Σres^2 = 0.4043.

The results obtained are consistent with the fractional crystallization hypothesis, representing an evolution from a less differentiated liquid to a more differentiated composition. These models provide a good fit to the main elements considering the reasonable proportions required and the low sum of square of residuals.

In order to test the evolution of these liquids since the crust assimilation associated with fractional crystallization (AFC) and its effect on the behavior of the trace elements during the rise of the magmas, the FC and AFC trends were calculated with an initial magma composition as less differentiated (samples 011-1B, 033A and 034H).

The selected contaminants were Neoproterozoic and Paleoproterozoic rocks of basement units geographically close to the studied area and for which geochemical information and Sr-Nd data were available in the literature.

The modeling was done using the Petrograph software (version 2.0 beta) in which the curves were arranged in the Ba-Rb, Rb-Y and Zr-Y diagrams (figure 10). These incompatible

trace elements were selected as good indicators of both fractional crystallization processes and crustal contamination. According to the observed behavior of these elements, only fractional crystallization would explain the evolution of the studied rocks. In the Rb vs. Ba diagram, the FC curve reaches the samples at about 37% to 50% crystallization. In Rb vs. Y and Zr vs. Th diagrams, the FC curves reach the samples at about 40% to 50% crystallization. Finally, in the Zr vs. Y diagram, the FC curve reaches the samples at about 29% to 45%.

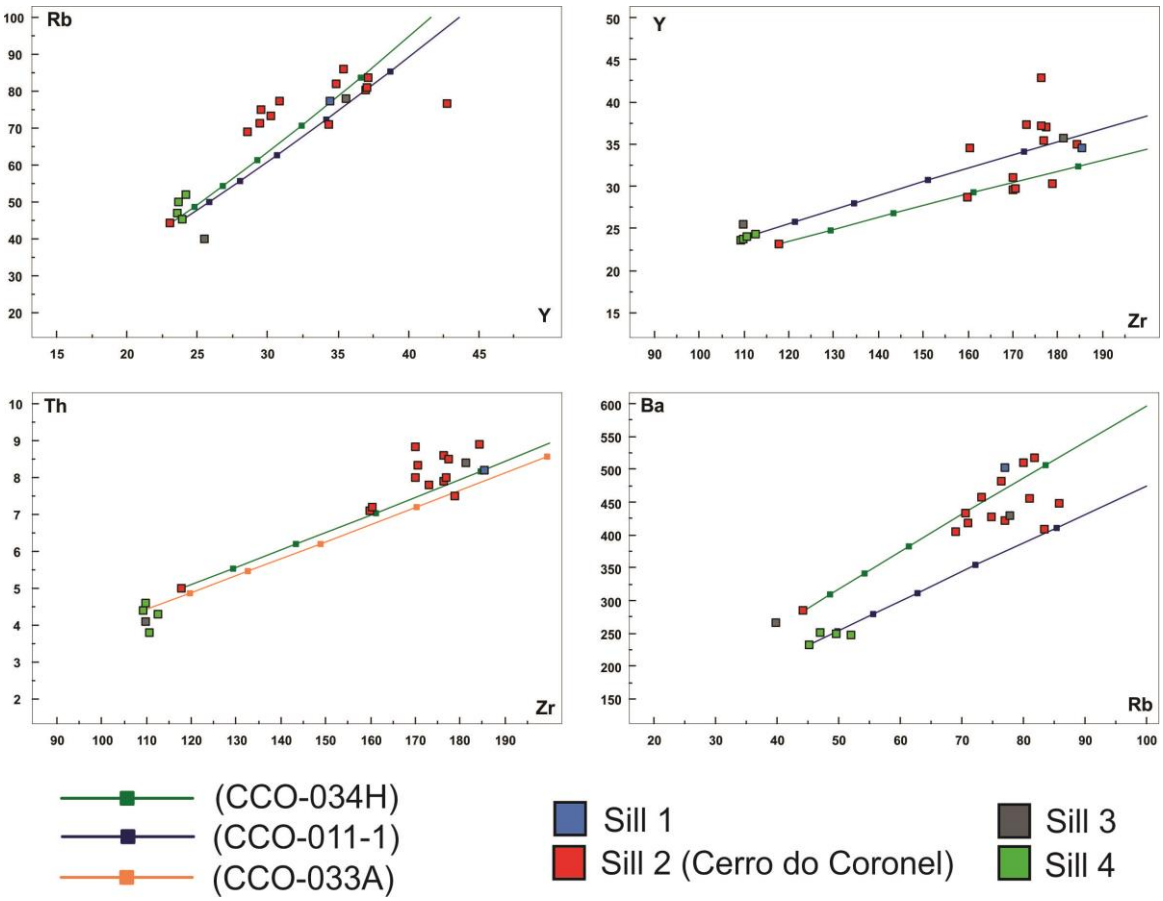

Figure 10. Variation diagrams of selected trace elements, illustrating the results of modelling of fractional crystallization (FC) of basaltic andesite rocks of Cerro do Coronel region. The squares in the lines represent increases of 10% in the crystallization degree.

The modeling of trace elements suggests that the evolution of the studied rocks occurred by fractional crystallization, but the high $^{87}Sr/^{86}Sr_i$ ratios of the Cerro do Coronel region implies that assimilation and crystallization (AFC, De Paolo 1981) were simultaneous processes in the residence of the magma inside the magma chamber or during the ascent of the magmas through the crust until the level of placement of the sills.

The contaminants selected for the construction of AFC curves in isotopic modeling are the Neoproterozoic units Ponta Grossa Granite (sample 630 from Philipp et al. 2007) and Capão do Leão Granite (sample 443C from Philipp et al., 2007). The chosen Paleoproterozoic

units are tonalites of the Arroyo dos Ratos Complex (samples TG-02O and TG-02G of Gregory, 2014).

Isotopic ratios were included in binary $^{87}Sr/^{86}Sr_i$ vs. Sr with r (assimilation/fractional crystallization rate) of 0.3 (30% assimilation) (Figure 11). The best results are shown as having one of the less developed samples of the base of the main sill in the southern portion (sample 011-1) and the Paleoproterozoic units, such as the Arroio dos Ratos Complex Tonalite (sample TG-02G) as a contaminant. Assimilation rates of 14% to 19% (crystallization from 35% to 57%). If Neoproterozoic units such as the Ponta Grossa Granite are used, the results are not satisfactory.

The FC and AFC models based on trace elements and Sr isotopes suggest that even with the domain of fractional crystallization at a local scale, there is an important role of the process of crustal assimilation in the petrogenesis of these rocks. A contribution of the Paleoproterozoic crust is considered. This condition is supported by the behavior of the AFC curve in the Sr isotope modeling (Figure 11), when using the Arroyo dos Ratos Complex units as a contaminant.

Negative Nb anomaly and enrichment in Th and U in relation to Ta and Hf (Figure 7), as well as increasing ratios of $^{87}Sr/^{86}Sr$ and constant Ba/Yb ratios (Figure 12) reinforce the important role of the upper crust assimilation. The $^{87}Sr/^{86}Sr$ versus Ba/Yb variations are analogous to the Nd-Sr isotope diagrams and define fairly similar trends (Wilson, 1989).

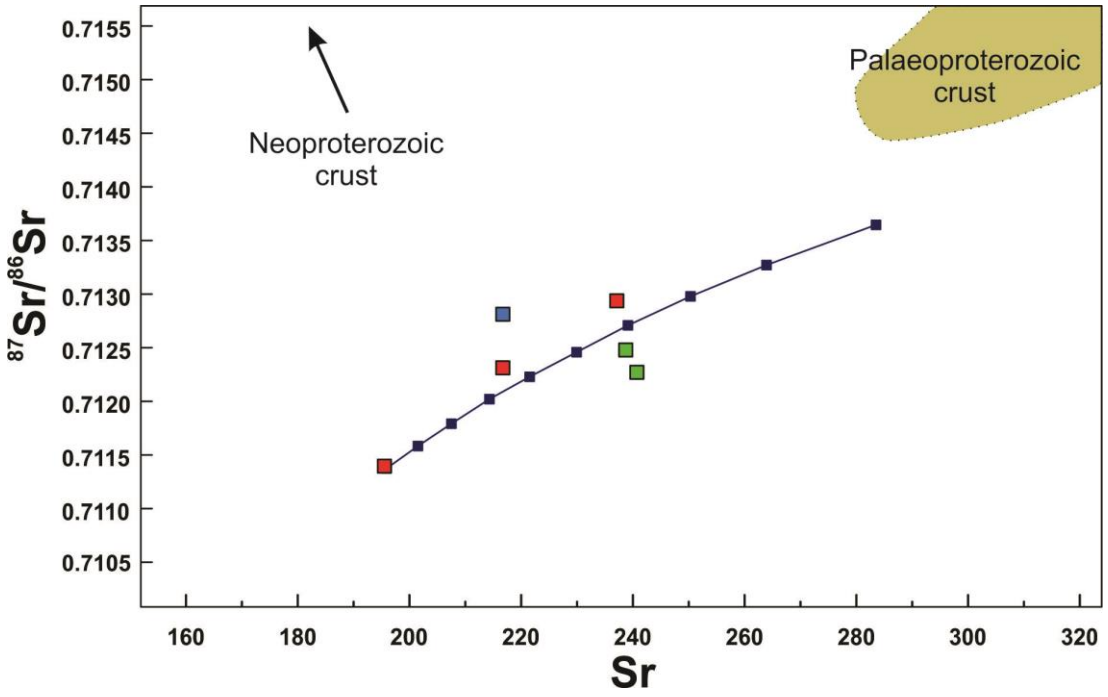

Figure 11. Modelling of assimilation-fractional crystallization (AFC) for the generation of basaltic andesite of the Cerro do Coronel region. The line represents AFC trajectory - The squares in the line represent increases of 10% in the crystallization degree. Degree of assimilation/degree of crystallization ("r") used = 0,3. Sr bulk distribution coefficient used = 0,924.

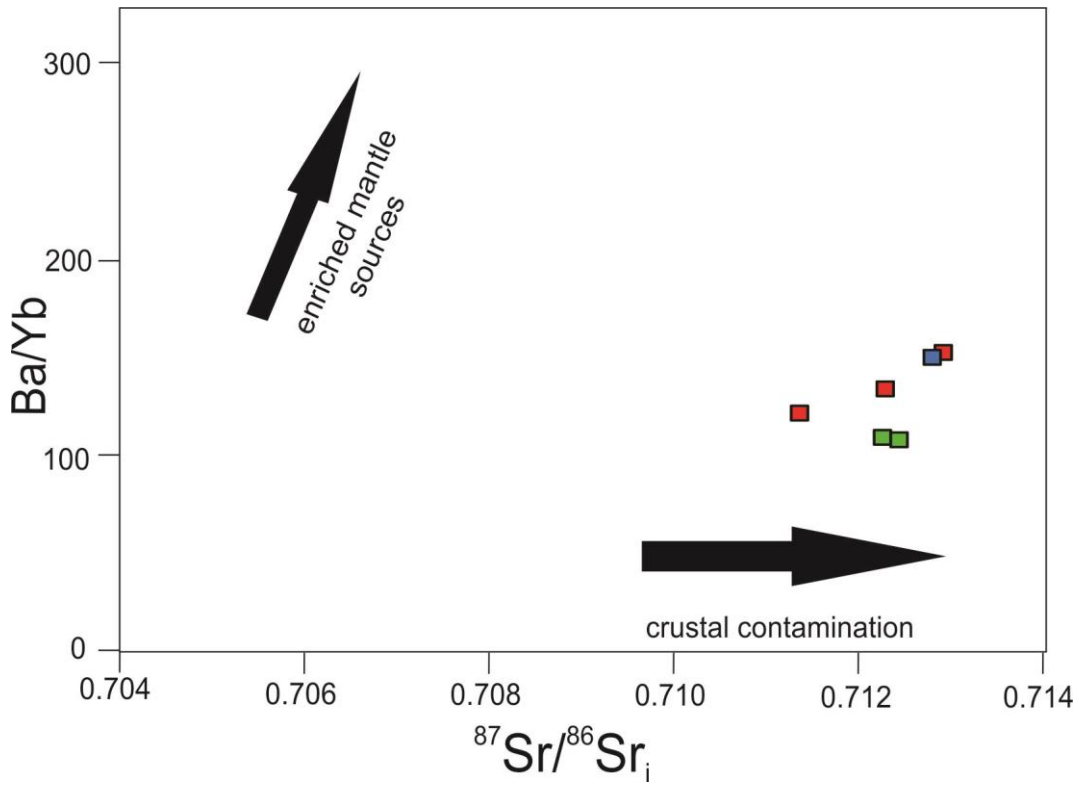

Figure 12. Ba/Yb versus 87Sr/86Sri diagram that reinforce the role of the upper crustal contamination. The vectors are taken from Wilson (1989) and they refer to open-system fractional crystallization (AFC) and closed-system fractional crystallization (FC).

8. CONCLUSIONS

The Cerro do Coronel region sills, located in the southernmost Brazil, form an alignment with NW-SE orientation and have contacts with sedimentary rocks of the Rio Bonito and Irati Formations of the Paraná Basin. The greater thickness found in the northern portion, assuming a semi-horizontal pattern and the uplift and erosion of the region due to the N70W fault of the sills suggest that the less differentiated terms are located in the basal portions of the intrusive bodies and that a slight evolution is observed toward its upper portions.

The geochemical signatures are similar to other mafic intrusions of the southern sub-province of the Paraná-Etendeka Magmatic Province.

The high initial $^{87}Sr/^{86}Sr$ ratios in these rocks indicate an intermediate continental crust source, but the Pb isotope data suggest a preference for EM-II source (enriched oceanic source or a subcontinental lithospheric source). The $^{144}Nd/^{143}Nd$ ratios appear slightly higher in samples from the southern portion when compared to those from the northern portion, suggesting that these bodies may have undergone fractionation and crust assimilation.

According to the modeling of major elements and incompatible trace elements, the fractional crystallization (FC) process plays the main role in the genesis of the investigated sills. However, Sr isotope modeling shows that there may also have been crustal assimilation. This indicates that fractional crystallization was the main factor on the local scale, but fractional crystallization with assimilation (AFC) of Paleoproterozoic crust may have been the predominant process for regional scale evolution in the rise of magma from the magma chamber to the placement of sills.

ACKNOWLEDGMENTS

Thanks to CAPES for the PhD research grant. This work had partial financial support to C.A. Sommer and E.F. Lima from CNPq (400724/2014-6, 441766/2014-5, 302213/2012-0, 303584/2009-2, 473683/2007, 5470641/2008-8, 470203/2007-2, 471402/2012-5, 303038/2009-8 and 470505/2010-9), and from the Rio Grande do Sul State Research Foundation (FAPERGS) 1180/12-8, and PRONEX 10/0045-6. We also thank the laboratory support from the IGEO/UFRGS.

REFERENCES

Allégre, C. (2008). Isotope Geology. Cambridge University Press, p. 512

Allégre, C. J., Lewin, E., Dupre, B. (1988). A coherent crust-mantle model for the uranium-thorium-lead isotopic system. *Chem. Geol*. 70, 211-234.

Almeida, F.F.M. (1986). Distribuição regional e relações tectônicas do magmatismo pós-paleozóico no Brasil. *Revista Brasileira Geciências,* 16(4), 325-349.

Almeida, V. V., Janasi, L. M., Heaman, L. M., Shaulis, Hollanda, M. H. B.M., Renne, P. R. (2017). Contemporaneous alkaline and tholeiitic magmatism in the Ponta Grossa Arch, Paraná-Etendeka Magmatic Province: Constraints from U-Pb zircon/baddeleyite and 40Ar/39Ar phlogopite dating of the José Fernandes Gabbro and mafic dykes. *Journal of Volcanology and Geothermal Research.* (Accepted Manuscript) doi: 10.1016/j.jvolgeores.2017.01.018

Barreto, C. J. S., Lima, E. F., Scherer, C. M., Rossetti, L. M. M. (2014). Lithofacies analysis of basic lava flows of the Paraná igneous province in the south hinge of Torres Syncline, Southern Brazil. *Journal of Volcanology and Geothermal Research*, 285, 81–99.

Bellieni, G., Comin-Chiaramonti, P., Marques, L. S.,Melfi, A. J.,Stolf A, D. (1984). Low-pressure evolution of basalt sills from bore-holes in the Paraná Basin, Brazil. *TMPM*, 33, 25-47.

Bryan, S.E.; Ernst, R.E (2008). Revised definition of Large Igneous Provinces (LIPs). *Earth Sciences Review* 86, 175-202.

Coffin, M. F. & Eldholm, O. (1992). Volcanism and continental break-up: A global compilation of large igneous provinces. In: Geological Society of London Special Publication, 68, 17-30.

Corval, A., Valente, S., Duarte, B. P., Famelli, N., Zanon, M. (2008). Dados petrológicos preliminares dos diabásios dos setores centro-norte e nordeste do Enxame de Diques da Serra do Mar. Geochimica Brasiliensis, 22, 159-177.

Corval, A. V. (2009). Petrogênese e Contexto Geodinâmico das Suítes Basálticas Toleíticas (de alto -TiO_2 e baixo - TiO_2) do Cretáceo Inferior da Formação Centro-oriental do Enxame de Diques da Serra do Mar. Tese (Doutorado) - Centro de Tecnologia e Ciências. Faculdade de Geologia. Universidade do Estado do Rio de Janeiro, Rio de Janeiro, RJ.

Coutinho, J.M.V. (2008). Dyke swarms of the Paraná triple junction, southern Brazil. Geol. Usp. Série Científica, 8 (2), 29-52.

Deckart, K., Féraud, G., Marques, L.S., Bertrand, H. (1998). New time constraints on dyke swarms related to the Paraná – Etendeka magmatic province, and subsequent South Atlantic opening, southeastern Brazil. Journal of Volcanology and Geothermal Research, 80, 67-83.

De Paolo, D.J. (1981). *Nd isotopic studies: Some new perspectives on Earth Structure and Evolution: EOS*, Transactions American Geophysical Union 62, 137–145. doi:10.1029/EO062i014p00137-01

De Paolo, D.J., Wasserburg, G.J. (1979). Sm-Nd age of Stillwater complex and mantle evolution curve for neodymium. Geochim. Cosmochim. Acta, 43, 999-1008.

Duncan, A.R., Newton, S. R., van den Berg, C., Reid, D. L. (1989). Geochemistry and petrology of dolerite sills in the Huab River Valley, Damaraland, north-western Namibia, Communs geol. Surv., Namibia, 5, 5-18

Duncan, A.R., Armstrong, R.A., Erlank, A.J., Marsh, J.S. and Watkins, R.T. (1990). MORB-related dolerites associated with the final phases of Karoo flood basalt volcanism in southern Africa. In: J.A.J. Parker, P. C. Rickwood and D.H. Tucker (Editors), Mafic Dikes and Emplacement Mechanisms, A.A. Balkema, Rotterdam, The Netherlands, 119-129.

Eick, N. C., Lisboa, N. A., Schuck, M. T. G. O. (1984). Geologia do Cerro Coronel, Rio Pardo, RS. XXXIII Congresso Brasileiro de Geologia, v. 5, 2450-2464. Rio de Janeiro: SBG.

Erlank, A.J., Marsh, J.S., Duncan, A.R., Miller, R.M., Hawkesworth, C.J., Betton, P.J. and Rex, D.C. (1984). Geochemistry and petrogenesis of the Etendeka volcanic rocks from SWA/ Namibia. In: A.J. Erlank (Editor), Petrogenesis of Volcanic Rocks of the Karoo Province. Special Publication of the Geological Society of South Africa 13, 195-245.

Ewart, A.J., Marsh, J.S., Duncan, A.R., Miller, R.M., Hawkesworth, C.J., Betton, P.J., Rex, D.C. (1984). Geochemistry and petrogenesis of the Etendeka volcanic rocks from SWA/ Namibia. In: Erlank, A.J. (Ed.), Petrogenesis of Volcanic Rocks of the Karoo Province, Geological Society of South Africa Special Publication, 13, 195–245.

Florisbal, L. M., Heaman, L. M., Janasi, V. A., Bitencourt, M. F. (2014). Tectonic significance of the Florianópolis Dyke Swarm, Paraná–Etendeka Magmatic Province: A reappraisal based on precise U–Pb dating. Journal of Volcanology and Geothermal Research 289, 140-150.

Florisbal, L. M., Janasi, V. A., Bitencourt, M. F., Nardi, L. V. S., Marteleto, N. S. (2017). Geological, geochemical and isotope diversity of ~ 134 Ma dykes from the Florianópolis Dyke Swarm, Paraná Magmatic Province: Geodynamic controls on petrogenesis. Journal of Volcanology and Geothermal Research. (Accepted Manuscript)

Frank, H. T., Gomes, M. E. B., Formoso, M. L. L. (2009). Review of the areal extent and the volume of the Serra Geral Formation, Paraná Basin, South America. Pesquisas em Geociências 36 (1), 49-57.

Gibb, F.G.F., Henderson, C.M.B. (1996). The Shiant Isles Main Sill: structure and mineral fractionation trends. Mineralogical Magazine 60, 67–98.

Gregory, T.R. (2014). Evolução Petrológica do magmatismo TTG Paleoproterozóico do Complexo Arroio dos Ratos, distrito de Quitéria, São Jerônimo/RS [PhD Thesis]: Porto Alegre, Universidade Federal do Rio Grande do Sul, 100 p.

Hart, S.R., (1984) A large-scale isotope anomaly in the southern hemisphere mantle: Nature 309, 753–757. doi:10.1038/309753a0

Hawkesworth, C.J., Marsh, J.S., Duncan, A.R., Erlank, A.J. and Norry, M.J. (1984). The role of continental lithosphere in the generation of the Karoo volcanic rocks: evidence from combined Nd- and Sr-isotope studies. Spec. Publ. geol. Soc. S. Afr. 13, 341-354.

Hawkesworth, C.J., Mantovani, M.S.M., Taylor, P.N., and Palacz, Z. (1986). Evidence from the Parana of south Brazil for a continental contribution to Dupal basalts: Nature 322, 356–359. doi:10.1038/322356a0

Hawkesworth, C., Gallagher, K., Kirstein, L., Mantovani, M.S.M., Peate, D.W., Turner, S.P. (2000). Tectonic controls on magmatism associated with continental break-up: an example from the Paraná–Etendeka Province. Earth Planet. Sci. Lett., 179, 335–349. http://dx.doi.org/10.1016/S0012-821X(00)00114-X.

Irvine, T.N., Baraguar, W.R.A. (1971). A guide to the chemical classification of the common volcanic rocks. Can. J. Earth Sci., 8 (5), 523-548.

Janasi, V. A., Freitas, V. A., Heaman, L. H. (2011). The onset of flood basalt volcanism, Northern Paraná Basin, Brazil: A precise U-Pb baddeleyite/zircon age for a Chapecó-type dacite. Earth and Planetary Science Letters, 302(1-2), 147-153.

Jerram, D.A., Bryan, S.E. (2015). *Plumbing systems of shallow level intrusive complexes*. In: Breitkreuz, C.H., Rocchi, S. (Eds.), Physical Geology of Shallow Magmatic Systems. Advances in Volcanology. Springer, Berlin, pp. 1-22. http://dx.doi.org/10.1007/11157_2015_8.

Jerram, D. A., Mountney, N., Howell, J., Long, D., Stollhofen, H. (2000). Death of a sand sea: an active aeolian erg systematically buried by the Etendeka flood basalts of NW Namibia. Journal of the Geological Society of London, 157(3), 513–516.

Jourdan, F., Bertrand, H., Scharer, U., Blichert-Toft, J., Feraud, G., and Kampunzu, B. (2007). Major and Trace Element and Sr, Nd, Hf, and Pb Isotope Compositions of the Karoo

Large Igneous Province, Botswana-Zimbabwe: Lithosphere vs Mantle Plume Contribution: Journal of Petrology 48(6), 1043–1077. doi:10.1093/petrology/egm010

Le Bas, M. J., LeMaitre, R. W., Streckeisen, A., Zannetin, B. A. (1986). Chemical classification of volcanic rocks based on the total alkali-silica diagram. Journal of Petrology 27(3), 745-750.

Lord, J., Oliver, G., Soulsby, J., 1996. Landsat MSS imagery of a Lower Cretaceous regional dyke swarm, Damaraland, Namibia: a precursor to the splitting of Western Gondwana. International Journal of Remote Sensing, 17, 2945–2954.

Ludwig, K.R., (2001). Isoplot: A ploting and regression program for radiogenic isotope data (version 2.50). United States Geological Survey. Open file Report, 88-542.

Machado, F. B., Nardy, A. J. R. & Oliveira, M. A. F. (2007). Geologia e aspectos petrológicos das rochas intrusivas e efusivas mesozóicas de parte da borda leste da bacia do Paraná no estado de São Paulo. Revista Brasileira de Geociências, 37(1), 64-80.

Maniesi Petersohn, V., Oliveira, M. A. F. (1997). Petrologia das soleiras de diabásio de Reserva e Salto do Itararé, PR. Geochimica Brasiliensis, 11(2), 153-169.

Mantovani, M.S.M., Marques, L.S., Souza, M.A., Atalla, L., Civeta, L., Inonocenti, F. (1985).Trace Element and Strontium Isotope Constrains of the Origin and Evolution of Paraná Continental Flood Basalts of Santa Catarina State (Southern Brazil). Journal of Petrology 26, 187-209.

Marques, L.S., Ernesto, M., (2004). *O Magmatismo Toleítico da Bacia do Paraná*. In: Mantesso-Neto, V., Bartorelli, A., Carneiro, C. D. R., Brito-Neves, B. B. (Eds), Livro Geologia do Continente Sul-Americano: Evolução da obra de Fernando Flávio Marques de Almeida. São Paulo: Editora Beca.

Marques, L.S., Figueiredo, A.M.G., Saiki, M., Vasconcellos, M.B.A. (1989). *Geoquímica analítica dos elementos terras raras - Aplicação da técnica de análise por ativação neutrônica*. In: Formoso, M.L.L.; Nardy, L.V.S. & L.A. Hartmann (Coords.), Geoquímica dos Elementos Terras Raras no Brasil. CPRM/DNPM, Sociedade Brasileira de Geoquímica, Rio de Janeiro, pp. 15-20.

Marsh, B.D. (2013). *On some fundamentals of igneous petrology*. Contributions to Mineralogy and Petrology 166, 665–690.

Marsh, J. S., Erlank, A. J., Duncan, A. R. (1991). Report: Preliminary geochemical data for dolerite dykes and sills of the southern part of the Etendeka Igneous Province, Communs geol. Surv., Namibia 7, 77-80.

McDonough, W. S., Sun, S. (1995). The composition of the Earth. Chemical Geology 120, 223-253.

Middlemost, E. A. K., (1975). The basalt clan. Earth Science Review, 11, 337-64.

Milani, E. J. (1997). Evolução tectono-estratigráfica da Bacia do Paraná e seu relacionamento com a geodinâmica fanerozóica do Gondwana Sul-Ocidental. 2 v. Tese (Doutorado). Porto Alegre: Instituto de Geociências – UFRGS.

Muzio, R., Scaglia, F., Masquelin, H. (2012). Petrochemistry of mesozoic mafic intrusions related to the Paraná Magmatic Province, Uruguay. Int. Geol. Rev. 54(7), 844-860.

Muzio, R., Peel, E., Porta, N., Scaglia, F. (2017). Mesozoic dykes and sills from Uruguay: Sr - Nd isotope and trace element geochemistry. Journal of South American Earth Sciences, 77, 92-107.

Owen-Smith, T. M., Ashwal, L. D. (2015). Evidence for multiple pulses of crystal-bearing magma during emplacement of the Doros layered intrusion, Namibia. Lithos, 238, 120-139.

Peate, D. W. Hawkesworth, C. J., Mantovani, M. S. M. (1992). Chemical stratigraphy of the Paraná lavas (South América): classification of magma types and their spatial distribution. Bulletin of Volcanology, 55 (1), 119-139.

Peate D.W. (1997). The Paraná–Etendeka province. In: Mahoney J.J., Coffin M.F. Large Igneous Provinces: Continental, Oceanic and Planetary Flood Volcanism. American Geophysical Union, Washington, DC, pp. 217-245.

Peate, D.W., Hawkesworth, C.J., Mantovani, M.S.M., Rogers, N.W., Turner, S.P. (1999). Petrogenesis and stratigraphy of the high-Ti/Y Urubici magma type in the Paraná flood basalt province and implications for the nature of ‘Dupal’- type mantle in the South Atlantic region. J. Petrol., 40, 451-473.

Peate, P.W., and Hawkesworth, C.J., (1996). Lihospheric to astenospheric transition in Low-Ti flood basalts from southern Paraná: Brazil. Chemical Geology. 127, 1–24.

Petersohn, E., Gouvea, E. M. (2009). Geologia e geoquímica da soleira de Reserva, Estado do Paraná. Revista Brasileira de Geociências, 39(4), 740-750.

Petersohn, E., Vasconcellos, E. M. G., Lopes, K. (2007). Petrologia de *sills* encaixados nas Formações Irati e Ponta Grossa (Bacia do Paraná) no Estado do Paraná. Geochimica Brasiliensis, 21, 58-70.

Philipp, R. P., Machado, R., Nardi, L. V. S., Lafon, J. M., (2002). O magmatismo granítico Neoproterozoico do batólito Pelotas no Sul do Brasil: Novos dados e revisão da geocronologia regional. Revista Brasileira de Geociências, 32(2), 277-290.

Philipp, R.P., Machado, R., and Junior, F.C. (2007). *A geração dos granitóides Neoproterozóicos do Batólito Pelotas: Evidências dos isótopos de Sr e Nd e implicações para o crescimento continental da Porção Sul do Brasil*. In: Iannuzzi, R., and Frantz, J.C., (Eds.),

50 anos de Geologia: Instituto de Geociências: Contribuicões, Comunicação e Identidade, 399p.

Piccirillo, E. M., Melfi A. J. (1988). *The Mesozoic flood volcanism of the Paraná Basin - petrogenetic and geophysical aspects.* USP, São Paulo.

Piccirillo, E. M., Civetta, L., Petrini, R., Longinelli, A., Bellieni, G., Comin-Chiaramonti, P., Marques, L. S., Melfi, A. J. (1989). Regional variations within the Paraná Flood Basalts (Southern Brazil): Evidence for subcontinental mantle heterogeneity and crustal contamination. Chemical Geology, 75, 103-122.

Piccirillo, E. M., Bellieni, G., Cavazzini, G., Comin-Chiaramonti, P., Petrini, R., Melfi, A. J., Pinesi, J. P. P., Zantadeschi, P., Demin, A. (1990). Lower Cretaceous tholeiitic dyke swarms from the Ponta Grossa (southeast Brazil): Petrology, Sr-Nd isotopes and genetic relationships whith the Paraná flood volcanic. Chemical Geology, Netherlands, 89, 19-48.

Raposo, M. I. B., Ernesto, M., Renne, P. R. (1998). Paleomagnetism and $^{40}Ar/^{39}Ar$ dating of the Early Cretaceous Florianópolis dike swarm (Santa Catarina Island), Southern Brazil. Physics of the Earth and Planetary Interiors, 108, 275-290.

Renne, P. R., Ernesto, M., Pacca, I. G., Coe, R. S., Glen, J. M., Prévot, M., Perrin, M. (1992). The age of Paraná Flood Volcanism, rifting of Gondwana land, and the Jurassic-Cretaceous boundary. Science, 258, 975-979.

Renne, P.R., Deckart, K., Ernesto, M., Féraud, G., and Piccirillo, E.M. (1996). Age of the Ponta Grossa dike swarm (Brazil), and implications to Paraná flood volcanism. Earth and Planetary Science Letters, 144, 199–211. doi: 10.1016/0012-821X(96)00155-0.

Renner, L.C. (2010). Geoquímica de sills basálticos da Formação Serra Geral, sul do Brasil, com base em rocha total e micro-análise de minerais. Tese (Doutorado) – Instituto de Geociências. Programa de Pós-Graduação em Geociências, Universidade Federal do Rio Grande do Sul, Porto Alegre, RS.

Rohde, J., Hoernle, K., Hauff, F., Werner, R., O'Connor, J., Class, C., Garbe Schonberg, D., and Jokat, W. (2013). 70 Ma chemical zonation of the Tristan-gough hotspot track. Geology. 41, 335–338. doi:10.1130/G33790.1

Sarmento, C.C.T., Sommer, C. A., Lima, E. F., Oliveira, D. S. (2014). Corpos hipabissais correlacionados à Formação Serra Geral naregião do Cerro do Coronel, RS: geologia e petrologia. Geologia USP, Série Científica, 14(2), 23-44.

Sarmento, C.C.T., Sommer, C. A., Lima, E. F. (2017). Mafic subvolcanic intrusions and their petrologic relation with the volcanism in the south hinge Torres Syncline, Paraná-Etendeka Igneous Province, southern Brazil. Journal of South American Earth Sciences, 77, 70-91.

Self, S., Widdowson, M., Thordarson, T., Jay, A. E. (2006). Volatile fluxes during flood basalt eruptions and potential effects on global environment: a Deccan perspective. Earth and Planetary Science Letters, 248, 518–532.

Stewart, K., Turner, S., Kelley, S., Hawkesworth, C. J., Kirstein, L., Mantovani, M. (1996). 3-D, Ar/Ar geochronology in the Paraná continental flood basalt province. Earth and Planetary Science Letters, 143, 95-109.

Steiger, R.H., Jäger, E. (1977). Subcommission on geochronology: convention on the use of decay constants in geo- and cosmochronology. Earth and Planetary Science Letters, 36(3), 359-362.

Stormer, J.C., and Nicholls, J., 1978, XLFRAC: *A program for the interactive testing of magmatic differentiation models: Computers & Geosciences*, v. 4. p. 143–159. doi:10.1016/0098-3004(78)90083-3

Thiede, D. S., Vasconcelos, P. M. (2010). Paraná flood basalts: Rapid extrusion hypothesis confirmed by new $^{40}Ar/^{39}Ar$ results. Geology, 38 (8), 747- 750.

Thompson, R. N., Gibson, S. A., Dickin, A. P. & Smith, P. M., (2001). Early Cretaceous basalt and picrite dykes of the southern Etendeka region, NW Namibia: windows into the role of the Tristan mantle plume in Parana-Etendeka magmatism. Journal of Petrology, 42, 2049-2081.

Thompson, R.N., Riches, A.J.V., Antoshechkina, P.M., Pearson, D.G., Nowell, G.M., Ottley, C.J., Dickin, A.P., Hards, V.L., Nguno, A.-K. and Niku-Paavola, V. (2007). Origin of CFB magmatism: multi-tiered intracrustal picriterhyolite magmatic plumbing at Spitzkoppe, western Namibia, during Early Cretaceous Etendeka magmatism. Journal of Petrology, 48, 1119-1154.

Tomazzoli, E.R. & Lima, E.F. (2006). Magmatismo ácido-básico na ilha do Arvoredo-SC. Revista Brasileira de Geociências, 36, 57–76.

Tomazzoli, E. E. & Pellerin, J. M., (2015). Unidades do mapa geológico da ilha de Santa Catarina: as Rochas. Florianópolis. Geosul, 60(30), 225-247.

Trumbull, R.B., Vietor, T., Hahne, K., Wackerle, R., Ledru, P. (2004). Aeromagnetic mapping and reconnaissance geochemistry of the early cretaceous Henties bay-Outjo mafic dike swarm, Etendeka igneous province, Namibia. J. Afr. Earth Sci., 40, 17-29.

Trumbull, R.B., Reid, D.L., Beer, C., Acken, D., Romer, R.L. (2007). Magmatism and continental breakup at the west margin of southern Africa: a geochemical comparison of dolerite dikes from northwestern Namibia and the Western Cape. South Afr. J. Geol., 110, 477-502.

Turner, S., Regelous, M., Kelley, S., Hawkesworth, C., Mantovani, M., (1994). Magmatism and continental break-up in the South Atlantic: high precision $^{40}Ar/^{39}Ar$ geochronology. Earth and Planetary Science Letters, 121, 333-348.

UFRGS. (2006). *Mapeamento Geológico de parte da Folha Quitéria SH22-Y-B-I-4 (MI2985/4) (1:25.000)*, RS. 1 vol., 2 mapas. Porto Alegre: Curso de Geologia, Instituto de Geociências da Universidade Federal do Rio Grande do Sul.

Valente, S.C.; Corval, A.; Duarte, B.P.; Ellam, R. L.; Fallick, A.E.; Dutra, T., (2007). Tectonic boundaries, crustal weakness zones and plume-subcontinental lithospheric mantle interactions in the Serra do Mar Dyke Swarm, SE Brazil. Revista Brasileira de Geociências, 37, 194-201.

Waichel, B. L., Lima, E. F., Viana, A., Scherer, C.M. S., Bueno, G., Dutra, G. (2012). Stratigraphy and volcanic facies architecture of the Torres Syncline, Southern Brazil, and its role in understanding the Paraná-Etendeka Continental Flood Basalt Province. Journal of Volcanology and Geothermal Research, 215, 74-82.

Wasserburg, G.J., Jacobsen, S.B., De Paolo, D.J., Mc Culloch, M.T., Wen, T. (1981). Precise determination of Sm/Nd ratios, Sm and Nd isotopic abundances in standard solutions. Geochimica et Cosmochimica Acta, 45, 2311-2323.

Wilson, M. (1989). *Igneous Petrogenesis a global tectonic approach*. Berlin: Springer.

Zalán, P. V., Conceição, J. C. J., Astolfi, M .A. M., Appi, V. T., Wolff, S., Vieira, I. S., Marques, A. (1985). Estilos estruturais relacionado às intrusões magmáticas básicas em rochas sedimentares. Rio de Janeiro, RJ. Boletim Técnico da PETROBRAS, 28 (4): 221 – 230.

Zindler, A., and Hart, S. (1986) *Chemical geodynamics: Annual Review of Earth and Planetary Sciences*, v.14, 493–571. doi:10.1146/annurev.ea.14.050186.002425

Table 1. Lithochemical results of representative samples of sills for major elements (wt.%), trace and REE (ppm).

	035	005	007	029	011-1	012B	017A	018B	030B	033B	034A
	Sill 1	Sill 2 (Cerro do Coronel)							Sill 3	Sill 4	
SiO_2	54.90	54.49	54.99	53.92	52.79	54.44	54.38	53.30	52.47	52.57	52.72
Al_2O_3	12.97	12.47	12.70	13.09	13.66	12.86	12.95	13.06	14.05	13.99	13.87
$Fe_2O_{3(T)}$	14.62	14.62	14.70	14.11	12.94	14.43	14.95	14.97	12.17	12.55	12.52
MnO	0.20	0.18	0.18	0.21	0.22	0.18	0.19	0.20	0.17	0.19	0.19
MgO	3.17	2.83	2.96	3.72	5.55	3.04	3.26	3.50	5.80	5.81	5.89
CaO	6.95	6.45	6.55	7.37	9.12	7.03	6.99	6.96	9.25	8.89	9.01
Na_2O	2.39	2.84	2.83	2.70	2.21	2.63	2.67	2.77	2.22	2.47	2.40
K_2O	2.12	2.26	2.16	1.91	1.34	2.12	2.12	1.98	1.14	1.37	1.33
TiO2	1.91	1.92	1.90	1.64	1.31	1.87	1.91	1.89	1.19	1.21	1.20
P_2O_5	0.22	0.21	0.21	0.19	0.14	0.20	0.20	0.18	0.13	0.14	0.14
PF*	0.30	1.50	0.60	0.90	0.50	1.00	0.20	1.00	1.2	0.6	0.5
Total	99.75	99.77	99.78	99.76	99.78	99.80	99.82	99.81	99.79	99.79	99.77
Rb	77.10	81.90	76.40	70.70	44.20	73.20	74.90	69.00	39.80	52.00	49.70
Ba	502	516	481	433	284	457	427	405	265	247	249.0
Sr	216.9	237.5	201.1	217	195.9	188.9	204.3	196.2	223.2	241.1	239.1
Ga	20.5	21.10	19.30	20.10	17.60	19.10	20.80	20.20	19.30	19.20	18.10
Zr	185.6	184.5	176.4	160.4	117.8	179.1	170.8	159.9	109.9	112.8	109.9
Y	34.5	34.9	42.8	34.4	23.1	30.3	29.6	28.6	25.5	24.2	23.7
Nb	13.8	12.90	13.20	11.40	8.50	12.40	11.90	11.70	7.80	7.70	7.90
Sc	40	39	39	40	43	40	41	42	43	43	43.00
V	514	553	510	433	373	502	593	634	376	372	361
Co	45.80	43.10	43.30	48	45.90	42.10	45.60	49.30	50.80	46.30	48.60
Cu	174.5	142.4	158.9	176.2	138.0	170.7	160.7	154.7	86.3	130.0	135.8
Zn	72	51	61	53	42	73	62	54	45	37	40
La	28.10	27.80	31.80	25.50	16.0	25.90	24.90	24.10	16.20	16.00	15.50
Ce	59.30	59.70	59.70	52.10	36.3	58.30	55.00	52.40	32.90	33.60	31.90
Pr	7.55	7.27	8.10	6.84	4.36	6.83	6.44	6.37	4.39	4.39	4.29
Nd	30.80	31.20	34.00	27.80	18.4	28.60	27.50	27.10	18.30	18.40	18.00
Sm	6.59	6.31	7.30	6.12	4.21	6.30	6.03	6.08	4.18	4.24	4.08
Eu	1.63	1.62	1.83	1.53	1.17	1.59	1.58	1.57	1.17	1.15	1.14
Gd	6.39	6.38	7.96	6.20	4.32	6.19	6.14	5.86	4.37	4.32	4.25
Tb	1.11	1.08	1.34	1.05	0.74	1.07	1.01	1.02	0.77	0.74	0.73
Dy	6.40	6.27	8.07	5.73	4.31	6.03	5.84	5.80	4.61	4.35	4.16
Ho	1.23	1.27	1.64	1.17	0.89	1.23	1.16	1.18	0.90	0.87	0.87
Er	3.58	3.71	4.77	3.45	2.54	3.53	3.39	3.33	2.59	2.53	2.55
Tm	0.54	0.48	0.64	0.52	0.32	0.45	0.44	0.42	0.38	0.39	0.36
Yb	3.30	3.35	4.58	3.20	2.30	3.30	3.20	3.02	2.42	2.23	2.28
Lu	0.49	0.52	0.71	0.48	0.35	0.47	0.47	0.45	0.37	0.36	0.34
Hf	5.30	5.00	4.80	4.70	3.3	5.40	4.80	4.80	3.00	3.60	3.10
Ta	0.90	0.90	0.80	0.80	0.5	0.90	0.90	0.80	0.50	0.40	0.40
Th	8.20	8.90	8.60	7.20	5.0	7.50	8.30	7.10	4.10	4.30	4.60
U	1.90	1.80	1.30	1.30	1.1	1.80	1.90	1.40	0.90	1.00	0.90

Table 2. Sr-Nd-Pb data for the sills of the Cerro do Coronel region.

Samples	CCO-035	CCO-005	CCO-029	CCO-011-1	CCO-033B	CCO-034A
$^{87}Sr/^{86}Sr$	0.71473(17)	0.71480(08)	0.7147(08)	0.71260 (09)	0.71343(12)	0.71358(08)
$^{87}Sr/^{86}Sr_{(i)}$	0.712801	0.71293	0.712297	0.711379	0.712257	0.712459
$^{143}Nd/^{144}Nd$	0.51234(20)	0.51234(30)	0.51231(30)	0.51241(36)	0.51242(32)	0.512426(28)
$^{143}Nd/^{144}Nd_{(i)}$	0.512235	0.51224	0.51220	0.51230	0.512310	0.512315
$eNd_{(i)}$	-4.61	-4.55	- 5.20	-3.30	-3.14	-3.04
T_{DM} (Ga)	1.17	1.16	1.23	1.11	1.11	1.10
$^{206}Pb/^{204}Pb$	18.815(158)	18.771(143)	18.723(395)	n.d.	n.d.	18.568(998)
$^{207}Pb/^{204}Pb$	15.702(135)	15.655(116)	15.649(331)	n.d.	n.d.	15.549(939)
$^{208}Pb/^{204}Pb$	38.961(329)	38.858(286)	38.863(827)	n.d.	n.d.	38.562(999)

Initial ratios for Sr and Nd and epsilon values corrected to 132 Ma; Pb ratios are measured; Measurement errors for Sr and Nd isotope ratios in parenthesis refer to last digits (2σ); n.d. = not determined

Table 3. Major element involving less evolved basic liquids and more evolved from the sills of the Cerro do Coronel region.

Test 1	L_o (CCO-011-1)	L_f (CCO-029)	Plag	Ti-mag	Cpx	Ol	XL-frac	Δ_0	Δ_f	residual (Δ_0-Δ_f)
SiO_2	53.17	54.54	54.62	0.04	50.72	39.56	51.01	1.369	1.415	-0.046
TiO_2	1.32	1.66	0.05	25.5	0.64	0.03	0.64	0.339	0.409	-0.069
Al_2O_3	13.76	13.24	27.98	1.07	1.07	0.06	14.20	-0.518	-0.384	-0.134
FeOtot	13.03	14.27	0.68	72.08	20.49	16.1	11.10	1.239	1.27	-0.031
MnO	0.22	0.21	0.01	0.5	0.53	0.25	0.25	-0.009	-0.016	0.006
MgO	5.59	3.76	0.04	0.75	10.99	43.7	8.23	-1.827	-1.785	-0.042
CaO	9.19	7.45	10.84	0.03	15.39	0.29	11.68	-1.731	-1.689	-0.042
Na_2O	2.23	2.73	5.34	0.01	0.16	0	2.69	0.505	0.016	0.489
K_2O	1.35	1.93	0.43	0.01	0.01	0	0.22	0.582	0.687	-0.104
P_2O_5	0.14	0.19	0	0	0	0	51.01	0.051	0.077	-0.026
TOT	100	100	100	100	100	100				
Σres^2										0.2802
subtracted phases (100%)			49.10	1.36	41.12	8.41				
fractionated total (%)										40.00

Ol= olivine; Plag= plagioclase; cpx= clinopyroxene; Ti-mag= titano magnetite; Lo= initial liquid; Lf= final liquid; XL-frac = crystallized fraction in the parental magma; Δ0 = observed difference between the magmas ; Δf = calculated difference between the magmas; Σres2 = sum of the squares of residuals.

Table 4. Major element involving less evolved basic liquids and more evolved from the sills of the Cerro do Coronel region.

Test 2	L_o (CCO-011-1)	L_f (CCO-005)	Plag	Ti-mag	Cpx	Ol	XL-frac	Δ_0	Δ_f	residual (Δ_0-Δ_f)
SiO_2	53.17	55.45	54.62	0.04	50.72	39.56	50.88	2.276	2.342	-0.065
TiO_2	1.32	1.95	0.05	25.5	0.64	0.03	0.72	0.634	0.635	-0.001
Al_2O_3	13.76	12.69	27.98	1.07	1.07	0.06	14.41	-1.07	-0.881	-0.188
FeOtot	13.03	14.88	0.68	72.08	20.49	16.1	11.12	1.844	1.926	-0.082
MnO	0.22	0.18	0.01	0.5	0.53	0.25	0.25	-0.038	-0.033	-0.005
MgO	5.59	2.88	0.04	0.75	10.99	43.7	8.06	-2.71	-2.658	-0.052
CaO	9.19	6.56	10.84	0.03	15.39	0.29	11.61	-2.623	-2.589	-0.034
Na_2O	2.23	2.89	5.34	0.01	0.16	0	2.73	0.664	0.082	0.582
K_2O	1.35	2.30	0.43	0.01	0.01	0	0.22	0.95	1.067	-0.117
P_2O_5	0.14	0.21	0	0	0	0	0	0.073	0.11	-0.037
TOT	100	100	100	100	100	100				
Σres^2										0.4043
subtracted phases (100%)			49.87	1.69	40.16	8.28				
fractionated total (%)										51.28

Ol= olivine; Plag= plagioclase; cpx= clinopyroxene; Ti-mag= titano magnetite; Lo= initial liquid; Lf= final liquid; XL-frac = crystallized fraction in the parental magma; Δ0 = observed difference between the magmas ; Δf = calculated difference between the magmas; Σres2 = sum of the squares of residuals.

4. SÍNTESE INTEGRADORA E CONSIDERAÇÕES FINAIS

Os diques investigados neste estudo, localizados na região centro-leste do Rio Grande do Sul e relacionados à ombreira sul da Calha de Torres, mesmo não tendo a característica clássica de “enxame de diques” , ocorrem sob uma direção preferencial NE-SW, quando intrusivo nas rochas sedimentares da Bacia do Paraná. Esta direção coincide com lineamentos tectono-magmáticos, relacionados a processos distensivos e sistemas de falhamentos que serviram de dutos para enxames de diques paralelos à costa brasileira e também a mesma direção do enxame de diques da costa da Namíbia. Sugere-se, portanto, que esses diques possam ter feito parte do sistema de junção tríplice relacionado à abertura do Atlântico Sul. Os diques intrusivos nos derrames do Grupo Serra Geral, ao longo da Calha de Torres, têm direções preferenciais NW-SE, semelhante às direções dos Arcos de Ponta Grossa, Rio Grande e da Calhal de Torres. Esta condição sugere que as origens desses diques possam estar relacionadas a um ou mais ciclos tectônicos que originaram essas estruturas regionais.

Os padrões morfológicos dos diques investigados (simétricos e assimétricos) indicam a possibilidade de ter havido dos condicionantes vinculados ao processo de colocação dos diques: (i) fraturamento prévio, no caso dos diques simétricos e (ii) fraturamento hidráulico, para os diques assimétricos, bem como os diques e *sills* secundários associados às intrusões principais, pois não seguem um padrão de preenchimento de fraturas pré-existentes.

A colocação das soleiras ocorre concordantemente às zonas de fraqueza das unidades sedimentares das Formações Rio Bonito, Iratí, Rio do Rastro, Pirambóia e Santa Maria, na borda sul da Bacia do Paraná.

A assinatura geoquímica de rocha total dos diques SSOT mostra similaridade com a composição do Complexo Básico Lomba Grande, RS, Brasil e com a das intrusões básicas de afinidade P-MORB com MgO > 6% relacionadas à Província Magmática Paraná-Etendeka, na Namíbia. Mostra a possibilidade destes diques fazerem parte de um sistema de condutos de alimentação. A geoquímica dos diques e *sills* do termo TSS indicam características típicas de andesitos basálticos e padrões de LILEs, HFSE e ETRs, semelhantes ao magmatismo das suítes de baixo-Ti de grandes províncias basálticas continentais, como são vinculadas as rochas vulcânicas da Província Magmática Paraná-Etendeka.

Quando correlacionados com as intrusões associadas à Formação Etendeka, o tipo SST é similar ao magma-tipo Tafelberg, correspondente ao magma-tipo Gramado da Província do Paraná, com assinaturas isotópicas e enriquecidos em elementos-traço como os dos derrames de lava da Província Basáltica Continental Paraná-Etendeka. Estes magmas seriam derivados em grande parte de uma fonte de manto litosférico, enriquecido com alguma assimilação crustal. Já os diques do tipo SSTO seriam derivados de uma fonte manto-litosférica enriquecida, com muita pouca contribuição crustal, possuindo composições isotópicas semelhantes aos magmas baixo Ti com MgO>7%, como o magma-tipo Nil Desperandum, sem correspondente na Província Paraná.

Fazendo uma correlação dos diques com a estratigrafia de derrames da calha sul da Sinclinal de Torres, os diques do tipo SST cortam os derrames das unidades basais: Formações Torres e Vale do Sol, podendo ser elimentadores dos derrames posteriores as estas unidades. Esta interpretação pode ser corroborada pelos dados químicos, onde o comportamento dos elementos maiores, traços e terras raras e as razões isotópicas Sr-Nd-Pb, sugerem que esses diques podem ter contribuido como parte de um sistema de alimentação dos derrames básicos estratigraficamente posicionados acima dos derrames encaixantes e basais do Grupo Serra Geral. Os diques SST intrusivos em derrames *ponded pahoehoe* e *pahoehoe*, com mais altas razões de Sr, sofreram um grau de assimilação crustal maior ou fazem parte do sistema de realimentação dos próprios derrames *ponded pahoehoe* da Formação Torres. O dique encontrado intrusivo nos derrames da Formação Vale do Sol, no topo da sequencia vulcânica, pode ter sido parte de um sistema condutor para os derrames do magma-tipo Esmeralda (Formação Esmeralda), por apresentar assinaturas isotópicas menos contaminadas e elementos-traço semelhantes.

Os diques do termo SSOT, intrusivos somente nos derrames *ponded pahoehoe* da Formação Torres, apesar de possuírem razões isotópicas com valores menores de Sr e Pb, poderiam fazer parte de um sistema de alimentação ou um componente dos diques que efetivamente alimentaram os derrames basálticos com olivina do tipo *compound pahoehoe* da Formação Torres, encontrados estratigraficamente acima dos derrames encaixantes. A variação dessas razões pode ter ocorrido pela contaminação no momento da ascensão e extrusão do magma.

Observações das modelagens de AFC e FC baseadas em elementos-traço e razões isótopicas sugerem que para os diques SSOT, o processo de FC foi o mais

importante para a petrogênese desses condutos. Modelagens para esses diques mais primitivos e os derrames de lava mostram que a assimilação crustal teve papel principal na petrogênese dessas rochas na ombreira sul da Calha de Torres. A assimilação tanto Paleoproterozoica quanto Neoproterozoica é considerada, porém uma maior contribuição de crosta Neoproterozoica foi constatada neste estudo.

Na investigação de processos petrogenéticos atuantes em soleiras, usou-se como estudo de caso, as soleiras da região do Cerro do Coronel, localizadas a sudeste da cidade de Pantano Grande, RS. Estes corpos formam um alinhamento com orientação NW-SE e apresentam contatos concordantes com rochas sedimentares das Formações Rio Bonito e Irati. Levando-se em conta a maior espessura encontrada na porção norte, assumindo-se um padrão semi-horizontal e o soerguimento e erosão da região em decorrência da falha N70W das soleiras, sugere-se que os termos menos diferenciados estejam situados nas porções basais dos corpos intrusivos e que uma leve evolução geoquímica é observada em direção às suas porções superiores.

As assinaturas geoquímicas são semelhantes a outras intrusões máficas da sub-província sul da Província Magmática Paraná.

As altas razões iniciais ^{87}Sr / ^{86}Sr dessas rochas indicam uma fonte de crosta continental intermediária, mas os dados isotópicos de Pb sugerem a preferência por uma fonte EM-II (fonte oceânica enriquecida ou a uma fonte de litosférica subcontinental). As razões $^{144}Nd/^{143}Nd$ se mostram levemente mais elevadas nas amostras da porção sul, quando comparadas às do porção norte, sugerindo também que estes corpos podem ter sofrido fracionamento e assimilação da crosta.

Conforme o modelamento de elementos maiores e elementos-traço incompatíveis, o processo de cristalização fracionada (FC) teria o papel principal na gênese das soleiras investigadas. Entretanto, o modelamento com isótopos de Sr mostram que pode ter havido também assimilação crustal. Isso indica que a cristalização fracionada foi o fator principal em escala local, mas a cristalização fracionada com assimilação (AFC) sendo de crosta Paleoproterozoica, pode ter sido o processo predominante para a evolução em escala regional. Na ascensão do magma da câmara magmática até a colocação das soleiras.

O estudo das intrusões vinculadas ao Grupo Serra Geral na porção centro-leste da Bacia do Paraná, no extremo sul do Brasil permitiu tecer considerações a respeito da sua origem e evolução magmática. Com isso, a investigação demonstrou a possibilidade de grande parte dos diques ser associada a sistemas de alimentação

para o vulcanismo da Calha Sul de Torres, refletindo na heterogeneidade litoestratigráfica e composicional entre os derrames. Contribui, portanto, para a evolução do conhecimento científico sobre o entendimento da dos processos evolutivos atuantes na sub-província sul da Província Magmática Paraná-Etendeka.

REFERÊNCIAS

Almeida, F.F.M. 1986. Distribuição regional e relações tectônicas do magmatismo pós-paleozóico no Brasil. Revista Brasileira Geciências, 16(4): 325-349.

Armstrong, R.A., Bristow, J.W., Cox, K.G., 1984. The Rooi Rand dyke swarm, southern Lebombo. In: Erlank, A.J. (Ed.), Petrogenesis of the Volcanic Rocks of the Karoo Province. Geological Society of South Africa Special Publication, 13: 77–86.

Arndt, N.T. & Christensen, U. 1992. The role of lithospheric mantle in continental Flood volcanism: thermal and geochemical constraints. J. Geophys. Res., 97(B7): 10967-10981.

Atkinson, B. K. 1987. Fracture Mechanics of Rock Academic Press. London. 380p.

Barreto, C. J. S., Lafon, J. M., Lima, E. F., Sommer, C. A., 2016. Geochemical and Sr–Nd–Pb isotopic insight into the low-Ti basalts from southern Paraná Igneous Province, Brazil: the role of crustal contamination. International Geology Review 59(1):1 DOI: 10.1080/00206814.2016.1147988

Barreto, C. J. S., Lafon, J. M., Lima, E. F., Sommer, C. A., 2016. Geochemical and Sr–Nd–Pb isotopic insight into the low-Ti basalts from southern Paraná Igneous Province, Brazil: the role of crustal contamination. International Geology Review 59(1):1 DOI: 10.1080/00206814.2016.1147988

Bear, G., M. Beyth, Z. & Reches, 1994. Dikes emplaced into fractured basement, Timna Igneous Complex, Israel. Journal of Geophysical Research, 99: 24039-24050.

Bellieni, G., Comin-Chiaramonti, P., Marques, L. S.,Melfi, A. J.,Stolf A, D. 1984. Low-pressure evolution of basalt sills from bore-holes in the Paraná Basin, Brazil. TMPM, 33: 25-47.

Bellieni, G., Comin-Chiaramonti, P., Marques, L. S., Melfi, A. J., Nardy, A. J. R., Papatrechas, C., Piccirillo, E. M., Roisenberg, A. 1986. Petrogenetic aspects of acid and basaltic lavas from the Paraná plateau (Brazil): geological, mineralogical and petrochemical relationships. Journal of Petrology, 27: 915-944.

Billings, M. P. 1972. Structural Geology. Prentice-Hall Inc. Englewood Cliffs, New Jersey, USA. 606 p.

Bondre, N.R., Hart, W.K. & Sheth, H.C., 2006. Geology and geochemistry of the Sangamner mafic dyke swarm, western Deccan volcanic province, India: implications for regional stratigraphy. Journal of Geology 114: 155–170.

Brandon, A. D., Hooper, P. R., Goles, G. G. & Lambert, R. St. J. 1993. Evaluating crustal contamination in continental basalts: The isotopic composition of the Picture Gorge Basalt of the Columbia River Basalt Group. Contrib. Mineral. Petrol. 114: 452–464

Bryan, S.E. 2007. Silicic Large Igneous Provinces. Episodes, 30: 20-31.

Bryan, S.E. & Ernst, R.E. 2006. Proposed Revision to Large Igneous Province Classification. http://www.mantleplumes.org/LIPClass2.html.

Bryan, S.E.; Ernst, R.E. 2008. Revised definition of Large Igneous Provinces (LIPs). Earth Sciences Review, 86: 175-202.

Bryan, S.E.; Peate, I.U.; Peate, D.W.; Self, S.; Jerram, D.A.; Mawby, M.R.; Marsh, J.S.; Miller, J.A. 2010. The largest volcanic eruptions on Earth. Earth Sciences. Review, 102: 207-229.

Brueseke, M. E., Heizler, M. T., Hart,W. K. & Mertzman, S. A. 2007. Distribution and geochronology of Oregon Plateau (U.S.A.) flood basalt volcanism: The Steens Basalt revisited. J. Volcanol. Geotherm. Res. 161: 187–214

Bosworth, W., Burke, K., Strecker, M. 2000. Magma chamber elongation as an indicator of intraplate stress field orientation: Borehole breakout mechanism and examples from the Pleistocene to Recent Kenya Rift Valley. In: Jessell M. V. & Urai J. L. (Eds.) Stress, Strain and Structure, A Volume in Honor of W. D. Means. Journal of Virtual Explorer 2.

Camp, V. E. & Ross, M. E. 2004. Mantle dynamics and genesis of mafic magmatism in the intermontane Pacific Northwest. J. Geophys. Res. 109 (doi:10.1029/2003JB002838).

Campbell, I.H. & Griffiths, R.W. 1990. Implications of mantle plume structure for the evolution of flood basalts. Earth Planet. Sci. Lett., 99: 79-93.

Coffin, M. F. & Eldholm, O. 1992. Volcanism and continental break-up: A global compilation of large igneous provinces. In: Geological Society of London Special Publication, 68: 17-30.

Coffin, M.F. & Eldholm, O. 1994. Large igneous provinces: Crustal structure, dimensions and external consequences. Rev. Geophy., 32(1): 1-36.

Comin-Chiaramonti, P.; Gomes, C. B.; Piccirillo, E. M.; Rivalente, G. 1983. High-TiO2 Basaltic Dykes in the coastline of São Paulo and Rio de Janeiro States (Brazil). Neues Jahrdbuch Miner. Abh. 146: 133-150.

Comin-Chiaramonti, P.; Cundari, A.; Piccirillo, E.M.; Gomes, C.B.; Castorina, F.; Censi, P.; De Min, A.; Marzoli, A.; Speziale, S.; Velaszquez, V.F. 1997. Potassic and sodic igneous rocks from Eastern Paraguay: their origin from the lithospheric mantle and genetic relationships with associated Paraná flood tholeiites. J. Petrol., 38: 495-528.

Corval, A., Valente, S., Duarte, B. P., Famelli, N., Zanon, M. 2008. Dados petrológicos preliminares dos diabásios dos setores centro-norte e nordeste do Enxame de Diques da Serra do Mar. Geochimica Brasiliensis, 22: 159-177.

Corval, A. V. 2009. Petrogênese e Contexto Geodinâmico das Suítes Basálticas Toleíticas (de alto -TiO_2 e baixo - TiO_2) do Cretáceo Inferior da Formação Centro-oriental do Enxame de Diques da Serra do Mar. Tese (Doutorado) - Centro de Tecnologia e Ciências. Faculdade de Geologia. Universidade do Estado do Rio de Janeiro, Rio de Janeiro, RJ.

Courtillot, V. E.1990. Deccan volcanism at the Cretaceous/Tertiary boundary: past climatic crises as a key to the future?. Palaeogeography, Palaeoclimatology, Palaeoecology, 189: 291-299.

Courtillot, V. E.1995. Mass extinctions in the last 300 million years: One impact and seven flood basalts. Israel Journal of Geology (in press).

Courtillot, V. E.1999. Evolutionary Catastrophes: The Science of Mass Extinction. Cambridge University Press, Cambridge, 173 p.

Courtillot, V. E., Besse, J., Vandame, D., Montigny, R., Jaegar, J. J., Cappetta, H. 1986. Deccan flood basalts at the Cretaceous/Tertiary boundary?. Earth and Planetary Science Letters, 80: 361-374.

Courtillot, V. E., Renne, P. R. 2003. On the ages of flood basalt events. Comptes Rendus Geoscience, 335: 113-140.

Coutinho, J. M. V. 2008. Dyke Swarms of the Paraná Triple Junction, Southern Brazil Enxame de Diques da Junção Tríplice do Paraná, Brasil Meridional. Geol. USP Sér. Cient., 8, (2), 29-52.

Cox, K. G. 1980. A model for flood basalt volcanism. Journal of Petrology. 21: 629-650.

Cox, K., Hawkesworth, C. J. 1985. Geochemical Stratigraphy of the Deccan Traps at Mahabaleshwar, Western Ghats, India, with implications fos open system magmatic processes. Journal of Petrology, 26(2): 335-377.

Curtis, M.L., Riley, T.R., Owens, W.H., Leat, P.T., Duncan, R.A., 2008. The form, distribution and anisotropy of magnetic susceptibility of Jurassic dykes in H.U. Sverdrupfjella, Dronning Maud Land, Antarctica. Implications for dyke swarm emplacement. Journal of Structural Geology 30: 1429–1447.

Daniels, K. A., Kavanagh, J. L., Menand, T., Sparks, R. S. J. 2012. The shapes of dikes: Evidence for the influenceof cooling and inelastic deformation. GSA Bulletin, v. 124; no. 7/8; p. 1102–1112; doi: 10.1130/B30537.1.

Deckart, K., Féraud, G., Marques, L.S., Bertrand, H. 1998. New time constraints on dyke swarms related to the Paraná – Etendeka magmatic province, and subsequent South Atlantic opening, southeastern Brazil. Journal of Volcanology and Geothermal Research, 80: 67-83.

Delaney, P. T. and A. E. Gartner, 1997. Physical processes of shallow mafic dike emplacement near the San Rafael Swell, Utha. Geologycal Society of America Bulletin, 109: 1117-1192.

Delaney, P. T., D. D. Pollard, J. I. Ziony and E. H. Mckee, 1986. Field relations between dikes and joints: emplacement processes and paleostress analyses. Journal of Geophysical Research, 91: 4920-4983.

De Paolo, D.J., 1981, Nd isotopic studies: Some new perspectives on Earth Structure and Evolution: EOS, Transactions American Geophysical Union 62, 137–145.doi:10.1029/EO062i014p00137-01

Duncan, A.R., Newton, S. R., van den Berg, C., Reid, D. L., 1989. Geochemistry and petrology of dolerite sills in the Huab River Valley, Damaraland, north-western Namibia, Communs geol. Surv. Namibia 5, 5-18

Duncan, A.R., Armstrong, R.A., Erlank, A.J., Marsh, J.S. and Watkins, R.T., 1990. MORB-related dolerites associated with the final phases of Karoo flood basalt volcanism in southern Africa. In: J.A.J. Parker, P. C. Rickwood and D.H. Tucker (Editors), Mafic Dikes and Emplacement Mechanisms, A.A. Balkema, Rotterdam, The Netherlands, 119-129.

Eick, N. C., Lisboa, N. A., Schuck, M. T. G. O. 1984. Geologia do Cerro Coronel, Rio Pardo, RS. In. CONGRESSO BRASILEIRO DE GEOLOGIA, 33., 1974, Anais, Rio de Janeiro, SBG, v. 5, 2450-2464.

Elliot, D.H., 1975. Tectonics of Antarctica: a review. American Journal of Science, 275: 45–106.

Encarnación, J., Fleming, T.H., Elliot, D.H., Eales, H.V., 1996. Synchronous emplacement of Ferrar and Karoo dolerites and the early breakup of Gondwana. Geology 24: 535–538.

Ernesto, M., Raposo, M. I. B., Marques, L. S., Renne, P. R., Diogo, L. A., De Mim, A. 1999. Paleomagnetism, geochemistry and 40Ar/39Ar dating of the North-eastern Paraná Magmatic Province: tectonic implication. Journal of Geodynamics, Netherlands, 28: 321-340

Ernst, R. E., and A. R. Duncan, 1995. Magma flow in the giant Botswana dyke swarm from analysis of magnetic fabric (abstract), Program & Abstracts for the Third International Dyke Conference, Sept. 4-8, 1995, Jerusalem, Israel, edited by A. Agnon and G. Baer, pp. 30.

Ewart A., Milner, S.C., Armstrong, R.A., Duncan, A.R., 1998. Etendeka volcanism of the Goboboseb Mountains and Messum Igneous Complex, Namibia. Part I: Geochemical evidence of early Cretaceous Tristan plume melts and the role of crustal contamination in the Parana-Etendeka CFB. Journal of Petrology 39, 191-225.

Ferreira, F. J. F. 1982. Alinhamentos estruturais magnéticos de região centro-oriental da Bacia do Paraná e seu significado tectônico. In: Geologia da Bacia do Paraná – reativação da potencialidade e prospectividade em hidrocarbonetos (143-166). São Paulo: Paulipetro – Consórcio CESP/IPT.

Fleming, T.H., Poland, K.A., Elliot, D.H., 1995. Isotopic and chemical constraints on the crustal evolution and source signature of Ferrar magmas, north Victoria Land, Antarctica. Contributions to Mineralogy and Petrology 121: 217–236.

Florisbal, L. M., Heaman, L. M., Janasi, V. A., Bitencourt, M. F., 2014. Tectonic significance of the Florianópolis Dyke Swarm, Paraná–Etendeka Magmatic Province: A reappraisal based on precise U–Pb dating. Journal of Volcanology and Geothermal Research 289, 140-150.

Florisbal, L. M., Janasi, V. A., Bitencourt, M. F., Nardi, L. V. S., Marteleto, N. S., 2017. Geological, geochemical and isotope diversity of ~ 134 Ma dykes from the Florianópolis Dyke Swarm, Paraná Magmatic Province: Geodynamic controls on petrogenesis. Journal of Volcanology and Geothermal Research. (Accepted Manuscript)

Frank, H. T., Gomes, M. E. B., Formoso, M. L. L. 2009. Review of the areal extent and the volume of the Serra Geral Formation, Paraná Basin, South America. Pesquisas em Geociências, 36 (1): 49-57.

Fúlfaro, V. J., Saad, A. R., Santos, M. V., Vianna, R. B. (1982). Compartimentação e evolução tectônica da bacia do Paraná. Revista Brasileira de Geociências, 12: 590–611.

Galerne, C. Y., Galland, O., Neumann, E., Planke, S. 2011. 3D relationships between sills and their feeders: evidence from the Golden Valley Sill Complex (Karoo Basin) and experimental modeling. Journal of Volcanology and Geothermal Research, 202: 189-199.

Galerne, C. Y., Neumann, E., Planke, S. 2008. Emplacement mechanisms of sill complexes: Information from the geochemical architecture of the Golden Valley Sill Complex, South Africa. Journal of Volcanology and Geothermal Research, 177: 425–440.

Gibson, S.A.; Thompson, R.N.; Dickin, A.P.; Leonardos, O.H. 1995. High-Ti and low-Ti mafic potassic magmas: key to plume-lithosphere interactions and continental flood-basalt genesis. Earth Planet. Sci. Lett., 136: 149-165.

Gibson, S.A.; Thompson, R.N.; Leonardos, O.H.; Dickin, A.P.; Mitchell, J.G. 1999. The limited extent of plume-lithosphere interactions during continental flood basalt genesis: geochemical evidence from Cretaceous magmatism in southern Brazil. Contrib. Mineral. Petrol., 137: 147-169.

Gibson, S.A., Thompson, R.N., Day J.A. 2006. Timescales and mechanisms of plume–lithosphere interactions: 40Ar/39Ar geochronology and geochemistry of

alkaline igneous rocks from the Paraná–Etendeka large igneous province. Earth and Planetary Science Letters, 251: 1-17.

Glen, W. 1994. The mass-extinction debates: How science work in a crisis. Stanford, Calif.: Stanford University Press, 370 p.

Goulty, N.R., 2005. Emplacement mechanism of the Great Whin and Midland Valley dolerite sills. Journal of the Geological Society 162: 1047–1056.

Haimson, B. C., 1975. Deep in-situ stress measurements by hydrofracturing. Tectonophysics, 29: 41-47.

Hall, A., 1987. Igneous petrology. John Wiley & Sons, Inc. New York., 573 p.

Hastie, W. W., Michael, K. W., Charles, A. 2014 Magma flow in dyke swarms of the Karoo LIP: Implications for the mantle plume hypothesis. Gondwana Research. 25: 736–755

Hawkesworth, C. J., Mantovani, M. S. M., Peate, D. W. 1988. Lithosphere remobilization during Parana CFB magmatism, in Oceanic and Continental Lithosphere; Similarities and Differences, edited by Menzies, M. A. & Cox, K. Joural of Petrology, special volume (1): 205-223.

Heilbron, M., Pedrosa-Soares, A. C., Campos Neto, M. C., Silva, L. C., Trow, R. A. J., Janasi, V. A. 2004. Província Mantiqueira. In: Mantesso-Neto, V., Bartorelli, A., Carneiro, C. D. R., Brito-Neves, B. B. (Eds) Livro Geologia do Continente Sul_Americano: Evolução da obra de Fernando Flávio Marques de Almeida. São Paulo: Editora Beca. p. 647.

Hills, E. S., 1975. Elements of structural geology. Chapman and Hall.Ltd., London. 501 p.

Hooper, P. R., Camp, V. E., Reidel, S. P. & Ross, M. E. 2007. The origin of the Columbia River flood basalt province: Plume versus nonplume models. Geol. Soc. Am. Special Paper 430: 635–668.

Hooper, P., Widdowson, M., Kelley, S., 2010. Tectonic setting and timing of the final Deccan flood basalt eruptions. Geology 38: 839–842.

Janasi, V. A., Freitas, V. A., Heaman, L. H. 2011. The onset of flood basalt volcanism, Northern Paraná Basin, Brazil: A precise U-Pb baddeleyite/zircon age for a Chapecó-type dacite. Earth and Planetary Science Letters, 302 (1): 147-153.

Jerram, D.A., Mountney, N., Holzforster, F., Stollhofen, H., 1999. Internal stratigraphic relationships in the Etendeka Group in the Huab Basin, NW Namibia: under- standing the onset of flood volcanism. J. Geodyn. 28, 393-418.

Jerram, D.A., Mountney, N., Howell, J., Long, D., Stollhofen, H. 2000. Death of a Sand Sea: an active erg systematically buried by the Etendeka flood basalts of NW Namibia. Journal of the Geological Society of London, 157: 513–516.

Jordan, B. T., Grunder, A. L., Duncan, R. A. & Deino, A. L. 2004a. Geochronology of age-progressive volcanism of the Oregon high lava plains: Implications for the plume interpretation of Yellowstone. J. Geophys. Res. 109 (doi:10.1029/2003JB002776).

Jourdan, F., Féraud, G., Bertrand, H., Kampunzu, A.B., Tshoso, G., Le Gall, B., Tiercelin, J.J., Capiez, P., 2004b. The Karoo triple junction questioned: evidence from Jurassic and Proterozoic 40Ar/39Ar ages and geochemistry of the giant Okavango dyke swarm (Botswana). Earth and Planetary Science Letters. 222: 989–1006.

Jourdan, F., Féraud, G., Bertrand, H.,Watkeys,M.K., Renne, P.R., 2007. Distinct brief major events in the Karoo large igneous province clarified by new 40Ar/39Ar ages on the Lesotho basalts. Lithos 98: 195–209.

Kelley, S. 2007. The geochronology of large igneous provinces, terrestrial impact craters, and their relationship to mass extinctions on Earth. Journal of the Geological Society of London, 164: 923-936.

Kumagai, I.; Kurita, K. 2005. A causal relationship between a superplume and a supercontinent: Which came first?. Geophysical Research Abstracts, v. 7, p. 9302.

Leeman,W. P., Oldow, J. S. & Hart,W. K. 1992. Lithosphere-scale thrusting in the western U.S. Cordillera as constrained by Sr and Nd isotopic transitions in Neogene volcanic rocks. Geology 20: 63–66.

Lima, E.F.; Philipp, R. P.; Rizzon, G.C.; Waichel, B.L.; Rossetti, L.M.M. 2012a. Sucessões Vulcânicas e Modelo de Alimentação e Geração de Domos de Lava Ácidos da Formação Serra Geral na Região de São Marcos-Antonio Prado (RS). Geol. USP. Série Científica, 12: 49-64.

Lima, E.F.; Waichel, B.L; Rossetti, L.M.M.; Viana, A.R.; Scherer, C.M.; Bueno, G.V.; Dutra, G. 2012b. Morphology and petrographic patterns of the pahoehoe and 'a'a flows of the Serra Geral Formation in the Torres Syncline (Rio Grande do Sul state, Brazil. Rev. Bras. Geoc., 42: 744-753.

Lister, J. R. and R. C. Kerr, 1991. Fluid-mechanical models of crack propagation and their application to magma transport in dykes. Journal of Geophysical Research, 96: 10049-10077.

Ludwig, K.R., 2001. Isoplot: A ploting and regression program for radiogenic isotope data(version 2.50). United States Geological Survey. Open file Report, 88-542.

Lugmair, G.W., Marti, K., 1978. Lunar initial $^{143}Nd/^{144}Nd$: Differential evolution of the lunar crust and mantle: Earth and Planetary Science Letters 39, 349–357. doi:10.1016/0012-821X(78)90021-3

Machado, F.B. 2005. Geologia e aspectos petrológicos das rochas intrusivas e efusivas mesozóicas de parte da borda leste da Bacia do Paraná no Estado de São

Paulo. 2005. Dissertação (Mestrado). Instituto de Geociências e Ciências Exatas, Universidade Estadual Paulista. Rio Claro, SP.

Machado, F. B., Nardy, A. J. R. & Oliveira, M. A. F. 2007. Geologia e aspectos petrológicos das rochas intrusivas e efusivas mesozóicas de parte da borda leste da bacia do Paraná no estado de São Paulo. Revista Brasileira de Geociências, 37(1): 64-80.

Mahoney, J. J., Sheth, H. C., Chandrasekharam, D. & Peng, Z. X. 2000. Geochemistry of flood basalts of the Toranmal section,Northern Deccan Traps, India: Implications for regional Deccan stratigraphy. Journal of Petrology 41(7): 1099-1120.

Maniesi, V., Oliveira, M. A. F. 1997. Petrologia das soleiras de diabásio de Reserva e Salto do Itararé, PR. Geochimica Brasiliensis , 11(2): 153-169.

Mantovani, M.S.M., Marques, L.S., Souza, M.A., Atalla, L., Civeta, L., Inonocenti, F. 1985.Trace Element and Strontium Isotope Constrains of the Origin and Evolution of Paraná Continental Flood Basalts of Santa Catarina State (Southern Brazil). Journal of Petrology, 26: 187-209.

Marques, L.S. 2001. Geoquímica dos diques toleíticos da costa sul-sudeste do Brasil: Contribuição ao conhecimento da Província Magmática do Paraná. 2001. Tese (Doutorado) – Instituto de Astronomia e Geofísica, Universidade de São Paulo.

Marques, L.S.; Dupré, B.; Piccirillo, E.M. 1999. Mantle source compositions of the Paraná Magmatic Province: evidence from trace element and Sr-Nd-Pb isotope geochemistry. J. Geodynamics, 28: 439-459.

Marques, L.S., Ernesto, M. 2004. O Magmatismo Toleítico da Bacia do Paraná. In: Mantesso-Neto, V., Bartorelli, A., Carneiro, C. D. R., Brito-Neves, B. B. (Eds), Livro Geologia do Continente Sul-Americano: Evolução da obra de Fernando Flávio Marques de Almeida. São Paulo: Editora Beca.

Marques, L.S., Figueiredo, A.M.G., Saiki, M., Vasconcellos, M.B.A. 1989. Geoquímica analítica dos elementos terras raras - Aplicação da técnica de análise por ativação neutrônica. In: Formoso, M.L.L.; Nardy, L.V.S. & L.A. Hartmann (Coords.), Geoquímica dos Elementos Terras Raras no Brasil (15-20), CPRM/DNPM, Rio de Janeiro, Sociedade Brasileira de Geoquímica.

Marsh, B.D., 2013. On some fundamentals of igneous petrology. Contributions to Mineralogy and Petrology 166, 665–690.

Melfi, A.J.; Nardy, A.J.R.; Piccirillo, E.M. 1988. Geological and magmatic aspects of the Paraná Basin: An introduction. In: Piccirillo, E.M. & Melfi, A.J. (eds.). The Mesozoic flood volcanism of the Paraná Basin: Petrogenetic and geophysical aspects. IAG-USP, p. 1-13.

Milani, E. J. 2004. Comentários sobre a origem e a evolução tectônica da Bacia do Paraná. In: Mantesso-Neto V, Bartorelli A, Carneiro Cdr & Brito Neves Bb (Eds.).

Geologia do continente sul-americano: evolução da obra de Fernando Flávio Marques de Almeida. São Paulo, Beca. p. 265-279.

Milani, E.J.; Fernandes, L.A.; França, A.B; Melo, J.H.G.; Souza, P.A. 2007. Bacia do Paraná. In: Milani, E.J. (ed.). Boletim de geociências da Petrobrás, Cartas estratigráficas. Petrobrás, 15 (2): 265-287.

Milner, S.C. & LeRoex, A.P. 1996. Isotope characteristics of the Okenyenya igneous complex, northwestern Namibia: constraints on the composition of the early Tristan plume and the origin of the EM 1 mantle componente. Earth Planet. Sci. Letters, 141: 277-291.

Motoki, A., 1986. Geologia e Petrologia do Maciço Alcalino da Ilha de Vitória, SP. Tese (Doutorado). Instituto de Geociências da Universidade de São Paulo.

Motoki, A., Sichel S.E., 2008. Hydraulic fracturing as a possible mechanism of dyke-sill transitions and horizontal discordant intrusions in trachytic tabular bodies of Arraial do Cabo, State of Rio de Janeiro, Brazil. Geofísica Internacional, 47 (1): 13-25.

Mountney, N., Howell, J., Flint, S., Jerram, D., 1998. Aeolian and alluvial deposition within the mesozoic Etjo sandstone formation, northwest Namibia. J. Afr. Earth Sci. 27 (2), 175-192.

Nakamura, K., 1977. Volcanoes as possible indicators of tectonic stress orientation; Principle and proposal. Journal of Volcanology and Geothermal Research, 115(2): 1-16.

Nakamura, K., Jacob, J. N. &. Davies, K. H. 1977. Volcanoes as possible indicators of tectonic stress orientation; Aleutians and Alaska, Pure and Application Geophysics, 115, 87-112.

Nardy, A. J. R. 1995. Geologia e petrologia do vulcanismo mesozóico da região central da Bacia do Paraná. Tese (Doutorado). Instituto de Geociências e Ciências Exatas, Universidade Estadual Paulista. Rio Claro, São Paulo.

Oliveira, E.C., Lafon, J.M., Gioia, S.M.C.L., and Pimentel, M.M., 2008, Datação Sm-Nd em rocha total e granada do metamorfismo granulítico da região de Tartarugal Grande: Amapá Central: Revista Brasileira Geociências 38, 116–129.

Owen-Smith, T. M., Ashwal, L. D. 2015., Evidence for multiple pulses of crystal-bearing magma during emplacement of the Doros layered intrusion, Namibia. Lithos 238, 120-139.

Parsons, T. & G. A. Thompson, 1992. The Role of magma overpressure in suppressing earthquakes and topography: worldwide examples. Science, 253: 1399-1402.

Parsons, T., Thompson, G. A. & Sleep, N.H. 1994. Mantle plume influence on the Neogene uplift and extension of the U.S. western Cordillera?. Geology, 22: 83-86.

Peate, D. & Hawkesworth, C.J. 1996. Lithospheric to astenospheric transition in low-Ti flood basalts from Southern Paraná , Brazil. Chem. Geol., 127: 1-24.

Peate, D. W. Hawkesworth, C. J., Mantovani, M. S. M. 1992. Chemical stratigraphy of the Paraná lavas (South América): classification of magma types and their spatial distribution. Bulletin of Volcanology, Berlin, 55 (1): 119-139.

Peate D.W. 1997. The Paraná–Etendeka province. In: Mahoney J.J., Coffin M.F. Large Igneous Provinces: Continental, Oceanic and Planetary Flood Volcanism (217-245). Washington, DC: American Geophysical Union.

Peate, D.W., Hawkesworth, C.J., Mantovani, M.M.S., Rogers, N.W., Turner, S.P. 1999. Petrogenesis and stratigraphy of the high Ti/Y Urubici magma type in the Paraná flood basalt province and implications for the nature of "Dupal"- type mantle in the South Atlantic region. Journal of Petrology, 40: 451-473.

Peng, Z. X., Mahoney, J. J., Hooper, P. R., Macdougall, J. D., Krishnamurthy, P. 1998. Basalts of the northeastern DeccanTraps, India: Isotopic and elemental geochemistry and relation to southwestern Deccan stratigrapy. Journal of Geophysical Research, 103 (B12): 29843-29865.

Petersohn, E. & Gouvea, E. M. 2009. Geologia e geoquímica da soleira de Reserva, Estado do Paraná. Revista Brasileira de Geociências, 39(4): 740-750.

Petersohn, E., Vasconcellos, E. M. G., Lopes, K. 2007. Petrologia de sills encaixados nas Formações Irati e Ponta Grossa (Bacia do Paraná) no Estado do Paraná. Geochimica Brasiliensis, 21, 58-70.

Petrini, R., Civetta, L., Piccirillo, E.M., Bellieni, G., Comin-Chiaramonti, P., Marques, L.S., and Melfi, A.J., 1987, Mantle heterogeneity and crustal contamination in the genesis of low-Ti continental flood basalts from the Paraná plateau (Brazil): Sr-Nd isotope and geochemical evidence. Journal of Petrology 28, 701–726. doi:10.1093/petrology/28.4.701

Phillips, W. J., 1974. The dynamic emplacement of cone sheets. Tectonophysics, 24: 69-84.

Piccirillo, E. M. & Melfi A. J. 1988. The Mesozoic flood volcanism of the Paraná Basin - petrogenetic and geophysical aspects. São Paulo: USP.

Piccirillo, E. M., Civetta, L., Petrini, R., Longinelli, A., Bellieni, G., Comin-Chiaramonti, P., Marques, L. S., Melfi, A. J. 1989. Regional variations within the Paraná Flood Basalts (Southern Brazil): Evidence for subcontinental mantle heterogeneity and crustal contamination. Chemical Geology, 75: 103-122.

Piccirillo, E. M., Bellieni, G., Cavazzini, G., Comin-Chiaramonti, P., Petrini, R., Melfi, A. J., Pinesi, J. P. P., Zantadeschi, P., Demin, A. 1990. Lower Cretaceous tholeiitic

dyke swarms from the Ponta Grossa (southeast Brazil): Petrology, Sr-Nd isotopes and genetic relationships whith the Paraná flood volcanic. Chemical Geology, Netherlands, 89: 19-48.

Pollard, D.D., Muller, O.H., 1976, The effect of gradients inregional stress and magma pressure on the form of sheetintrusions in cross section: Journal of Geophysical Research,v. 81, p. 975–984, doi:10.1029/JB081i005p00975.

Rampino, M. R., Haggerty, B. M. 1996. Impact crises and mass extinctions: A working hypothesis. Geological Society of America Special Papers, 307: 11-30.

Rampino, M. R., Stothers, R. B. 1988. Flood basalt volcanism during the past 250 million years. Science, 241: 663-668.

Raposo, M. I. B., Ernesto, M., Renne, P. R. 1998. Paleomagnetism and 40Ar/39Ar dating of the Early Cretaceous Florianópolis dike swarm (Santa Catarina Island), Southern Brazil. Physics of the Earth and Planetary Interiors, 108: 275-290.

Ray, R., Sheth, H.C., Mallik, J., 2007. Structure and emplacement of te Nandurbar-Dhule mafic dyke swarm, Deccan Traps, and the tectonomagmatic evolution of flood basalts. Bulletin of Volcanology 69: 531–537.

Renne, P. R., Ernesto, M., Pacca, I. G., Coe, R. S., Glen, J. M., Prévot, M., Perrin, M. 1992. The age of Paraná Flood Volcanism, rifting of Gondwana land, and the Jurassic-Cretaceous boundary. Science, 258: 975-979.

Renne, P. R., Glen, J. M., Milner, S. C., Duncan, A. R. 1996. Age of the Ponta Grossa dyke swarm (Brazil), and implications to Paraná flood volcanism. Earth and Planetary Science Letters, Netherlands, 144: 199-211.

Renner, L. C., Hartmann, L. A.,Wildner, W. 2008. Caracterização geoquímica de sills da região de Manoel Viana e Agudo, porção sul da Formação Serra Geral e comparação com os sills da porção leste e norte da Bacia do Paraná. IV Simpósio de Vulcanismo e Ambientes Associados. (1 CD.ROM) SBG. Foz do Iguaçu, PR.

Renner, L.C. 2010. Geoquímica de sills basálticos da Formação Serra Geral, sul do Brasil, com base em rocha total e micro-análise de minerais. Tese (Doutorado) – Instituto de Geociências. Programa de Pós-Graduação em Geociências, Universidade Federal do Rio Grande do Sul, Porto Alegre, RS.

Ricommini, C., L. G. Sant'anna and A. L. Ferrari, 2004. Evolução geológica do rift continental do Sudeste do Brasil. In Mantesso-Neto, V., Bartorelli, A., Carneiro, C.D.R., Brito-Neves, B.B. Ed. Geologia do Continente Sul-Americno: Evolução da obra de Fernando Flávio Marques de Almeida. São Paulo. Editora Beca, 385-405.

Ricommini, C., 1997. Arcabouço estrutural e aspectos do tectonismo gerador e deformador da bacia Bauru no estado de São Paulo. Revista Brasileira de Geociências, 27(2), 153-162.

Riley, T.R., Curtis, M.L., Leat, P.T., Watkeys, M.K., Duncan, R.A., Millar, I.L., Owens, W.H., 2006. Overlap of Karoo and Ferrarmagma types in KwaZulu-Natal, South Africa. Journal of Petrology, 47: 541–566.

Rossetti, L. M., Lima, E. F., Waichel, B. L., Scherer, C. M., Barreto, C. J., 2014. Stratigraphical framework of basaltic lavas in Torres Syncline main valley, southern Parana-Etendeka Volcanic Province. Journal of South American Earth Sciences 56, 409-421.

Rossetti, L. M., Lima, E. F., Waichel, B. L., Hole M. J., Scherer, C. M., Simões, M. S., 2017. Lithostratigraphy and volcanology of the Serra Geral Group, Paraná-Etendeka Igneous Province in Southern Brazil: Towards a formal stratigraphical framework. J. Volcanol. Geotherm. Res., In Press, http://dx.doi.org/10.1016/j.jvolgeores.2017.05.008

Sarmento, C.C.T., Sommer, C. A., Lima, E. F., Oliveira, D. S. 2014. Corpos hipabissais correlacionados à Formação Serra Geral naregião do Cerro do Coronel, RS: geologia e petrologia. Geologia USP, Série Científica, 14(2): 23-44.

Self,S.; Keszthelyi, L.; Thordarson, T. The importance of pahoehoe. 1998. Annual Reviews Earth Planetary Science, 26: 81-110.

Self, S., Widdowson, M., Thordarson, T., Jay, A.E., 2006. Volatile fluxes during flood basalt eruptions and potential effects on global environment: a Deccan perspective. Earth and Planetary Science Letters, 248: 518–532.

Scherer, C.M.S. 2002. Preservation of aeolian genetic units by lava flows in the Lower Cretaceous of the Paraná Basin, southern Brazil. Sedimentology, 49: 97–116.

Schmitt, S. R. & N. Stanton, 2007. Cronologia relativa das estruturas rúpteis e diques meso-cenozóicos na porção on shore do alto do Cabo Frio - Região costeira e ilhas adjacentes, RJ. Anais do SIMPÓSIO NACIONAL DE ESTUDOS TECTÔNICOS, 5TH INTERNACIONAL SYMPOSIUM ON TECTONICS OF THE SBG. 221-223.

Smith, R. B. & Braile, L. W. 1993 The Yellowstone hotspot : physical properties, topographic and seismic signature, and space-time evolution (abstract), Eos Trans. AGU 1993 Fall Meeting Suppl, p. 602, 1993

Sen, G. 2001. Generation of Deccan Trap magmas. Proceedings of the Indian Academy of Science. Earth and Planetary Science, 110(4):409-431.

Sheth, H.C. 2007. 'Large Igneous Provinces (LIPs)': Definition, recommended terminology, and a hierarchical classification. Earth-Sci. Rev., 85(3-4): 117-124.

Sheth, H.C., Ray, J.S., Ray, R., Vanderkluysen, L., Mahoney, J.J., Kumar, A., Shukla, A.D.,Das, P., Adhikari, S., Jana, B. 2009. Geology and geochemistry of Pachmarhi dykes and sills, Satpura Gondwana Basin, central India: problems of dyke-sill flow correlations in the Deccan Traps. Contributions to Mineralogy and Petrology, 158: 357–380.

Sheth, H. C., Zellmer, G. F., Demonterova E. I., Ivanov, A. V., Kumar, R., Patel, R. K. 2013. The Deccan tholeiite lavas and dykes of Ghatkopar–Powai area, Mumbai, Panvel flexure zone: Geochemistry, stratigraphic status, and tectonic significance. Journal of Asian Earth Sciences. http://dx.doi.org/10.1016/j.jseaes.2013.05.007

Soares, P. C. 1981. Estratigrafia das Formações Jurássico-Cretáceas na Bacia do Paraná, Brasil. In: Cuencas Sedimentares De Jurássico Y Cretáceo De América Del Sur, Comitê Sul Americano del Jurássico Y Cretáceo., 1, 271- 304. Buenos Aires

Steiger, R.H., Jäger, E., 1977. Subcommission on geochronology: convention on the use of decay constants in geo- and cosmochronology. Earth and Planetary Science Letters 36(3), 359-362.

Stewart, K., Turner, S., Kelley, S., Hawkesworth, C. J., Kirstein, L., Mantovani, M. 1996. 3-D, Ar/Ar geochronology in the Paraná continental flood basalt province. Earth and Planetary Science Letters, 143, 95-109.

Subbarao, K. V., Hooper, P. R., Dayal, A. M., Walsh, J. N., Gopalan, K. 1999. Narmada dykes. In: Subbarao, K. V. (ed.) Deccan Volcanic Province. Memoir of the Geological Society of India 43:891-902.

Swanson, D., Wright, T. L., Hooper, P. R., Bentley, R. D. 1979. Revisions in stratigraphic nomenclature of the Columbia River Basalt Group. US Geol. Survey. Bull. 1457-G, 59p.

Thiede, D. S., Vasconcelos, P. M. 2010. Paraná flood basalts: Rapid extrusion hypothesis confirmed by new 40Ar/39Ar results. Geology, 38 (8): 747- 750.

Thompson, R. N., Gibson, S. A., Dickin, A. P. & Smith, P. M., 2001. Early Cretaceous basalt and picrite dykes of the southern Etendeka region, NW Namibia: windows into the role of the Tristan mantle plume in Parana-Etendeka magmatism. Journal of Petrology 42, 2049-2081.

Thompson, R.N., Riches, A.J.V., Antoshechkina, P.M., Pearson, D.G., Nowell, G.M., Ottley, C.J., Dickin, A.P., Hards, V.L., Nguno, A.-K. and Niku-Paavola, V., 2007. Origin of CFB magmatism: multi-tiered intracrustal picriterhyolite magmatic plumbing at Spitzkoppe, western Namibia, during Early Cretaceous Etendeka magmatism. Journal of Petrology 48, 1119-1154.

Tomazzoli, E.R. & Lima, E.F., 2006. Magmatismo ácido-básico na ilha do Arvoredo-SC. Revista Brasileira de Geociências 36, 57–76.

Tomazzoli, E. E. & Pellerin, J. M., 2015. Unidades do mapa geológico da ilha de Santa Catarina: as Rochas. Florianópolis. Geosul 60(30), 225-247.

Trumbull, R.B., Vietor, T., Hahne, K., Wackerle, R. and Ledru, P., 2004. Aeromagnetic mapping and reconnaissance geochemistry of the Early Cretaceous Henties Bay-Outjo mafic dike swarm, Etendeka Igneous Province, Namibia. Journal of African Earth Sciences 40, 17-29.

Trumbull, R.B., Reid, D.L., Beer, C., Acken, D., Romer, R.L., 2007. Magmatism and continental breakup at the west margin of southern Africa: a geochemical comparison of dolerite dikes from northwestern Namibia and the Western Cape. South Afr. J. Geol. 110, 477-502.

Turner, S., Regelous, M., Kelley, S., Hawkesworth, C., Mantovani, M. 1994. Magmatism and continental break-up in the South Atlantic: high precision 40Ar/39Ar geochronology. Earth and Planetary Science Letters, 121: 333-348.

UFRGS. 2006. Mapeamento Geológico de parte da Folha Quitéria SH22-Y-B-I-4 (MI2985/4) (1:25.000), RS. 1 vol., 2 mapas. Porto Alegre: Curso de Geologia, Instituto de Geociências da Universidade Federal do Rio Grande do Sul.

Vanderkluysen, L., Mahoney, J.J., Hooper, P.R., Sheth, H.C., Ray, R., 2011. The feeder system of the Deccan Traps (India): insights from dyke geochemistry. Journal of Petrology 52:315–343.

Valente, S.C.; Ellan, R. L., Meighan, I. G., Fallick, A. E. 1998. Geoquímica isotópica, modelo geodinâmico e petrogênese dos diabásios do Cretáceo Inferior no enxame de diques máficos da Serra do Mar (EDSM) na área do Rio de Janeiro, RJ. In: 40º CONGRESSO BRASILEIRO DE GEOLOGIA, Belo Horizonte. Boletim de Resumos do 40º Congresso Brasileiro de Geologia. Sociedade Brasileira de Geologia. p. 471.

Valente, S.C.; Meighan, I. G., Fallick, A.E.; Ellam, R.L. 2002. The assessment of post-magmatic processes in the Serra do Mar Dyke Swarm SE, BRAZIL: proposals for acid leaching techniques and criteria for petrognetic interpretations. Revista da Universidade Rural-Série Ciências Exatas e da Terra, Seropédica, 21: 1-21.

Valente, S.C.; Corval, A.; Duarte, B.P.; Ellam, R. L.; Fallick, A.E.; Dutra, T. 2007. Tectonic boundaries, crustal weakness zones and plume-subcontinental lithospheric mantle interactions in the Serra do Mar Dyke Swarm, SE Brazil. Revista Brasileira de Geociências, 37: 194-201.

Valentine, A. G. & K. E. C. Krogh, 2006. Emplacement of shallow dikes and sills beneath a small basaltic volcanic center - The role of pre-existing structure (Paiute Ridge, southern Nevada, USA). Earth and Planetary Science Letters, 246: 217-230.

Viero, A. P. & Roisenberg, A. 1992. Petrologia e geoquímica do Complexo Básico Lomba Grande. Pesquisas em Geociências, 19 (1): 41 – 54.

Waichel, B.L., Scherer, C.M.S., Frank, H.T. 2008. Basaltic lavas covering active Aeolian dunes in the Paraná Basin in Southern Brazil: features and emplacement aspects. Journal of Volcanology and Geothermal Research, 169: 59–72.

Waichel, B. L., Lima, E. F., Viana, A., Scherer, C. M. S., Bueno, G., Dutra, G. 2012. Stratigraphy and volcanic facies architecture of the Torres Syncline, Southern Brazil, and its role in understanding the Paraná-Etendeka Continental Flood Basalt Province. Journal of Volcanology and Geothermal Research, 215: 74-82.

Wasserburg, G.J., Jacobsen, S.B., De Paolo, D.J., Mc Culloch, M.T., Wen, T., 1981.

Precise determination of Sm/Nd ratios, Sm and Nd isotopic abundances in standard solutions. Geochimica et Cosmochimica Acta 45, 2311-2323.

White, R. S.; Mckenzie, D. 1989. Magmatism at rift zones: The generation of volcanic continental margins and flood basalts. Journal of Geophysical Research, Cambridge, 94: 7685–7729.

White, R. S.; Mckenzie, D. Mantle plumes and flood basalts. 1995. Journal of Geophysical Research, Cambridge,. 100 (9) : 17.543-17.585.

Wignall, P. B. 2001. Large igneous provinces and mass extinctions. Earth-Science Reviews, 53: 1-33.

Wignall, P. B. 2005. The link between Large Igneous Province eruptions and mass extinctions. Elements, 1: 293-297.

Wolff, J. A., Ramos, F. C., Hart G. L., Patterson, J. D., Brandon, A. D. 2008. Columbia River flood basalts from a centralized crustal magmatic system. Nature Geoscience, 1: 177-180.

Zalán, P. V., Conceição, J. C. J., Astolfi, M .A. M., Appi, V. T., Wolff, S., Vieira, I. S., Marques, A. 1985. Estilos estruturais relacionado às intrusões magmáticas básicas em rochas sedimentares. Boletim Técnico da PETROBRAS, Rio de Janeiro, RJ, 28 (4): 221 – 230.

Zalán P.V., Wolff S., Conceição J.C., Astolfi M.A.M., Vieira I.S., Appi C.T, Zanotto O.A. 1987. Tectônica e sedimentação da Bacia do Paraná. In: SBG, SIMP. SUL-BRAS. GEOL. (3), Atas, 1, p. 441-447.

Zhang, X., Luttinen, A.V., Elliot, D.H., Larsson, K., Foland, K.A., 2003. Early stages of Gondwana breakup: the 40Ar/39Ar geochronology of Jurassic basaltic rocks from western Dronning Maud Land, Antarctica, and implications for the timing of magmatic and hydrothermal events. Journal of Geophysical Research, 108: 2449–2468.

Zoback, M . L., McKee, M. L., Blackely, R. J., Thompson, G. A. 1994. The northern Nevada riff: Regional tectono-magmatic relations and middle Miocene stress direction. Geol. Soc. Am. Bull., 106: 371-382.